MESOZOIC TO RECENT EVOLUTION OF THE ANDEAN FOREARC, NORTHERN CHILE (22-24°S).

ADRIAN JOHN HARTLEY

Doctor of Philosophy

THE UNIVERSITY OF ASTON IN BIRMINGHAM

OCTOBER 1987

The University of Aston in Birmingham

Mesozoic to Recent Evolution of the Central Andean Forearc, Northern Chile (22-24°S).

ADRIAN JOHN HARTLEY
DOCTOR OF PHILOSOPHY

1987

The Andean forearc of northern Chile comprises four morphotectonic units, which include from east to west:
1) The Cordillera de la Costa: composed of Jurassic granites and andesites, thought to represent a volcanic arc, the Mejillones terrane, an accreted allochthonous terrane, and the Lower Cretaceous Coloso basin, which formed through forearc extension along the suture between the Mejillones terrane and the Jurassic arc. Palaeomagnetic studies of the above units have identified approximately 29+/-11 degrees of clockwise rotation. Rotation is due to extension (caused by subduction roll back and slab pull), at an angle to the direction of absolute motion of the South American Plate.
2) The Central Depression: a large arid basin containing isolated fault-bounded blocks of pre-Mesozoic metamorphosed igneous rocks, Triassic sediments and volcanics, and Jurassic carbonates, deposited in a back-arc basin setting. The isolated blocks formed through extension along previous thrust faults, these originated through compression of the back-arc basin due to accretion of the Jurassic volcanic arc.
3) The Precordillera: composed of Permian-Triassic rift-related sediments and volcanics, Jurassic continental sediments synchronous with back-arc basin sedimentation, and Cretaceous and Oligo-Miocene continental sediments deposited in foreland basins. Palaeomagnetism has identified clockwise rotation in rocks ranging in age from Jurassic-Miocene. Rotation in the Precordillera affected larger structural blocks than in the Cordillera de la Costa.
4) The Salar Depression: a series of arid continental basins developed on continental crust. These basins may have originated in the Triassic, when rifting of the South American craton is thought to have taken place.

In conclusion, palaeomagnetic and geological evidence is consistent with the view that the north Chilean forearc was largely under an extensional stress regime. However, the presence of extensive compressional structures in Palaeocene and older rocks in the forearc together with the currently active foreland thrust belt of Argentina, indicate that throughout the evolution of the Andean Orogen, a delicate balance between compressional and extensional tectonic regimes has existed.

ANDES FOREARC PALAEOMAGNETISM ROTATION CHILE

ACKNOWLEDGEMENTS

I would especially like to thank Pete Turner who initiated and supervised this research project (funded by NERC), and without whose knowledge and continuous encouragement, the project would not have succeeded. Steve Flint contributed a great deal to the project, particularly in the desert, and provided a valuable proof reading service. Andy Chambers helped with igneous and metamorphic petrology. Graham Williams added considerably to my knowledge of structural geology. Rob Ixer helped with reflected light microscopy. The friendship and logistical support of many people in Chile (particularly Guillermo Chong and Jaime Morales), enabled fieldwork to proceed smoothly.

I would like to thank Dr. D. W. Collinson for the use of the Nuffield palaeomagnetic laboratory at the University of Newcastle upon Tyne. Rob Wilson and Dave Plant are gratefully acknowledged for the use of electron microprobe facilities at the Universities of Leicester and Manchester respectively. Thanks are also due to the technical staff in the Department of Geological Sciences at Aston, for help throughout the project, and in particular Beverley Parker, who considerably aided the production of diagrams for this thesis.

The thesis has benefited considerably from discussion (in either the Department or Sacks of Potatoes) with, Jeremy Prosser, Chris Cornelius, Mandy Turner and other postgradute students (both past and present) from Aston geology.

Finally, the most important acknowledgement is to my fiancee Jo, without whose love and continued support, the completion of this thesis would not have been possible (and fudge).

List of Contents

List of Figures

Page

Chapter 3

Page

Chapter 4

Chapter 5

List of Tables

List of Plates

CHAPTER 1

INTRODUCTION

1.1 Preface

The first description of the geology of the Andes was provided by Darwin (1876), since then, many workers have attempted to describe and characterise this distinctive Orogen. The advent of the plate tectonic theory resulted in the Andes being regarded as the classic "simple" Orogen, formed at a convergent plate boundary, with uplift due to subduction and melting of the oceanic plate.

Recent work has shown however, that many features of the Andean margin vary considerably along strike, particularly: seismicity, volcanicity (Barazangi and Isacks,1976), topography (Jordan et al.,1983) and mineralisation (Sillitoe,1974). These variations have been correlated with changes in the dip of the subducting segments of the Nazca Plate beneath the continental margin (Barazangi and Isacks,1976; Jordan et al.,1983).

From the above work, the Andean margin has been subdivided into 5 segments, related to variations in the angle of subduction along strike (Fig. 1.1). The junctions between these segments may be abrupt or gradual (James, 1978).

The geology above each individual segment varies considerably. In this thesis the geology of the southern part of the Central Andean segment is considered (Fig. 1.1).

1.2 Study Area

This thesis is particularly concerned with the evolution of the Andean forearc in northern Chile between 20 and 26°S, with the main study area lying between 22 and 24°S. Although the following work concentrates on northern Chile, the Andean Orogen also extends into southwest Bolivia and northwest Argentina between 20 and 26°S. Consequently, the geological history of these areas is also considered.

Between 20-26°S. and 70-65°W. the Andes can be split into 8 separate morphological provinces, which strike N/S (Fig. 1.2a). From east to west these are:

1) The Cordillera de la Costa. This area comprises a narrow mountain range, adjacent to the Pacific Ocean, which is up to 2000m. high and 50-70km. wide. The area is bounded to the east by the Atacama fault zone.

2) The Central Depression. A major sedimentary basin, which contains a large part of the Atacama Desert. The area is up to 150km. wide and rises gently from west to east, from 1100-1700m.

3) The Precordillera. A narrow mountain range up to 4800m. high, known locally as the Cordillera de Domeyko.

4) The Salar Depression. A narrow, discontinuous belt of large, internally drained basins, with an average elevation of approximately

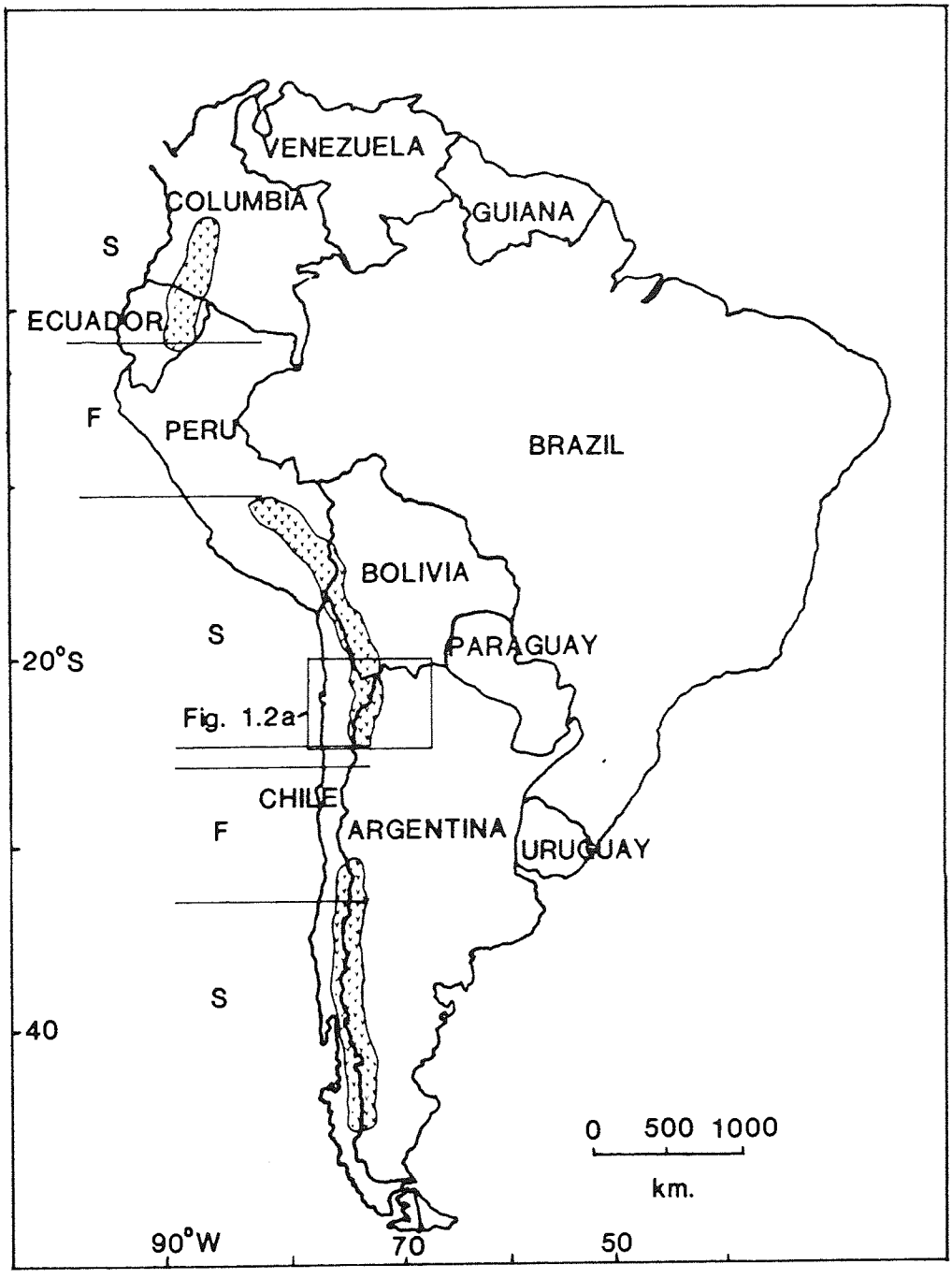

Fig. 1.1 Map of South America showing the sub-horizontal (F) and steeply dipping (30-40 degrees; S), segments of the subducted Nazca Plate. The areas overlying steeply dipping Benioff zones are characterised by Neogene-Recent volcanism (v ornament) and a narrow seismic zone, whereas areas overlying shallowly inclined Benioff zones have little Neogene-Recent volcanism and are seismically active over a broad area (Jordan et al.,1983). The box corresponds to the area covered by Fig. 1.2a.

1500m. This area contains the Salar de Atacama and other smaller salt pans such as the Salar de Punta Negra (Fig. 1.2b).

5) The Cordillera de los Andes. The high Andes, which comprise an extensive chain of Miocene-Recent volcanoes, over 6000m. high in places.

6) The Altiplano/Puna. This area forms a barren, extensive plateau with an average elevation of 3800m., extending as far north as Peru. It contains several extensive salt pans and lakes (Salar de Uyuni, Lake Titicaca). The plateau is arid and scoured by cold winds.

7) The Cordillera Oriental. The area to the east of the Altiplano/Puna, with peaks up to 6000m. in height, and parts of the dissecting valleys dropping to 1200m. The average peak height is 4000m. The climate is arid and cold with strong winds in the western part from the Puna/Altiplano.

8) The Sierras Subandinas. The eastern Andean foothills, generally below 3000m. in height. They show a steady decrease in elevation to the east and are heavily vegetated. The area currently forms a seismically active foreland thrust zone (Allmendinger et al.,1983).

1.2.1 Climate, Demography and Logistics

West of the Cordillera de los Andes between 22 and 24°S., the area below 3000m. (Fig. 1.2b) is completely arid, with summer temperatures up to 40°C., and a large diurnal temperature range. Above 3000m. (in the east of the area), ephermal snow fed rivers provide

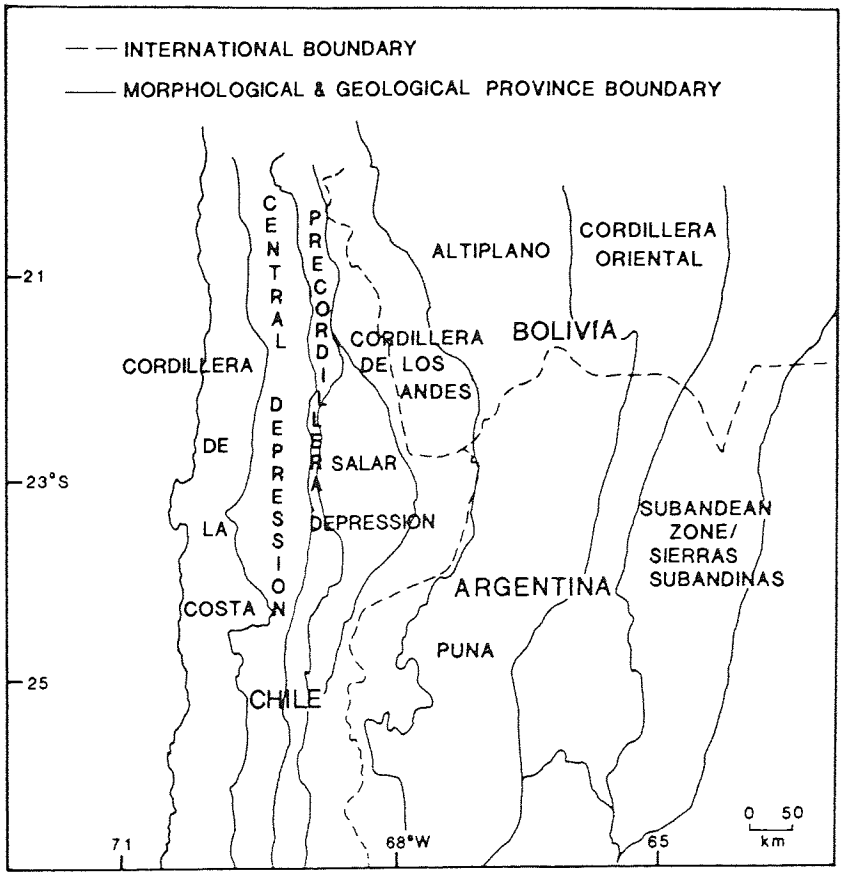

Fig. 1.2a Map of the morphological provinces present across the Andean orogen between 20-26°S. and 65-70°W.,

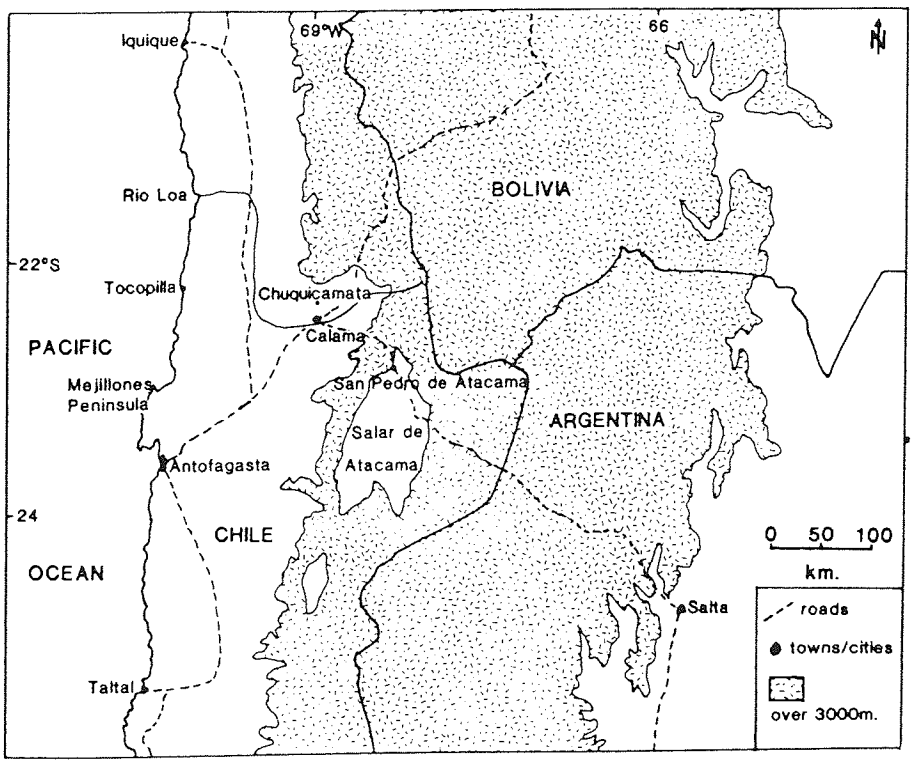

Fig. 1.2b Map of the general geography of the study area and surround-

water for intermittent scrubby vegetation.

Habitation is concentrated in the oasis town of San Pedro de Atacama, the regional capital Calama (adjacent to the large Chiquicamata porphyry copper deposit), the provincial capital Antofagasta and small isolated villages (Fig. 1.2b). Water for the towns situated on the coast, is supplied by pipeline from the Cordillera de los Andes.

The Antofagasta-Salta international "highway" which passes through San Pedro de Atacama provides access to the area (Fig. 1.2b). However, a 4 wheel drive vehicle is required for off road work, and many areas are only accessible on foot. Exposure in the study area is generally good.

1.3 Thesis Aims and Layout

Despite recent work, the regional geology and evolution of the Andean orogen between 20 and 26°S. is poorly understood. Chapter 2 of this thesis attempts to summarise literature relevant to the study area, and discuss the current views concerning the evolution of the Andean Orogen. Particular attention is paid to the Mesozoic-Recent evolution of the area. This Chapter is also concerned with the little known pre-Mesozoic history of the area, as a background to the development of the Andean Orogen.

Previous palaeomagnetic work in northern Chile, has revealed a marked discordance in Mesozoic palaeomagnetic poles derived from the Cordillera de la Costa and the apparent polar wander path for the stable shield area of South America (Palmer et al.,1980a,b; Turner et al.,1984a). One of the aims of this thesis was to investigate and

account for this discrepency. Palaeomagnetic samples ranging from Precambrian-Miocene in age, were collected from across the forearc, in order to approach this problem. This work is presented in Chapters 3 (Cordillera de la Costa) and 5 (Precordillera/Central Depression).

A major problem concerning the evolution of the andean forearc in northern Chile, is the presence of the Mejillones Peninsula (Fig. 1.2b). The Peninsula comprises a crystalline massif, which has yielded Precambrian radiometric dates (Damm et al.,1986), in contrast to the dominantly Jurassic-Cretaceous Cordillera de la Costa. The western margin of North America is almost entirely composed of accreted allochthonous terranes (Beck et al.,1980), yet no evidence for the presence of accreted terranes has been found in the Central Andes. In Chapter 4, the possibility that the Mejillones Peninsula forms part of an accreted allochthonous terrane is considered using palaeomagnetic, geochronological and geological evidence.

Sedimentary basin formation in the Andean forearc is very poorly constrained. Using facies analysis, structural data and a regional geological knowledge of the study area, a palaeogeographic reconstruction of the Andean forearc is attempted, and presented in Chapter 6.

Chapter 7 is concerned with the diagenesis of 4 of the units studied in Chapter 6. The constant aridity of the climate in the study area, throughout the Mesozoic (Turner et al.,1984a), allows a comparison to be made between units of different ages, with similar source areas, all deposited in internally drained basins.

The generalised conclusions from the previous Chapters are presented in Chapter 8.

CHAPTER 2

THE TECTONIC EVOLUTION OF THE CENTRAL ANDES

2.1 Introduction

The tectonic evolution of the Central Andes between 20-26°S. and 71-65°W. (Fig. 2.1), from the Precambrian to Recent is considered in this chapter. An understanding of the regional tectonic framework of the area, is especially important for the geological interpretation of palaeomagnetic data presented in later chapters.

In order to give a more complete picture of the known tectonic history of the Central Andes, the geology of southwest Bolivia, northwest Argentina (and to a lesser extent southern Peru) are described, in addition to northern Chile. The area considered has a unique evolution, distinctive from adjacent segments of the Andean orogenic belt (Coira et al.,1982).

Two major orogenic cycles have been recognised in the Central Andes:

1) The "Hercynic" cycle comprising the Palaeozoic, which can be divided into two stages separated by three periods of deformation, and is developed on Precambrian basement.

2) The Andean cycle comprising the Mesozoic to Recent, developed on Hercynic cycle basement.

The Palaeozoic/Mesozoic boundary separates the two cycles, and is coincident with a relocation of the focus of igneous activity, associated with a change in tectonic setting.

Fig. 2.1 Map showing the morphotectonic provinces of the study area and a generalised geological cross-section. The morphotectonic units comprise from W to E:

1) The Cordillera de la Costa composed of dominantly Jurassic granites, granodiorites and dacitic and andesitic lavas of the La Negra Formation, as well as the Palaeozoic Mejillones Peninsula and Moreno Complex (Chapters 3 and 4).

2) The Central Depression a large basin containing isolated blocks of Palaeozoic metamorphics, Triassic sediments and volcanics, Jurassic carbonates and continental sediments, and Tertiary to Recent continental sediments.

3) The Precordillera comprising mainly Mesozoic marine and continental sediments.

4) The Salar Depression, a series of extensive internally drained continental basins, the origin of which is uncertain, btu have probably existed from the mid-Tertiary at least.

5) Cordillera de los andes, Miocene to Recent volcanics and volcanoes.

6) The Puna/Altiplano an extensive plateau composed of lava flows and isolated pockets of continental sediments.

7) Cordillera Oriental an extensive foreland thrust belt which was active in the Miocene.

8) Sierras Subandinas currently a seismically active foreland thrust belt.

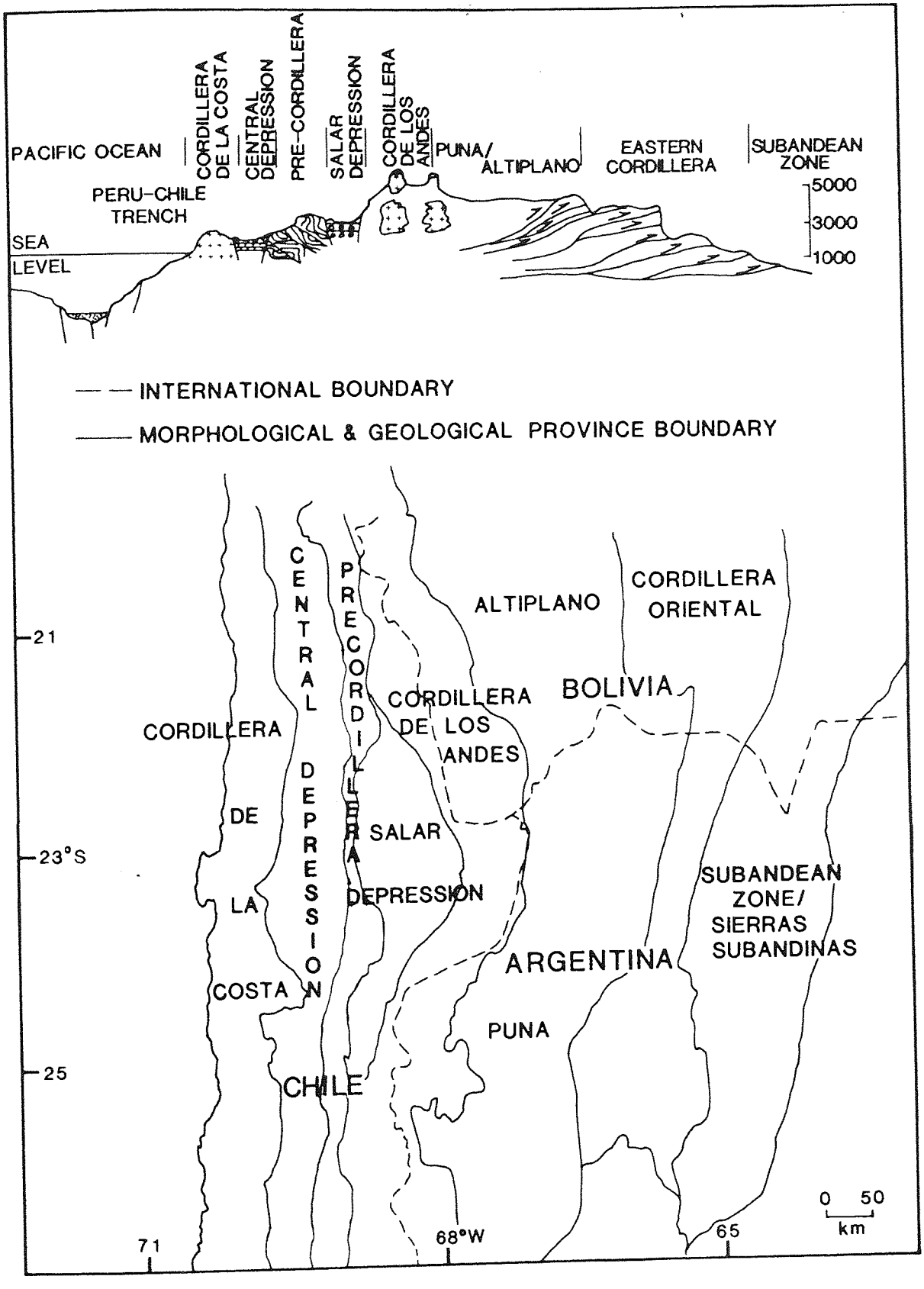
PACIFIC OCEAN
CORDILLERA DE LA COSTA
CENTRAL DEPRESSION
PRE-CORDILLERA
SALAR DEPRESSION
CORDILLERA DE LOS ANDES
PUNA/ ALTIPLANO
EASTERN CORDILLERA
SUBANDEAN ZONE
PERU-CHILE TRENCH
SEA LEVEL
5000
3000
1000
INTERNATIONAL BOUNDARY
MORPHOLOGICAL & GEOLOGICAL PROVINCE BOUNDARY
CENTRAL DEPRESSION
PRECORDILLERA
ALTIPLANO
CORDILLERA ORIENTAL
CORDILLERA DE LOS ANDES
BOLIVIA
CORDILLERA DE LA COSTA
SALAR DEPRESSION
SUBANDEAN ZONE/ SIERRAS SUBANDINAS
ARGENTINA
PUNA
CHILE
21
23°S
25
71
68°W
65
0 50
km

2.2 Precambrian Basement

Metamorphosed Precambrian basement rocks are exposed in two belts striking N-S (Fig. 2.2). These are:

1) A belt coincident with longitude 69°W. in northern Chile, forming a narrow horst extending for 200km. (Breitkreuz and Zeil,1984),

2) A belt along longitude 66°W. in northwest Argentina, known as the "Faja Eruptiva de la Puna" (Coira et al.,1982). A N-S oriented fault associated with periodic igneous activity throughout the Lower Palaeozoic, which formed a major positive tectonic feature throughout the Central Andes during this period.

The Precambrian basement of northern Chile consists of gneisses and migmatites, plus a series of phyllites, intruded by Ordovician/Silurian granites. U-Pb dates give a 1260±30my age for the migmatites (Breitkreuz and Zeil,1984). Evidence for the existence of Precambrian basement beneath northern Chile is provided by Damm et al.(1981), who dated zoned zircons at 1730Ma. from late Palaeozoic plutons of the Cordillera de la Costa. It has also been postulated that the Mejillones Peninsula (Fig. 2.2), may be an inlier of Precambrian basement, a possible southerly extension of the Arequipa Massif, Peru. A recent U-Pb date thought to represent an original age (Damm et al.,1986), assigns part of the Peninsula to the Lower Cambrian (534+/-120Ma.).

The Precambrian basement of northwest Argentina (Puncoviscana Formation, Fig. 2.2), consists dominantly of alternating metamorphosed greywackes and shales, interbedded with ultrabasic volcanics (Acenolaza and Durand,1986). The metamorphic grade of the sediments

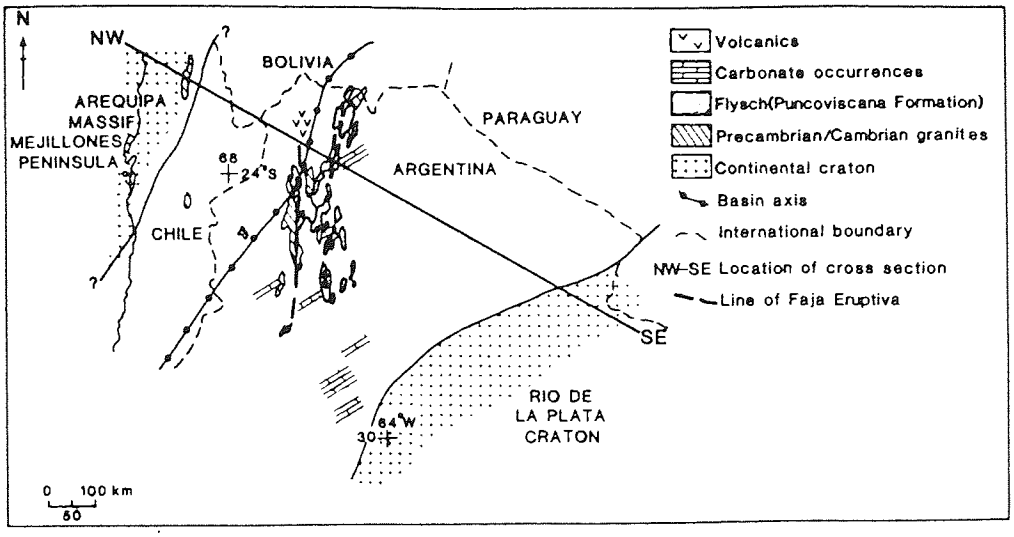

Fig. 2.2 Precambrian-Cambrian outcrop distribution and inferred palaeogeography.

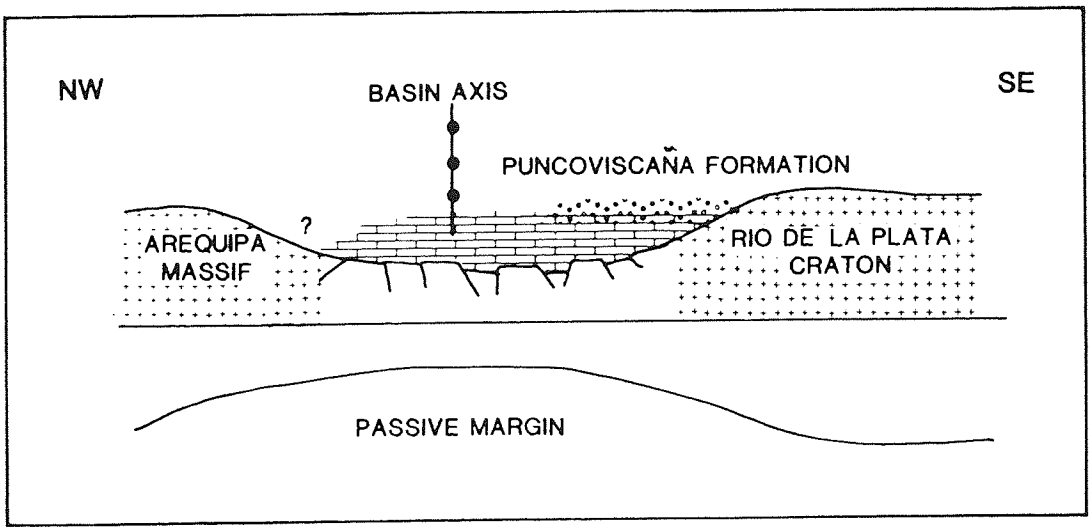

Fig. 2.3 Envisaged Precambrian-Cambrian plate tectonic setting.

increases from greenschist facies in the north, to medium to high grade facies southwards (Coira et al.,1982). Recent work on the biota and sedimentology of the Puncoviscana Formation (Acenolaza and Durand,1984,1987), has given a better understanding of Precambrian-Lower Cambrian palaeogeography and tectonics. The Puncoviscana Formation is thought to have been deposited in a NE-SW trending basin, bounded by the Arequipa Massif to the west and the Brazilian Shield to the east (Fig. 2.2). It has been postulated, that the basin formed as a result of rifting within the original South American craton (Dalmayrac et al.,1980). However no associated rift volcanics have been recorded from the area.

The Puncoviscana Formation is intruded by granodioritic and granitic plutons (Turner,1970), which were assigned to the Precambrian/Cambrian boundary by Turner and Mon (1979) and Halpern and Latorre (1973). However the reliability of these dates has been questioned by Breitkreuz (1986).

In conclusion, if the envisaged tectonic setting for late Precambrian times is correct (Fig. 2.3), ie. rift basin formation within the South American craton, it may follow that the Central Andes (20-26°S. and 70-65°W.) are underlain by Precambrian basement (see section 6.5). It is not clear however, whether the basement represents a southerly extension of the Peruvian Arequipa Massif, or an easterly extension of the Puncoviscana Formation.

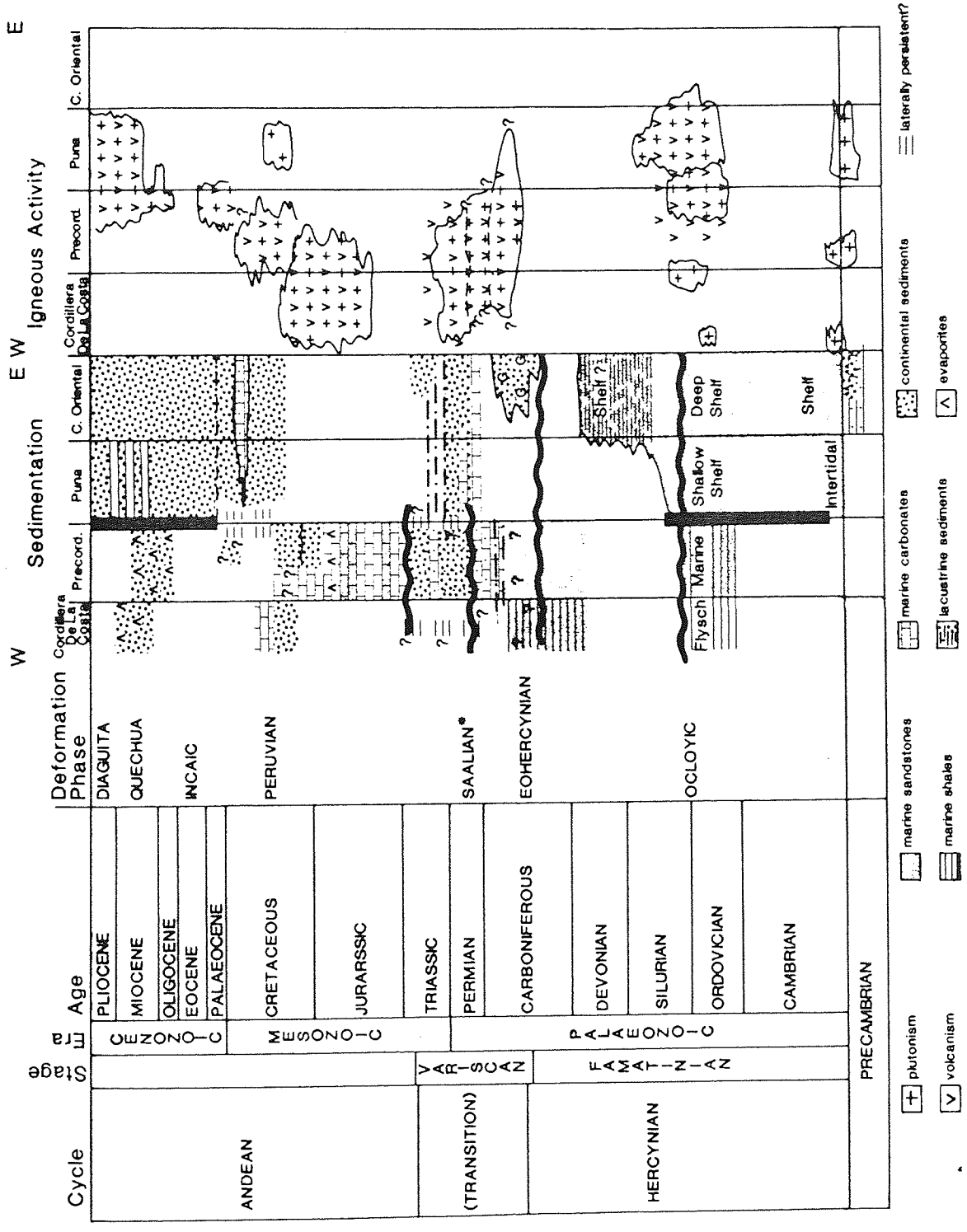

Table 2.1 Schematic presentation of the geology of the Central Andes. *Saalian is used in this thesis, as there is no suitable South American equivalent to this European term.

2.3 Hercynic Cycle (Palaeozoic)

2.3.1 Introduction

The Hercynic cycle, has been divided into two stages : 1) the Famatinian stage (Cambrian-Devonian), and 2) the Variscan (Carboniferous to early Triassic) stage. Three phases of deformation were recorded during the Palaeozoic:

a) The Ocloyic phase (Coira et al.,1982) at the end of the Ordovician,

b) The late Devonian-early Carboniferous Eohercynic phase (Dalmayrac et al.,1980), and

c) The early-mid Permian Saalian phase (Coira et al,1982).

The Palaeozoic of the Central Andes will be considered in two areas separated by the Faja Eruptiva, owing to differences in tectonic evolution. Northern Chile and northwest Argentina west of the Faja Eruptiva, have a markedly different Palaeozoic tectonic history than the area east of the Faja Eruptiva.

Until recently most work on the Palaeozoic rocks of this area has been of a stratigraphic, radiometric or metamorphic nature, with little attention paid to the tectonic and palaeogeographic setting. This has been due mainly to problems concerning the overprinting of Palaeozoic rocks by younger igneous activity, giving a sporadic outcrop distribution (Fig. 2.4). Work has also been hampered by the often poorly exposed, strongly folded and altered nature of the rocks.

2.3.2 The Famatinian Stage (Cambrian-Ordovician)

Cambro-Ordovician sediments are well documented east of the Faja Eruptiva (eg. Cuerda,1974; Barth,1972; Turner,1970; Zeil,1979; Fig. 2.4). Sections west of the Andes are, however, poorly exposed and

discontinuous. The main localities (Fig. 2.4), have been documented by Herve et al.(1981). Plutonic rocks of mainly Ordovician age occur in two main longitudinal belts coincident with the Precambrian basement along longitudes 69 and 66°W. Volcanism was extensive in northwest Argentina and southern Bolivia during the Ordovician (Coira et al.,1982).

Sedimentation (Table 2.1): East of the Faja Eruptiva de la Puna in northwest Argentina, a thick sequence (3100m.) of shallow marine Cambrian sediments (Meson Group), has been documented by Turner (1970). Abundant cross-laminae, ripple marks, dessication cracks and Skolithus burrows indicate an intertidal environment.

Extension and subsidence of the basin resulted in a transition from the Cambrian intertidal environment to a dominantly shallow marine environment during the Tremadocian (Turner, 1970). From the beginning of the Ordovician to the Arenig, a west-east facies zonation can be recognised, with shallow continental shelf facies in the west grading into a more distal shelf facies to the east. The largest extension of the Ordovician sea throughout southern Peru and southern Bolivia, occurred in Arenig to Llanvirn times (James, 1971).

No Cambrian sediments have been recorded west of the Faja Eruptiva de la Puna. Coira et al.(1982), document a typical flysch facies from Ordovician rocks in northern Chile. They concluded that the Ordovician facies distibution represented the eastern border of a deep marine basin, which may have passed westwards into the shallow platform facies of northwest Argentina. Observations by Breitkreuz (1985), indicate the possible presence of a shallow marine sequence in some parts of northern Chile (Sierra de Argomedo, Fig. 2.4). Most

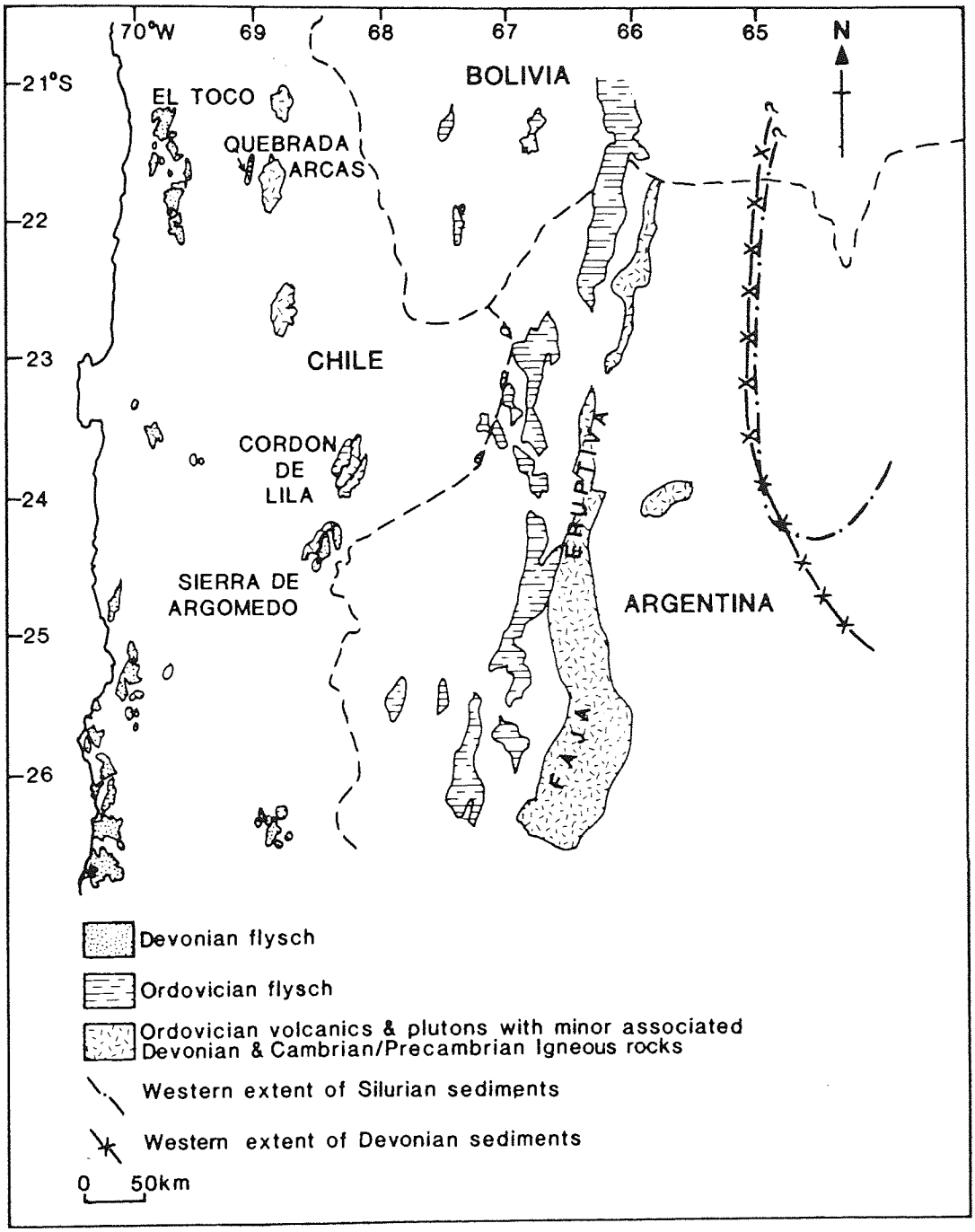

Fig. 2.4 Cambrian-Lower Carboniferous outcrop distribution.

sedimentation during the Ordovician in northern Chile however appears to have been dominated by flysch facies (Table 2.1). All sediments are interbedded with extensive volcanics, probably derived from the Faja Eruptiva (Bahlberg et al.,1986).

Igneous Activity (Table 2.1): No Cambrian igneous activity has been recorded in the Central Andes (Breitkreuz,1986). Major plutonism and associated volcanism took place throughout the Ordovician climaxing at the Ordovician/Silurian boundary, associated with the Ocloyic deformation phase.

Two belts of plutonic rocks dated as Ordovician/Silurian (Heute et al.,1977; Halpern,1978; Rapela et al.,1982; Breitkreuz,1986), crop out in the Central Andes. They occur along longitudes 66 and 69°W. coincident with the Precambrian basement and have diffuse to migmatitic contacts with the basement. The plutons are of a calc-alkaline nature, and are thought to have been intruded syn-, late- and post-tectonically (Breitkreuz,1986). A small Ordovician pluton has been recorded by Breitkreuz (1986), from the Mejillones Peninsula (Fig. 2.2). The tectonic significance of which is uncertain and will be discussed later within the context of paleomagnetic studies (see Chapter 4 and also section 2.3.4).

Extensive acid to intermediate volcanism was contemporaneous with Ordovician sedimentation and plutonism in northwest Argentina and southern Bolivia (Turner,1970; Allmendinger et al.,1983). Due to the large aerial extent of volcanism, Coira et al.(1982) proposed the existence of a 1300km. long island arc through Bolivia and Argentina, centered on the Faja Eruptiva.

2.3.3 The Famatinian Stage (Silurian-Early Carboniferous)

The end of the Ordovician is marked by tectonic and plutonic activity, connected with the Ocloyic deformation phase (Table 2.1). This resulted in the emergence of the "Arco Puneno" (Coira et al.,1982), a positive feature centered in northwest Argentina for much of the Silurian. This topographic high formed a sedimentary divide between northwest Argentina and northern Chile, in much the same way as the Faja Eruptiva in the early Palaeozoic.

Sedimentation (Table 2.1): East of the "Arco Puneno" no Silurian-Devonian sediments have been recorded from the Puna. However mid-Silurian to mid-Devonian sediments have been found in the Cordillera Oriental. They are represented by the 30m. thick Mecoyita Formation a sequence of quartzitic sandstones and matrix-supported conglomerates, overlain conformably by the Lipeon Formation, 1600m. of shaley sandstones (Turner, 1970). The base of the Lipeon Formation contains oolitic ironstones. The two formations are thought to represent the gradual deepening of a restricted shallow marine basin (Turner, 1970). Lower Devonian sedimentation is very similar and represented by 2400m. of shallow marine sandstones and shales of the Baritu Formation (Turner,1970), which conformably overlie the Lipeon Formation. The age of the Baritu Formation was assigned through macrofossil character (Harrington,1967). Similar facies are also developed extensively in southern Bolivia and southern Peru (Isaakson,1975). The eastern boundary of the Lower Devonian basin is unknown (Coira et al.,1982).

No proven Silurian sediments are exposed West of the "Arco Puneno", possibly through its emergence (Bahlberg et al.,1986). Chong (1977) however, does record possible Silurian sediments from the

Precordillera of northern Chile (Fig. 2.1). Devonian to early Carboniferous sediments are well documented west of the "Arco Puneno" (see Herve et al.,1981), and can be split into two broad facies associations:

1) A shallow marine, continental shelf sequence exposed in the eastern part of northern Chile (Sierra de Almeida, Fig. 2.4). Interpreted by Davidson et al.(1981), as a prograding delta sequence with a source area to the east/southeast ie. the "Arco Puneno". Periodic emergence of the shelf led to red bed deposition represented by the Cordon de Lila sequence (Bahlberg et al.,1986, Fig. 2.4). Bahlberg et al.(1986), also document the occurrence of a terrestrial clastic succession (Quebrada Arcas, Fig. 2.4), thought to represent coastal sedimentation in a limnic/brackish environment.

2) A flysch sequence exposed in the Chilean Cordillera de la Costa. This sequence outcrops throughout much of the coastal region of the Central Andes as the 2300m. thick El Toco Formation (Bahlberg 1985, Fig 2.4). Deposition took place in a N-S oriented basin. Palaeocurrent data indicates source areas to the north/northwest and south (Bahlberg,1985), rather than from the easterly "Arco Puneno". The palaeocurrent evidence for sedimentation being restricted to a N-S oriented trough, led Bahlberg et al.(1986) to suggest that the trough was limited to the west by an elevated area. This is in accord with the view of Isaakson (1975), who proposed such a landmass to account for the apparent lack of source area for Peruvian and southern Bolivian Devonian sediments. A theory discussed in section 2.3.4.

Igneous Activity (Table 2.1): Silurian to early Carboniferous igneous activity appears to be mainly related to the late Devonian/early

Carboniferous "Eohercynian" deformation phase (Dalmayrac et al.,1980). Some alkaline and tholeiitic (ultra-) basic volcanics interfinger with Palaeozoic sediments in the Chanaral area (Bahlberg et al.,1986). Most igneous activity however, appears to be post-tectonic, with little or no plutonic/volcanic activity during the Devonian. Large quantities of Carboniferous acid to intermediate, mainly calc-alkaline melts are found throughout the Chilean Andes, Argentine Puna and Cordillera Oriental (Heute et al.,1977; Coira et al.,1982; Rogers,1985; Fig. 2.4), including the reactivation of the Faja Eruptiva (discussed below) in late Devonian times (Omarini et al.,1979).

2.3.4 Discussion of the Tectonic Evolution of the Central Andes During the Famatinian Stage

The palaeogeographic setting and tectonic style of the Central Andes remained broadly unaltered throughout Cambrian to early Carboniferous times (Figs. 2.5a,c). The emergence of the "Arco Puneno", maintained the topographic high first associated with the Faja Eruptiva during the Cambrian and Ordovician in northwest Argentina.

Coira et al.(1982), and Allmendinger et al.(1983), suggested that the Faja Eruptiva formed the root of a volcanic arc during the Ordovician, based on its association with extensive acid to intermediate volcanism. Dalmayrac et al.(1980), interpreted the arc as an orogenic suture between the Brazilian Shield and a Pacific "mini-continent". A relict of which may be represented by the Arequipa Massif.

The latter suggestion is consistent with the distribution of the pre-Silurian sedimentary facies in the Central Andes. To the west of

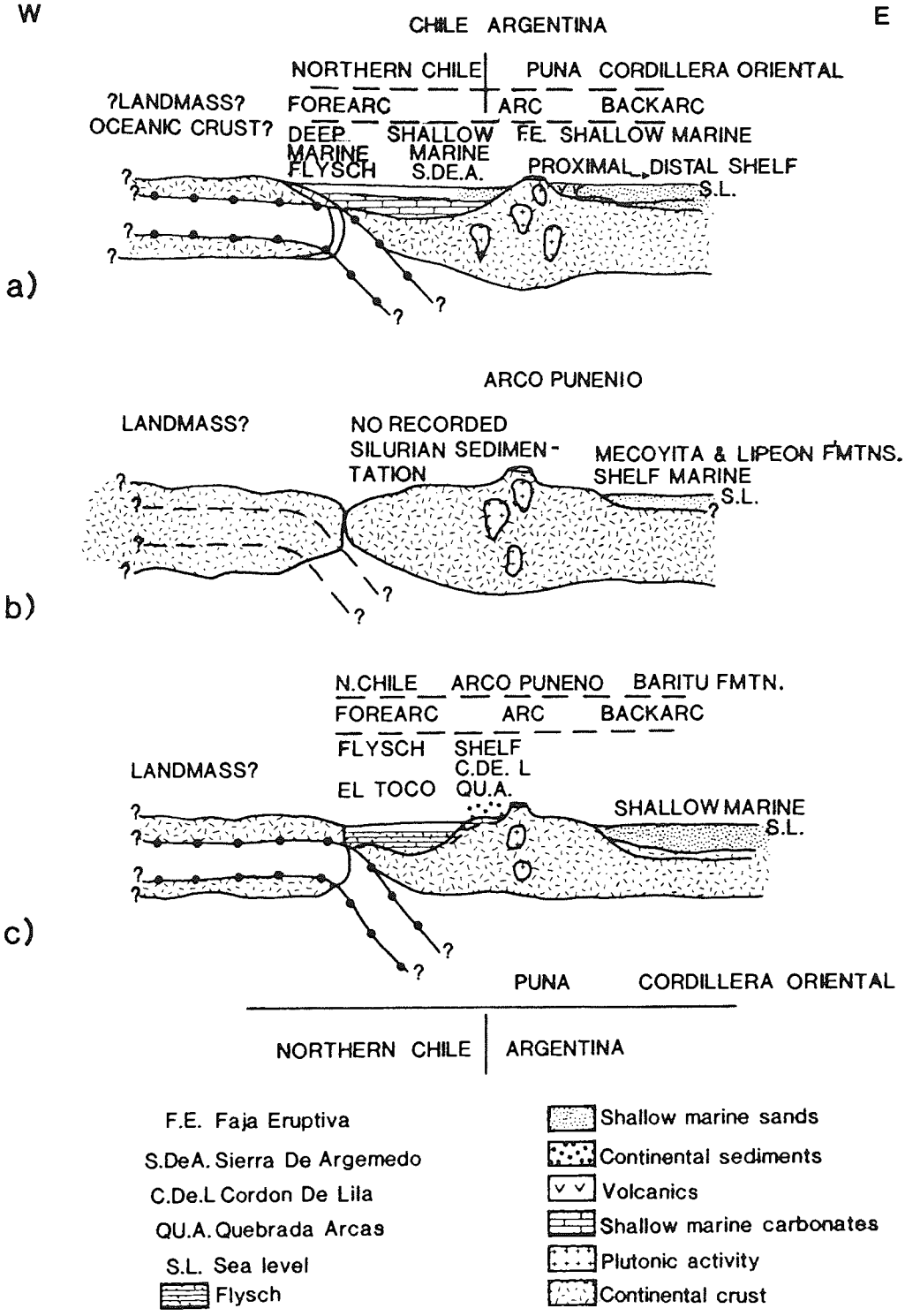

Fig. 2.5a Envisaged Ordovician plate tectonic setting.

b Envisaged Silurian plate tectonic setting.

c Envisaged Devonian plate tectonic setting.

the Faja Eruptiva, deposition of a turbiditic flysch sequence took place in a forearc basin (Fig. 2.5a). Evidence for the forearc nature of the flysch basin, is provided by the presence of a tectonic melange to the immediate west of the Faja Eruptiva (Allmendinger et al.,1983).

To the east of the Faja Eruptiva deposition of shallow marine sediments took place throughout Cambrian and Ordovician times. Although the eastern margin of the Faja Eruptiva is represented by a faulted contact, Allmendinger et al.(1983), nevertheless felt that this was still consistent with the interpretation of this sequence as being deposited in a back arc basin.

The post-Ordovician emergence of the "Arco Puneno" (Fig. 2.5b), continued to divide sedimentation in the Central Andes, but did not broadly alter the sedimentary facies distribution. To the west of the "Arco Puneno", flysch deposition took place throughout the Devonian in the coastal region of northern Chile, comparable to Ordovician sedimentation. Unlike Ordovician sedimentation however, the Devonian flysch passed eastwards into a shallow marine shelf sequence (Fig. 2.5c).

The tectonic setting of a Cambro-Ordovician forearc basin (flysch deposition-northern Chile), magmatic arc (Faja Eruptiva), back-arc basin (shallow marine sedimentation-northwest Argentina), extended throughout the Silurian and Devonian to early Carboniferous times. The main difference being the presence of a shallow marine shelf sequence to the immediate west of the magmatic arc after the Ocloyic deformation phase (Figs. 2.5a,c).

Throughout the Devonian the presence of a landmass to the west of the area has been postulated. Reasons include the restriction of sedimentation in the forearc basin based on palaeocurrent data

(Bahlberg,1985; Bahlberg et al.,1986), and lack of evidence for the source area required to supply the 4000m. thickness of observed Devonian sediment (Isaakson,1975). Dalmayrac et al.(1980) and Coira et al.(1982), have included a western landmass in plate reconstructions for this period of South American tectonism, the landmass being a possible southerly and westerly extension of the Peruvian Arequipa Massif.

Some problems associated with the above interpretations of Cambrian-early Carboniferous Central Andean tectonics include:

1) The distribution of Ordovician/Silurian plutons,

2) Palaeocurrent data for flysch of both Ordovician and Devonian ages,

3) Lateral facies relationships.

4) Poor evidence for a western landmass,

5) The role of the Faja Eruptiva,

6) The aerial extent of the "Arco Puneno",

1) The extensive distribution of Ordovician/Silurian plutonism in the Central Andes (Breitkreuz,1986, Fig. 2.4), makes it difficult to envisage a linear suture/volcanic arc for this period as proposed by Coira et al.(1982), Allmendinger et al.(1983) and Dalmayrac et al.(1980). However, on close examination of the Lower Palaeozoic plutonic outcrop distribution a possible solution may exist. In particular the most westerly outcrop, the Mejillones Peninsula, may be unrelated to the early Palaeozoic tectonic evolution of the Central Andes (for further discussion see Chapter 4). The other major discrepency is the prominent magmatic belt along 69°W. which maybe related to later tectonic activity (Chong and Reutter,1985), as it appears not to affect the sedimentary facies distribution.

2) Palaeocurrent data is not consistent with an expected easterly source area, as indicated by southerly and northwesterly-derived palaeocurrents for both Ordovician and Devonian flysch sequences. An easterly source however, is recorded for the limited, proximal shallow marine Devonian sediments (Bahlberg et al.,1986).

3) Sedimentary facies relationships should also be examined more closely. More evidence is required to confirm the presence of a pre-Silurian shallow marine sequence. If it was present has it been subducted? Has it been accreted? What is the relationship between the Devonian flysch basin and the shallow marine succession? If the two depositional centres are laterally equivalent, why are no easterly (connecting) palaeocurrents recorded?

4) The presence of a landmass to the west of the turbidite trough during the Devonian was postulated by Bahlberg et al.(1986), to account for the apparent restriction of turbidity currents (roughly paralleling the N-S tectonic strike). However the landmass presumably would also have been a sediment source, and westerly-derived palaeocurrents have not been documented.

5) It seems probable that the Faja Eruptiva de la Puna was the locus of igneous activity during the Cambrian-Ordovician. However it also appears that it was reactivated during the Devonian (and possibly in the Triassic), if this is the case why did the volcanic arc remain stationary? Considering that there appears to have been considerable variation in the position and type of prevailing Palaeozoic regime (Fig. 2.5).

6) Uplift of the "Arco Puneno" occurred at the end of the Ocloyic deformation phase, but what caused the uplift? The size of the "Arco Puneno" (covering 4-5^{o} of latitude, and probably more taking into

account the amount of younger crustal shortening), would require some considerable force eg. continental collision. Why is no relict of this continental collision preserved? Has it been subducted? Is the Mejillones Peninsula a relict of such a continent? If so why has it been preserved?. Also, if uplift did occur why are no continental sediments and only a limited shallow marine sequence preserved?

It is clear that the Cambrian-early Carboniferous evolution of the Central Andes is still poorly understood, and that much more work must be undertaken to improve our present understanding of the area. Particularly as due to later tectonic movements, the present day distribution of Palaeozoic rocks in northern Chile, almost certainly does not reflect the true Palaeozoic palaeogeography.

2.3.5 The Variscan Stage (Carboniferous-Early Triassic)

The Eohercynian tectonic event took place in late Devonian-early Carboniferous times, and is characterised by folding and plutonism throughout the Central Andes (Table 2.1). It has been linked to a major change in Palaeozoic palaeogeography (Coira et al.,1982). This may have formed the beginning of a transitional period during the late Carboniferous to early Triassic, with the relocation of the locus of igneous activity.

Two distinct phases can be distinguished during the Carboniferous-early Triassic (Coira et al.,1982). Firstly, a quiescent period of sediment deposition up to the middle Permian, after which followed the development of a volcanic arc, possibly centered on longitude 69 W. The Saalian tectonic event (Table 2.1), separates these phases (Coira et al.,1982).

Sedimentation (Table 2.1): Northwest Argentina and southwest Bolivia:

Shallow marine and continental sediments were dominant in this area. Acenolaza et al.(1972), record shallow marine limestones and sandstones from the Argentine Puna. To the east in the Cordillera Oriental and Sierras Subandinas (Fig. 2.1), continental and lacustrine sediments are recorded (Mingramm et al.,1979; Coira et al.,1982). The eastward gradation of shallow marine to continental sediments in northwest Argentina, is in contrast to the westwardly deepening marine basin of Cambrian-Early Carboniferous times. Southern Peru has similar Permian facies associations to northwest Argentina (James, 1971), indicating the large aerial extent of the Permian sedimentary basin.

Northern Chile: Carboniferous-Lower Permian sediments although poorly exposed consist of limestones and clastics. These were interpreted by Bahlberg et al.(1986), as a limnic/brackish sequence. Deposition took place on a shallow marine platform, formed as a consequence of the Eohercynian deformation phase.

Permo-Triassic rocks, deposited after the Saalian deformation phase, are relatively well documented from northern Chile, particularly in the Chilean Precordillera (Cordillera de Domeyko, Fig. 2.1). Sequences include the Agua Dulce, El Bordo, Tuina and Peine Formations (Fig. 2.6). These sequences are composed of continental sediments and shallow marine siliciclastics and limestones, interbedded with extensive silicic volcanics. See Chapter 6 for a more detailed discussion of Triassic palaeogeography.

Igneous Activity (Table 2.1): Plutonism and volcanism from this period is widely recorded in the Chilean Andes, and the Argentine Puna and Cordillera Oriental (Breitkreuz,1986; Coira et al.,1982).

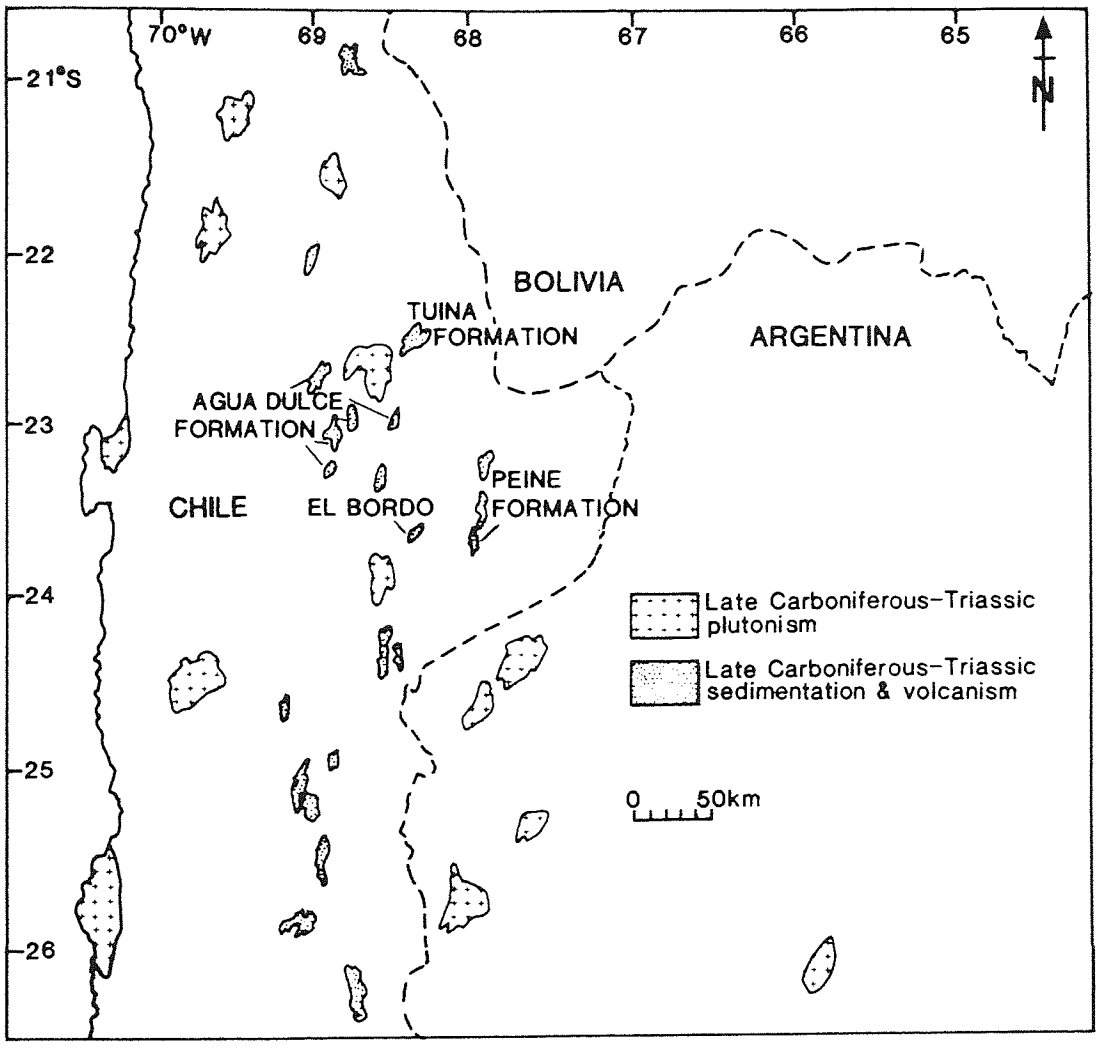

Fig. 2.6 Late Carboniferous-Triassic outcrop distribution.

Large quantities of intermediate to acid (mainly calc-alkaline) melts were intruded post-tectonically into all areas of the Central Andes during the Carboniferous. Coira et al.(1982), document an extensive magmatic belt on the western margin of northern Chile for much of the Permian to mid-Triassic. Rhyolites and dacites coupled with granites and granodiorites characterise the belt, and are usually associated with continental red beds. They formed part of an extensive magmatic belt developed during the Permian which extended 4000km. from southern Argentina to northern Chile. The relationship to rocks of southern Peru and southern Bolivia is however, uncertain.

Permo-Triassic batholiths of southern Peru and southern Bolivia show some geochemical characteristics of a rift association (Pitcher,1984), and may have developed within a back arc spreading regime (Noble et al.,1978). The extension of this rift association into northern Chile is an interesting possibility, but as yet unproven.

2.3.6 Discussion of the Tectonic Evolution of the Central Andes During the Variscan Stage

Sedimentation during this period appears to have been broadly similar across the Central Andes, reflecting a similar tectonic setting for the whole of the area during this period. In contrast to the early Palaeozoic sedimentation in back arc and forearc basin settings, which were separated by positive tectonic features. Two theories exist as to the prevailing tectonic setting during this period:

1) A volcanic island arc could have been the main tectonic feature, with shallow marine/continental sediments reflecting fluctuating sea-level (Fig. 2.7). Coira et al.(1982), placed the island arc

towards the western margin of present day Chile at 69°W. Bahlberg et al.(1986) however, located it on the western edge of the Puna. Volcanic and plutonic activity has been recorded throughout the Central Andes during this period, therefore the exact position of a volcanic arc at this time appears to be distinctly problematical.

2) The possibility exists that north Chilean igneous rocks may form a southerly extension of the Peruvian rift association (Breitkreuz,1986). If this is the case, this period may record the relocation of the focus of igneous activity in the Central Andes. If rifting took place at this time in northern Chile, it may have initiated the extensive back arc basin system present throughout the Andean margin in Jurassic times (see Chapter 6 for further discussion).

Previous authors (Coira et al.,1982; Dalziel,1986), have stated that the Carboniferous-Triassic period, records a transition from a passive Palaeozoic continental margin to an active Mesozoic continental margin. The presence however, of volcanic/magmatic arcs throughout the Palaeozoic, would appear to indicate that the Palaeozoic continental margin was active.

The Carboniferous-Triassic period is a transitional period however, as it records the relocation of the locus of igneous activity from the interior (between 69°W. and the Puna), to the Jurassic volcanic arc which forms the present day Cordillera de la Costa.

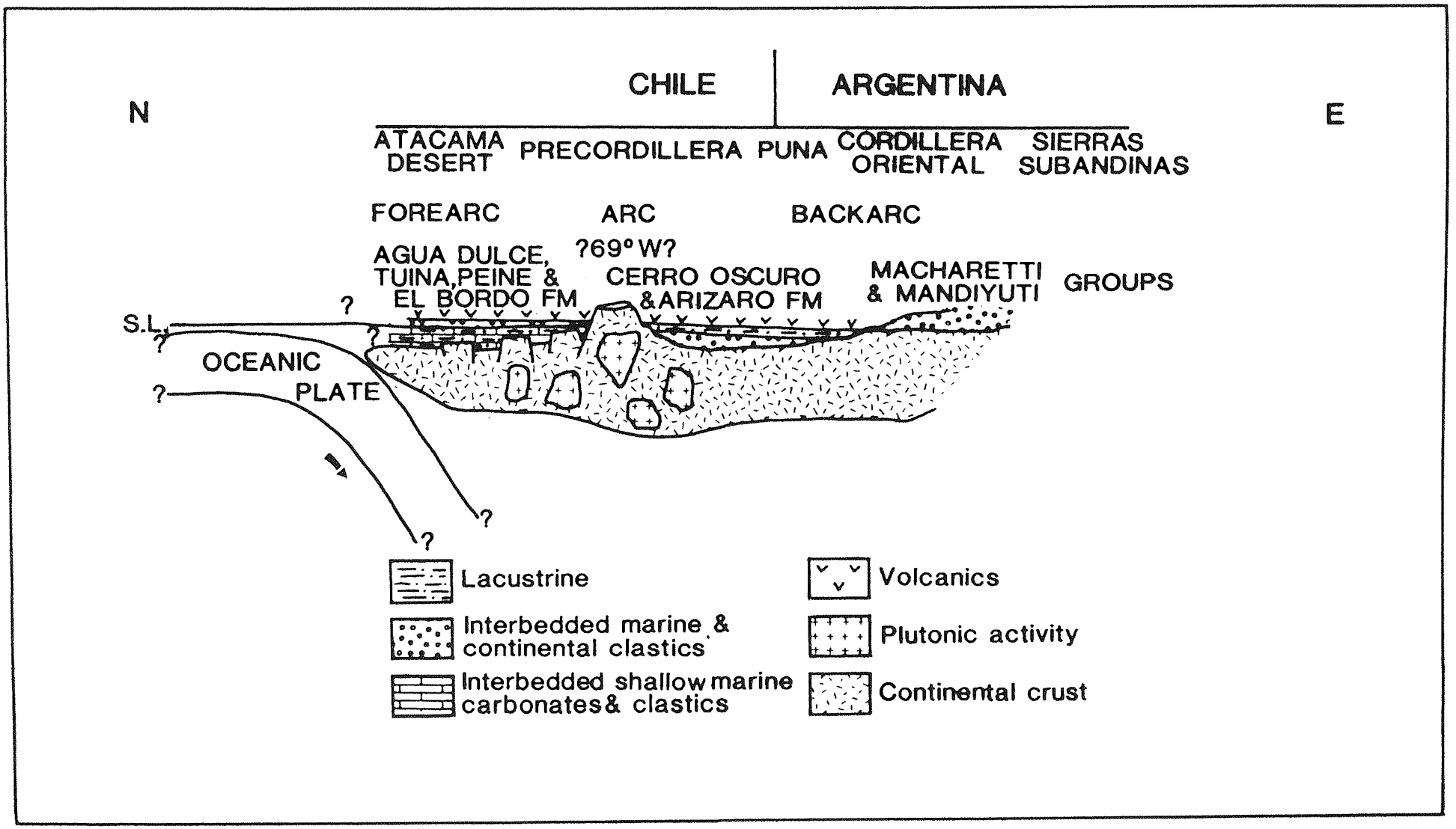

Fig. 2.7 Envisaged Triassic plate tectonic setting.

2.4 Andean Cycle

2.4.1 Introduction

The Andean cycle developed from the late Triassic onwards, following the late Carboniferous-early Triassic transitional period.

The main theme in South American plate tectonic configurations from the Mesozoic onwards, is the subduction of the oceanic (Pacific) plate beneath the continental South American plate. Two distinct tectonic regimes can be recognised:

1) Jurassic to early Cretaceous, characterised by a well defined volcanic arc/back arc basin geometry.

2) Late Cretaceous to Present, characterised by a well defined eastwardly migrating magmatic arc, with no extensive marine back arc basin.

2.4.2 Jurassic to Early Cretaceous

The tectonic setting for the Central Andes at this time was a paired island arc/back-arc basin. Consequently, most igneous activity was related to the formation of the volcanic arc, the relicts of which are now extensively exposed in the Cordillera de la Costa of northern Chile (Figs. 2.8,2.9).

Sedimentation was restricted to interbedded shallow marine and continental facies deposited in the back-arc basin. Evidence for sedimentation in a contiguous forearc basin is absent, possibly due to subduction. Some sediments have been recorded interbedded with the lavas of the volcanic arc (La Negra Formation).

Sedimentation (Table 2.1): During this period extensive sequences of

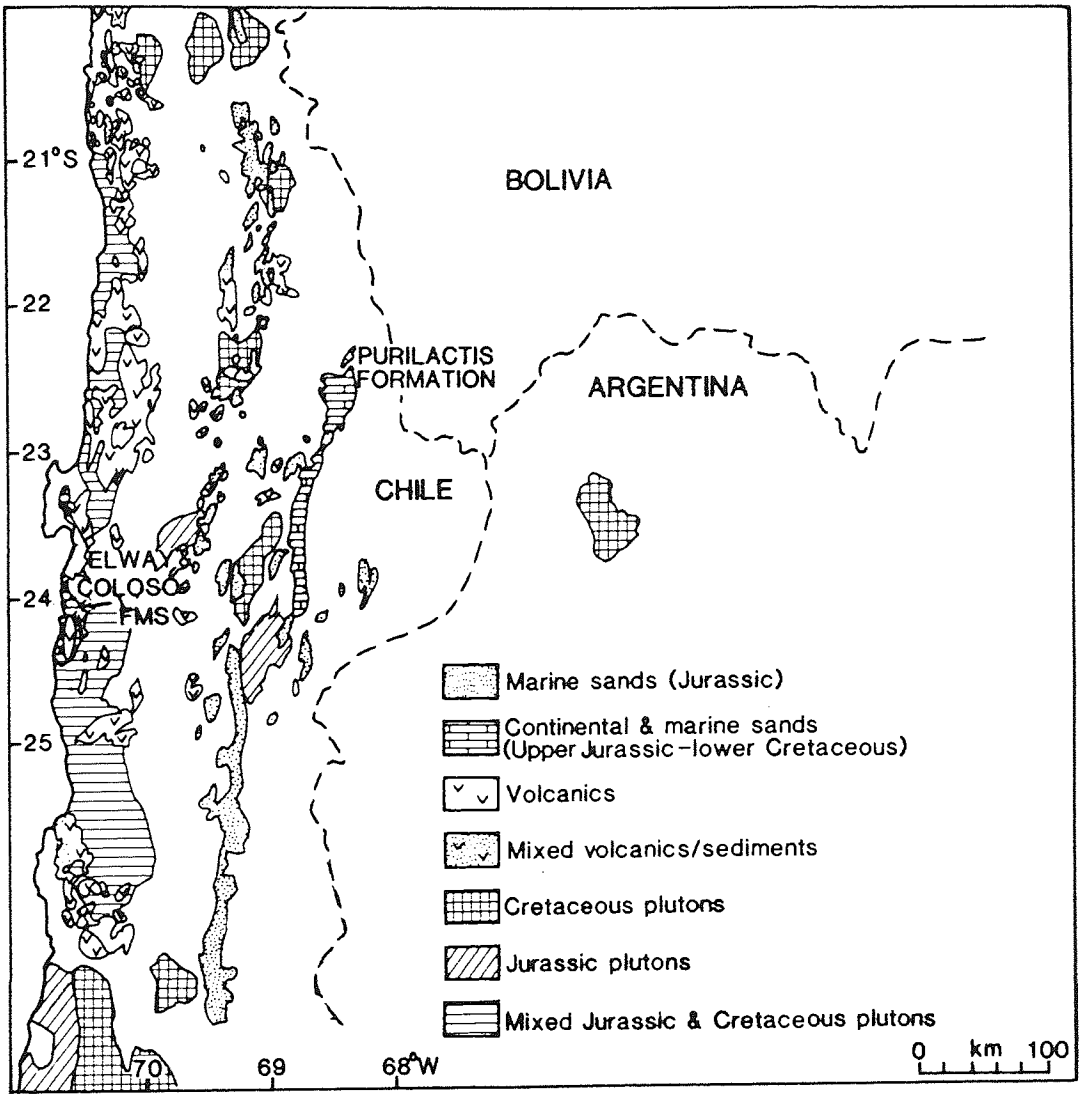

Fig. 2.8 Jurassic-Cretacous outcrop distribution.

carbonates, evaporites, marine sandstones and red beds were deposited with interbedded volcanics. These are now well exposed in the Central Depression and Precordillera (Cordillera de Domeyko, Fig. 2.8), of northern Chile. The rocks have been described by Biese (1957), Harrington (1961), Dingman (1963; 1965; 1967), Hollingworth and Rutland (1968), Moraga et al. (1974), Baeza (1976), Chong (1977) and further south by Hillebrandt (1973).

The Cordillera de Domeyko and its southern extension form a continuous ridge 400km. long (22-27°S.), and contain a virtually uninterrupted succession of Triassic to Palaeogene sediments and occasional volcanics. Jurassic to early Cretaceous sediments have been extensively described by Chong (1977), and only a brief summary will be given here.

Back arc basin sedimentation began in the Hettangian with a marked transgression over Palaeozoic granites, and Triassic continental and volcanic rocks. A continuous, dominantly shallow marine environment existed from the Hettangian to the Callovian (the Sinemurian saw the largest extension of the basin, resulting in deeper water black shale sedimentation), dominated by carbonates with subordinate sandstones, conglomerates and occasional evaporites. Oxfordian-Kimmeridgian evaporites represent shallowing of the basin. Silicic volcanics appear on the western margin particularly during the Callovian recording the continuous activity of the volcanic arc (when they may have contributed to the infilling and subsequent shallowing of the basin prior to the Oxfordian). A Neocomian marine to continental transition records the later stages of sedimentation prior to the closure and uplift of the back arc basin, associated with the mid-Cretaceous (Peruvian) deformation phase. Throughout the Jurassic

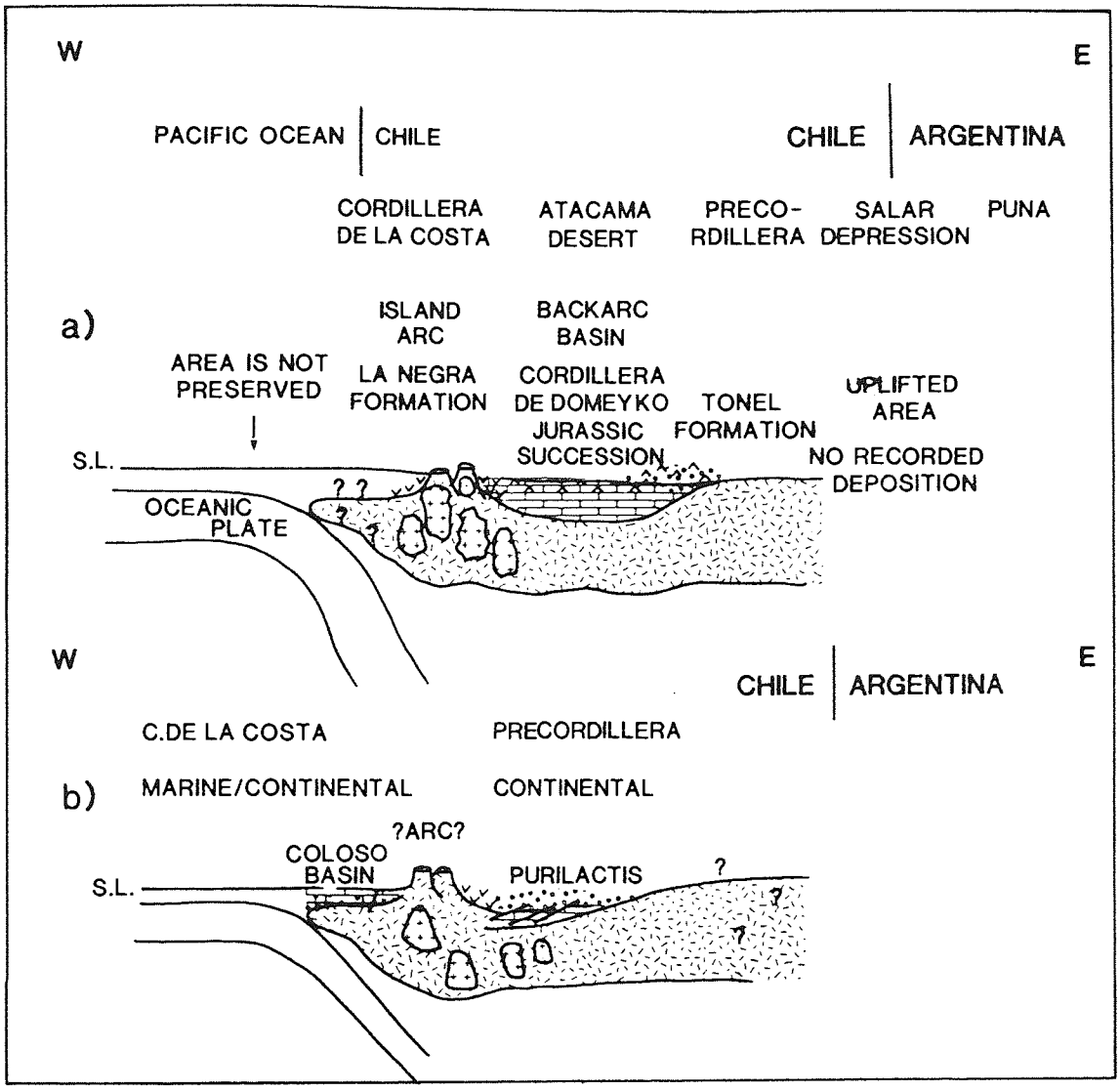

Fig. 2.9a Envisaged Mid-Jurassic plate tectonic setting.

b Envisaged Early Cretaceous plate tectonic setting.

and early Cretaceous the extent of marine deposition appears to have been variable, as continental sediments are common in the northern part of the area (Fig. 2.8); in particular the Coloso, Tonel and Purilactis Formations (see Chapters 5, 6 and 7, for a discussion of the palaeomagnetism, sedimentology and diagenesis of these Formations). No Jurassic to early Cretaceous sediments have been recorded from northwest Argentina or southwest Bolivia.

Igneous Activity (Table 2.1): James (1971) documents the beginning of the Jurassic island arc system, with rocks exposed in the Cordillera de la Costa of southern Peru and northern Chile (Fig. 2.8). The rocks consist largely of tuffs, pillow lavas, breccias and agglomerates of basaltic to andesitic composition, and are thought to represent the initial stage of island arc development. Further extension of the island arc system is represented by the lower Jurassic La Negra Formation (Fig. 2.8, see Chapter 3 for palaeomagnetic results). A 10 km. thick (Garcia,1967), aerially extensive sequence of dacites, andesites and basalts, erupted in both submarine and subaerial environments (Ferraris and Di Biase,1978).

Middle Jurassic to early Cretaceous plutonism in the area was extensive (Table 2.1, Fig. 2.8, see chapter 3 for palaeomagnetic results). Chilean magmatism reached a climax in the production of mantle material during the early Cretaceous (Berg and Breitkreuz,1983). The plutons are thought to form the root of the volcanic island arc. Pluton geochemistry at this time is typical of a subduction zone beneath thin continental crust, resulting in the production of both basic and acid I-type magmas (Pichowiak and Breitkreuz,1984; Breitkreuz,1986). During Jurassic to early Cretaceous

times both a west to east migration of magmatism and a magmatogenetic connection with contemporaneous volcanism can be partly confirmed (Farrar et al., 1970; Berg and Breitkreuz,1983; Breitkreuz,1986).

2.4.3 Late Cretaceous to Recent

A mid-Cretaceous (Peruvian) phase of deformation in the Central Andes (Dalmayrac et al.,1980; Zeil,1979, Table 2.1), accompanied this important and major change in tectonic style. The island arc/back-arc basin setting of Jurassic to early Cretaceous times was replaced by a single, eastwardly-migrating magmatic arc, which has remained active to the present day (Coira et al.,1982, Fig. 2.10). More localised deformation phases associated with Andean uplift occurred in the Middle Eocene (Incaic phase), Upper Miocene (Quechuan phase) and mid-Pliocene (Diaguita phase).

Sedimentation during this period was mainly confined to marine incursions located on or near the present day coastline and continental deposition in uplifted intermontane basins (Fig. 2.11). These continental sediments appear to reflect quiescent periods between tectonic and associated volcanic events

Sedimentation (Table 2.1): Sedimentation throughout the Central Andes from the late Cretaceous onwards was essentially similar to present day sedimentation. The sediments, mostly terrestrial in nature, were deposited in intermontane basins, and consist of conglomerates, sandstones, siltstones, mudstones and evaporites, reflecting alluvial fan, fluvial and playa lake facies (Fig. 2.11).

Three periods of basin formation have been recognised in the Cenozoic (Jordan and Alonso,1987). Basin formation took place between

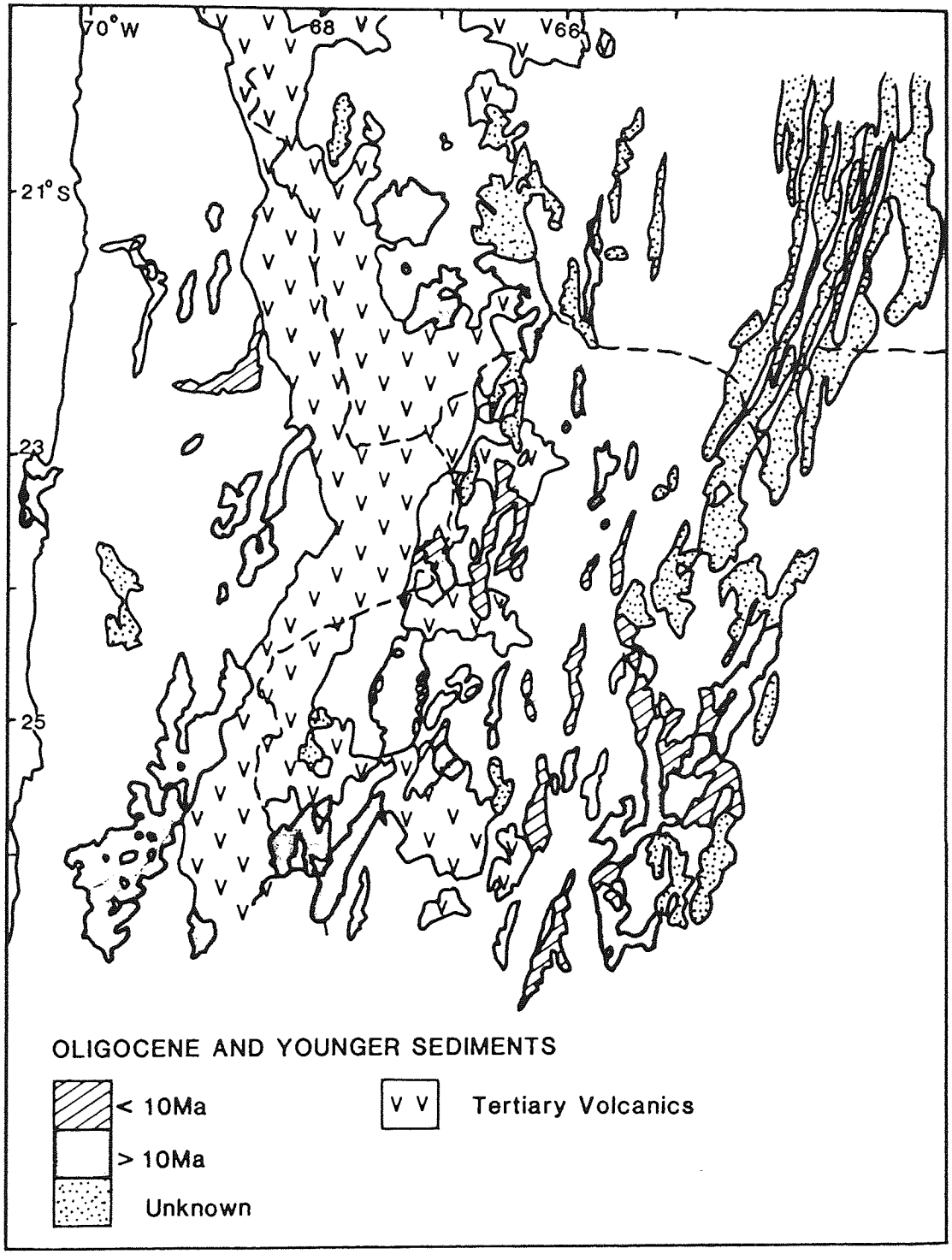

Fig. 2.10 Tertiary outcrop distribution.

phases of deformation (Table 2.1). From 40-25Ma. continental deposition occurred throughout the Central Andes in northwest Argentina (Salta Group, Turner,1970), northern Chile (Paciencia Group, Flint,1985a,b) and southwest Bolivia (Potoco and Lower Quechua Formation, Kussmaul et al.,1977). Between 25-10Ma. continental sedimentation was restricted to the Puna and further east, where a marine intercalation has been recorded from the Salta Group (Turner, 1970). Volcanic activity was dominant in the western part of the Puna at this time.

At approximately 10Ma. crustal shortening resulted in compression, forming two separate depositional centres. Sediments were deposited in small isolated basins within a widening volcanic arc, and in a foreland basin on the eastern flank of the volcanic arc.

Igneous Activity (Table 2.1): This period of igneous activity (particularly volcanism) in the Central Andes has been intensively researched, and extensive reviews are given by Coira et al.(1982) and Thorpe et al.(1982). Thus a brief summary with respect to Andean evolution will be presented here.

Plutonism was active throughout this period and has continued up to the present day. Small plutonic and subvolcanic bodies can be found in all regions of the Central Andes but more commonly in the Precordillera (Fig. 2.11). In common with the associated volcanics the plutons are mostly intermediate to acid in composition. An eastward migration of plutonic activity has been recorded from the late Cretaceous Peruvian coastal batholith (Cobbing et al.,1981) towards the younger Cordillera Occidental (Pitcher,1984). Tertiary magmatism in Peru reflects a large degree of crustal contamination

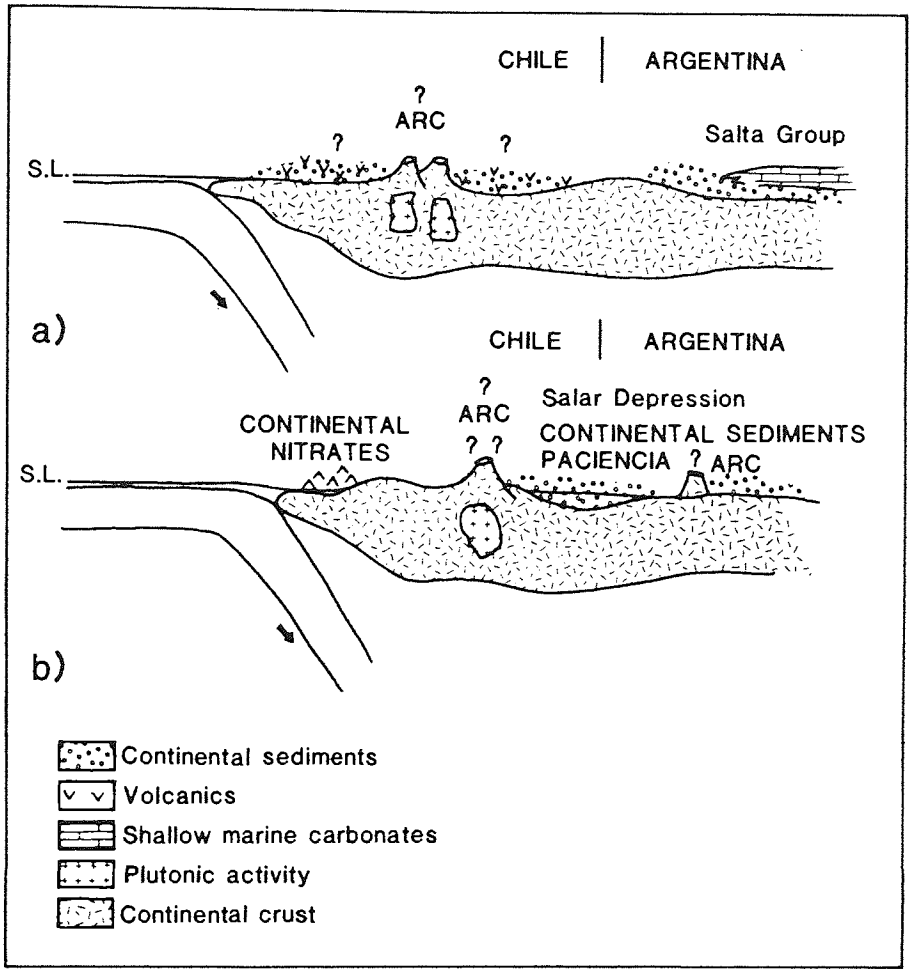

Fig. 2.11a Envisaged Late Cretaceous tectonic setting.

b Envisaged Oligocene tectonic setting.

(Pitcher,1984), and may be associated with the thickening of the Andean crust, which has continued through to the present day (James,1982). Cretaceous granites are also recorded from northwest Argentina (Halpern and Latorre,1973). During the Oligo-Miocene in the Bolivian Cordillera Oriental and Cordillera Real, the Triassic intrusion line was reactivated (McBride et al.,1983). A westward migration of volcanic activity has been recorded for this area during the Cenozoic (Kussmaul et al.,1977), this is in contrast to the Peruvian and Chilean eastward migration of igneous activity during the Cenozoic.

Volcanism during the late Cretaceous to Recent, was very extensive in the Central Andes (Fig. 2.11). Volcanics are usually pyroclastic in nature with andesitic to rhyolitic compositions, and are commonly interbedded with the Tertiary molasse sequences.

2.4.4 Discussion of Jurassic to Recent Tectonic Evolution of the Central Andes

The tectonic setting of the Central Andes during this period is relatively well known (Figs. 2.9,2.10), in contrast to the pre-Jurassic evolution of the area.

Throughout the Jurassic and early Cretaceous a well documented island arc/back-arc basin pair developed over the entire Andean margin (Dalziel,1986). Development of the back-arc basin took place in an extensional tectonic setting, with rifting developed on continental crust. This contrasts with the southern Andes (below 40°S.), where continuous extension resulted in the development of a basin floored by oceanic crust (Dalziel et al.,1974), and the northern Andes and

Central Peru, where a marginal forearc basin was developed on oceanic crust (Atherton et al.,1978; Dalziel,1986).

A major change in pole position between Africa and South America from 120-110my. (Rabinowitz and La Breque,1979), is coincident with a global increase in sea-floor spreading rates (Kominz,1984, Dalziel,1986). The increase in convergence (probably coincident with the breakup of Gondwana), of the Pacific margin of South America would have increased the horizontal component of compressive stress in the overriding continental lithosphere (Mendiguren and Richard,1978); resulting in uplift and compression (Peruvian deformation phase), and the development of foreland/intermontane basins. This compressive phase was accompanied by the rewelding of the Jurassic zone of weakness (Dalziel,1986), ie. the back-arc basin. Increasing the rate of sea-floor spreading however, would only result in the increased subduction of the oceanic plate at the continental margin. This is due to the difference in density between oceanic and continental crust, consequently a compressive stress regime would not be created. Also if a compressive stress regime was dominant, how did basin formation (an extensional process) take place? Palaeomagnetic results (Chapters 3, 4 and 5) also indicate a dominantly extensional stress regime.

Increased subduction due to rapid sea-floor spreading may be responsible for the eastward migration of magmatic foci in most of the Central Andes. An idea which supports the theory of Rutland (1971), that tectonic erosion of the continental margin as a result of subduction, took place from the late Cretaceous onwards.

The development of subsidence and rifting associated with a probable extensional tectonic regime in Jurassic and early Cretaceous times, may be related to the breakup of Gondwana (Dalziel,1986). The

gradual closure of the back-arc basin is recorded by the retreat of the sea southwards (Rutland, 1971), and the deposition of early Cretaceous continental sediments. The very large thicknesses of these continental sediments (Salta Group 10km.), record basin formation and subsequent rapid Andean uplift and erosion. This is reflected by the late Cretaceous Salta Group which contains a Maastrichtian marine incursion (Turner,1970), and is now some 3000-4000m. above sea-level.

The mid Cretaceous Peruvian deformation phase, accompanied the change in tectonic style, from the island arc/back arc basin pair to an eastwardly migrating magmatic arc. This major mid-Cretaceous compressional event is recorded throughout most of the Central Andes, however, evidence for its presence in northern Chile is limited.

The position of the post mid-Cretaceous volcanic arc is however uncertain (see Chapter 6 for further discussion). Other important questions regarding the late Cretaceous magmatic arc include: 1) How did the arc move eastwards? Was it a gradual movement, or did it take place in small rapid jumps? 2) How did this affect basin formation and sedimentation? 3) Is the model for sediment deposition in the late Cenozoic proposed by Jordan and Alonso (1987), ie. sedimentation in small isolated basins within the volcanic arc, applicable to the late Cretaceous?

2.5.5 General Remarks on the Tectonic Evolution of the Central Andes

Despite much recent attention, many aspects of Central Andean tectonics and geological evolution remain distinctly problematical. Some specific problems have been addressed in sections 2.3.4, 2.3.6 and 2.4.4. More general problems will be discussed below. In particular problems associated with:

1) Volcanic arcs and igneous rock composition.

2) Tectonism and the prevailing tectonic regime.

1) Igneous rock composition appears to have remained broadly similar throughout the Phanerozoic in the Central Andes. Acid to intermediate calc-alkaline plutonism and volcanism predominated, suggesting a volcanic arc association. The main variation in the igneous geology of the Central Andes during the Phanerozoic, being the position of the arc through time. The only periods of time in which there is any certainty (or agreement) on the location of the volcanic arcs, are those of the Jurassic (the Cordillera de la Costa of northern Chile), and the present day Cordillera de los Andes. The location of the Triassic and Palaeozoic arcs is very poorly defined, and even the position of the mid-Cretaceous arc is uncertain.

2) The prevailing tectonic regime throughout the Mesozoic in the Central Andes has always been considered to be compressive (Dalziel,1986; Coira et al.,1982). Undoubtedly compression has played a significant role, as demonstrated by crustal shortening in the form of thrust and reverse faulting. It is hoped in later chapters however, to demonstrate the prevalence of extensional tectonics in the development of the Central Andes throughout the Mesozoic-Recent, particularly with regard to basin formation.

Other problems include the relationship between extension and compression during the tectonic hisrtory of the Central Andes. Deformation phases in the Central Andes were periodic (and appear to be almost cyclic, Table 2.1), and associated with igneous activity.

What is the cause of this almost cyclic occurrence of major deformation? Can these phases be related to changes in the global sea-floor spreading rate? Or changes in the configuration of Gondwanaland? What effect did the breakup of Gondwanaland have? What connection is there between deformation, and processes active at the subduction zone? Do accreted terranes have a role to play in Andean tectonism? What caused the major changes in tectonic style, associated with the transitional periods of early Carboniferous-early Triassic and mid-Cretaceous times?

In the following chapters it is hoped to answer some of the problems outlined above, and addressed in sections 2.3.4, 2.3.6 and 2.4.4. The problems have been approached using the separate techniques of palaeomagnetism, sedimentology and diagenesis. The results have then been integrated and together with an understanding of the regional geology, an attempt has been made to solve these problems. Particular attention will be paid to the prevailing tectonic regime, tectonism and the related sedimentary response, tectonism and basin formation, it is hoped to demonstrate that the above approach has revealed a valuable insight into the Mesozoic-Recent tectonic evolution of the Central Andes.

CHAPTER 3

PALAEOMAGNETISM OF THE CORDILLERA DE LA COSTA, NORTHERN CHILE: EVIDENCE FOR FOREARC ROTATION

3.1 Introduction

Palaeomagnetic studies on the western margin of both North and South America have produced contrasting results. The western margin of North America consists of accreted, allochthonous terranes (Coney et al.,1980; Beck,1980; May et al.,1983; Jones et al.,1986). Palaeomagnetic work on the Andean forearc however, indicates that both clockwise and anticlockwise rotation of the forearc with respect to the stable shield area of South America has taken place (Palmer et al.,1980a,b; Heki et al.,1983,1984; Turner et al.,1984a; May and Butler,1985; Beck,1985; Beck et al.,1986). Although evidence has recently emerged that the Andean forearc may contain accreted terranes (McCourt et al.,1984; McGeary and Ben-Avraham,1985; Ramos et al.,1986; Feininger,1986), the subduction of the Nazca Plate along the Andean margin is nearly normal to the stable shield area; consequently differences between Mesozoic palaeomagnetic poles derived from the stable shield and continental margin should be relatively slight. Previous palaeomagnetic work in northern Chile (Palmer et al.,1980a,b; Turner et al.,1984a), appears to indicate local tectonic rotations of structural blocks with respect to the stable shield area.

The object of this study was to confirm that rotation of the forearc has taken place, to identify the amount, age, origin and

possible method of rotation, and to define the extent of these palaeomagnetically identified structural blocks.

A wide selection of palaeomagnetic samples was collected, ranging in age from ?Precambrian to Cretaceous. Collecting was also undertaken in the Central Depression, the Precordillera and Salar Depression (Fig. 2.1), in order to make a comparative study of palaeomagnetic results from rocks of similar ages. The results from these samples are presented in Chapter 5.

This chapter is limited to the Cordillera de la Costa, as it is a separate morphological and geological province (Fig. 2.1), of which the geological and tectonic evolution are relatively well understood (section 2.4.2).

3.2 Geology

The Cordillera de la Costa, Antofagasta Province, contains rocks ranging in age from Precambrian to Quaternary (Fig. 3.1a, Table 3.1). It is dominated by the 10km. thick volcanic La Negra Formation (Garcia, 1967); and associated acid to intermediate Jurassic and Cretaceous plutons.

Pre-Jurassic rocks exposed in the area include the Mejillones Peninsula and Bolfin Complex (Figs. 3.1a, 3.1b). The age, geology, palaeomagnetism and origin of the Mejillones Peninsula is complex, and treated separately in Chapter 4.

The Bolfin Complex comprises a layered intrusion of dioritic to gabbroic composition, with local anorthositic and amphibolitic layers. The main part of the Complex was originally regarded as Palaeozoic in

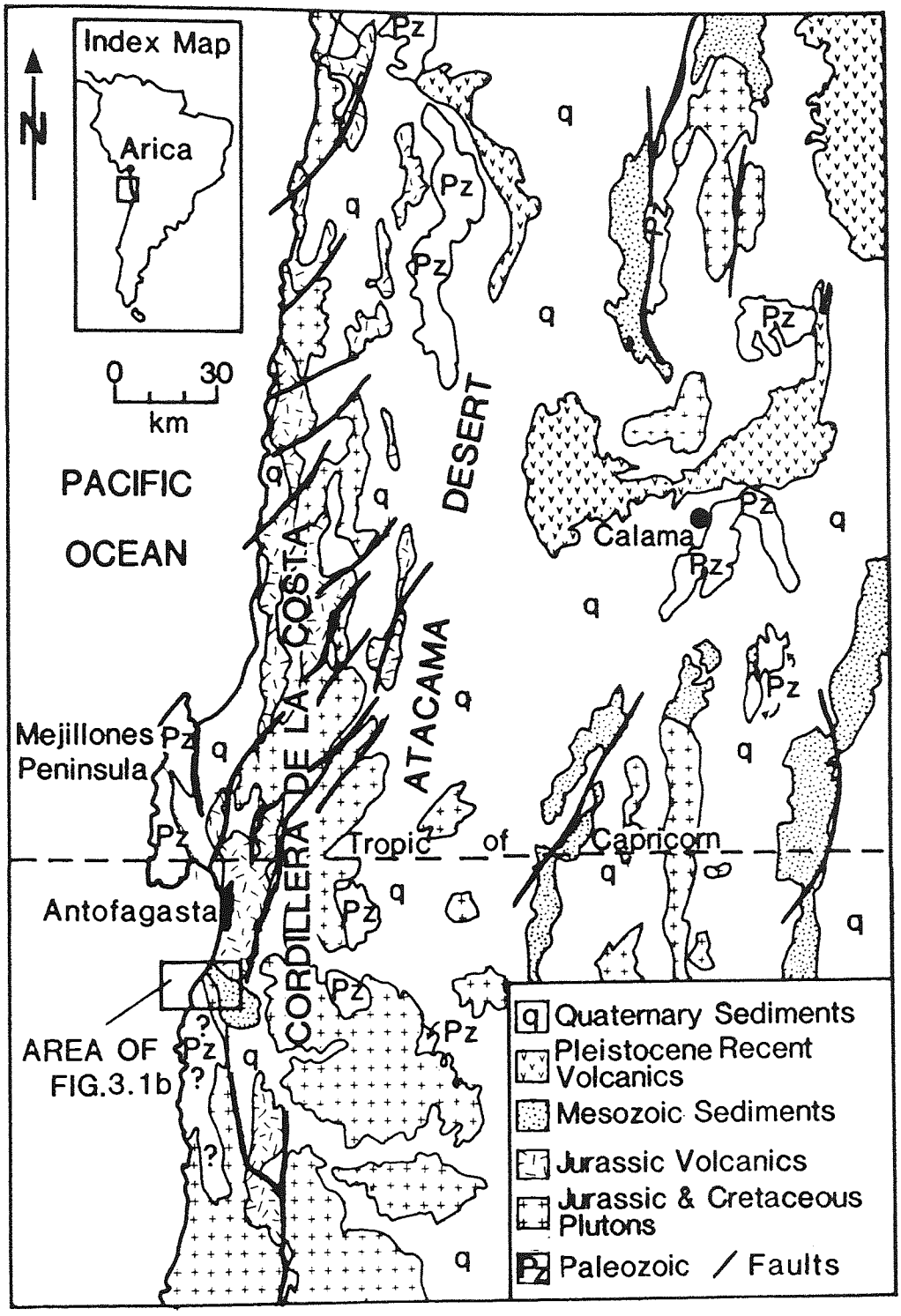

Fig. 3.1a Geological map of the Cordilera de la Costa, northern Chile, with an inset of the study area (Fig. 3.1b).

ERA	PERIOD	LITHOLOGY	UNIT
CENOZOIC	Quaternary	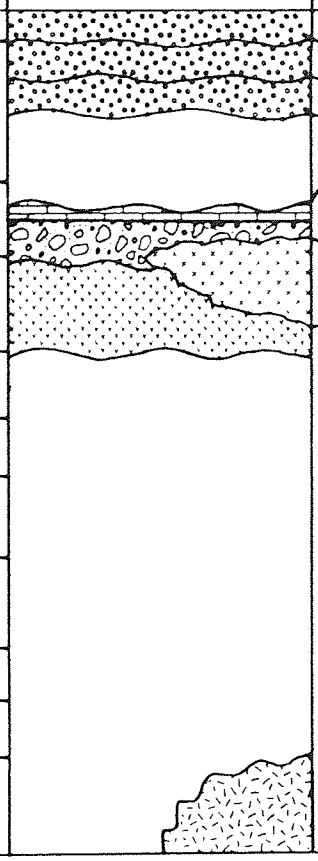	Unamed Late Tertiary -Recent sediments
	Tertiary		Mejillones Formation La Portada Formation
MESOZOIC	Cretaceous		El Way Formation Lombriz Formation Coloso Formation
	Jurassic		Jurassic Granodiorite
	Triassic		La Negra Formation
PALAEOZOIC	Permian		
	Carboniferous		
	Devonian		
	Silurian		
	Ordovician		
	Cambrian		Bolfin Complex

Table 3.1 Schematic presentation of the geology of the Cordillera de la Costa, Coloso area.

age on the basis of comparison with the Precambrian-Jurassic Mejillones Peninsula (Ferraris and Di Biase,1978; Espinoza,1983). Seven radiometric dates from the Complex indicate a Lower Jurassic-Lower Cretaceous age (206-134Ma., Ferraris and Di Biase,1978; D. Rex pers. comm.,1985; Damm et al.,1986). However, this probably reflects a resetting of the original age, as Damm et al. (1986), have obtained Precambrian (583+/-14Ma.) dates from the eastern edge of the Bolfin Complex. Petrographic observations indicate a gradation from unaltered gabbro to amphibolitized gabbro, resulting in a rock of dioritic composition, indicating a probable metamorphic event. The event is probably related to the emplacement of Jurassic granodioritic plutons (159-150Ma., Ferraris and Di Biase,1978; Rogers,1985), thought to be the surface expression of a granitic batholith emplaced along the Cordillera de la Costa, and also seen further south between 25-29°S. (Ulriksen,1979; Berg et al.,1983; Damm et al.,1986).

The Jurassic granodiorite plutons intrude the basaltic-andesitic mid-Jurassic La Negra Formation (186+/-14Ma., Rogers,1985). The La Negra Formation and the associated granodiorite plutons, are thought to represent the relicts of a volcanic island arc (James,1971; Palacios,1978; Coira et al.,1982). Rogers (1985) however, considers the La Negra Formation to have been erupted through fissures in an ensialic back arc basin, based on morphology and similarities with the Peruvian Puente Piedra Formation.

In Antofagasta Province, the La Negra Formation is overlain unconformably by the Lower Cretaceous Coloso and Lombriz Formations (Table 3.1). These Formations comprise an approximately 3000m. thick continental conglomerate sequence, dominated by proximal to distal alluvial fan facies, with interbedded playa lake sediments (Flint et

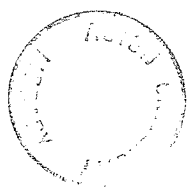

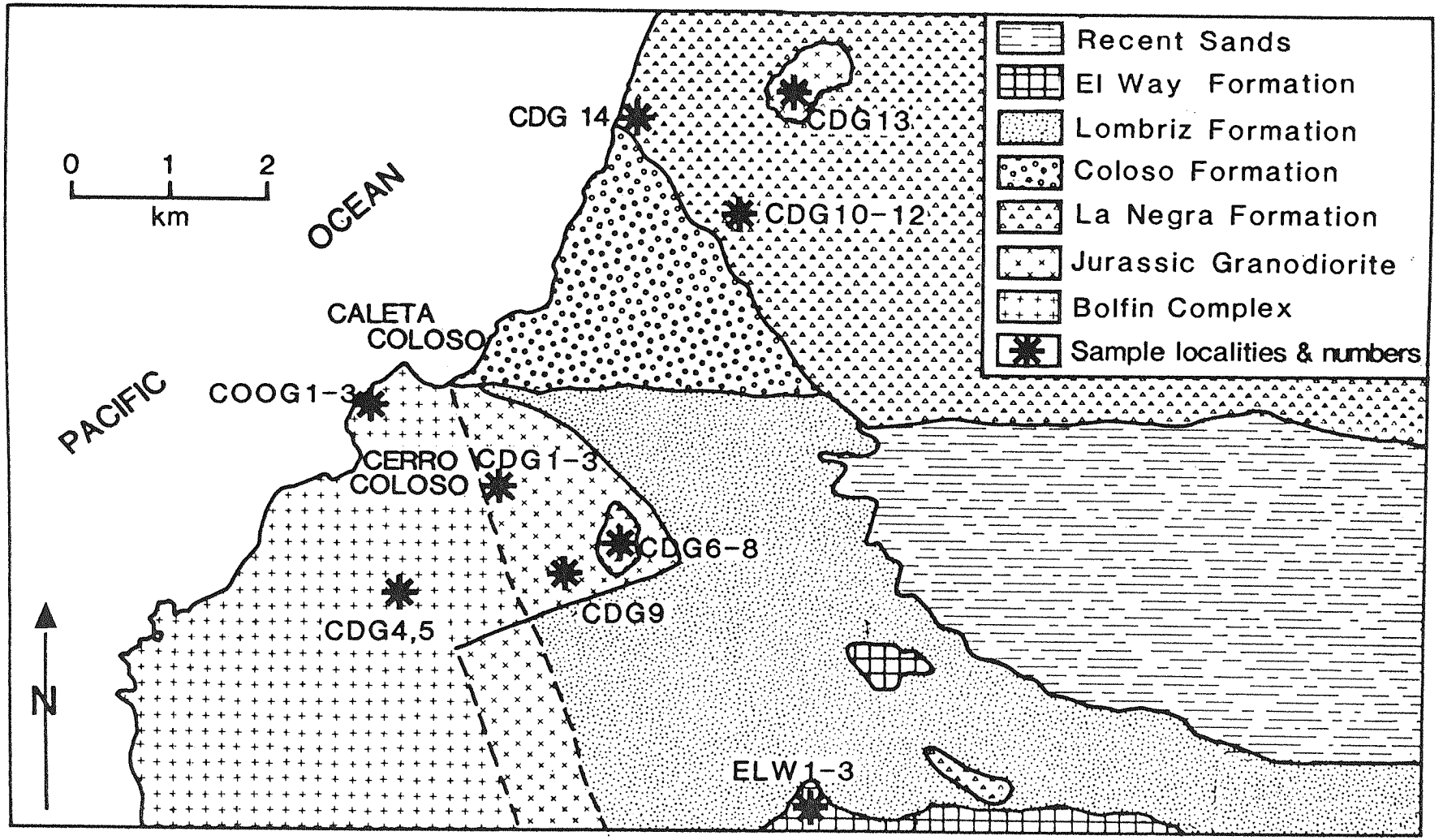

Fig. 3.1b Geological map of the Cordillera de la Costa (Coloso area), with palaeomagnetic sampling localities.

al.,1986; Flint and Turner,1988). A Lower Cretaceous age was assigned to the Coloso and Lombriz Formations based on their sequential position, as the conformably overlying shallow marine sandstones and limestones of the El Way Formation contain Hauterivian macrofossils (Jurgan,1974).

Along the coastal margin, the Tertiary La Portada and Mejillones Formations comprising aeolian and shallow marine sandstones, unconformably overlie all older rocks. Quaternary marine and alluvial gravels overlie the La Portada and Mejillones Formations, completing the stratigraphy of the Cordillera de la Costa (Table 3.1).

Normal faults with a NE-SW trend predominate in the Cordillera de la Costa (Fig. 3.1). No evidence for thrust faulting has been found. However, it is possible that the Cordillera de la Costa originally comprised a sequence of stacked thrust sheets, which were subsequently inverted through later extension (G. Williams, pers. comm.,1987). Regionally the rocks dip 15 degrees southwards.

3.3 Sampling and Laboratory Methods

Block and drilled samples oriented in the field were collected from the Bolfin Complex, the Lombriz and Coloso Formations (Turner et al.,1984), the Jurassic granodioritic plutons, the La Negra Formation, and the El Way Formation (Fig. 3.1b). The samples were oriented using both magnetic and sun compasses, orientation was accurate to within 5 degrees.

From sites drilled in the field and block samples drilled in the laboratory, 4 to 6 oriented specimen cores were obtained (2.54cm. in

diameter and height). One polished thin section was made for each site, in order to determine the magnetic mineralogy.

The initial natural remanent magnetization (NRM), was measured using a Digico balanced fluxgate magnetometer. Specimens were treated using a stepwise thermal demagnetization technique, in order to remove secondary components of magnetization, and establish discrete magnetic components (Stephenson,1967). All palaeomagnetic results have been tectonically corrected for the local dip of the La Negra and Coloso Formations. A palaeomagnetic fold test (McFadden and Jones,1981) which involved comparing isolated magnetic components of magnetization which had been structurally corrected with uncorrected components was applied to all samples, but proved inconclusive (Table 3.2).

Thermal demagnetization was undertaken at the University of Newcastle upon Tyne using the Nuffield Palaeomagnetic laboratory. Demagnetization was carried out using a non-inductive furnace and Hemholtz coil system in which the field is continuously monitored. Ambient magnetic fields during heating can be controlled to less than 2γ using this method. NRM measurements after each heating cycle were made using a two axis cryogenic magnetometer for weakly magnetized specimens, and a Digico balanced fluxgate magnetometer for strongly magnetized specimens.

The results were plotted using the following techniques which enabled careful analysis of individual specimens to be made:

a) a normalized intensity decay curve,

b) a stereographic projection of directional changes,

c) a Zijderveld orthogonal diagram, from which the stable component of magnetization can best be estimated (Dunlop,1979),

d) a least squares fit (LSF)/bulk demagnetisation method used to extract stable components of magnetization over different temperature ranges.

Stable components identified using the LSF technique are derived from a computer programme based on the work of Kirshvink (1980). The programme uses the same data points used for the Zijderveld diagrams. It scans from the origin, taking the next two successive values working from the highest demagnetization level to the inital NRM value. The programme tests that these three or more points lie within a box with a diagonal value of less than 10 degrees, if linear at this value it tries the next value and so on. Having established a line, the direction is given which is then taken as a stable component over the demagnetization range which the data points cover. A problem with this technique, is that it fails to account for individual data points which may be statistically significant when combined with data points from other samples derived at the same demagnetization step. The grouping of data points with similar orientations at or over similar demagnetization steps is referred to as the bulk demagnetization technique.

The bulk demagnetization technique has only been used if a grouping is statistically valid. Throughout this thesis the term statistically valid is taken to indicate a group of directions or components of magnetization which, when combined, have an angular error value of less than 20 degrees at the 95% significance level (Fisher, 1953).

Results presented in this thesis have only utilised specimens which at any time during demagnetization had an intensity of magnetization 10x greater than the noise level of the magnetometer used.

The isothermal remanent magnetization (IRM) technique was also used to determine the magnetic mineralogy of selected samples (Dunlop,1972). This technique allows a discrimination to be made between rocks containing low coercivity minerals such as magnetite, which normally saturate in fields of less than 0.3 Tesla, and high coercivity minerals such as haematite, for which fields in excess of 5 Tesla may be required for saturation (Turner et al.,1984b).

3.4 Palaeomagnetic Results

3.4.1 The Bolfin Complex (COOG1,2,3,CDG4,5)

Initial sample measurement (n=28) revealed large variations in both initial intensity values and directions of NRM. Initial intensities vary between 1432 and $2.9 \times 10^{-3} Am^{-1}$. NRM directions show a large degree of scatter, but are dominantly upwardly inclined in the northern quadrants (Fig. 3.2a).

During thermal demagnetization all samples display a rapid initial loss in intensity (50-80% between 0-150 deg.C.). The isolated component over this temperature range has random orientations and is considered to be a viscous component of magnetization of no palaeomagnetic significance.

Examination of the normalised intensity decay curves reveals some variation (Fig. 3.3a). Analysis of the isolated components (LSF, Zijderveld diagrams and stereographic projections), revealed the presence of a normal component of magnetization (upwardly inclined in

a)

c)

Fig. 3.2 Equal angle stereographic projection, showing fiducially corrected ● and fiducially and structurally corrected ▲ initial directions of NRM, for: a) the Bolfin Complex, b) the La Negra Formation, c) Jurassic granodioritic plutons, and d) the El Way Formation. Open symbols = upward inclination, closed symbols = downward inclination. ' = present axial dipole field.

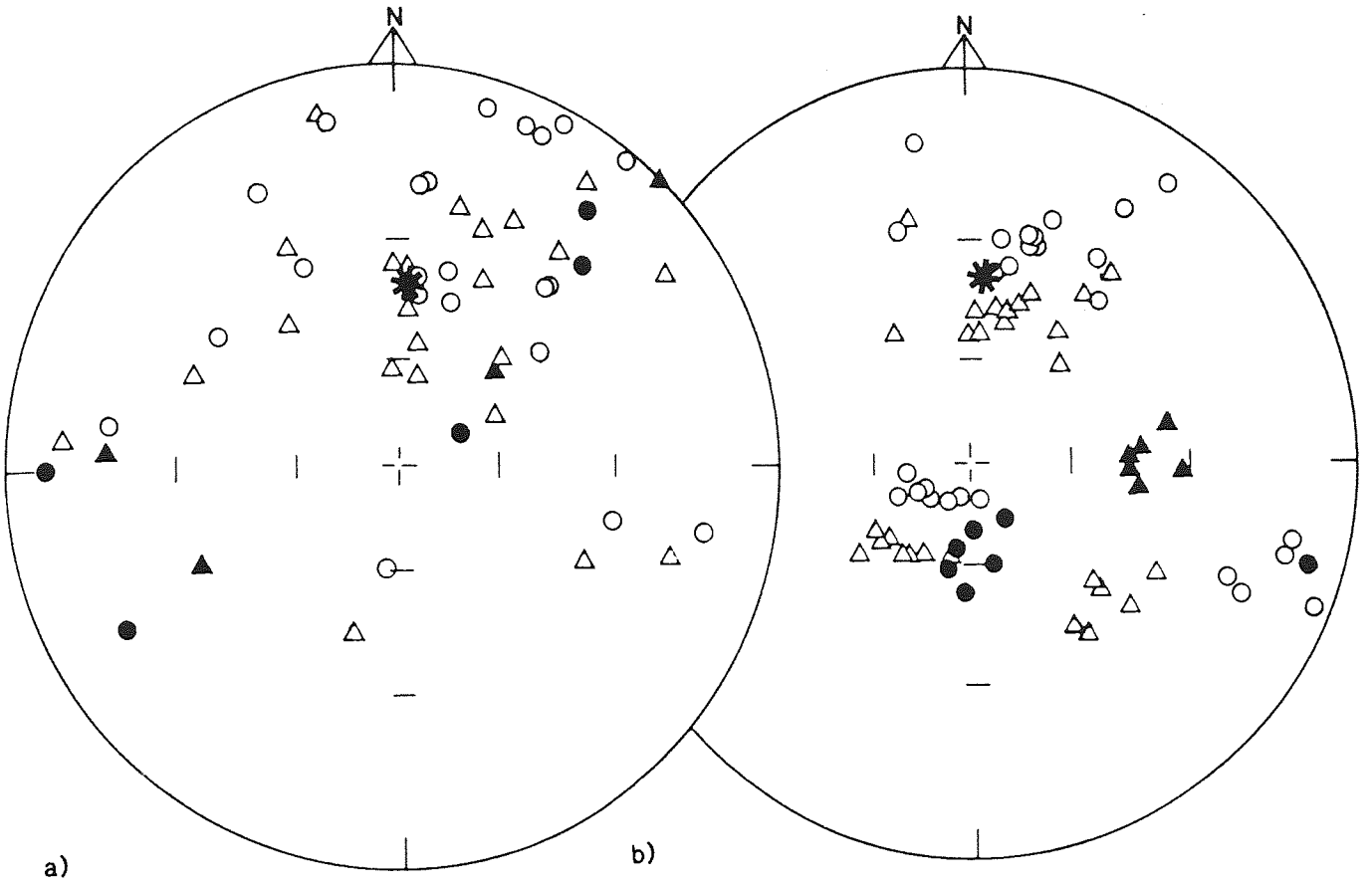
N
N
a)
b)

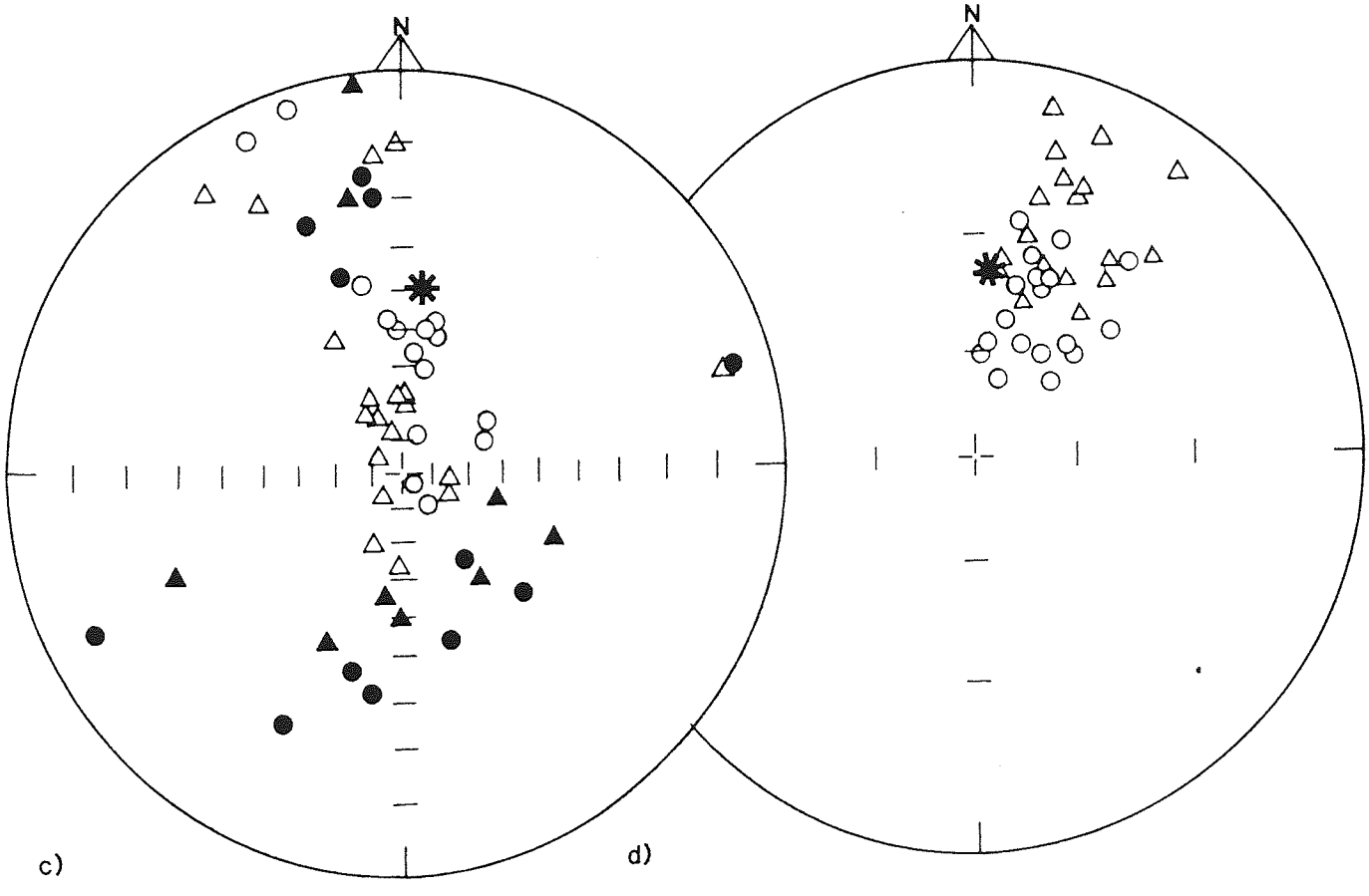
N
N
c)
d)

the northeast quadrant, Dec=40, Inc=-24; Table 3.2) between 150-500 deg.C. in 4 sites (COOG1,2,CDG4,5). Above 500/550 deg.C. and coincident with a marked blocking temperature (Fig. 3.3a), a strong reversed component (downward inclination in the southwest quadrant, Dec=238, Inc=+34; Table 3.2; Fig. 3.3b), was extracted from COOG1 and CDG5. This component is poorly defined in COOG2 and CDG4 (α_{95}>20 degrees). COOG3 has a relatively stable normal component over all temperature ranges. Isolated components are presented in Table 3.2.

IRM acqisition curves for CDG4 and 5 (Fig. 3.3c), indicate that haematite and magnetite are present in both samples. The presence of magnetite is shown by saturation of the samples in fields greater than 0.3 Tesla. Above 0.6 Tesla a progressive increase in the intensity of IRM, indicates that haematite is present.

Interpretation: A correlation can be made between the degree of metamorphism and isolated components. COOG3 has been strongly amphibolitized (Plate 3.1), and contains a single normal component. COOG2 and CDG4 are not as strongly altered as COOG3, and contain a strong normal component, with a very weak high temperature reversed component of poor statistical validity (α_{95}>20 degrees). COOG1 and CDG5 are virtually unaltered, and contain both normal and reversed components at low and high temperatures respectively (Table 3.2).

The high temperature component present in COOG1 and CDG5 (between 550 and 680 deg.C.; Fig. 3.3b), must be carried by haematite, as it is present above 580 deg.C. (the Curie temperature of magnetite). Haematite however, does not only form as a primary magmatic phase in igneous rocks, but can also form through the oxidation of magnetite in the magma chamber, or at a later date associated with late stage

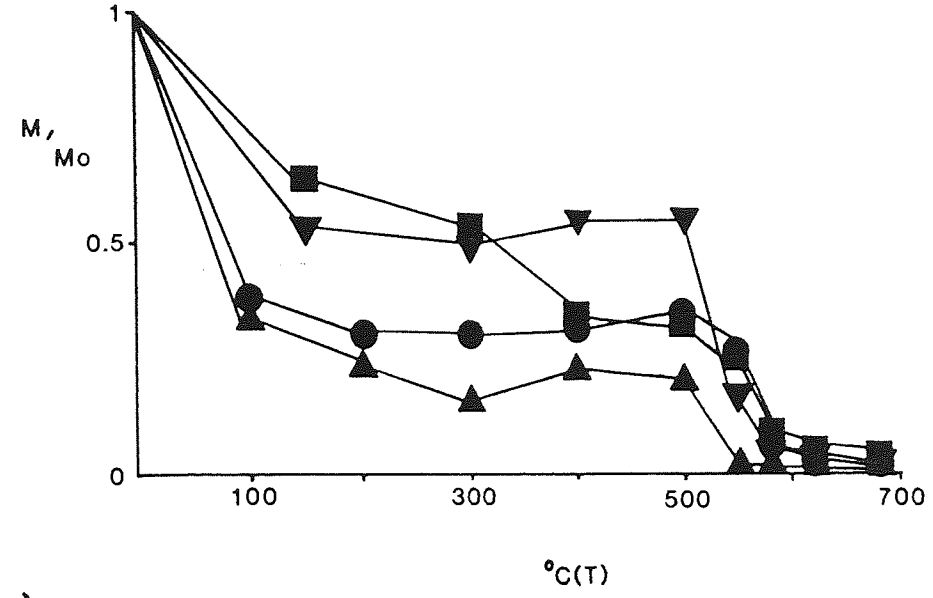
1
M,
Mo
0.5
0
100
300
500
700
°C(T)

a)

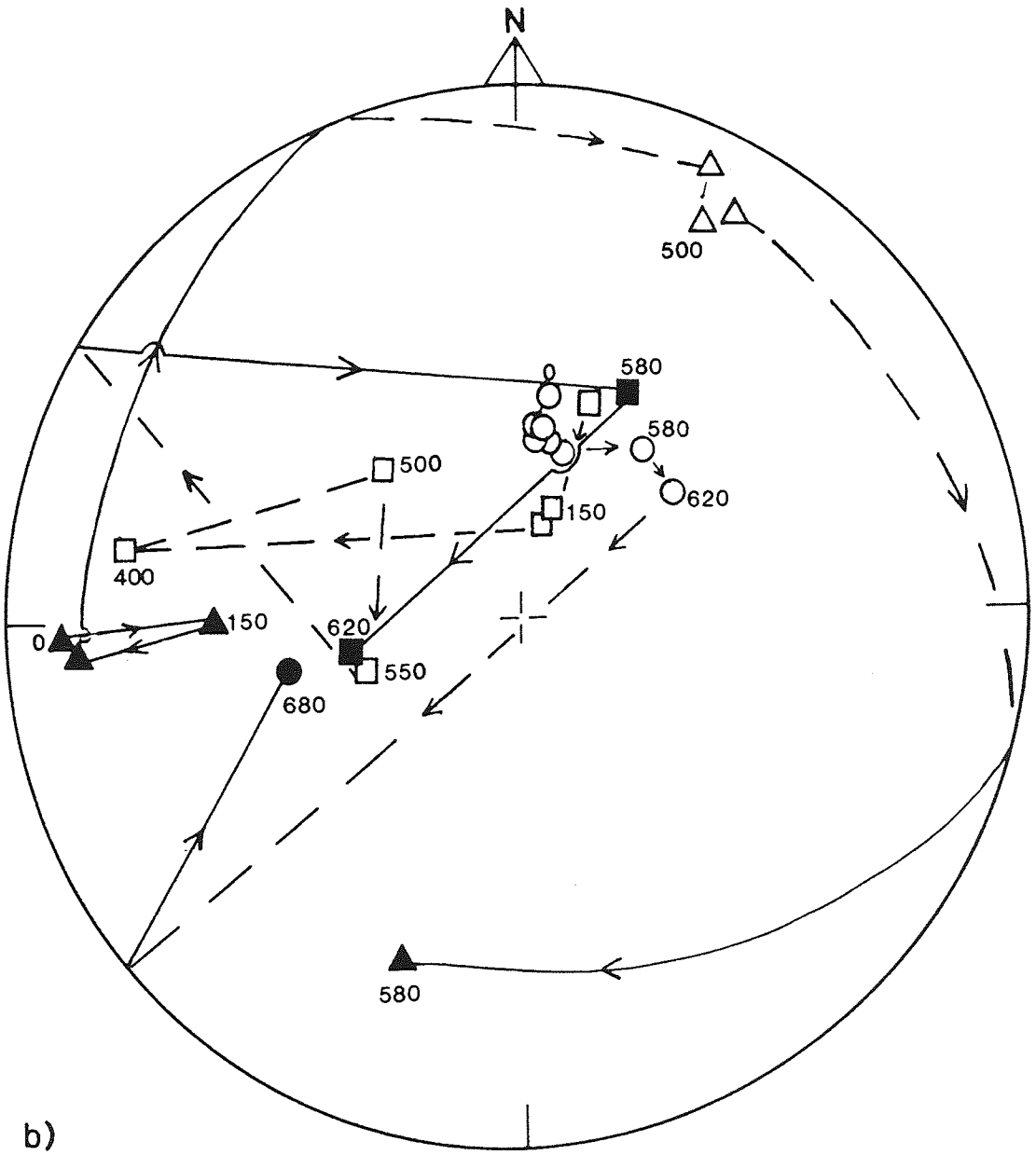
N
500
0
580
580
620
500
150
400
0
150
620
550
680
580

b)

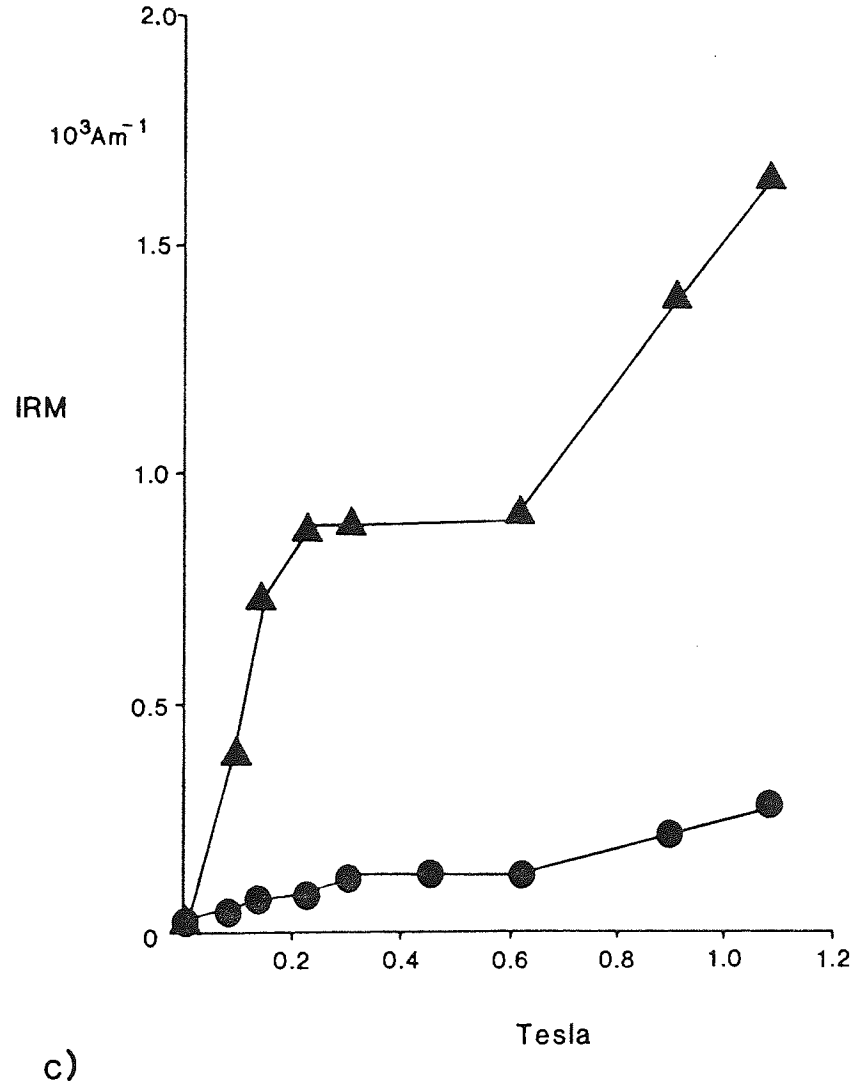

Fig. 3.3 Palaeomagnetic analysis of the Bolfin Complex, a) normalised intensity decay curves for COOG1.2●, COOG2.3▲, CDG4.1▼ and CDG5.2■, b) equal area stereographic projections of directional change for COOG1.3▲, CDG5.1 ● and CDG5.1A■, showing the presence of a high temperature reversed direction, c) IRM acquisition curves for CDG4▲ and CDG5●. Numbers=deg.C. Other details as Fig. 3.2.

NB All stereographic projections of directional change, and all Zijderveld diagrams presented in this thesis have been corrected for bedding (where possible).

magmatic fluids or metamorphism. In order to assign an age to the reversed component, it is important to determine whether it is of primary or secondary origin. Consequently, polished thin sections were examined which confirmed that the haematite present was of a primary magmatic origin, and not present in secondary (metamorphic textures).

The normal component present in the Bolfin Complex is due to remagnetization associated with a metamorphic event. Metamorphism is indicated by granoblastic recrystallistation textures (Plate 3.1), and the development of porphyroblastic hornblende, magnetite, biotite mica and the alteration of primary feldspar and muscovite mica (Plate 3.2). The most strongly metamorphosed site (COOG3), has been completely remagnetized. Partially metamorphosed sites (COOG2,CDG4), retain a weak reversed component, whereas unmetamorphosed sites (COOG1,CDG5), retain a strong reversed component, having only been partially remagnetized.

The Bolfin Complex does not reflect a simple magnetic polarity reversal. The correlation between metamorphism and remagnetization would not be present, if the NRM of the Complex had been acquired whilst cooling during a reversal of the Earth's magnetic field. Also, no stable transitional components have been identified; these would be present, if the Complex had cooled during a reversal.

Although the last point is not conclusive evidence of remagnetization. Both the Jurassic granodiorites and the La Negra Formation (sections 3.4.2,3.4.3), contain polarity reversals thought to reflect cooling during a reversal of the Earth's magnetic field. These units contain very steeply inclined components, interpreted as transitional in nature, which are absent from the Bolfin Complex.

In summary, the Bolfin Complex has been remagnetized during a

Plate 3.1 CCCG3 Metamorphic texture (amphibolitisation). Light grey porphyroblastic horneblende encloses and partially encloses crystals of magnetite (opaque). The magnetite crystals are embayed (top left), but appear pristine, suggesting formation after a metamorphic event. The white mineral is poryhroblastic plagioclase feldspar, again probably newly formed as alteration is limited (unlike Plate 3.2). Transmitted light, field of view=3.4mm.

Plate 3.2 Alteration CCCG2. The opaque mineral in the centre of the photomicrograph is magnetite, which is intergrown with quartz (Q). A chlorite alteration rim (C) surrounds the magnetite crystal, and is well developed in the bottom left of the photomicrograph. Plagiocalse feldspar is recognised by its marked cleavage (running from top to bottom), which often shows evidence of alteration to clay minerals (PA). Hornblende (H) is present in the bottom right and is slightly darker than the feldspar. Transmitted light, field of view=3.4mm.

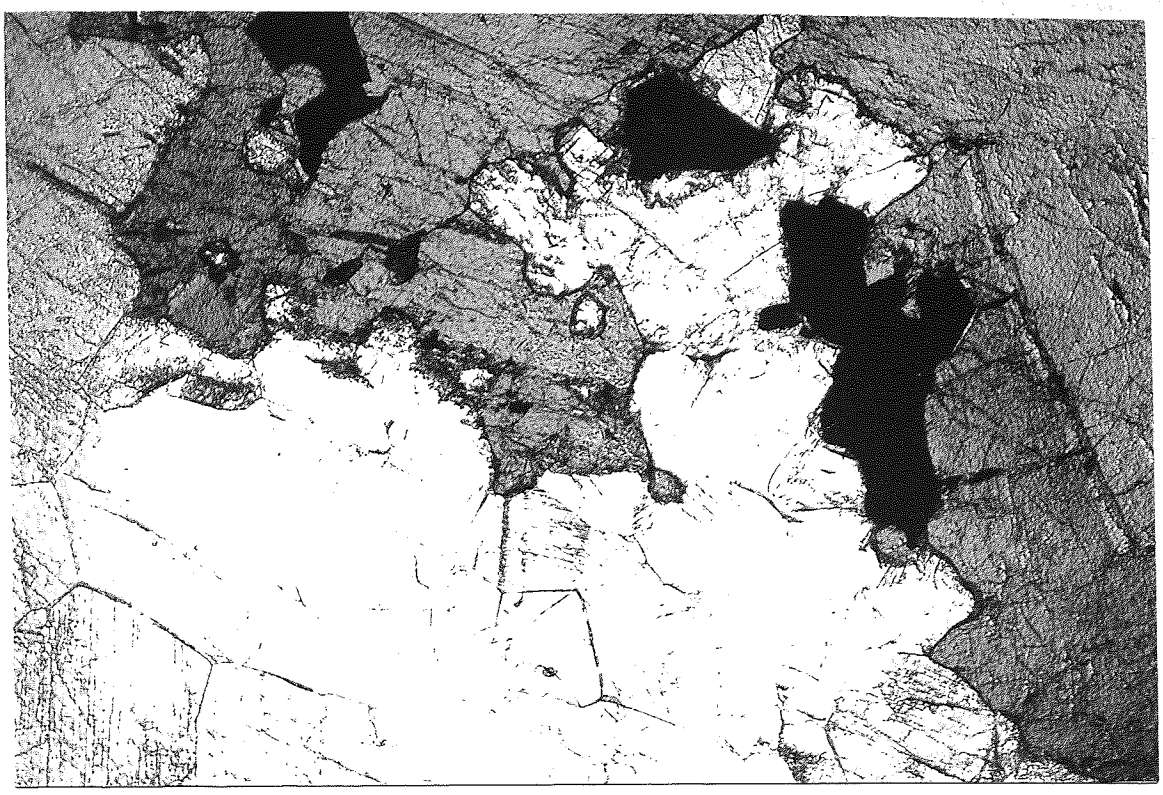

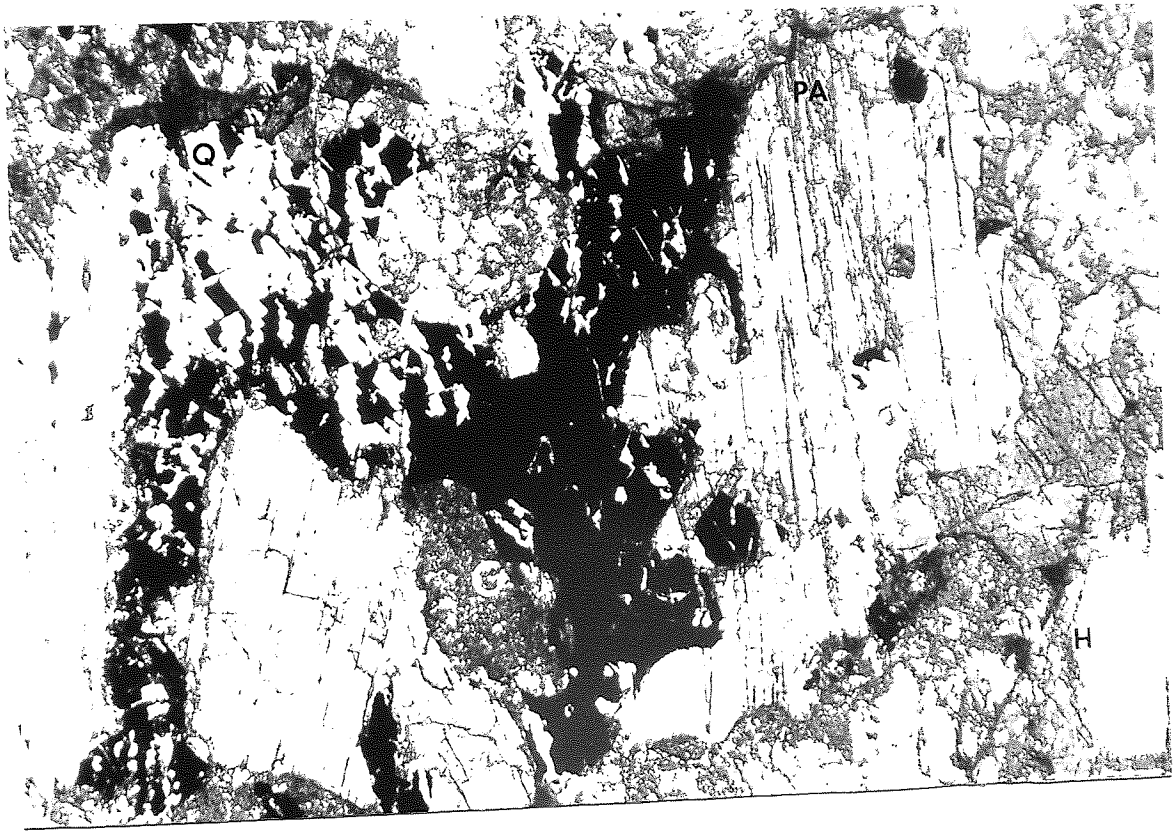
Q
PA
H

period of normal polarity of the Earth's magnetic field. The reversed component (carried by haematite) is pre-remagnetization of the Complex, and may reflect the original magnetization of the Complex. (The age of both the normal and reversed components is discussed in section 3.5.1).

3.4.2 The La Negra Formation (CDG6,7,8,10,11,12,14)

Seven sites (n=35), from the La Negra Formation were demagnetized. Within-site grouping was good, but much variation was apparent between sites. NRM directions are scattered (Fig. 3.2b), and initial intensities of NRM varied between 15.4 and 205.4x$10^{-3}$$Am^{-1}$.

Of the four analytical techniques employed, only LSF analysis (and to a lesser extent Zijderveld orthogonal diagrams), allowed any discrimination between sites. Using the LSF technique the seven sites were split into three groups. The groupings were derived from the variation in site behaviour, during demagnetization over certain temperature ranges. Total intensity behaviour during demagnetization and stereographic projections of directional changes are described below within the context of the identified groups. Extracted components from the La Negra Formation are presented in Table 3.2.

Group 1 (CDG7,8,12,14): Both CDG8 and 12 contain reversed components removed between 0-150 deg.C., individual specimens of CDG7 and 14 contain this component. The component is characterised by a sharp increase in intensity up to 150 deg.C. where half the NRM is lost between 300 and 500 deg.C., as shown by the normalised intensity decay curves (Fig. 3.4a). A component of normal polarity (Dec=24, Inc=-31) predominates between 150-500/580 deg.C. (Table 3.2). Above 500/580 deg.C. a reversed component is isolated (Dec=217, Inc=+50),

Table 3.2 Components of magnetization extracted from the studied units of the Cordillera de la Costa, and the respective temperature ranges. CDG1,3,13-Jurassic Granodiorite; CCOG1,2,3;CDG4,5-Bolfin Complex; CDG6,7,8,12,14-La Negra Formation (normal and reversed); ELW1,2,3-El Way Formation. CDG2,9,10,11 have been excluded as they contain stable intermediate components. N=Number of specimens per site. R=Resultant vector (Fisher,1953). K=estimated precision parameter (Fisher,1953). CSD=Circular Standard Deviation. A95=Angular radius of 95% cone of confidence about the observed mean. DEC=Declination of the isolated component in degrees (structurally corrected). INC=Inclination of the isolated component in degrees (structurally corrected), with north seeking directions down taken as positive. Figures in brackets correspond to the same extracted component which has not been structurally corrected, enabling a fold test to be applied.

Table 3.2

SITE	N	R	K	CSD	ALPHA 95		DEC		INC		RANGE (DEG. C.)
CDG1	5	4.80	20	18.0	17.4	(17.7)	203	(201)	+20	(+40)	620-680
CDG3	5	4.87	32	14.3	13.7	(13.7)	226	(231)	+28	(+47)	0-680
CDG13	5	4.67	12	20.1	19.9	(21.5)	207	(205)	+36	(+55)	300-680
COOG1	7	6.46	11	24.4	19.0	(19.0)	53	(59)	-24	(-41)	0-400
COOG2	3	2.95	41	12.6	19.5	(19.6)	26	(28)	-35	(-55)	0-400
CDG4	6	5.81	26	16.0	13.5	(13.5)	39	(41)	-16	(-36)	550-620
CDG5	6	5.71	17	19.6	16.7	(16.7)	23	(21)	-30	(-49)	0-400
CDG6	4	3.97	117	7.5	8.5	(8.5)	16	(328)	-22	(-52)	600-680
CDG8	6	5.98	223	5.4	4.5	(4.5)	24	(22)	-38	(-58)	500-680
CDG12	3	2.99	3365	1.4	2.1	(2.8)	32	(77)	-38	(-32)	400-550
CDG14	6	5.75	20	18.1	15.1	(15.1)	29	(29)	-32	(-52)	0-550
CDG7	6	5.97	156	6.5	5.4	(5.3)	189	(107)	+48	(+48)	500-680
CDG8	5	4.94	67	9.9	9.4	(9.3)	223	(242)	+58	(+77)	0-150
CDG12	3	2.99	356	4.3	6.5	(6.5)	236	(247)	+37	(+54)	0-150
ELW1	6	5.93	72	9.6	8.0	(8.4)	10	(8)	-29	(-52)	0-580
ELW2	6	5.91	54	11.0	9.2	(9.1)	25	(28)	-33	(-54)	0-550
ELW3	6	5.79	24	16.5	13.9	(14.1)	24	(28)	-32	(-54)	0-550

this polarity change is coincident with a marked blocking temperature at 500-580 deg.C. (Fig. 3.4a, Table 3.2). Fig. 3.4b shows the large directional changes which occur from an initial position in the NE quadrant, to a steep southerly direction as a lower blocking temperature component is removed. The Zijderveld orthogonal diagrams do allow a better definition of the normal and reversed components, as shown by Fig. 3.4c which has three components defined by linear segments, and with sharp breaks in their respective blocking temperature spectra (0-150 deg.C.=viscous component, 150-500 deg.C.=normal component, 500-620 deg.C.=reversed component).

Group 2 (CDG10,11): This group contains one dominant component, interpreted as transitional in nature, since it has steep inclinations, which fall directly between the normal and reversed components (Dec=243, Inc=-79). All four analytical techniques indicate a one component system; straight line Zijderveld orthogonal diagrams, stable stereographic projections, similar isolated components over all temperature ranges and normalised intensity decay curves with no marked blocking temperature and a gradual decrease in NRM, with 75% lost by 500 deg.C. (Fig. 3.4a).

Group 3 (CDG6): CDG6 displays much different behaviour to the other groups (Table 3.2). A rapid decrease in NRM with 80% lost by 150 deg.C. is shown by the normalised intensity decay curve (Fig. 3.4a), corresponding to the removal of a low blocking temperature component. The group also contains a 0-500 deg.C. component interpreted as transitional in nature characterised by a marked blocking temperature at 500 deg.C. (Fig. 3.4a), and a 580-680 deg.C. normal component. The 0-500 deg.C. component is thought to be transitional as both the stereographic projections and LSF analysis indicates continuous

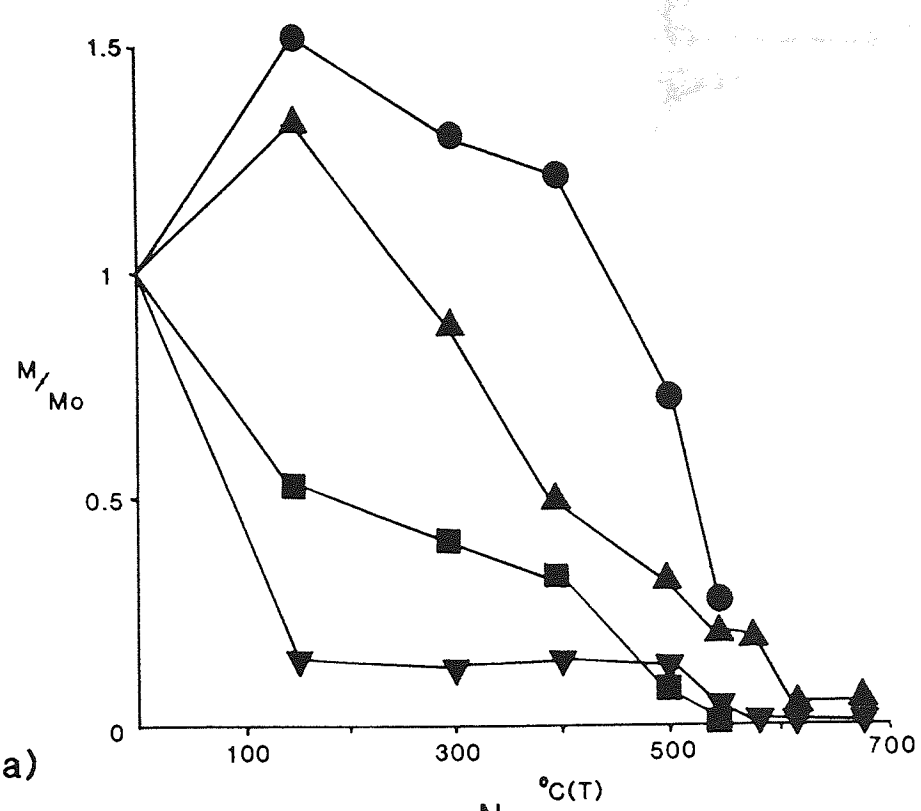
1.5
1
0.5
0
M/Mo
100
300
500
700
°C(T)

a)

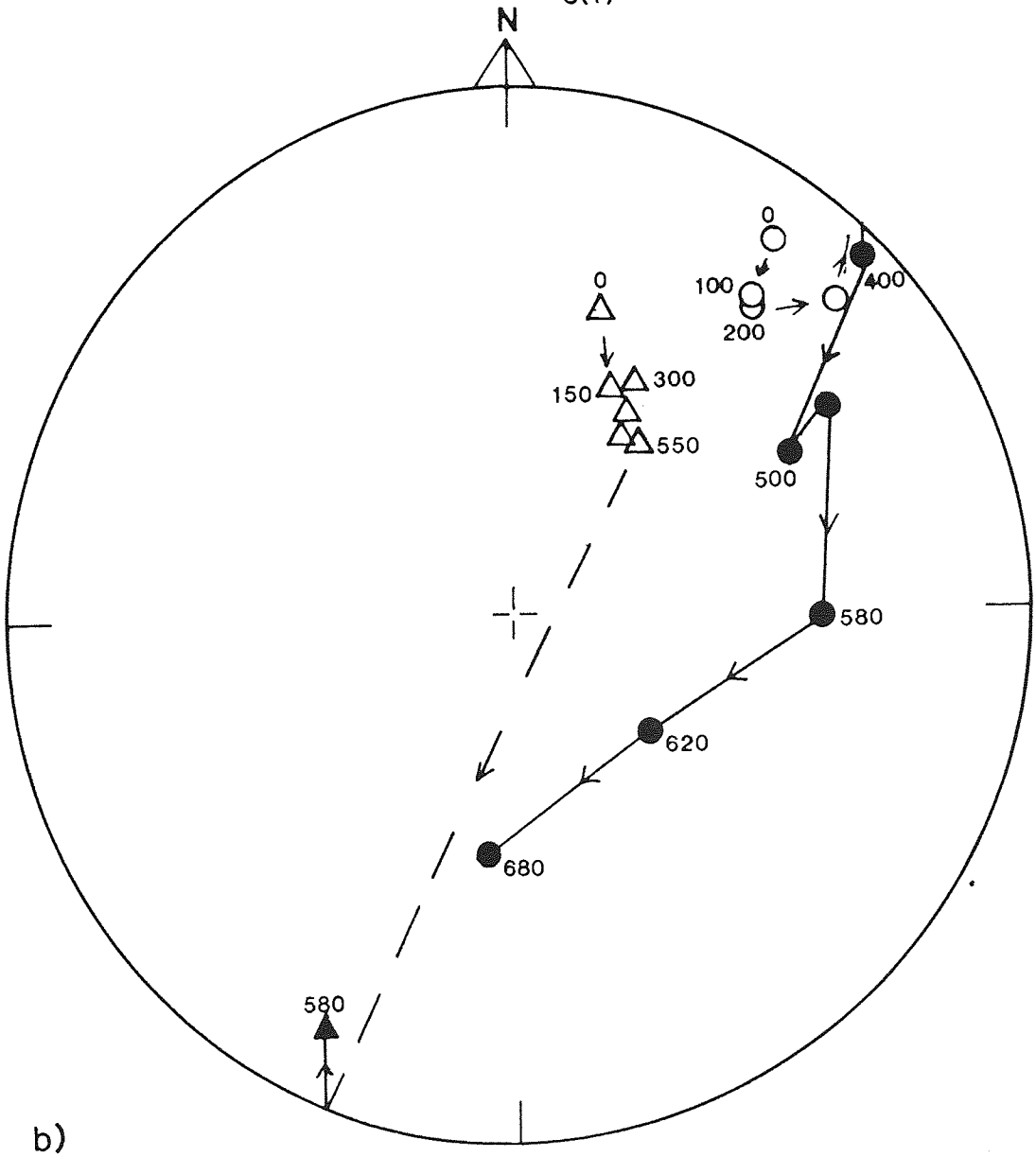
N
0
100
200
400
0
150
300
550
500
580
620
680
580

b)

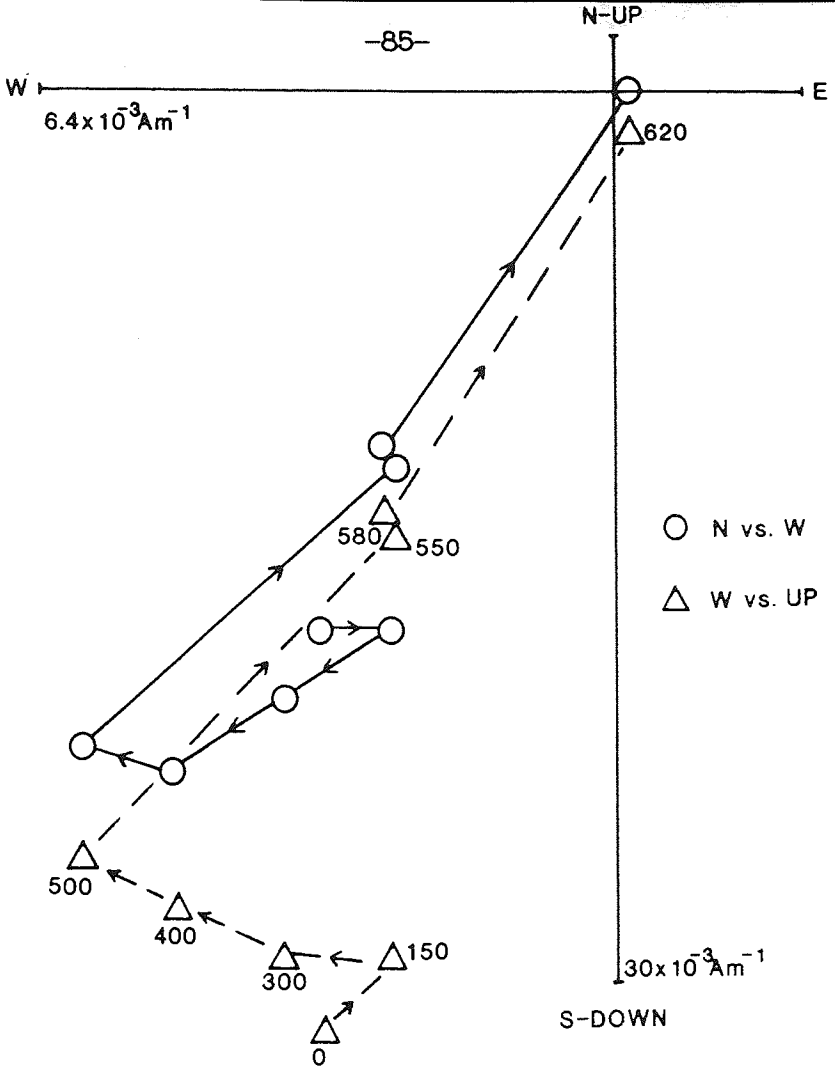
N-UP
W
E
$6.4 \times 10^{-3} Am^{-1}$
620
580
550
500
400
300
150
0
N vs. W
W vs. UP
$30 \times 10^{-3} Am^{-1}$
S-DOWN

c)

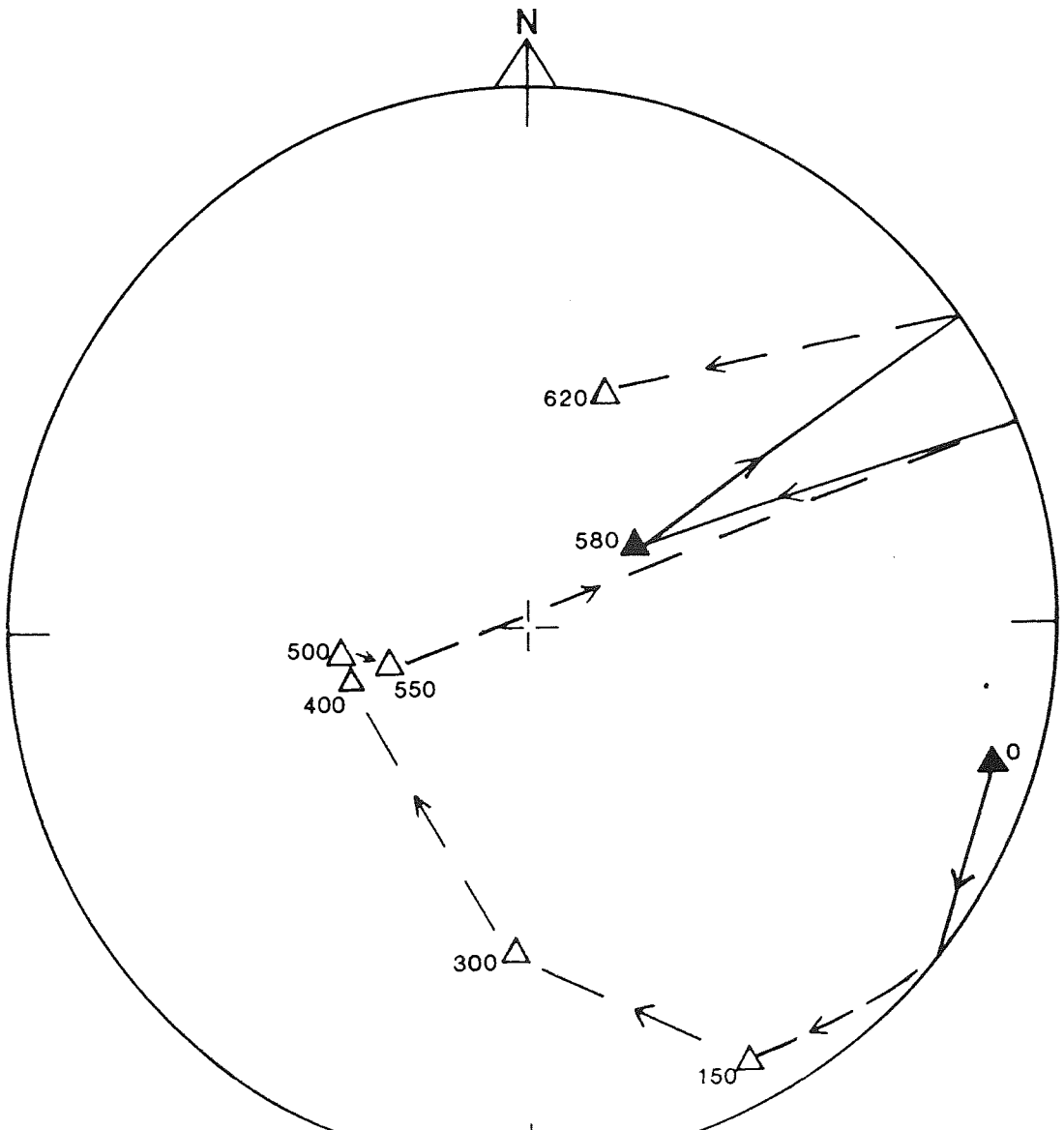
N
620
580
500
400
550
0
300
150

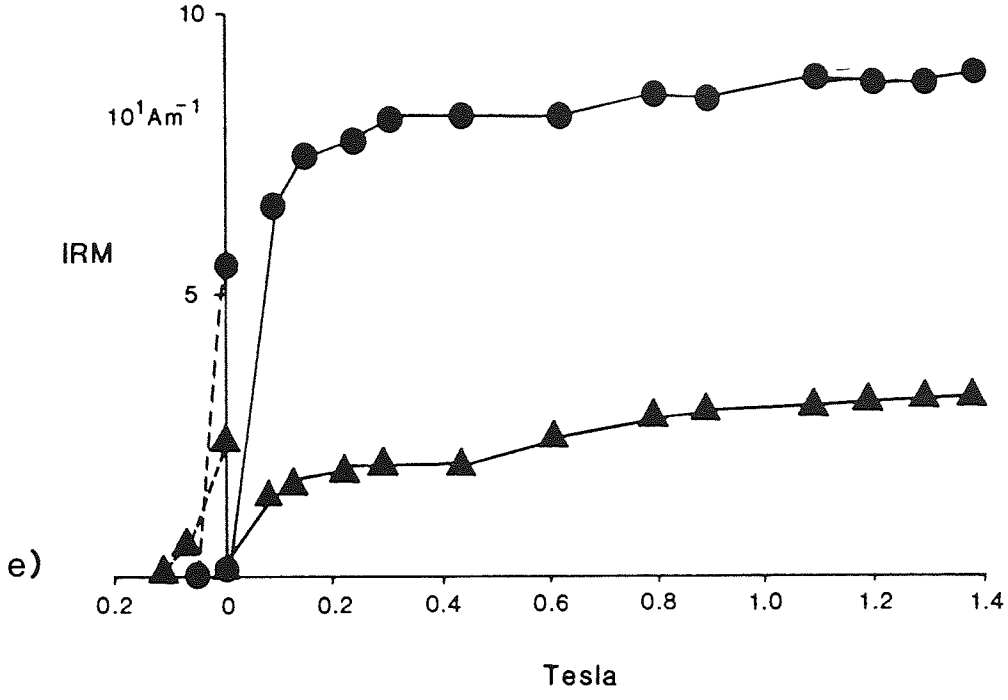

Fig. 3.4 Palaeomagnetic analysis of the La Negra Formation, a) normalised intensity decay curves for CDG6.3A▼, CDG8.2▲, CDG11.1■ and CDG12.2●, b) equal area stereographic projections of directional change for CDG8.1 ▲ and CDG14.3a ●, c) Zijderveld orthogonal diagram for CDG7.2A, and d) equal area stereographic projection of directional change for CDG6.4, e) IRM acquisition curves for CDG8● and CDG14▲. Other details as Fig. 3.3.

movement of the isolated components throughout demagnetization, finishing in the northeast quadrant (Fig. 3.4d).

IRM acquisition curves (Fig. 3.4e) and reflected light microscopy indicate that magnetite and haematite are present as discrete grains in all three groups. However, group 3 also contains cross-cutting veins of haematite, thought to be secondary in origin. It should be noted that high temperature components may have been present in CDG10,11 and 12, but due to disintegration of the specimens betwee" 500-580 deg.C., measurement was impossible.

Interpretation: Group 1 is thought to have been erupted during a normal period of the Jurassic magnetic field, producing a normal remanence carried by magnetite. Cooling resulted in fracturing of the lavas allowing the oxidation of iron bearing detritus to form haematite. This produced both high and low blocking temperature components, which are antiparallel to the normal component (Table 3.2), indicating that oxidation took place soon after eruption.

The rocks comprising group 2 contain a transitional component, resulting from eruption and cooling during a transitional period of the Jurassic magnetic field. The difference in the behaviour of group 3 to the other groups may be attributed to a subsequent localised metamorphic event. The presence of cross-cutting veins of haematite, suggests probable remagnetization of the site. The isolated normal component is however, similar to other isolated components from the La Negra Formation (Table 3.2), and may therefore be of a similar age (see section 3.5.1).

3.4.3 Jurassic Granodioritic Plutons (CDG1,2,3,9,13)

Three granodioritic plutons were sampled from the Cordillera de la Costa (Fig. 3.1), these yielded 28 specimen cores from 5 sites. Initial NRM directions are scattered (Fig. 3.2c), and initial intensities vary between 7.4 and 488.1x10 Am.. Of the 5 sites, 3 show similar behaviour during demagnetization (CDG1,2 and 13), whereas CDG3 and 9 which have been altered and mineralized, show different behaviour.

Normalised intensity decay curves reveal a marked blocking temperature, coincident with a high temperature polarity change for CDG1,2,9 and 13 at 500/550 deg.C. (Fig. 3.5a). Table 3.2 lists the relationship between component polarity and temperature range. Normal components dominate at low temperatures and reversed at high temperatures. The components were extracted using LSF analysis and Zijderveld orthogonal diagrams (Fig. 3.5b). Examination of IRM acquisition curves (Fig. 3.5c), indicate that the plutons contain both magnetite and haematite.

Interpretation: All 5 sites were intruded during a reversed magnetic field, indicated by the high temperature reversed component. An intermediate component was acquired during cooling. The normal, low temperature component records the change in remanence acquisition from reversed-intermediate-normal. CDG3 and 9 were subsequently altered and mineralized. CDG3 was remagnetized and acquired a very stable reversed component (with similar orientations to CDG1 and 13; Table 3.2). CDG9 was partially remagnetized, acquiring a possible Recent overprint.

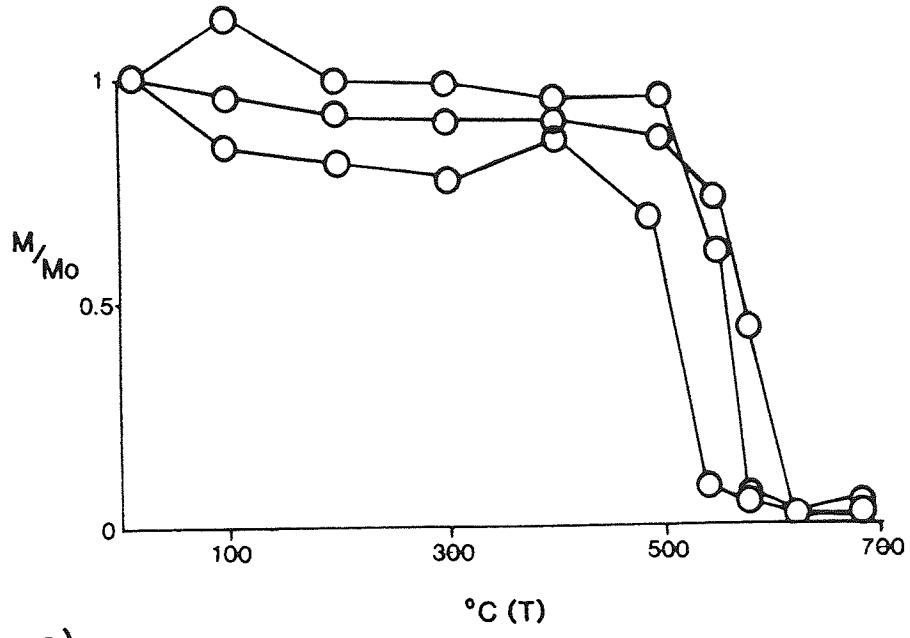
1
0.5
0
M/Mo
100
300
500
700
°C (T)

a)

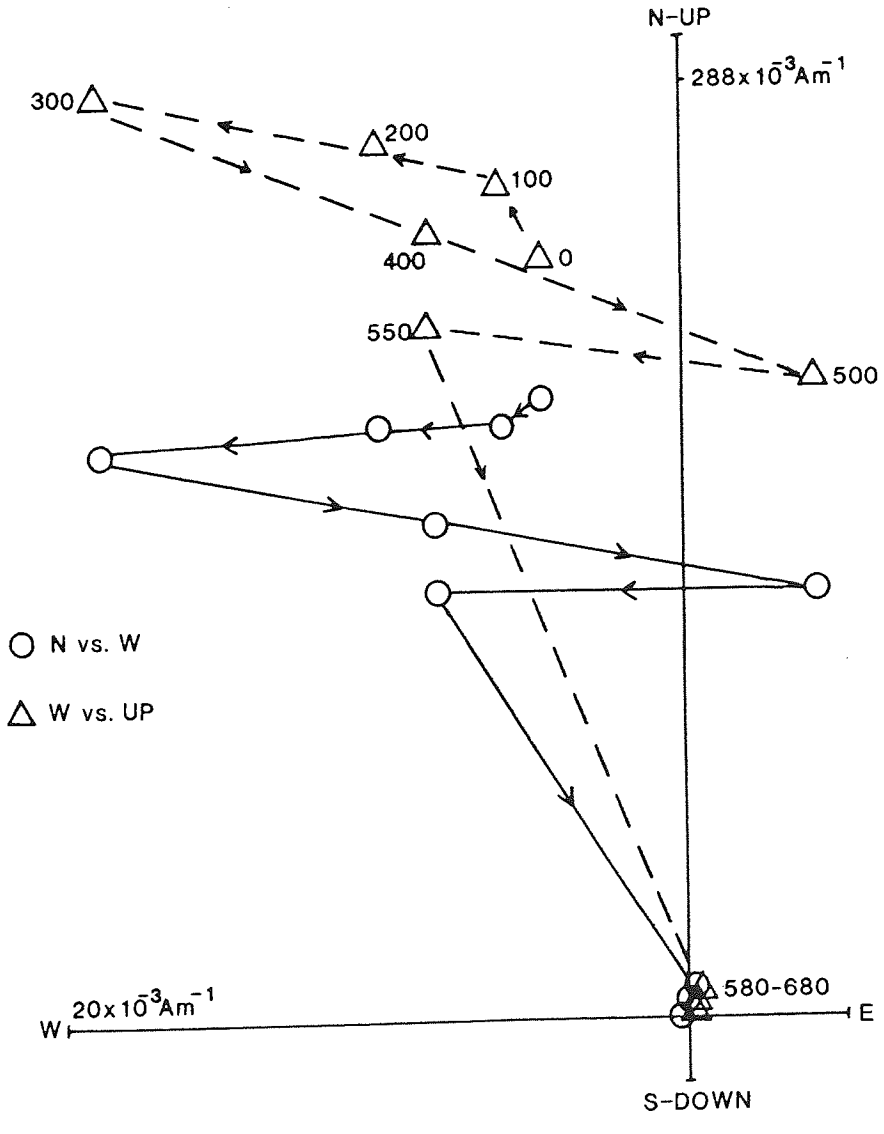
N-UP
288x10⁻³Am⁻¹
300
200
100
400
0
550
500
N vs. W
W vs. UP
580-680
20x10⁻³Am⁻¹
W
E
S-DOWN

b)

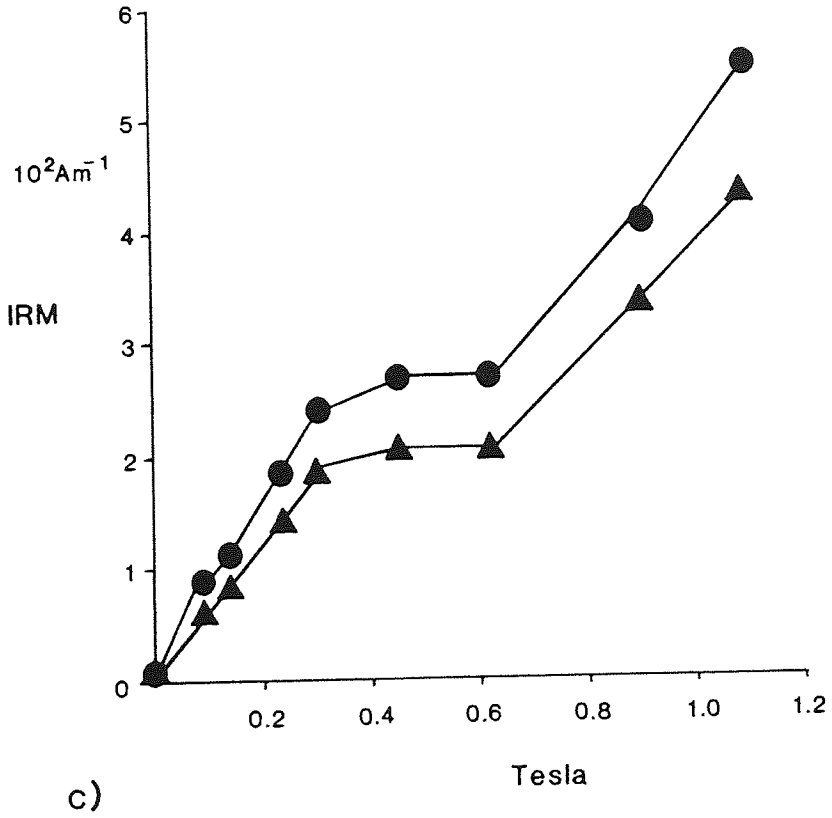

Fig. 3.5 Palaeomagnetic analysis of Jurassic granodioritic plutons, a) normalised intensity decay curve for specimens from sites CDG1, 2 and 13. b) Zijderveld orthogonal diagram for CDG2.1A, with 3 linear components which correspond to the following isolated components: 100-300 deg.C.=Normal, 300-500 deg.C.=Intermediate and 580-620 deg.C.=Reversed c) IRM acquisition curves for CDG1● and CDG2▲.

3.4.4 The Coloso and Lombriz Formations

The palaeomagnetism of the Coloso and Lombriz formations, has been described by Turner et al. (1984a).

The Formations have a complex magnetic history related to the diagenesis of arid zone alluvium. Both polarities are present, and magnetization is considered to have been acquired diagenetically, shortly after deposition. A Lower Cretaceous age is inferred on the basis of comparison with other South American Cretaceous palaeomagnetic results, and the probable rapid remanence acquisition.

3.4.5 The El Way Formation (ELW1,2,3)

The Hauterivian El Way Formation (Fig. 3.1), conformably overlies the Lombriz Formation, therefore, isolated magnetic components from these Formations should have similar orientations.

Two limestones (ELW2,3) and a calcareous sandstone (ELW1), were drilled in the field. Initial intensities of NRM varied considerably from 1.91(ELW2) to 157(ELW1)x$10^{-3}$$Am^{-1}$. Initial NRM directions are grouped predominantly in the NE quadrant with an upward inclination (Fig. 3.2d).

Examination of the normalised intensity decay curves, reveals similar behaviour for all three sites (Fig. 3.6a). They show a steady drop in intensity (75% is lost by 400 deg.C.) with a marked blocking temperature at 580 deg.C. for ELW1 and at 500-550 deg.C. for ELW2 and 3. Analysis of the stereographic projections allows a correlation with the decay curve observations. Specimens from all three sites have a stable normal component which only moves when the respective blocking temperature is reached (Fig. 3.6b). Inspection of the orthogonal Zijderveld diagrams reveals the same behaviour, straight one component

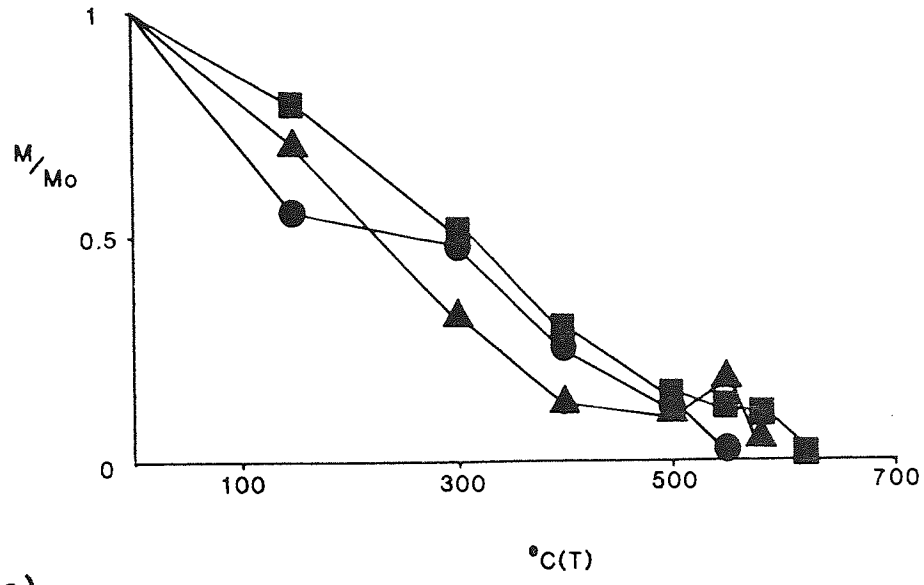

a)

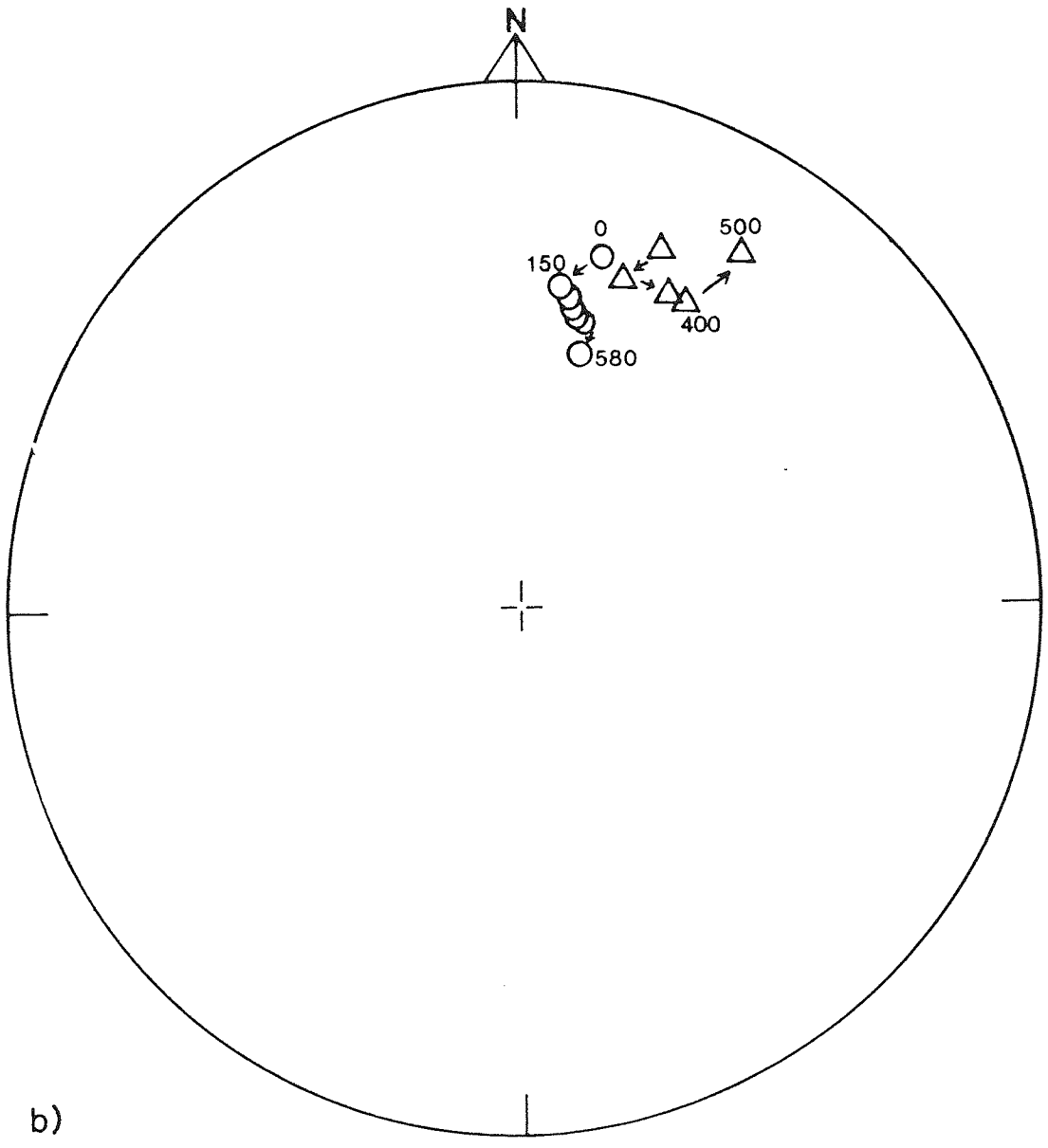

b)

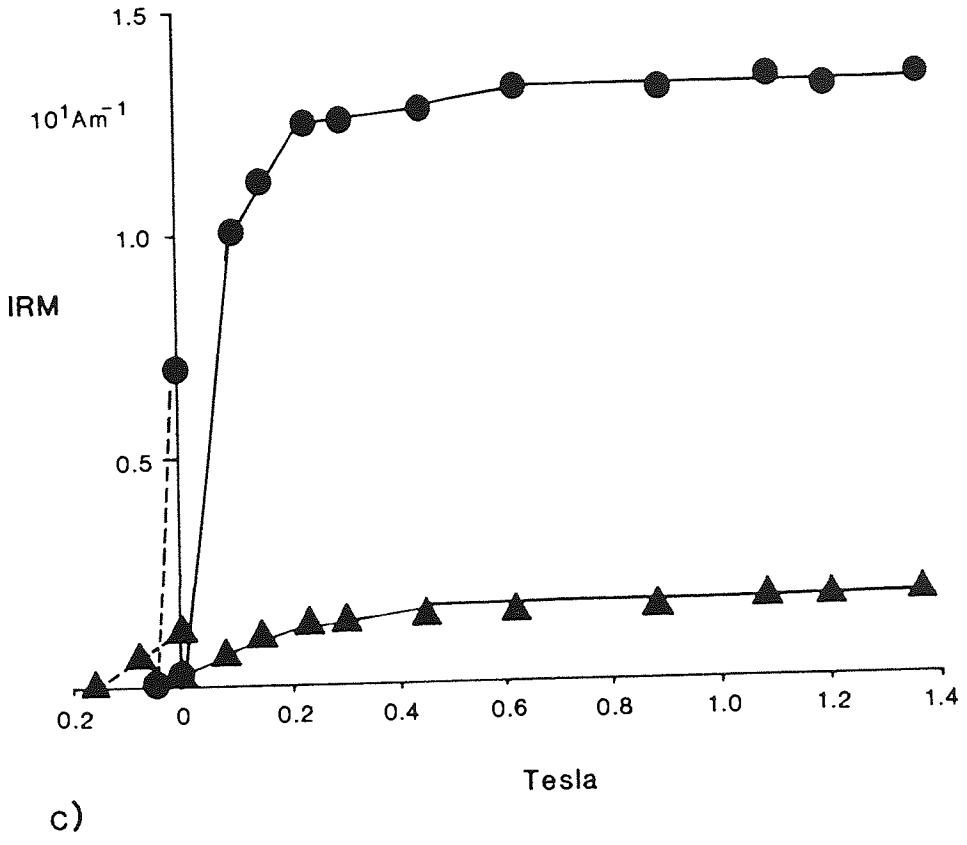

Fig. 3.6 Palaeomagnetic analysis of the El Way Formation, a) normalised intensity decay curves for ELW1.3■, ELW2.2● and ELW3.2▲, b) equal area stereographic projection of directional change for ELW1.5 ● and ELW2.2 ▲. c) IRM acquisition curves for ELW1● and ELW2▲. Other details as Fig 3.3.

demagnetization until the respective blocking temperature is reached. Components below the blocking temperature have a normal direction of magnetization.

Polished section microscopy and IRM acquisition curves (Fig. 3.6c), indicate that the magnetic carrier is detrital magnetite, with a larger amount in ELW1 (sandstone) than ELW2 and 3 (limestones), and is probably responsible for the large variation in the initial intensity of NRM between the sandstone and limestones.

Interpretation: The NRM of the El Way Formation was acquired during a period of normal polarity during the Hauterivian. Detrital magnetite, the principle magnetic carrier, imparted to the sediments a depositional remanent magnetization (DRM), or post depositional remanent magnetization (PDRM). The DRM/PDRM was not altered during diagenesis, as early calcite cementation (identified petrographically), would have prevented the oxidation of magnetite grains. Furthermore in these organic-rich sediments the interstitial conditions during early diagenesis can be expected to be reducing. The one stable component (Table 3.2) also indicates that the Formation has not been remagnetized.

3.5 Discussion

3.5.1 Age of Magnetization

Any discussion of the significance of palaeomagnetic results, is dependent on knowledge of the age of the magnetization of the sampled rocks.

Radiometric dates obtained from the Bolfin Complex range beween 206-134Ma. (Ferraris and Di Biase,1978; D. Rex, pers. comm.,1985; Damm et al.,1986). The majority of the dates fall between 158-150Ma. coincident with the radiometric age of the granodiorites (156-152Ma.; Halpern,1978; Damm et al.,1986), and other plutons of similar composition located further north in the Cordillera de la Costa (159-150Ma.; Ferraris and Di Biase,1978; Rogers, 1985). Damm et al. (1986), have also obtained a Lower Cambrian date (583+/-14Ma.), from the eastern edge of the Bolfin Complex (Fig. 4.8). It appears, therefore, that the radiometric age of the Bolfin Complex has been reset by the intrusion of the Mid-Upper Jurassic coastal batholith. This is consistent with petrographic evidence that indicates that the Bolfin Complex has been metamorphosed. Consequently, the Bolfin Complex is interpreted as having been remagnetized at this time, as the isolated normal components of the Complex and the granodiorites are virtually identical (Fig. 3.7). The high temperature reversed component present in the Bolfin Complex is probably pre-Jurassic in age, and has not been included in the calculation of a Mid-Upper Jurassic palaeomagnetic pole.

The La Negra Formation has been dated at 186+/-14Ma. (Rogers,1985). The history of magnetization of the Formation is complex, and it may not reflect an original Aalenian magnetization.

TABLE 3.3

UNIT	AGE	AGE OF MAGNETIZATION
Bolfin Complex	?Lower Cambrian	207-130Ma.
La Negra Formation	186-150Ma.	186-150Ma.
Granodiorites	159-150Ma.	159-150Ma.
Coloso/Lombriz Fms.	Lower Cretaceous	Lower Cretaceous
El Way Formation	Hauterivian	Hauterivian

Table 3.3 The age and probable age of magnetization of the units studied.

TABLE 3.4

UNIT	No (n)	R	K	CSD	α_{95}	DEC	INC	POLE (LAT. LONG)
GRANOD.	3 (15)	2.945	36.0	13.5	20.8	212	+28	59S. 189E.
BOLFIN C.	4 (22)	3.706	31.8	14.4	16.6	36	-27	55S. 191E.
LA NEGRA N	4 (19)	3.958	70.8	9.6	11.0	25	-33	66S. 190E.
LA NEGRA R	3 (14)	2.884	17.2	19.5	26.4	217	+50	57S. 220E.
COLOSO N	(17)	16.435	28.3	15.2	6.8	21	-36	70S. 192E.
COLOSO R	(9)	7.948	7.6	29.4	20.0	217	+31	55S. 195E.
EL WAY	3 (18)	2.983	117.1	7.5	11.4	20	-32	70S. 184E.
COMBINED	7	6.925	80.0	9.0	6.8			62S. 195E.

Table 3.4 Statistics for the isolated components from the units studied (Table 3.2), the Coloso Formation (Turner et al.,1984a) and palaeomagnetic pole. GRANOD.-Jurassic Granodiorite; COM-complex; N-Normal; R-Reversed. No=number of sites per unit. (n)=number of specimens per site. For explanation of other symbols used see Table 3.2.

The La Negra Formation may have been remagnetized during the emplacement of the Mid-Upper Jurassic coastal batholith. This is supported by the fact that there is little variation between the isolated magnetic components of the La Negra Formation, Bolfin Complex and the granodiorites (Fig. 3.7).

The age of the NRM of the Coloso and Lombriz Formations is less ambiguous. The Formations are Lower Cretaceous in age and the isolated magnetic components are thought to represent a rapidly acquired PDRM.

The NRM of the El Way Formation is considered to be a DRM/PDRM and virtually contemporaneous with deposition and cementation; representative of an Hauterivian magnetic field.

Although Cretaceous plutonic activity is recorded from the Cordillera de la Costa, none has been recorded from the Coloso area. Despite the fact that CDG3 and 9 have been altered after intrusion, the isolated components are not significantly different from the other Granodiorite results. Alteration was therefore relatively soon after intrusion. Both CDG3 and 9 show evidence of copper mineralization and could therefore be associated with the local mineralization present in the Coloso Formation, described by Espinoza (1983) and Flint et al. (1986b). See Table 3.3 for a summary of the age of the rocks studied and their probable age of magnetization.

3.5.2 Implications of the Palaeomagnetic Results

The similarity of isolated magnetic components (Tables 3.2,3.4) between rocks ranging from Lower Jurassic to Hauterivian in age (Fig. 3.7), indicates that the Cordillera de la Costa (Coloso area) acted as a discrete structural block, assuming no later remagnetization.

Figure 3.8 shows the position of the palaeomagnetic pole for the

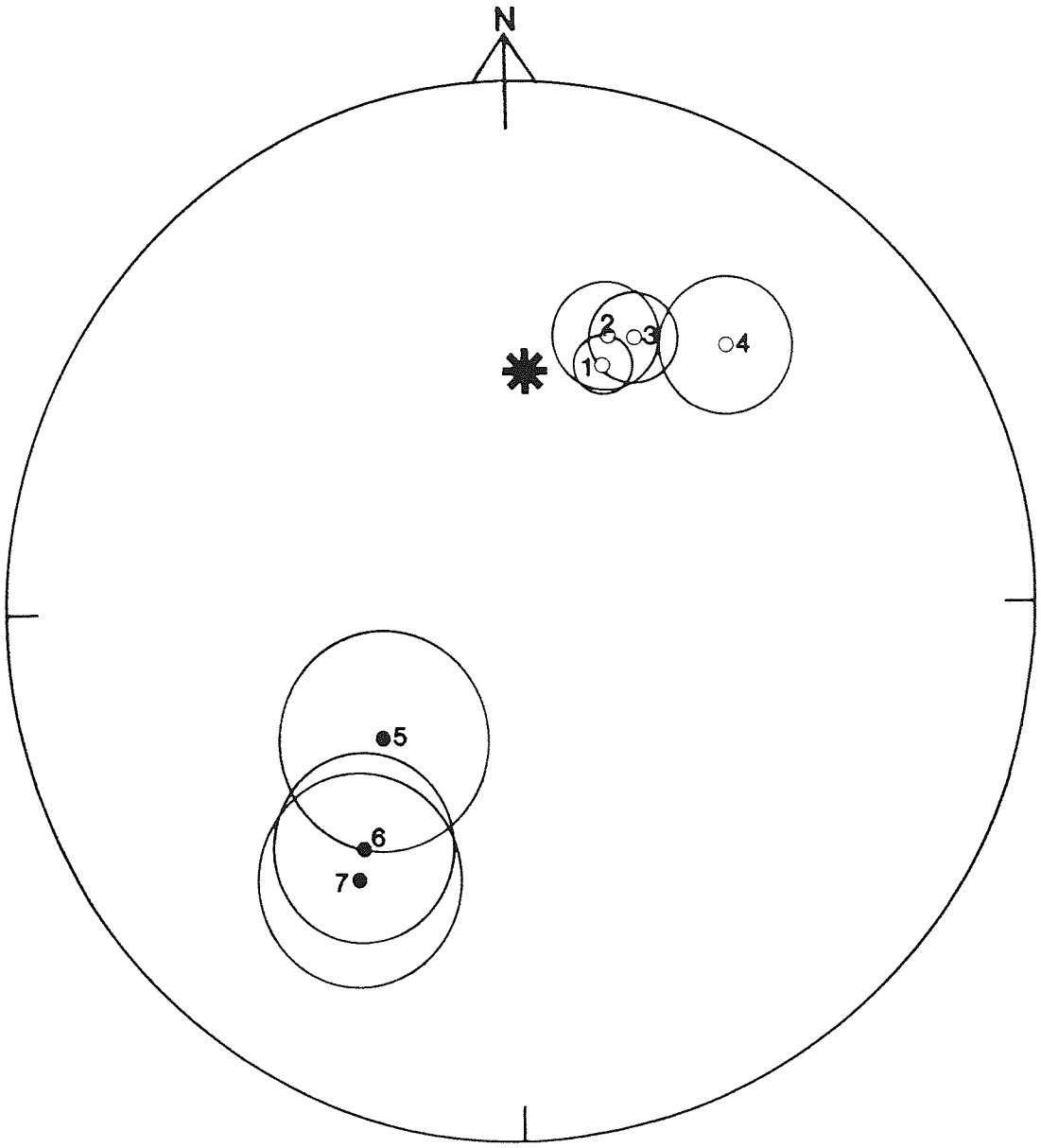

Fig. 3.7 Equal angle stereographic projection of extracted components from the Cordillera de la Costa (Coloso area), taken from Table 3.3. 1=Coloso Formation (normal), 2=El Way Formation, 3=La Negra Formation (normal) 4=Bolfin Complex, 5=La Negra Formation (reversed), 6=Jurassic granodiorite plutons and 7=Coloso Formation (reversed). Other details as Fig. 3.2.

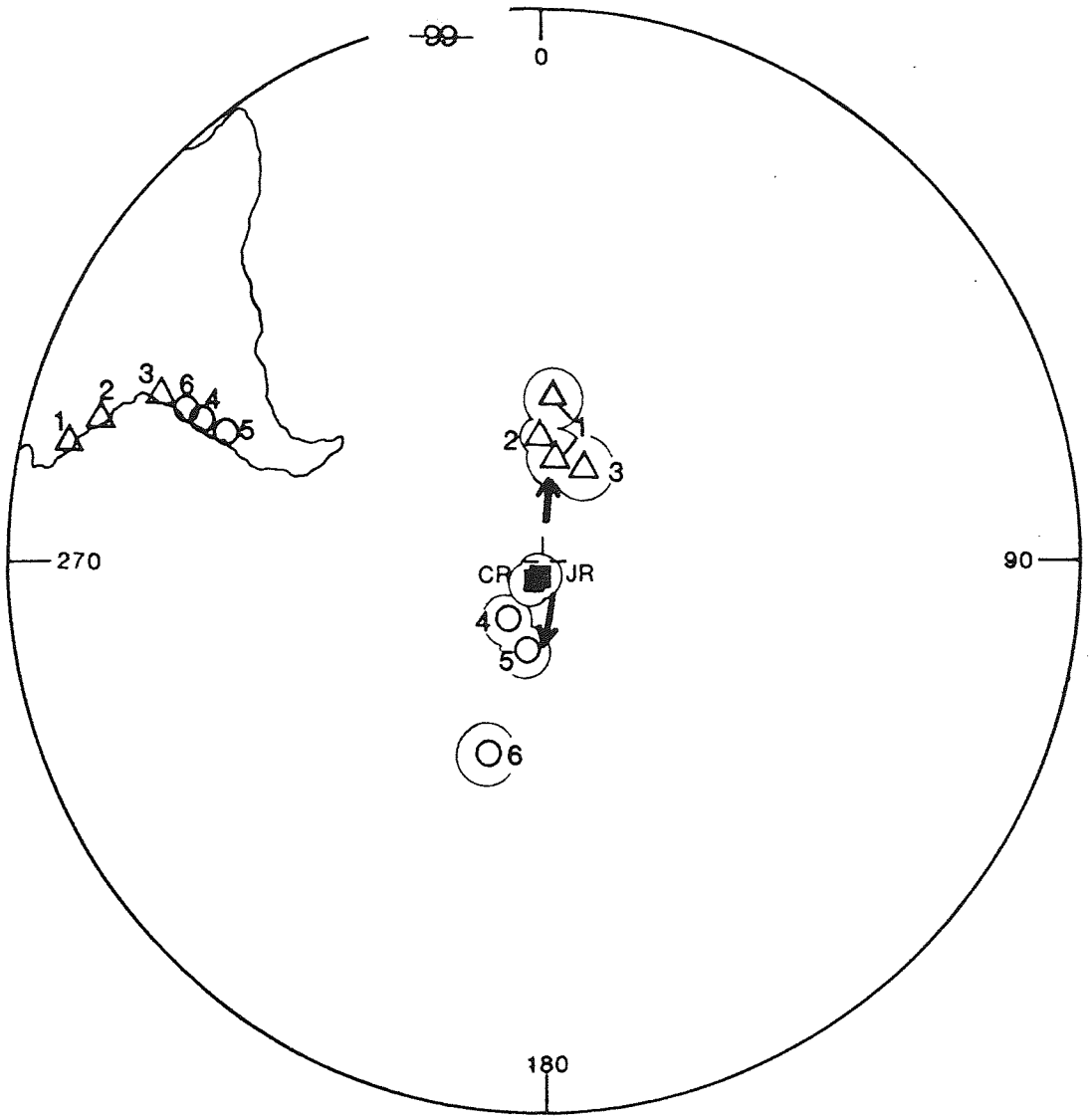

Fig. 3.8 Equal area stereographic projection of Mesozoic palaeomagnetic poles derived from the Andean forearc, compared to the Upper Jurassic (JR) and Mid Early-Mid Late Cretaceous (CR) reference poles derived from the stable shield area of South America (Appendix A), with 95% error limits. Triangles show poles rotated anticlockwise, circles show poles rotated clockwise with respect to the reference poles as viewed from South America. 1=Cretaceous coastal volcanics. Central Peru (Heki et al.,1984), 2=Cretaceous Puente Piedra Formation, Central Peru (May and Butler,1985), 3=Jurassic Camaraca Formation, northern Chile (Palmer et al.,1980b), 4=Cretaceous sediments and volcanics from the La Serena area, Central Chile (Palmer et al.,1980a), Cretaceous tuffs, Central Chile (Beck et al.,1986), and 6=Cordillera de la Costa, northern Chile (this study). Numbers also show the location of the sampled areas. Arrows indicate the sense of rotation.

Cordillera de la Costa (60°S. 192°E), with respect to the Upper Jurassic palaeomagnetic pole derived from the stable shield area of South America (89°S. 217°E.; see Appendix A, for reference pole derivation). The pole for the Cordillera de la Costa was computed using the combined poles from the units studied (Table 3.4), together with those from the Coloso Formation (Turner et al.,1984a). Figure 3.8 clearly shows that substantial clockwise rotation of the Cordillera de la Costa has taken place (approximately 29+/-11 degrees of rotation, Table 3.5). This rotation must be post-Hauterivian in age.

Other Chilean palaeomagnetic data also indicate substantial clockwise rotation of the Andean forearc. Palmer et al. (1980a), identified 15 degrees of clockwise rotation from the La Serena area, and Beck et al. (1986), found 14 degrees of clockwise rotation from the Santiago area. North of 18°45'S, 70°3'W. however, anticlockwise rotation of Mesozoic rocks in the Andean forearc has been identified; from the extreme north of Chile (Palmer et al.,1980b), and southern and central Peru (Heki et al.,1983,1984; May and Butler,1985).

Rotation of the Andean forearc has been identified between 7 and 34°30'S. A change in the angle of rotation takes place at approximately 18°45'S., with anticlockwise rotation north of and including this point, and clockwise rotation south of it. Figure 3.8 summarises all rotational palaeomagnetic data from the Andean forearc.

Age of Rotation: The post-Hauterivian rotation of the forearc must be examined within a tectonic context. Major deformation took place in the Central Andes during the ?mid-Cretaceous, mid-Eocene, mid-Miocene and mid-Pliocene (Table 2.1). Deformation in the Cordillera de la Costa is minor, and post-Cretaceous deformation in

TABLE 3.5

LAT.	LONG.	α_{95}	PALAEOPOLE	dp	dm	ROTATION
23.7S.	70.5W.	6.8	62S. 195E.	6.5	8.9	29+/-11

Table 3.5 Amount of rotation undergone by the Cordillera de la Costa (Coloso area) with respect to the stable shield area of South America (see Fig. 3.14 and Appendix A). dm=the radius of the ellipse of 95% confidence along the direction of the magnetic meridian from the site to the vertical pole. dp=the radius of the ellipse of 95% confidence at the pole perpendicular to the meridian.

Angular amounts of rotation as presented in this thesis have been calculated as follows:

1) The palaeomagnetic pole for northern Chile together with an equivalently aged reference pole from the stable shield area of South America (Appendix A) were plotted on an equal area stereographic projection of the southern hemisphere (Fig. 3.8).

2) The 95% significance error limits were plotted around the respective poles (Fig. 3.8).

3) The difference between the poles was then measured visually, along a great circle, to give the amount of rotation.

4) A +/- error was then measured visually as the angular distance covered by the respective 95% confidence limits along the great circle used for the rotation calculation (above).

Cordillera de la Costa is minor, and post-Cretaceous deformation in northern Chile is concentrated in the Precordillera and Altiplano/Puna (Jordan and Alonso,1987). Cenozoic deformation appears to have been much greater in southern Peru (Noble et al.,1974,1979; Tosdal et al.,1984; Megard et al.,1984,1985) although present in northern Chile (Jordan and Alonso, 1987). Consequently, the clockwise rotation of the Cordillera de la Costa could be associated with the major mid-Cretaceous deformation event. However, there is little evidence for this event in the Cordillera de la Costa, as the Coloso basin sediments were only mildly deformed prior to Tertiary sedimentation.

Method of Rotation: Most theories regarding rotation of the Andean forearc, agree that rotation has probably resulted from the "in situ" movement of discrete crustal blocks. Whatever the dominant stress regime (discussed below), the "in situ" rotation of discrete crustal blocks could be accomodated by the distributed deformation model of McKenzie and Jackson (1986), where "en echelon" faulting with a small strike-slip component accounts for block rotation (Fig. 3.9). It is interesting to note that this predicted fault pattern has been mapped in the Cordillera de la Costa, Antofagasta region (Fig. 3.1). A similar pattern of faulting and block rotation has been identified in oceanic (Cowan et al.,1986), and continental plates (Ron et al.,1984), within a predominantly compressive tectonic regime, with extensive strike-slip faulting. This is the first study of such a phenomenon from a convergent plate boundary, not dominated by strike-slip faulting.

It should also be noted that the uniformity of direction and degree of rotation precludes small-scale/local tectonic events as a

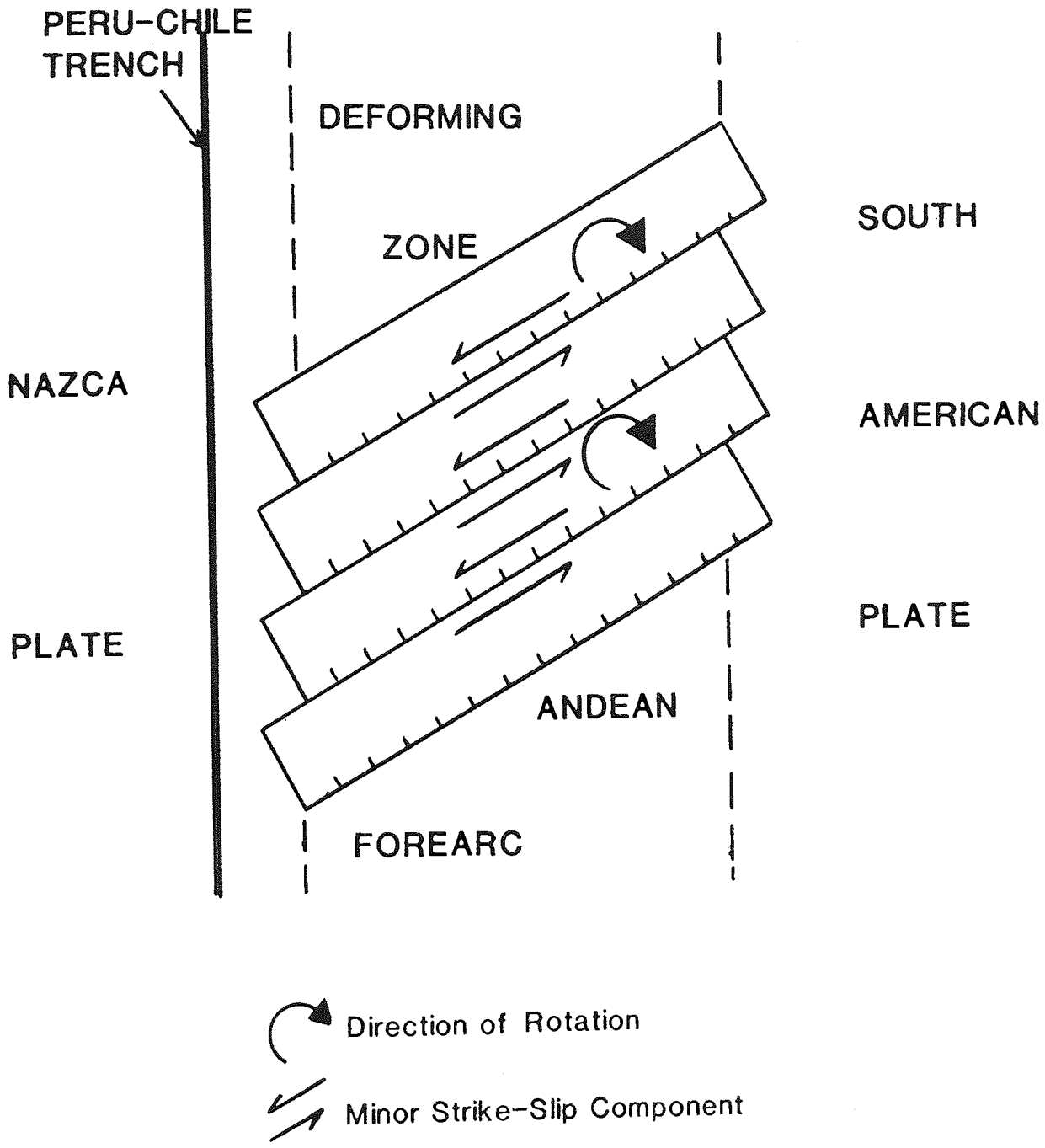

Fig. 3.9 Envisaged model for Andean forearc rotation (after Jackson and McKenzie,1986), resulting in NE-SW oriented faults with a small strike-slip component. The rotation mechanism is discussed in the text.

cause of rotation. However, the exact method of Andean forearc rotation is uncertain, and any theory must take into account: 1) The difference in palaeomagnetically identified rotation between north and central Chile (clockwise rotation), and south and central Peru (anticlockwise rotation), and 2) The extent of rotation in the Andean forearc; as rotation has been identified from rocks 200km. inland of the Pacific coast (Beck et al.,1986; Chapter 5).

Mechanism of rotation: The Andean margin has traditionally been regarded as compressional in nature (Coira et al.,1982; Damm et al.,1986; Dalziel,1986). Although there is no doubt that the eastern foreland of the Cordillera de los Andes is currently under a compressional tectonic regime, as demonstrated by the well known sub-Andean thrust zone (Allmendinger et al.,1983; Jordan et al.,1983 Jordan and Alonso,1987), the westwards extension of this compressional zone into the forearc has not been proven.

Any model attempting to define the stress regime in the Andean forearc must take into account the prevalence of normal faulting in the Cordillera de la Costa, the formation of sedimentary basins (the Coloso basin, Central Depression), and the presence of Palaeocene volcanoes (Ferraris and Di Biase,1978) 100km. east of the trench.

Rotation in the Andean forearc must be related to the dominant stress regime which is determined by the interaction of the oceanic and continental plates at the subduction zone of a convergent plate margin. The following section will attempt to identify the parameters which affect the stress regime in the Andean forearc, this should enable the determination of a possible mechanism for rotation. The main parameters include:

1) Subduction roll back. The oceanward movement of the hinge of the oceanic plate (Molnar and Atwater,1978), created through the gravitational pull on the sinking ocean slab, and consequently, dependent on the buoyancy of the slab. Roll back is the sum of the absolute motion of the overriding plate and the amount of back-arc spreading in the plate (Jarrard,1986).

2) Slab pull force (trench suction). The force created through the sinking of the oceanic slab at the subduction zone. The sinking slab exerts a pull on the overriding plate, causing tension in the plate due to the negative buoyancy of the slab (Bott,1982). The slab pull force is a function of the convergence rates at the plate boundary, the age of the subducting slab and slab dip (England and Wortel,1980).

3) Absolute motion (plate motion relative to a non plate reference point)-the absolute motion of the continental plate, determined using some form of inert or slowly moving asthenosphere as a reference point (Dewey,1980), and resulting from ridge push (the force produced from the creation of new lithosphere at mid-oceanic ridges; Bott,1982).

The subduction process involves a complex interplay of forces, and although the above parameters are thought to best describe the Andean forearc, the influence of asthenospheric flow and the effects of friction between the oceanic and continental plates cannot be discounted. Also, the relative influence and interaction of the above parameters is difficult to determine.

Subduction roll back is currently active in northern Chile (Jarrard,1986). This confirms the observations of Mendiguren and Richter (1978), who suggested that the absence of tensional earthquake focal mechanisms in the Nazca Plate near the trench, implied that the

gravitational sinking of the oceanic plate was compensated for through local forces, ie subduction roll back. Roll back in northern Chile is thought to be equivalent to the absolute motion of the overriding plate (Jarrard,1986), this indicates that the South American plate is currently moving oceanwards. The interaction between roll back and absolute motion of the South American plate should determine the morphology of the Peru-Chile trench, and the thickness of adjacent oceanic crust. Hayes (1966), found pronounced thinning of the oceanic crust immediately to the west of the Peru-Chile trench. This observation implies that roll back is more rapid than the absolute motion of the South American plate, as, if roll back was less than the absolute motion of the South American plate, the oceanic crust should be thickened in the area to the west of the trench, not thinned.

The direction of roll back is related to the sinking oceanic slab. Assuming that the oceanic slab sinks relatively uniformly along its length, it will result in a direction of roll back directly opposite to the direction of movement of the oceanic plate.

The slab pull force currently acting on the South American plate in northern Chile is considerable, and eqivalent to areas in the western Pacific, where extension has resulted in back-arc spreading (for example, New Britain; Jarrard,1986). A combination of slab pull and roll back, will result in the South American plate being placed under a considerable amount of extensional stress. This is consistent with the work of England and Wortel (1980), who predicted an extensional regime for the Andean forearc using convergence rate, age of subducted lithosphere, dip of the angle of the Benioff zone and descent velocity as parameters.

The vectors of absolute motion for the South American plate (Chase,1978; Minster and Jordan,1978), are slightly oblique to the direction of roll back and associated slab pull (assuming the direction of roll back is directly opposite to the direction of subduction of the Nazca plate). Consequently, the South American plate is subject to an extensional stress regime, applied at an angle to the direction of absolute motion of South America. This could be accommodated through the rotation of discrete crustal blocks in the Andean forearc (Fig. 3.10).

This theory would account for the the extensional normal faulting seen in the Cordillera de la Costa, the formation of extensive sedimentary basins (the Coloso basin and the Central Depression), and provide a conduit for Pleistocene volcanoes located 100km. inland of the trench.

The interaction between extension created through roll back, slab pull and absolute motion of the overriding plate, should be manifested in the direction of longitudinal trench slope. It is interesting to note that a northerly direction of longitudinal slope for the trench is inferred for Chile between 18 and 45°S., and that between 4 and 18° S. the longitudinal slope of the trench changes to a southerly direction (Dewey,1980). If the longitudinal slope of the trench can be taken as a valid pointer to the direction of extension along the Andean margin, the resulting interaction between slab pull, roll-back and the overriding South American plate would produce clockwise rotation of the Andean forearc between 18 and 45°S., and anticlockwise rotation between 4 and 18°S.

It follows from the above argument that extension and associated rotation should be dependent on the angle of subduction of the oceanic

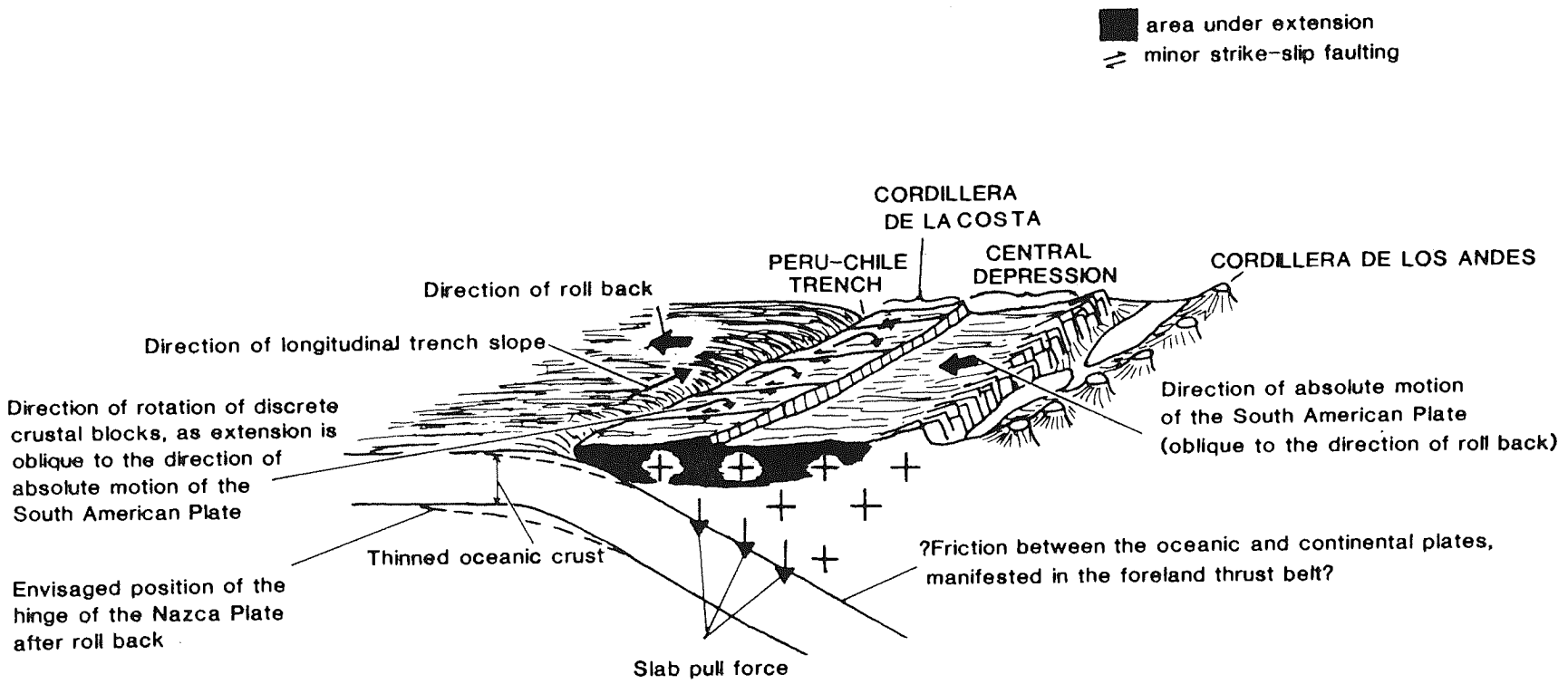

Fig. 3.10 Schematic diagram of the Andean forearc, showing the effects and processes resulting from the extension of the South American plate at an oblique angle to its direction of absolute motion.

plate. ie. the steeper the slab dip, the more influence slab pull and subduction roll-back have over the edge of the continental plate, this would be reflected in a larger extensional stress regime inland of the plate junction, as opposed to areas overlying shallower dipping slabs. It is interesting to note that Mercier (1981) working in Peru, found a correlation between the stress regime and angle of subduction zone. In northern Peru which overlies a shallow dipping slab, a compressional regime is currently active, in Central and Southern Peru (overlying the same steeply dipping subduction zone as northern Chile), an extensional regime is currently active. As it is probable that rotation is related to extension, it follows that a larger amount of rotation should take place in areas overlying steep subduction zones than in areas overlying shallow ones. No apparent correlation has yet emerged between the angle of subduction and the amount of palaeomagnetically identified forearc rotation. Rotation takes place over both shallow and steeply dipping subduction zones, and both clockwise (Turner et al.,1984a) and anticlockwise (Palmer et al.,1980a), rotation occurs within an area of the forearc overlying a steeply dipping subduction zone. It should also follow, that areas overlying shallow dipping slabs show limited evidence of rotation, but, rotation has been recorded up to 200km. inland, from Central Chile (Beck et al.,1986).

For the envisaged tectonic regime presented above to be applicable to northern Chile, a small amount of oblique stress is required in the forearc, due to the oblique angle of extension (Fig. 3.9). However, a large angle of oblique subduction would result in a significant amount of strike-slip faulting. A method favoured by Beck (1985), who accounted for the "in situ" rotation of discrete crustal blocks through shearing, created by subduction against a buttress

located near Arica. Beck postulated that north of the buttress sinistral shearing predominated and was associated with anticlockwise rotation, whilst south of the buttress clockwise rotation could be explained by dexteral shear.

However, evidence for extensive strike-slip movement in the Andean forearc is absent. Studies by Arabasz (1968,1970), Okada (1971) and Ulriksen (1979), on the major Atacama fault zone found only a minor strike-slip component. This is in contrast to the western margin of North America where subduction is at an oblique angle to the continental plate, a situation ideal for significant amounts of strike-slip displacement.

From the above discussion, it appears that an extensional tectonic regime would best explain the observed geological phenomena of the Andean forearc, and that rotation is, therefore, not related to compression. However, this does not discount the possibility that the Andean Orogen is subjected to an overall compressional tectonic regime. The prevailing stress regime is probably a matter of scale, with extension dominant in the forearc of the Andes, whilst an overall compressive regime is manifested in the foreland thrust belt of Argentina and Bolivia.

CHAPTER 4

THE MEJILLONES PENINSULA, NORTHERN CHILE: GEOLOGICAL AND PALAEOMAGNETIC EVIDENCE FOR AN ACCRETED TERRANE

4.1 Introduction

The recent confirmation of the role of accreted terranes in the orogenesis of the North American Cordillera (Coney et al.,1980; Beck,1980; May et al.,1983; Jones et al.,1986), has led to interest in possible "suspect" terranes emplaced in the Andean forearc and, if present, their influence on Andean orogenesis.

Recent work has confirmed the presence of accreted terranes in the Colombian Andes (McCourt et al.,1984; McGeary and Ben-Avraham,1985), northwestern Peru and Ecuador (Feininger,1986), and the possibility of accreted Palaeozoic terranes in the Central Andes (29-33 S.), has been postulated by Ramos et al.(1986).

Speculation regarding the origin of the Mejillones Peninsula, northern Chile (Miller,1970; Howell et al.,1985; Ramos et al.,1986; Breitkreuz,1986; Damm et al.,1986), has led to the emergence of two main theories:

1) That the Mejillones Peninsula forms part of the South American Precambrian Basement, as either a southerly extension of the Arequipa Massif or a westerly extension of the Argentinian Basement (see section 2.2),

or 2) that the Peninsula is a "suspect" terrane.

Firm evidence in support of either theory has yet to emerge.

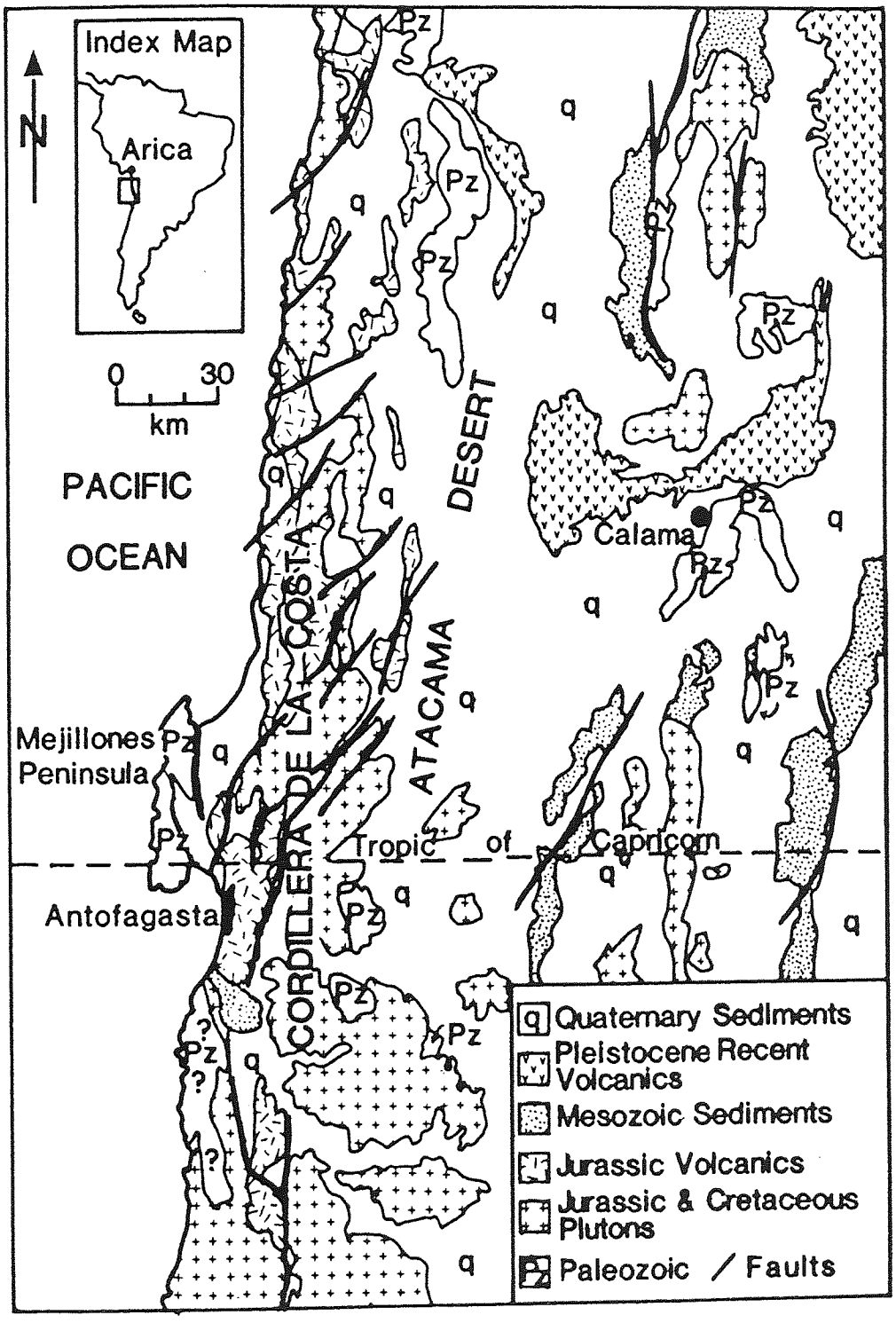

Fig. 4.1 Location map showing the position of the Mejillones Peninsula and Arequipa.

Using palaeomagnetism, petrology, radiometric dating and familiarity with the regional geology, it is hoped herein to prove that the Mejillones Peninsula forms part of an accreted terrane. The relationship of the Peninsula to the Cordillera de la Costa, particularly the Bolfin Complex (Fig. 4.1), will also be investigated.

4.2 Geology

The Mejillones Peninsula (Fig. 4.1) situated on the Tropic of Capricorn, forms a prominent topographic feature of the North Chilean coastline, 60km. long, 20km. wide and up to 1km. high.

The Peninsula comprises igneous and metamorphosed igneous (and ?sedimentary) rocks of probable oceanic crustal origin (section 4.5). The geology, geochemistry and geochronology of the area have been described by Baeza and Venegas (1984,1985) and Damm et al. (1986). The rocks are exposed in three fault-bounded blocks trending NW-SE. The blocks are separated by marine and continental sandstones and gravels ranging from Upper Tertiary to Quaternary in age (Figs. 4.1,4.2). The outcrop distribution allows the partitioning of the Peninsula into northern, central and southern parts. The Peninsula is separated from the Chilean mainland by an extension of the Atacama fault zone.

Geochronological data allows the division of the Peninsula into two areas: 1) The northern and central parts comprising rocks yielding Cambrian radiometric dates (534-521Ma.; Damm et al.,1986), and 2) The southern part which yields radiometric dates ranging from 297-126Ma. (Damm et al.,1986; D. Rex, pers. comm.1985). The range in radiometric

Plate 4.1 MEJ3 Metamorphic texture. Porphyroblastic horneblende completely encloses altered biotite mica (BM), and altered plagioclase feldspar (P). The biotite mica has been altered to chlorite (light grey), haematite (opaque) and replaced by quartz (Q). The plagioclase feldspar is altering to clay minerals (?sericite) along its cleavage planes. The other opaque minerals are magnetite and ilmenite. Hornblende is characteristically intergrown with rounded quartz crystals (top right, bottom left). A texture thought to be characteristic of recrystallisation. Transmitted light, field of view=3.4mm.

Plate 4.2 MEJ12 Alteration. The opaque mineral is magnetite, which appears to be associated with biotite mica (BM). The magnetite crystal at the top of the photomicrograph is altering to chlorite. Biotite mica crystals (bottom left, middle right), show no evidence of alteration, which probably indicates that they formed after a metamorphic event. The small oriented crystals of magnetite (bottom right, running diagonally from top right to bottom left), are forming at the expense of pyroxene, which is also being altered to chlorite. The light mineral (P), is plagioclase feldspar, which shows some evidence of alteration to clay minerals. Transmitted light, field of view=3.4mm.

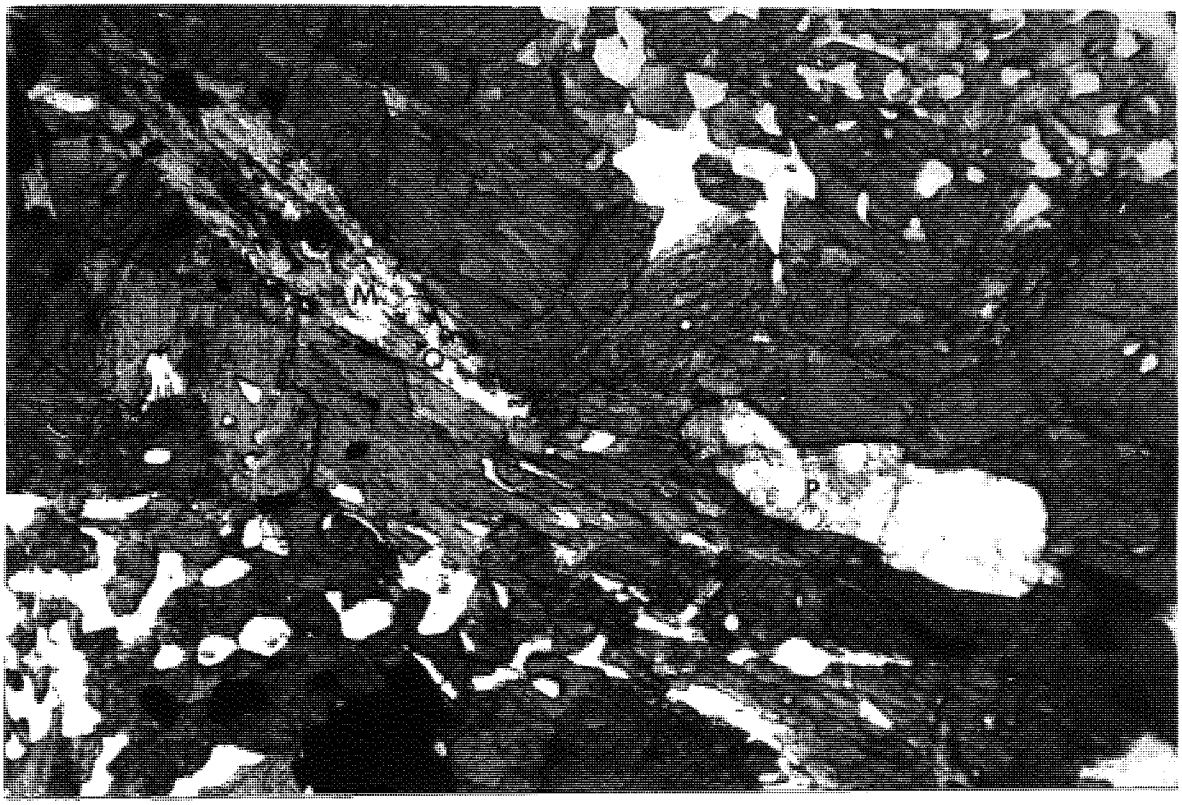
M
P

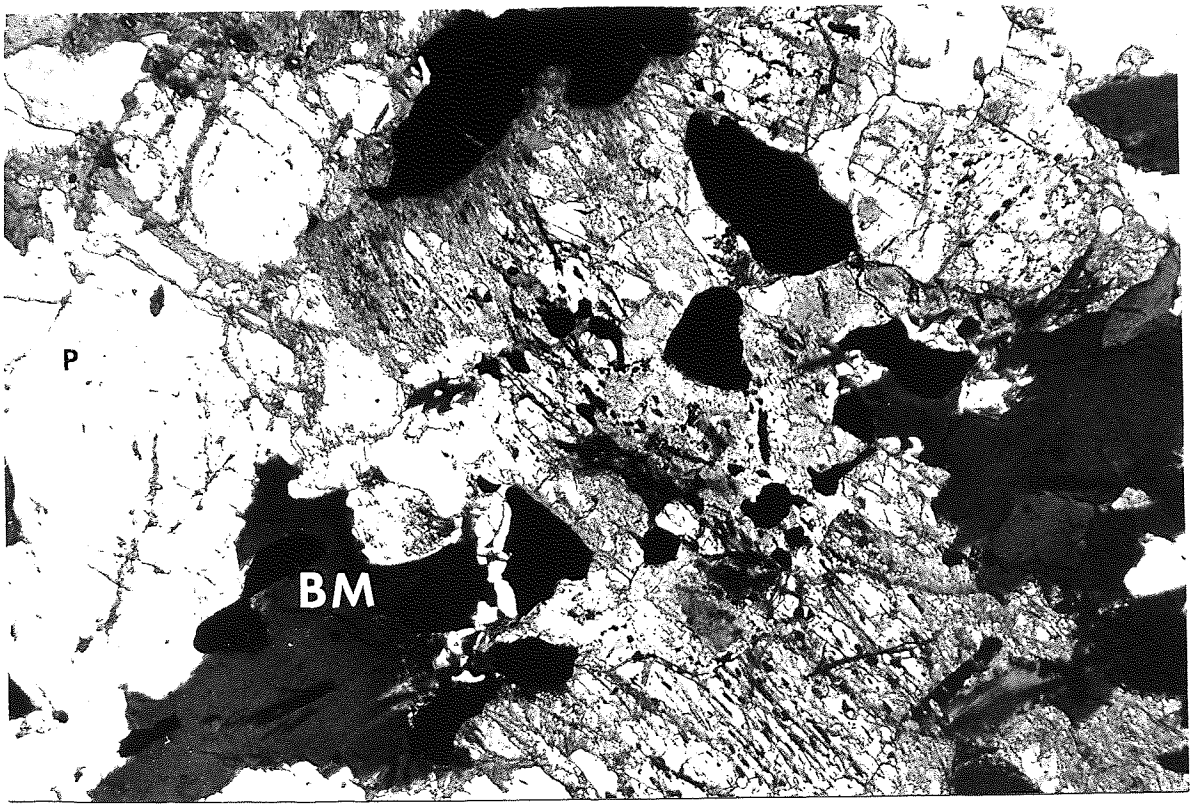
P
BM

dates within the southern area is probably the result of a metamorphic event, which may have reset the original radiometric age of the rocks. Petrographic work indicates the presence of granoblastic and porphyroblastic textures indicative of recrystallisation, as well as the growth of new minerals (hornblende, ilmenite, magnetite, quartz, chlorite, biotite with occasional calcite and pyrite), and alteration of primary minerals, particularly feldspar biotite mica and pyroxene (Plates 4.1,4.2). The above petrographic observations were undertaken on rocks which have been mapped as separate lithologies (Baeza and Venegas,1984; Damm et al.,1986). It appears however, that the variation in both lithology and range of radiometric dates is due to varying degrees of metamorphism; rocks of originally gabbroic composition have been metamorphosed, producing different lithologies and radiometric dates. This dominantly gabbroic-amphibolitic area will be referred to as the Moreno Complex (Fig. 4.2). The variation in lithology, metamorphism and geochronology, has important implications for the magnetic history of the Moreno Complex.

The southern part of the Peninsula has been tilted approximately 30 degrees southwestwards since the Lower Cretaceous, recorded by the presence of an outlier of the Coloso Formation on the southeastern tip of the Peninsula (Fig. 4.2).

4.3 Sampling and Laboratory Methods

Block and drilled samples oriented in the field were collected from the central and southern parts of the Peninsula (Fig. 4.2), the northern part is a military zone with limited access. Samples were

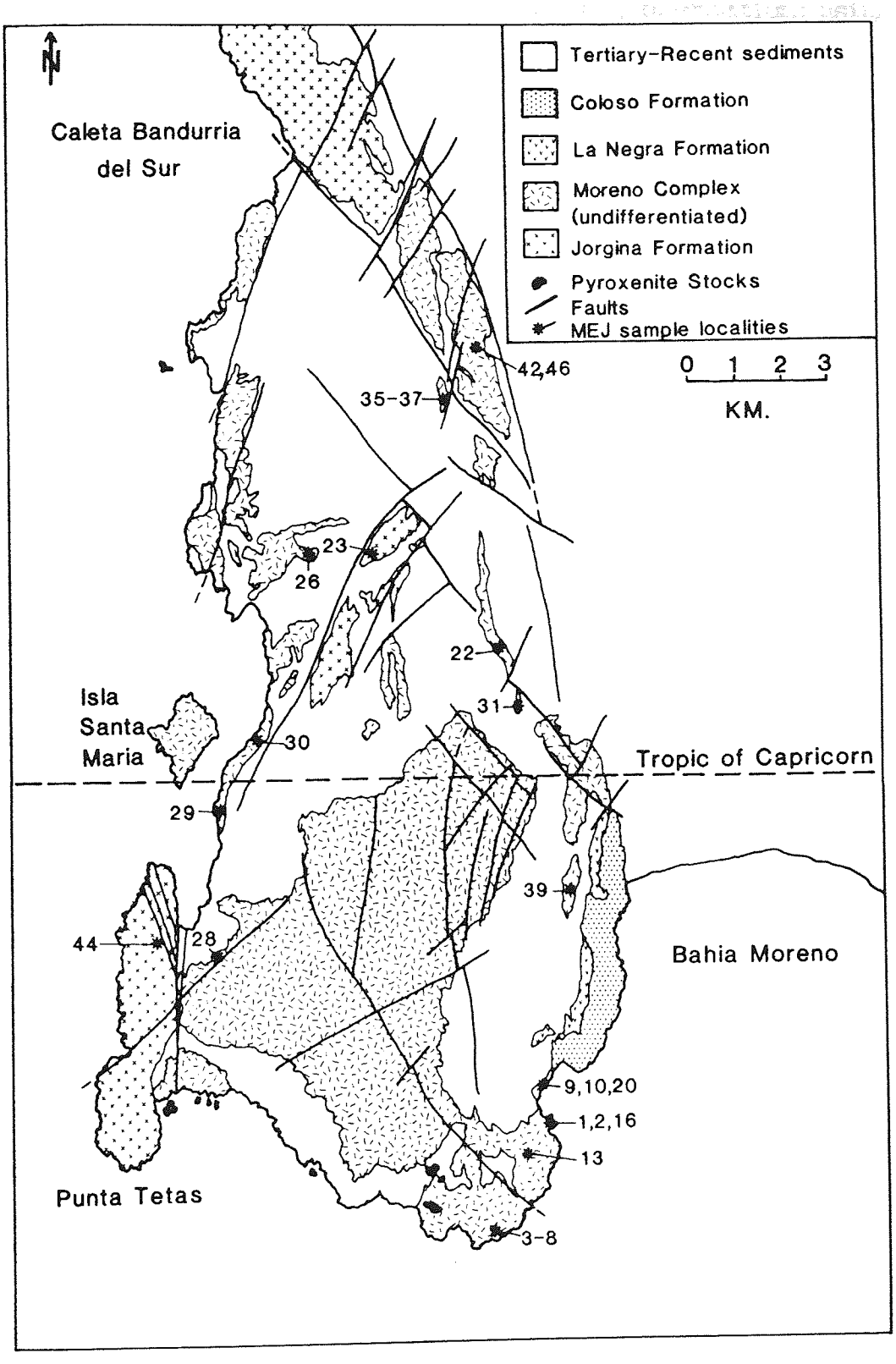

Fig. 4.2 Geological map of the southern half of the Mejillones Peninsula (after Baeza and Venegas,1985; Buchelt and Zeil,1986), with palaeomagnetic sampling localities.

orientated using both magnetic and sun compasses, orientations using both techniques agreed to within 3 degrees.

The samples were prepared, demagnetized and analysed using the techniques described in section 3.3, with the addition of the alternating field (AF) demagnetization technique. AF demagnetization was carried out in steps of 5 or 10mT. up to a peak field of 100mT., using a two axis reciprocating tumbler and a digitally controlled AF demagnetizer as described by Widdowson and de Sa (1975).

All the results have been corrected for the tectonic dip of the overlying Coloso Formation, which is in agreement with the regional tectonic tilt encountered on the Chilean mainland. A palaeomagnetic fold test (McFadden and Jones,1981), was applied to all sites, but proved inconclusive (see Table 4.1).

No lithological grouping of sites was possible, as the lithological subdivision of the southern and central parts of the Peninsula is not considered valid (as outlined in section 4.2), with the exception of the Jorgina Formation (Fig. 4.2)

4.4 Palaeomagnetic Results

Initial sample measurement (27 sites, n=130), revealed large variations in both initial intensity values and directions of NRM. Initial intensities varied between 0.08 and 1115.2x$10^{-3}$$Am^{-1}$. NRM directions show a wide degree of scatter (Fig. 4.3). The palaeomagnetic results will be described using the 4 analytical techniques outlined in section 3.3 (with the exception of site MEJ3, which proved unstable during demagnetization), together with a

Fig. 4.3 Equal angle stereographic projection of initial NRM directions for the Mejillones Peninsula, a) fiducially and b) fiducially and structurally corrected. Open symbols=upward inclination, closed symbols=downward inclination.

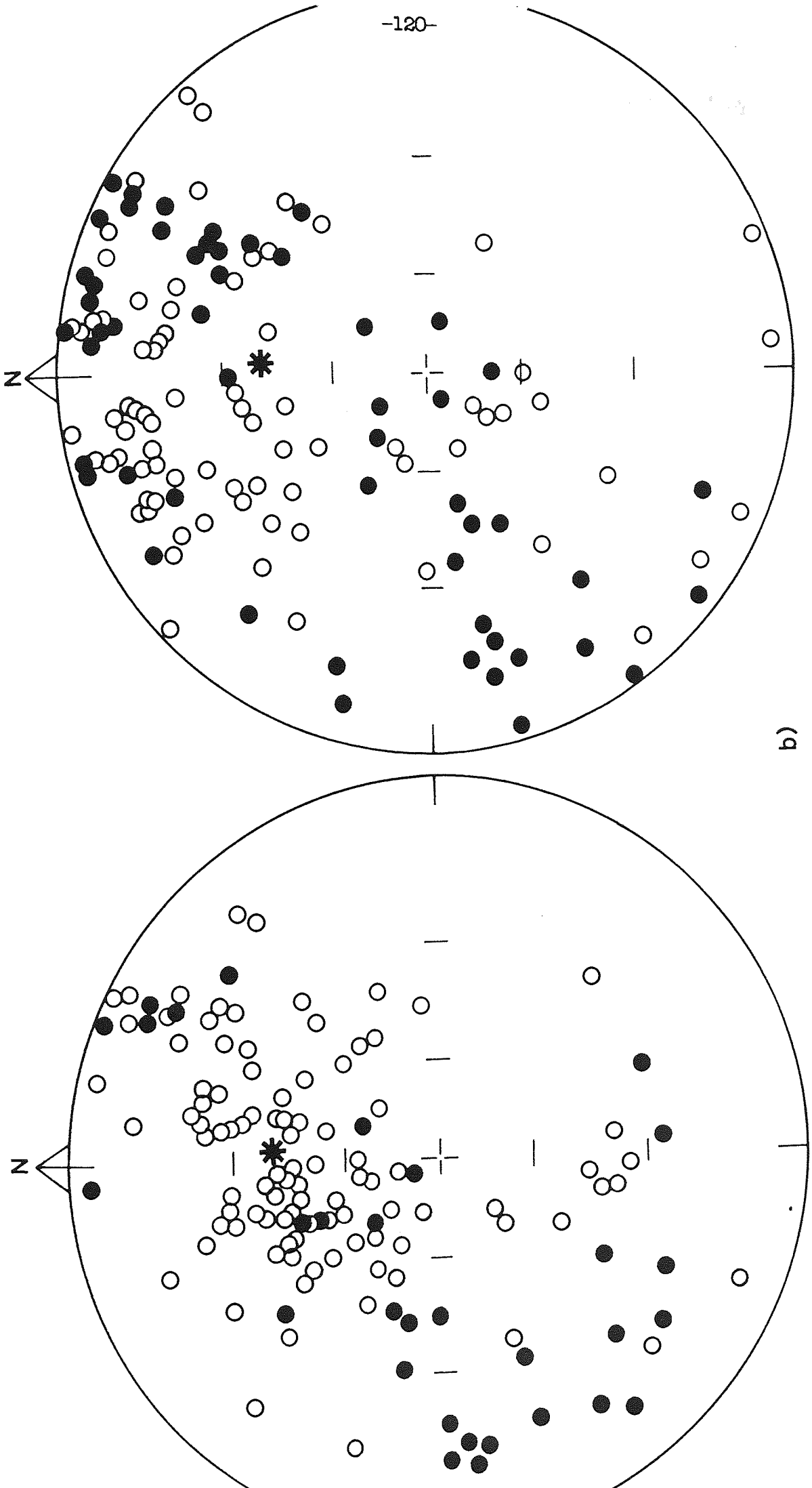

b)

description of the magnetic mineralogy of all sites, determined by reflected light microscopy and IRM acquisition curves.

Normalised Intensity Decay Curves:

Examination of the normalised intensity decay curves for individual sites, reveals a wide variety of behaviour during demagnetization. Thermally demagnetized specimens display three main types of behaviour (Fig. 4.4). In both Figures 4.4a and 4.4b, the specimens are characterised by a marked blocking temperature at 550 deg.C., a rapid intensity increase present in Figure 4.4a at 580 deg.C., is absent in Figure 4.4b. This blocking temperature spectrum corresponds to the removal of a component carried by magnetite at 580 deg.C. Above 580 deg.C. the presence of a haematite carrying component is indicated in Figure 4.4a by a rapid intensity increase, but absent in the specimens illustrated in Figure 4.4b. Figure 4.4c features the other type of intensity decay curve commonly seen in the samples, this is characterised by a steady decrease in intensity up to 550 deg.C., where a small but marked blocking temperature is present, all remaining NRM is gradually lost up to 680 deg.C. The behaviour displayed in Figure 4.4c, implies that both magnetite and haematite bearing components are present, but show a small degree of overlap as the blocking temperature is much less marked than the other illustrated intensity decay curves, although haematite is still present above 580 deg.C.

Specimens subjected to AF demagnetization showed a very rapid initial loss in NRM up to 10mT. (Fig. 4.4d), with a median destructive field of about 7-12mT. Above 10mT. the intensity of NRM gradually decreases up to the peak field of 100mT.

Fig. 4.4 Shows the variation in normalised intensity decay curves for thermally demagnetized samples from the Mejillones Peninsula: a) MEJ16.1● and MEJ29.1A▲, b) MEJ31.3●, MEJ36.4▲ and MEJ42.6■, c) MEJ8.1A▲, MEJ13.1● and MEJ20.3A■, and AF demagnetized samples: d) MEJ1.4●, MEJ6.3▲ and MEJ10.2A■.

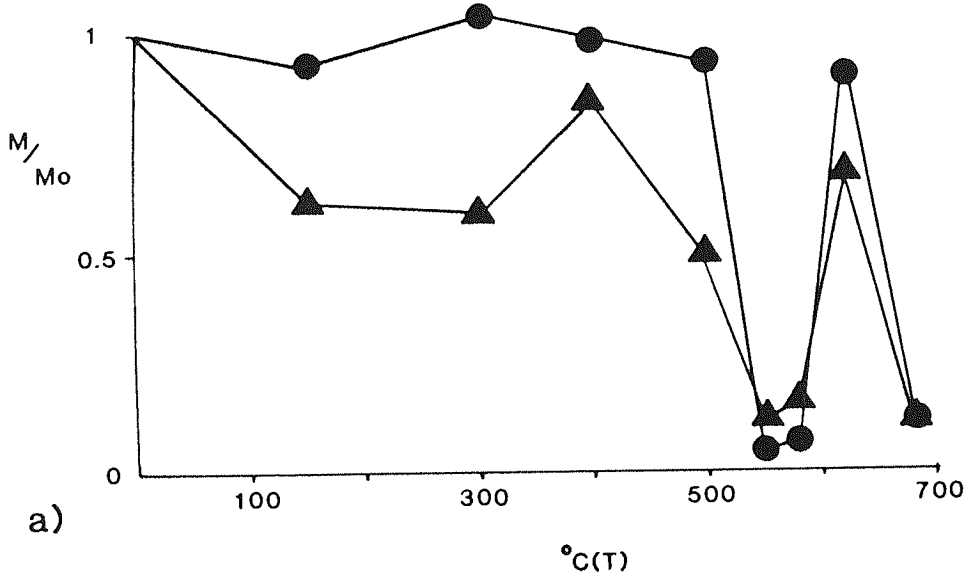
1
0.5
0
M/Mo
100
300
500
700
°C(T)

a)

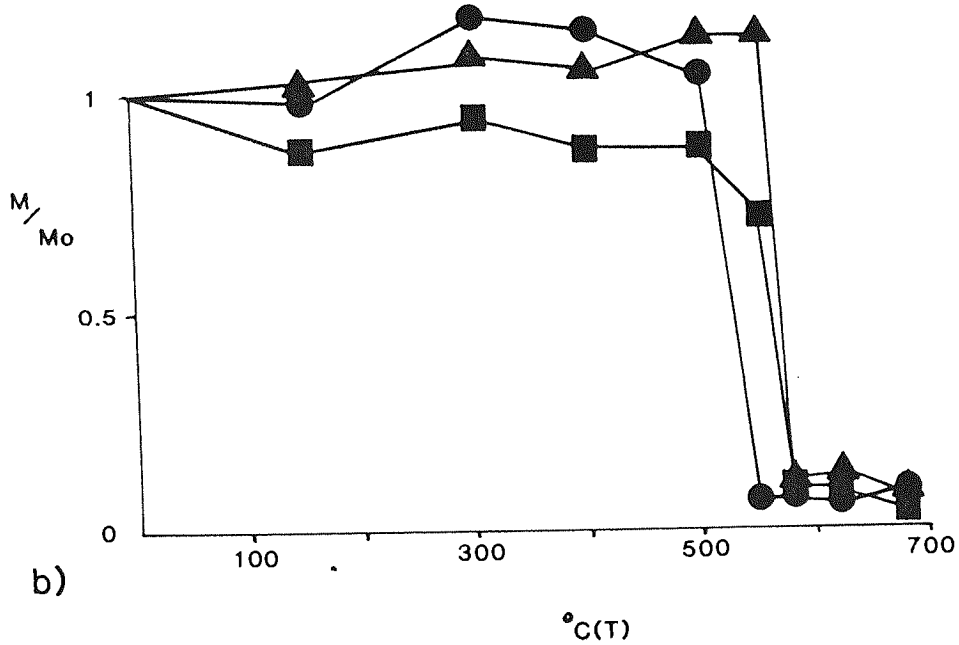
1
0.5
0
M/Mo
100
300
500
700
°C(T)

b)

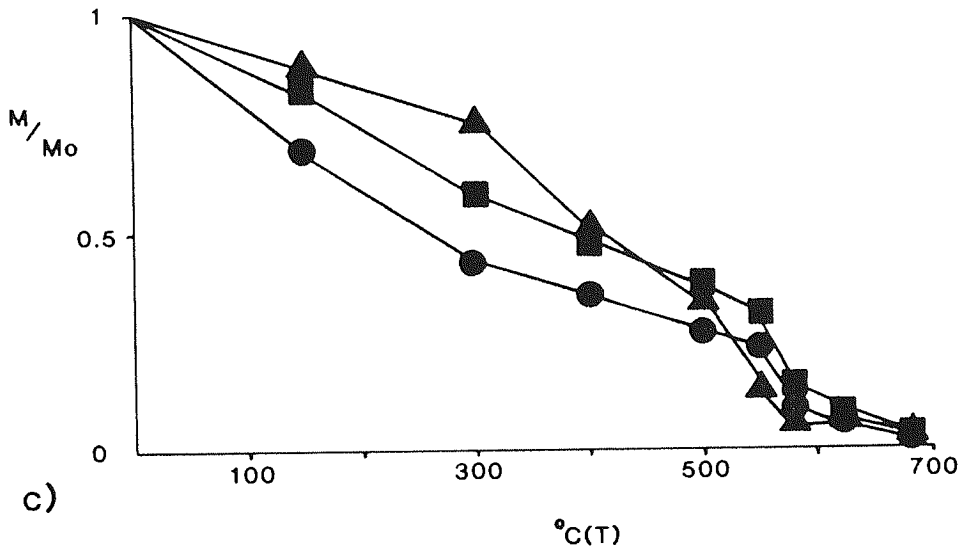
1
0.5
0
M/Mo
100
300
500
700
°C(T)

c)

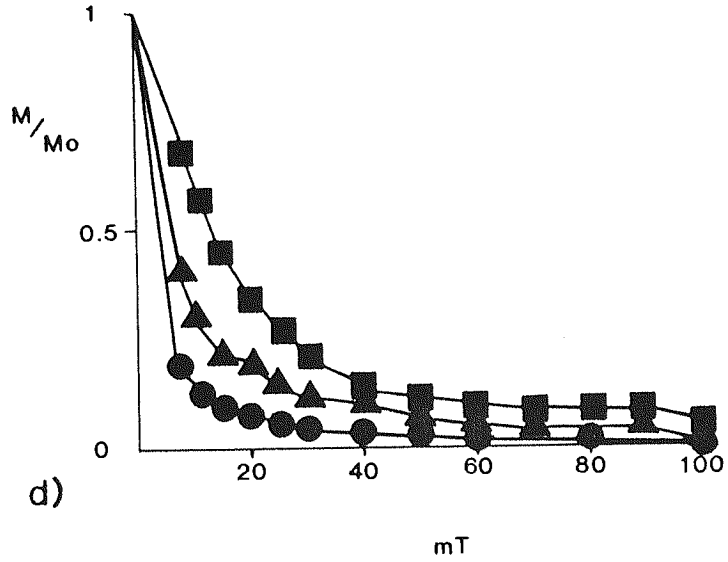
1
0.5
0
M/Mo
20
40
60
80
100
mT

d)

Stereographic Projections:

From examination of the stereographic projections (Fig. 4.5), two dominant patterns of directional change during demagnetization can be identified. Figure 4.5a shows sites which display a normal/intermediate to reversed directional change during demagnetization. This is in contrast to the behaviour displayed by sites illustrated in Figure 4.5b, which contain stable normal/intermediate components with little or no directional change throughout demagnetization.

MEJ6 and 8 displayed very variable behaviour, individual samples revealed no stable characteristic component during demagnetization. Site MEJ16 shows a reversed to normal directional change during demagnetization, in contrast to other sites. Petrographic work indicates that this site has been almost totally altered unlike the other sites, this is probably reflected by the variation in behaviour during demagnetization.

Zijderveld Orthogonal Diagrams:

Examination of the Zijderveld diagrams allows the definition of one, two and three component systems of magnetization, defined during demagnetization, except for sites MEJ5,8,22,26 and 44 which contained no identifiable stable linear components of magnetization.

One component systems show a straight line demagnetization path to the origin from 0-680 deg.C. (Fig. 4.6a), and often contain a low blocking temperature component removed between 0-150 deg.C. Two component systems present in 11 sites, have a low temperature component removed between 0 and 500 deg.C., and a high temperature component grouped closely around the origin removed between 550 and

Fig. 4.5 Equal angle stereographic projections of directional change for thermally demagnetized samples from the mejillones Peninsula: a) specimens containing two components of magnetization, MEJ1.1A ●, MEJ31.4 ■ and MEJ42.5 ▲, and b) specimens with one component of magnetization, MEJ13.2▲ and MEJ7.1● Numbers=deg.C. Other details as Fig. 4.3.

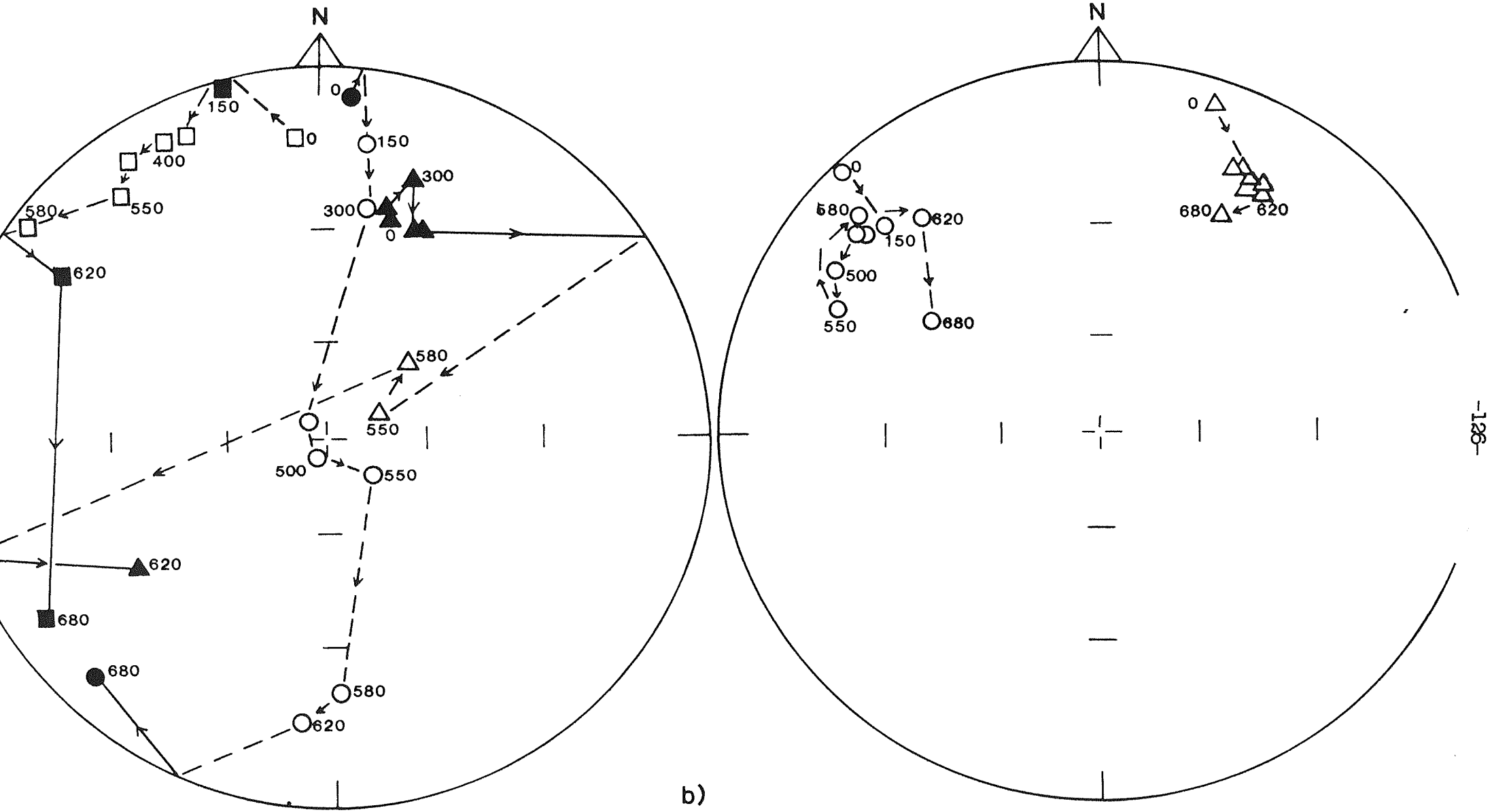
N
0
150
0
400
550
580
620
680
300
300
0
580
550
500
550
620
680
580
620
N
0
580
620
150
500
550
680
0
680
620

b)

Fig. 4.6 Orthogonal Zijderveld diagrams for: a) MEJ13.1, b) MEJ31.3, c) MEJ35.3 and d) MEJ36.2. Numbers=deg.C.

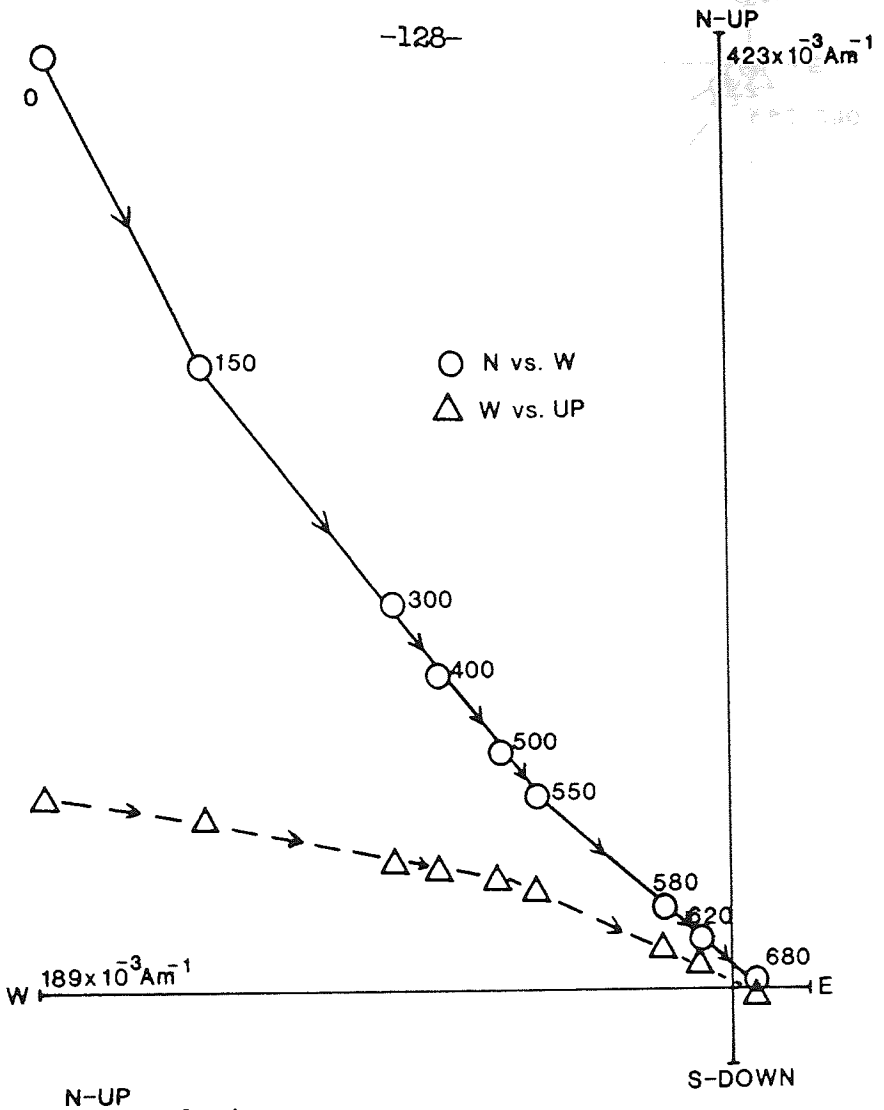
N-UP
423x10⁻³Am⁻¹
0
150
300
400
500
550
580
620
680
N vs. W
W vs. UP
W
189x10⁻³Am⁻¹
E
S-DOWN

a)

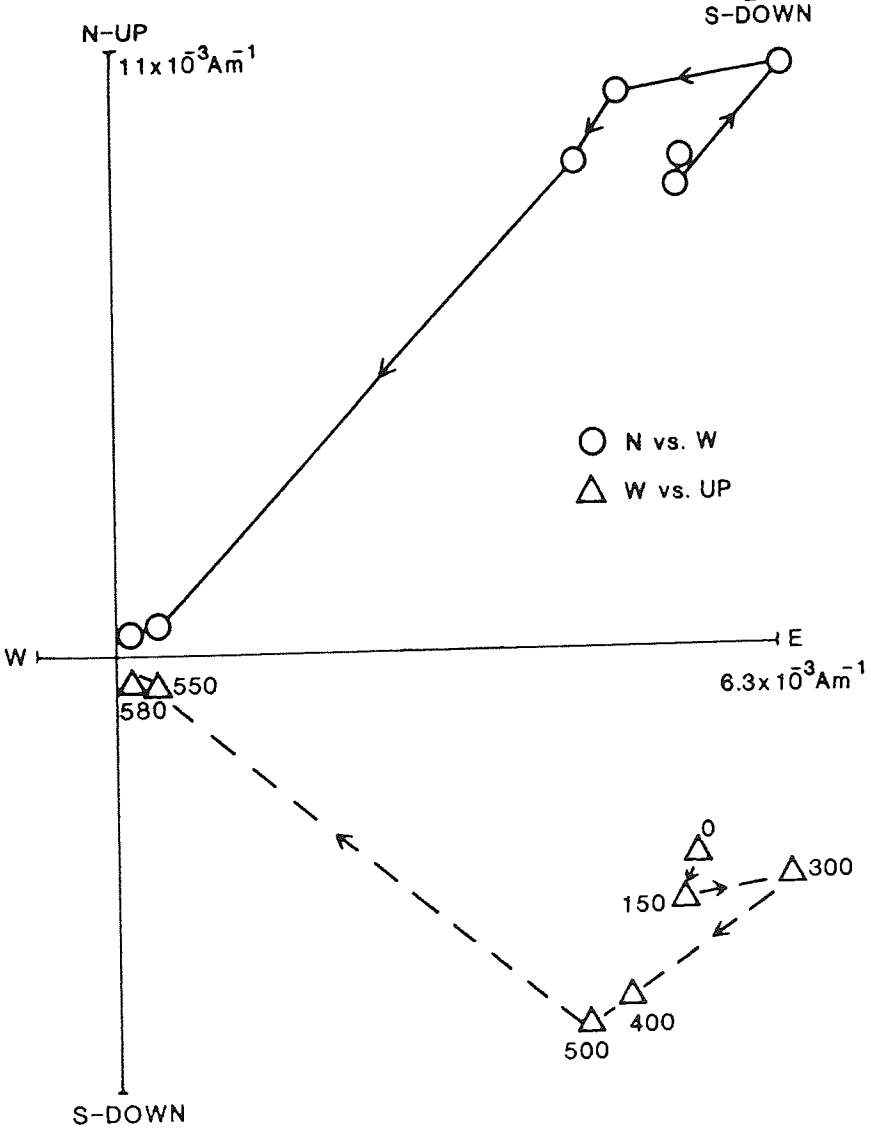
N-UP
11x10⁻³Am⁻¹
N vs. W
W vs. UP
W
E
6.3x10⁻³Am⁻¹
550
580
0
150
300
400
500
S-DOWN

b)

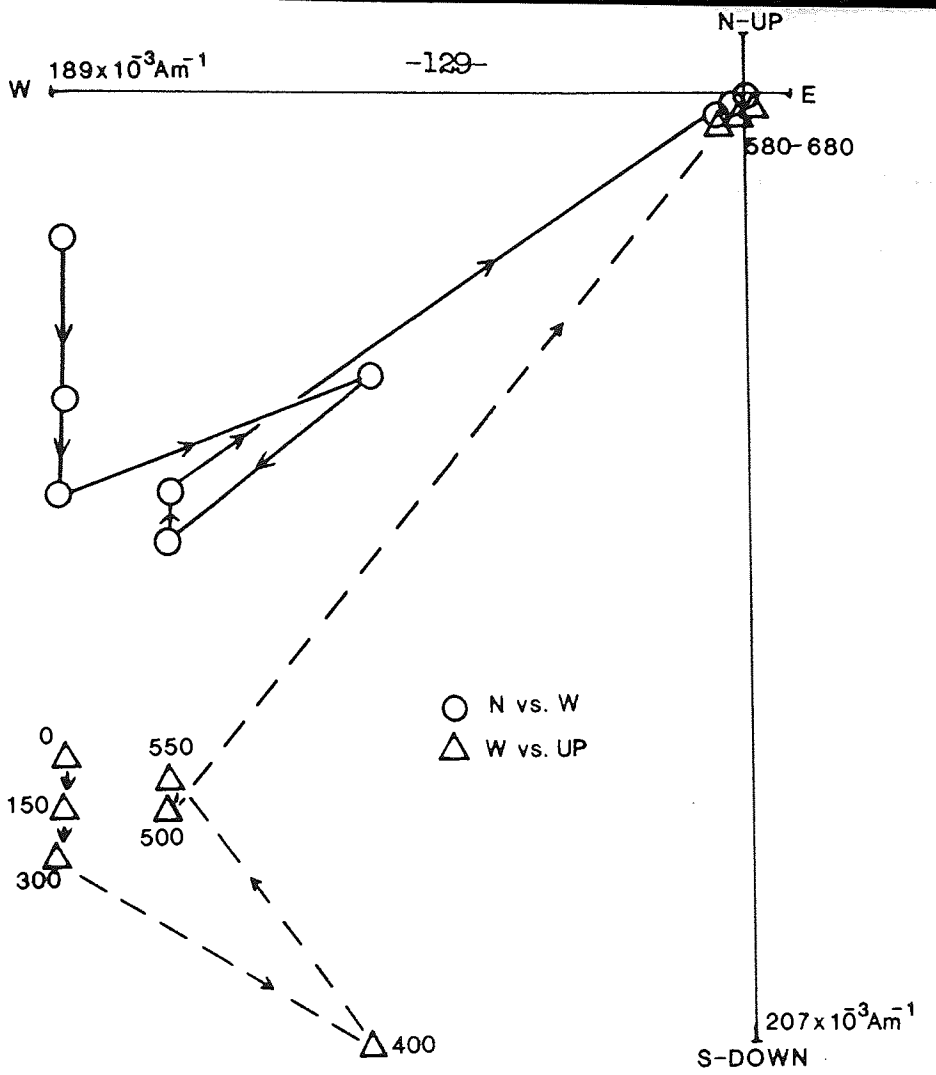
N-UP
W
189x10⁻³Am⁻¹
E
580-680
N vs. W
W vs. UP
0
150
300
550
500
400
207x10⁻³Am⁻¹
S-DOWN

c)

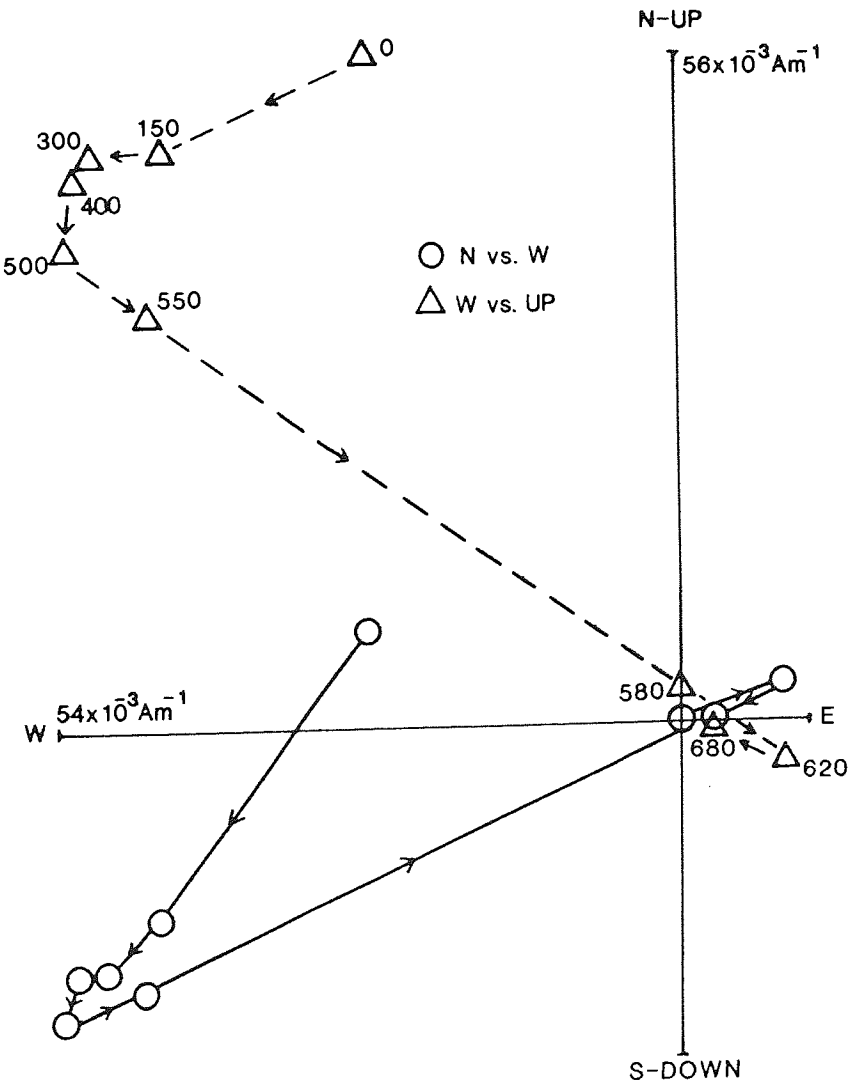
N-UP
56x10⁻³Am⁻¹
0
300
150
400
500
550
N vs. W
W vs. UP
W
54x10⁻³Am⁻¹
E
580
680
620
S-DOWN

d)

680 deg.C. (Fig. 4.6b). Three component systems are present in sites MEJ9,16 and 42, where components were removed between 0 to 300 deg.C., 400 to 550 deg.C. and 580 to 680 deg.C. (Figs. 4.6c,d).

Isolated Components (LSF analysis):

Isolated components using LSF analysis and the bulk demagnetization technique outlined in section 3.3, show normal, transitional and reversed components (Table 4.1). Sites MEJ4,6 and 13 are dominated by an intermediate component, and consequently are not used for statitistical analysis. Fourteen sites have one stable component, 10 of which are normal and dominant over low temperature ranges (0-500 deg.C.), 4 are reversed and dominant at higher temperatures (550-680 deg.C.), with the exception of MEJ22 where the reversed component is removed between 0 and 150 deg.C. Three components of magnetization have been isolated from MEJ5,6 and 16, however these sites do not display similar behaviour; different components are isolated over the same temperature ranges.

Some correlation was possible between components isolated using Zijderveld orthogonal diagrams and LSF analysis, similar components were isolated over the same temperature ranges using both techniques.

Magnetic Mineralogy:

Petrographic observations allow the definition of two site groupings based on the textural characteristics displayed by the magnetic minerals: 1) sites which contain primary textures involving magnetic minerals and 2) sites containing secondary or metamorphic textures involving magnetic minerals. However, some textures are ambiguous and may belong to either group, also some sites show

TABLE 4.1

NORMAL UNCORRECTED FOR BEDDING

SITE	N	R	K	CSD	DEC	INC	α_{95}
MEJ2	4	3.968	93.5	8.4	21	-42	9.6
MEJ5	4	3.917	36.1	13.5	47	-55	15.5
MEJ7	5	4.975	162.5	6.4	34	-30	6.0
MEJ10	5	4.920	50.1	11.4	29	-50	10.9
MEJ16	5	4.872	31.4	14.5	38	-46	13.9
MEJ20	5	4.892	37.1	13.3	29	-40	12.7
MEJ23	6	5.893	46.5	11.9	16	-42	9.9
MEJ28	6	5.898	49.0	11.6	20	-46	9.8
MEJ29	3	2.965	56.8	10.7	95	-47	16.5
MEJ30	4	3.935	45.9	12.0	15	-44	13.7
MEJ31	5	4.822	22.4	17.1	80	-64	16.5
MEJ39	6	5.785	23.3	16.8	30	-47	14.2
MEAN	12	11.463	20.5	17.9	35	-48	9.8

REVERSED UNCORRECTED FOR BEDDING

MEJ8	4	3.899	29.8	14.8	248	+17	17.1
MEJ16	5	4.970	132.4	7.0	261	+13	6.7
MEJ22	3	2.973	74.3	9.4	266	+56	14.4
MEJ26	3	2.944	35.8	13.5	244	+32	20.9
MEJ30	4	3.963	80.6	9.0	236	+40	10.3
MEJ35	4	3.979	141.2	6.8	262	+42	7.8
MEJ42	6	5.741	19.3	18.4	211	+34	15.6
MEAN	7	6.588	14.6	21.2	247	+35	16.4

TABLE 4.1 (continued)

NORMAL BEDDING CORRECTED								TEMP.
SITE	N	R	K	CSD	DEC	INC	α_{95}	(DEG. C.)
MEJ2	4	3.966	88.7	18.6	13	-15	9.8	0-620
MEJ5	4	3.918	36.7	13.4	25	-34	15.4	500-680
MEJ7	5	4.973	146.2	6.7	27	-7	6.4	0-150
MEJ10	5	4.916	47.7	11.7	16	-25	11.2	300-620
MEJ16	5	4.873	31.6	14.4	24	-23	13.8	550-620
MEJ20	5	4.897	39.0	13.0	20	-15	12.4	100-680
MEJ23	6	5.889	45.1	12.1	10	-14	10.1	0-300
MEJ28	6	5.891	45.9	12.0	21	-42	10.0	0-150
MEJ29	3	2.972	70.8	9.6	56	-44	14.8	0-400
MEJ30	4	3.936	47.1	11.8	8	-16	13.5	150-500
MEJ31	5	4.821	22.3	17.1	34	-51	16.6	300-580
MEJ39	6	5.887	27.3	15.5	19	-22	13.0	150-500
MEAN	12	11.487	21.5	17.5	22	-26	9.6	
REVERSED BEDDING CORRECTED								
MEJ8	4	3.899	29.6	14.9	241	+9	17.2	500-680
MEJ16	5	4.968	123.7	7.3	254	+11	6.9	550-620
MEJ22	3	2.974	77.6	9.2	227	+48	14.1	0-500
MEJ26	3	2.960	49.4	11.5	231	+18	17.7	300-500
MEJ30	4	3.963	81.8	9.0	220	+24	10.2	500-580
MEJ35	4	3.978	138.6	6.9	237	+37	7.8	550-680
MEJ42	6	5.743	19.5	18.4	204	+10	15.6	300-680
MEAN	7	6.590	14.6	21.2	231	+23	16.3	

Table 4.1. Extracted normal and reversed components of magnetization from the Mejillones Peninsula. For symbols used see Table 3.2.

transitional textures common to both groups.

Group 1 (primary igneous textures): In this group magnetite is present as discrete grains which may be euhedral to anhedral in shape often containing embayments usually with haematite (and less commonly ilmenite) exsolution lamellae (Plate 4.3). Haematite is also present as a "spongy" intergrowth with ilmenite, occurring as small exsolution blebs (Plate 4.4). Another primary texture is the aggregation of grains of magnetite with haematite exsolution and grains of ilmenite with haematite exsolution (Plate 4.4).

Group 2 (secondary metamorphic textures): This group includes myrmekitic intergrowths of magnetite (sometimes with haematite exsolution lamellae) and hornblende (Plate 4.5). Haematite is also common as an alteration product of biotite (Plate 4.6). Magnetite may be present as small euhedral to anhedral grains, but unlike the similar primary texture these grains are scattered uniformly throughout the polished section and not concentrated in one particular area.

IRM acquisition curves for sites with primary or secondary textures indicates that hamatite and magnetite are present in both groups. (Fig. 4.7a). This is shown by the saturation of magnetite in fields of over 0.3 Tesla, above 0.6 Tesla a progressive increase in the intensity of IRM testifies to the presence of unsaturated haematite. It should also be noted that some sites (with either primary or secondary textures), only contain magnetite (Fig. 4.7b).

4.4.1 Interpretation

The presence of metamorphic textures in the sites studied, indicates that the analysed sites have almost certainly been

Plate 4.3 MEJ36 Primary magmatic texture. Photomicrograph of an embayed magnetite crystal (dark grey), with well developed exsolution lamellae of haematite (light grey), oriented along cleavage planes. Ilmenite lamellae are also present (running diagonally from right to left (I) at the bottom of the magnetite crystal), they form form slightly larger exsolution lamellae than haematite and are darker than haematite. Reflected light, field of view=1.13mm.

Plate 4.4. MEJ29 Primary magmatic texture. Photomicrograph of a composite grain of ilmenite with haematite exsolution (the light area which forms most of the grain), and magnetite (the dark part of the grain, in the centre of the field of view) with haematite exsolution seen at the edges of the grain. A contrast can be seen between haematite exsolution in magnetite, which is needle-like and oriented along cleavage planes, and haematite exsolution in ilmenite, which is not orientated, and forms a patchy globule-like texture. Reflected light, field of view=0.56mm.

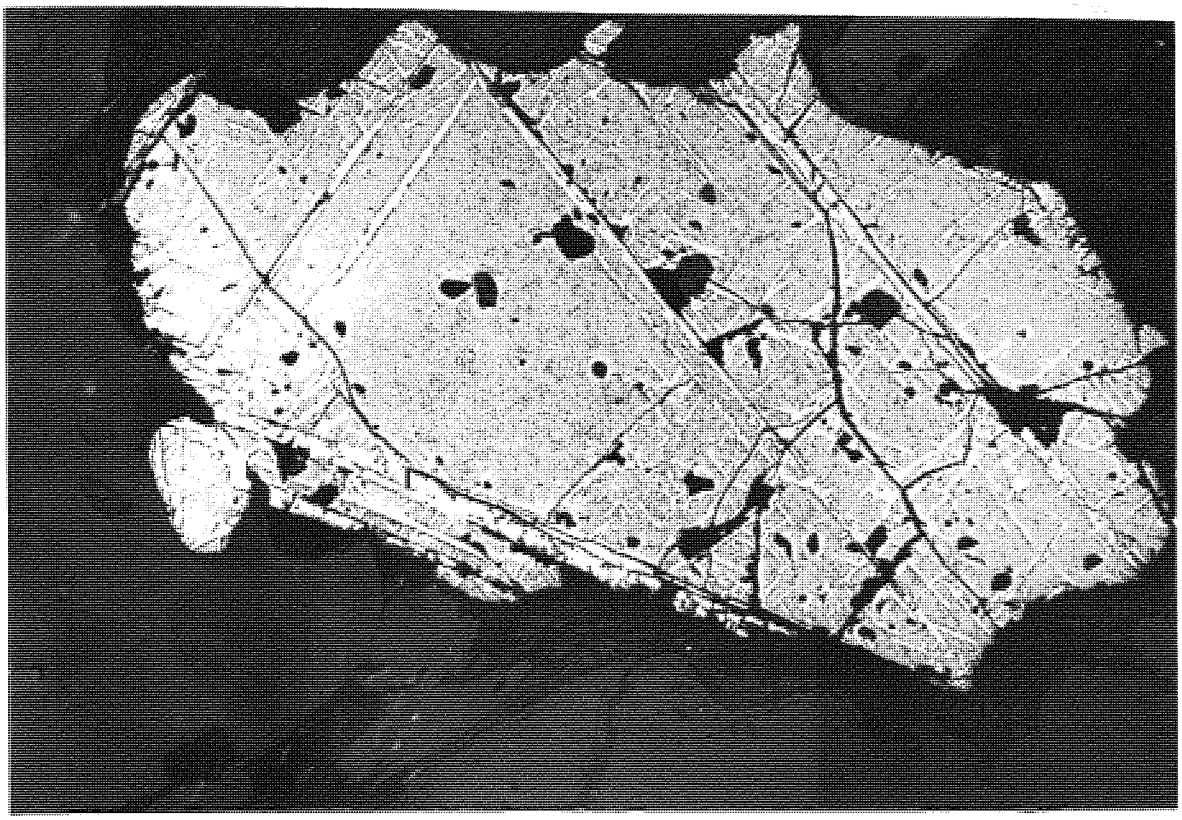

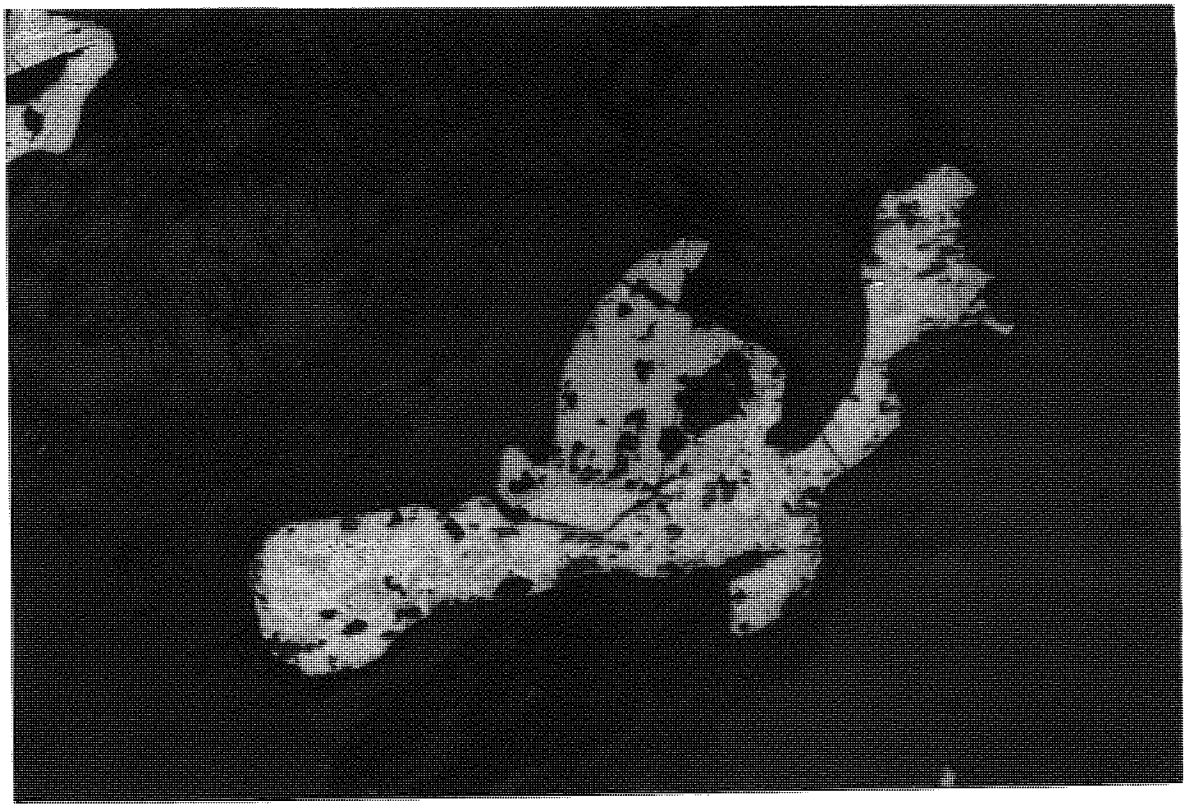

Plate 4.5 MEJ8 Secondary metamorphic texture. Symplectic texture (centre) caused by the worm-like intergrowth of magnetite and quartz (also seen between magnetite and hornblende in other sites). Porphyroblastic hornblende is present in the bottom left of the photomicrograph, enclosing grains of magnetite. The elongate texture seen in the middle right and running from the top of the photomicrograph, results from the alteration of biotite to haematite. Transmitted light, field of view=3.4mm.

Plate 4.6 MEJ30 Secondary metamorphic texture. Haematite (the light mineral), has completely pseudomorphed a biotite mica. The darker euhedral grains are magnetite, which have been partially altered to haematite. Reflected light, field of view=0.56mm.

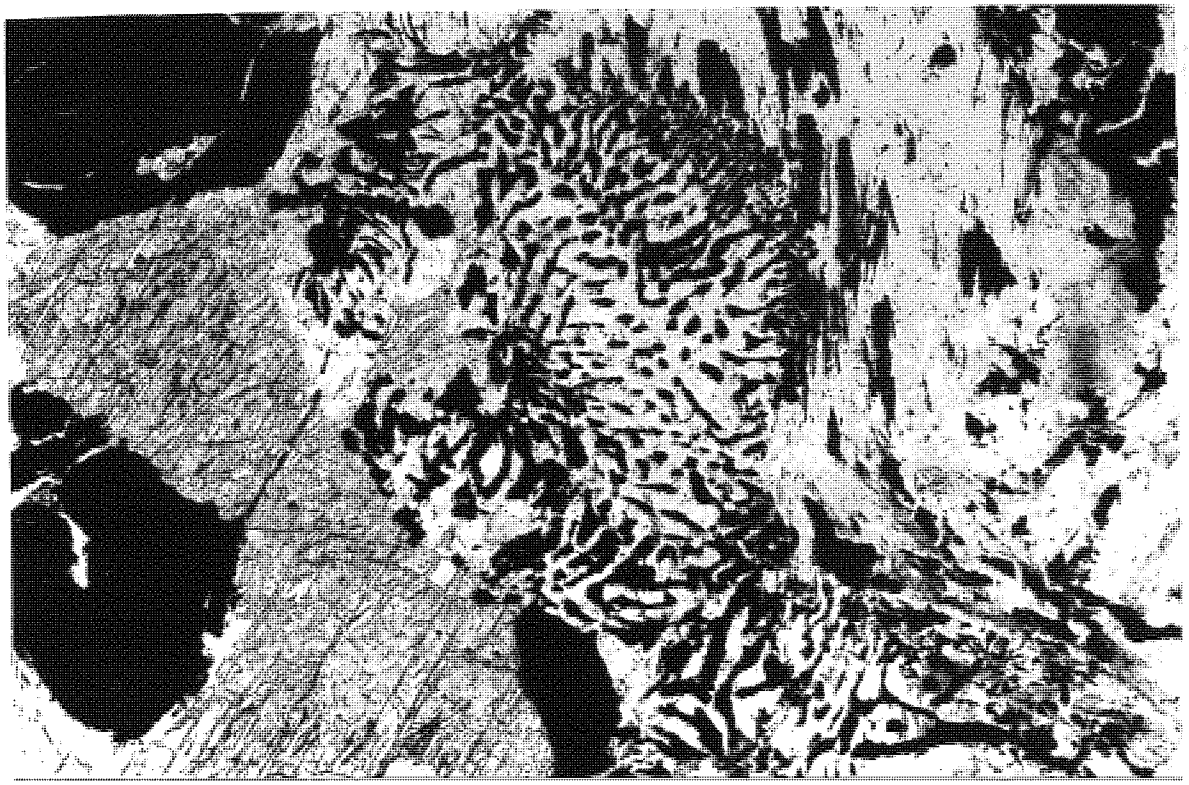

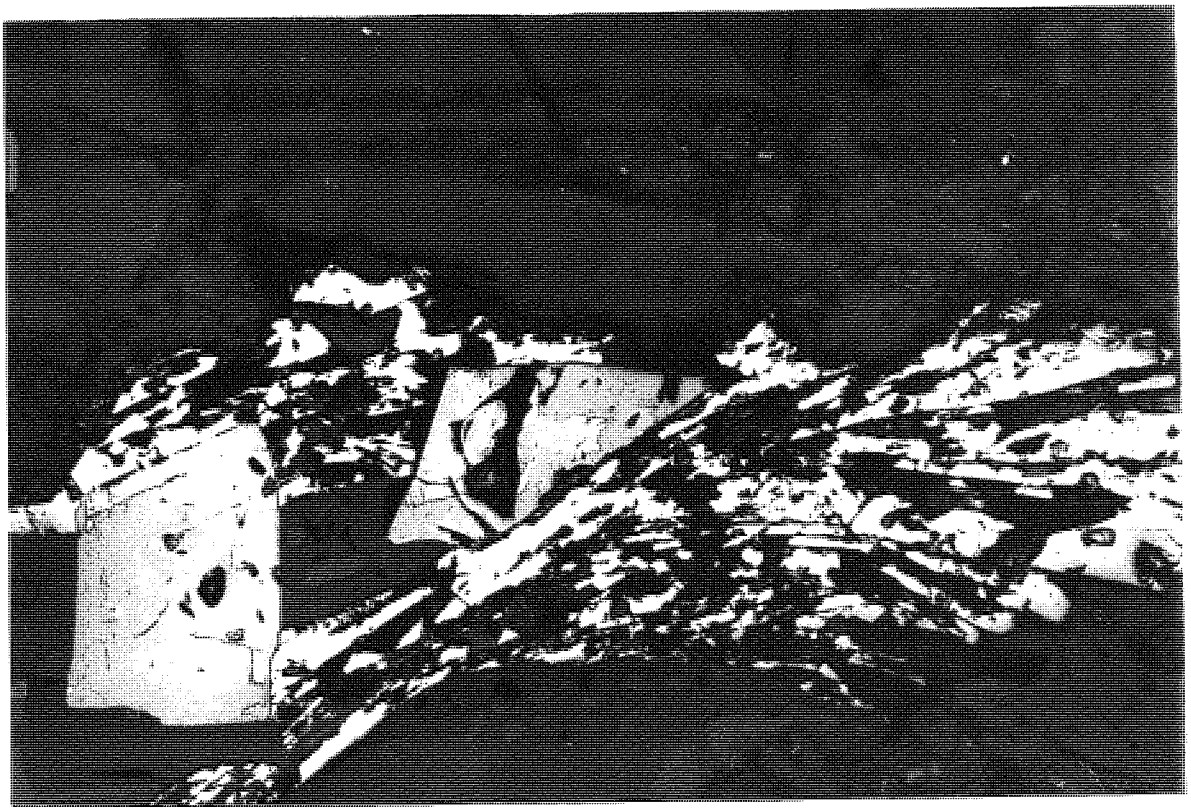

Fig. 4.7 IRM acquisition curves for a) sites contianing haematite and magnetite MEJ1●, MEJ6▲ and MEJ9■, and b) sites containing only magnetite, MEJ3● and MEJ4▲.

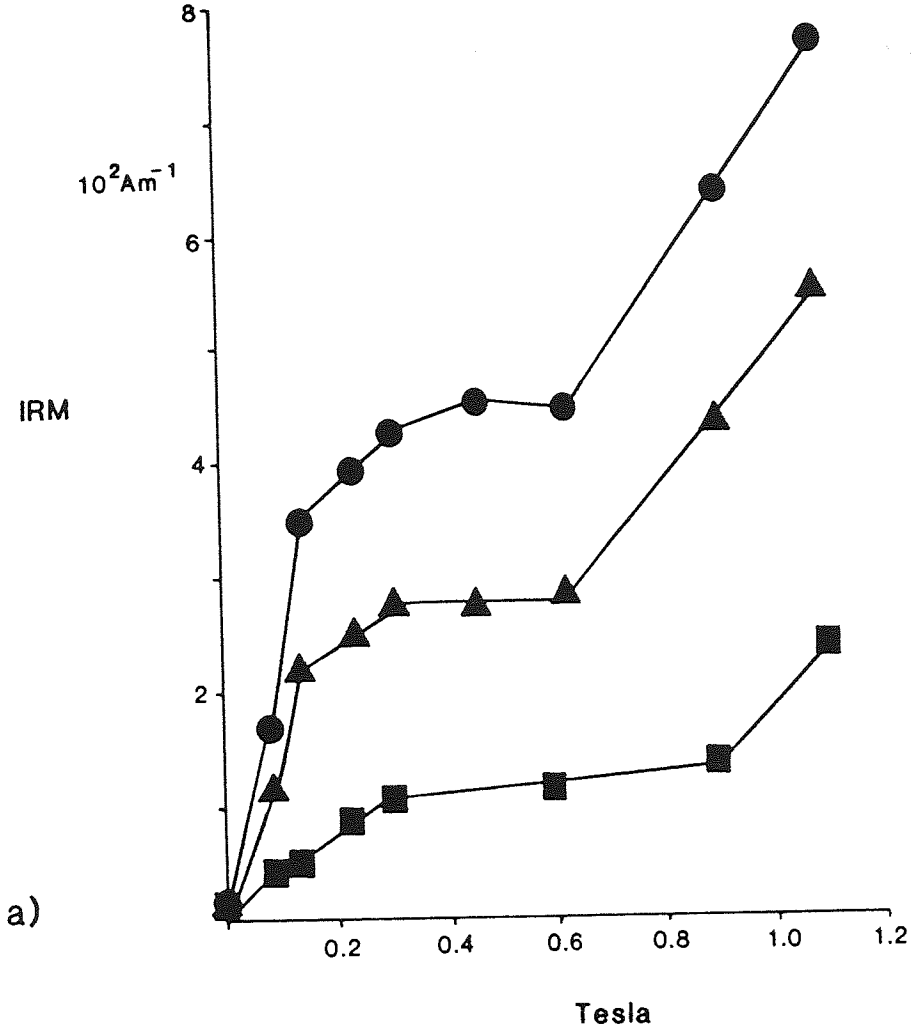
8
$10^2 Am^{-1}$
6
IRM
4
2
a)
0.2
0.4
0.6
0.8
1.0
1.2
Tesla

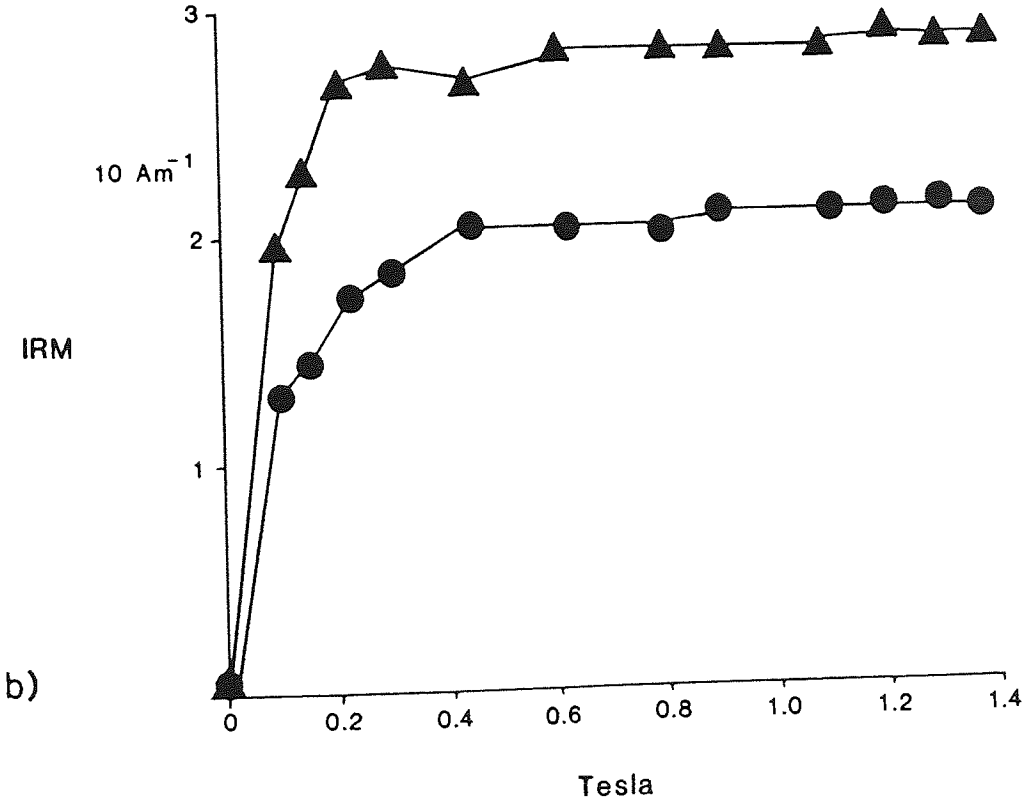
3
10 Am^{-1}
2
IRM
1
b)
0
0.2
0.4
0.6
0.8
1.0
1.2
1.4
Tesla

remagnetized. The difference in the degree of metamorphism between sites, is reflected in the variation in palaeomagnetic results, particularly the lack of site to site correlation between individual analytical techniques.

A correlation can be made between the magnetic mineralogy and isolated components. The reversed component present between 500 and 680 deg.C. must be carried by haematite, and/or magnetite with a high blocking temperature (500-580 deg.C.). Haematite occurs in both primary magmatic and secondary metamorphic textures. There is no significant statistical difference between reversed components derived from sites with primary textures and components derived from sites with secondary textures. Consequently, it can be assumed that there is no significant age difference between the acquisition of the normal and reversed components, particularly as the components are statistically antiparallel (Table 4.1).

4.5 Discussion

4.5.1 Age of Magnetization

Field, petrographic and radiometric evidence (large scatter in dates from similar rock types: 296-121Ma.; Fig. 4.8), indicate that the Moreno Complex has been metamorphosed. Most of the radiometric dates from the Moreno Complex range between 196 and 153Ma., indicating a major period of igneous/metamorphic activity. This range in radiometric dates is coincident with the age of intrusion of the north Chilean coastal batholith and extrusion of the La Negra Formation (186-150Ma., Ferraris and Di Biase,1978; Rogers,1985), both connected

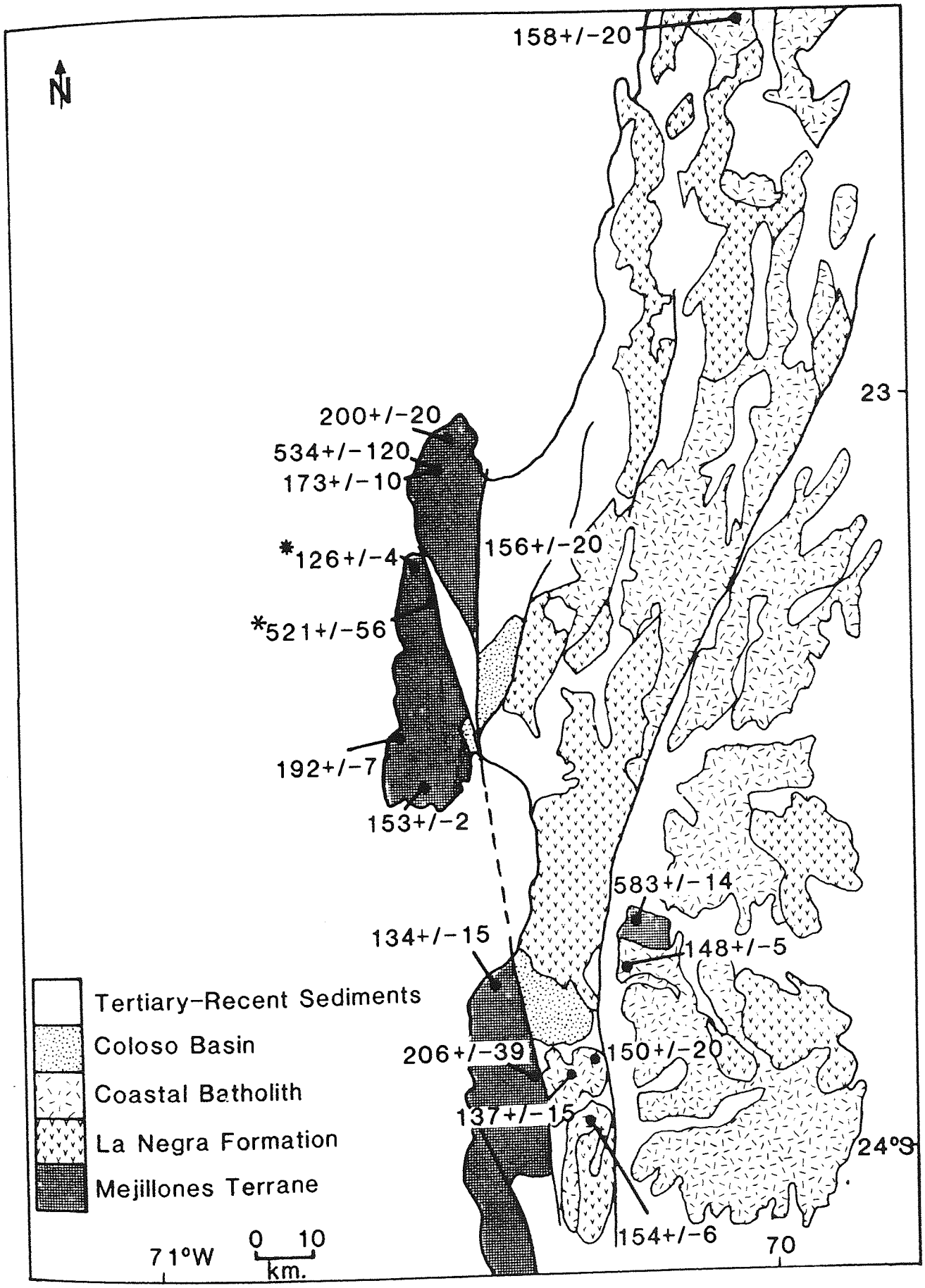

Fig. 4.8 Geological map showing fault trends, extent of the Coloso basin outcrop and radiometric dates for the Cordillera de la Costa and Mejillones Terrane. All dates are Pb/α , except for *K/Ar and *Nd/Sm.

to the activity of the Jurassic volcanic island-arc. It is probable therefore, that the Moreno Complex was remagnetized, acquiring a reversed component of magnetization during this time period. The normal component may reflect later remagnetization associated with younger igneous/metamorphic activity, possibly coincident with the youngest radiometric date from the Peninsula (121+/-6Ma., Damm et al.,1986).

4.5.2 Relationship of the Mejillones Peninsula to the Cordillera de la Costa (Coloso area)

Many similarities exist between the Cordillera de la Costa (Coloso area) and the Mejillones Peninsula, in particular the similarity between the Moreno and Bolfin (Chapter 3) Complexes. They include:

1) Lithology: Both the Moreno and Bolfin Complexes were originally gabbroic in composition and have suffered subsequent amphibolitization during a metamorphic event.

2) Radiometric dates: a) Both the Moreno and Bolfin Complexes have yielded Mid-Upper Jurassic radiometric dates (Halpern, 1978; Ferraris and Di Biase,1978; D. Rex, pers. comm.,1985; Damm et al.,1986; Fig. 4.8). b) The north and central parts of the Mejillones Peninsula and associated rocks from the eastern edge of the Bolfin Complex have yielded Lower Cambrian radiometric dates (Damm et al.,1986; Fig. 4.8), subsequently reset by later metamorphic/igneous activity.

3) Age of remagnetization: Both the Moreno and Bolfin Complexes appear to have been remagnetized as a result of a metamorphic event (almost certainly coincident with the activity of the Jurassic

TABLE 4.2

	DEC	INC	N	R	K	CSD	α_{95}
BEDDING CORRECTED	32	-26	19	17.627	13.1	22.4	9.6
UNCORRECTED	50	-44	19	17.588	12.7	22.7	9.8
POLE (LONG., LAT.)	187.9	57.0					

Table 4.2 Statistics for the combined normal and reversed components of magnetization extracted from the Mejillones Peninsula, and the palaeomagnetic pole, derived from Table 4.1. For symbols used see Table 3.2.

volcanic island-arc).

4) Palaeomagnetic poles: Fig. 4.9 shows the virtually identical nature of palaemagnetic poles derived from the Moreno Complex (Table 4.2), and the Bolfin Complex. The pole from the Cordillera de la Costa (Coloso area), was interpreted as having been rotated clockwise 29+/-11 degrees with respect to the stable shield area of South America (section 3.5). To reach its present position, the Moreno Complex has undergone a similar amount of clockwise rotation.

5) Tectonic trends: The three outcrops forming the north, central and southern parts of the Mejillones Peninsula are bounded by NW-SE oriented faults. The Bolfin Complex is bounded by NW-SE trending faults which if extrapolated northwards along their current orientation, connect with those of the Mejillones Peninsula (Fig. 4.8).

6) Sedimentary basin formation: Fig. 4.8 shows the outcrop distribution of the Coloso and Lombriz Formations. If the outliers present on the eastern flank of the Mejillones Peninsula are taken to define the previous extent of the Coloso basin, a NW-SE elongate basin (along the tectonic trend outlined above), would result. This would be bounded by the La Negra Formation to the east and a hypothetical connection between the Bolfin and Moreno Complexes to the west. This idea is supported by the observations of Flint et al. (1986a) and Flint and Turner (1988), who noted that the Coloso Formation was derived from the west, with sedimentological evidence indicating a very proximal source area. Clasts contained in the Upper Coloso Formation include: amphibolitised gabbro which often show evidence of copper mineralization (both of these features are present in the Moreno and Bolfin Complexes), and basaltic andesite of the La Negra

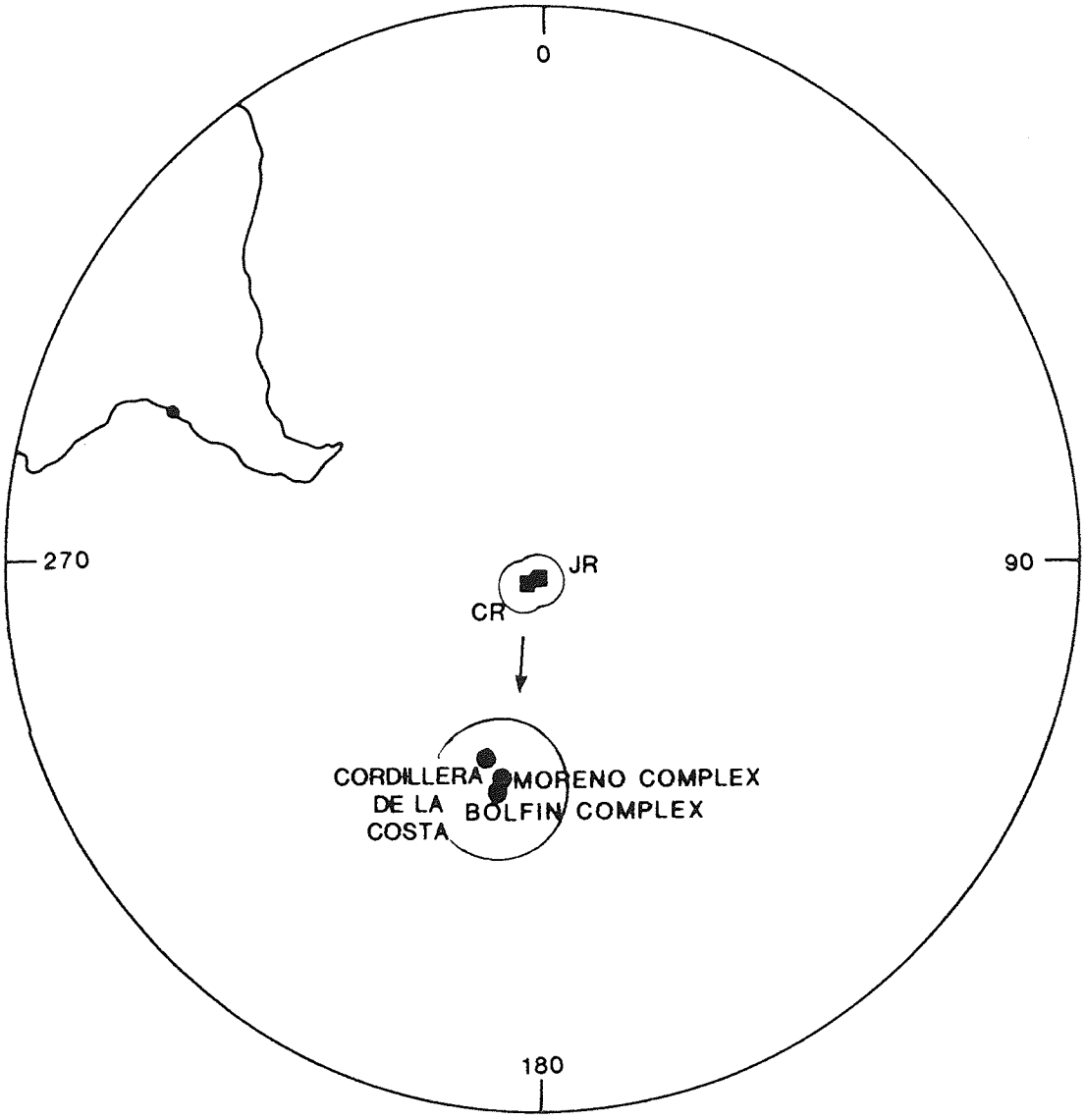

Fig. 4.9 Equal angle stereographic projection of palaeomagnetic poles derived from the Cordillera de la Costa (Chapter 3), the Moreno Complex (Table 4.2) and the Bolfin Complex (Table 3.3), relative to Mid Early-Mid Late Cretaceous (CR) and Upper Jurassic (JR) reference poles (see Appendix A), and 95% error limits.

Formation.

The above points appear to suggest that the Mejillones Peninsula and Bolfin Complex formed part of the same landmass at least as far back as the Lower Cretaceous. The centre of this positive area has subsequently been eroded.

Palaeomagnetic, geological and radiometric evidence confirms that the Mejillones Peninsula (the whole of the Peninsula is considered to be a single unit) and the Bolfin Complex (Cordillera de la Costa), acted as a single rigid block. This block is tentatively interpreted as an accreted terrane (the Mejillones terrane).

4.5.3 Tectonic Implications: Evidence for an accreted terrane

Palaeomagnetism has been used to good effect in the identification of accreted terranes in North America (Beck,1980), however, accreted terranes can only be identified palaeomagnetically, if a significant amount of discordance can be displayed between a reference pole, (usually derived from a stable shield area), and a pole of the same age derived from a "suspect" terrane. Palaeomagnetic work in the Central Andes must also take into account that subduction in the area is, currently, nearly normal to the plate margin, consequently any differences in pole position could be due to rotation of the Andean forearc (discussed in section 3.5). Also it is impossible to detect terranes emplaced along lines of latitude, as palaeomagnetism cannot determine the palaeolongitude of rocks.

Palaeomagnetic poles from the Mejillones terrane are significantly different when compared to poles derived from the stable shield area of South America (Fig. 4.9). Virtually identical palaeomagnetic poles have been derived from Mesozoic rocks located on

the continental margin unrelated to the Mejillones terrane (Fig. 4.9). The discordance in pole position between the continental margin and the stable shield area, was interpreted as the result of clockwise rotation attributed to forearc extension related to subduction roll back, slab pull and the absolute motion of the South American Plate (section 3.5). Therefore, both the Mejillones terrane and the north Chilean continental margin have been rotated. Consequently, any significant variation in pole position between "suspect" terranes, and palaeomagnetic poles derived from the stable shield area of South America, is not considered relevant in the identification of Andean accreted terranes.

An alternative view, is that the entire Andean forearc is comprised of an accreted terrane or a series of accreted terranes. Although the forearc does contain significant amounts of palaeomagnetically identified rotation, all the results are from Mesozoic rocks located on the continental margin, which geological evidence suggests are autochthonous in nature. Furthermore, rotation of the forearc north of 18°S. is anticlockwise, which would not comply with a margin composed of accreted terranes, as palaeomagnetic poles should be markedly discordant, and not display uniform clockwise or anticlockwise rotation.

The NW-SE fault pattern dominant in the Mejillones terrane is thought to represent an original tectonic trend present in the terrane prior to its emplacement. NE-SW oriented faulting is present in the Mejillones terrane (Fig. 4.8), but is thought to be superimposed, being the response of the terrane to the clockwise rotation of the forearc, evidence for this theory is supported by the NE-SW fault trend cutting the pre-existing NE-SW fault trend (Fig. 4.2).

Evidence for the allochthonous nature of the terrane is provided by the presence of rocks yielding Lower Cambrian radiometric dates. Although not conclusive evidence, other Lower Cambrian rocks west of the Cordillera de los Andes include an elongate belt of metamorphosed igneous rocks which outcrop along longitude 69°W. This is almost certainly structural in origin (G. Williams, pers. comm.,1987), and probably represents extension along pre-existing thrust faults (section 6.4.5). The only other exposures of Precambrian/Lower Cambrian age include: 1) The Arequipa Massif, located on the coast of southern Peru, the origin of which is uncertain (for discussion see Shackleton et al.,1979; Dalmayrac et al.,1980; Coira et al.,1982; Howell et al.,1985), and 2) The Chanaral melange, which forms the Cordillera de la Costa between 25 and 28°S, and is "suspect" in nature, having many similarities to the Mejillones terrane (Fig. 4.10).

The presence of Lower Cambrian rocks along the north Chilean coastline does not comply with the regional tectonic setting during the Mesozoic (the probable time of terrane accretion, see below). The Mesozoic tectonic setting of the Central Andes is relatively well known (section 2.4.2.), and involved a back-arc basin/island arc pair. The back-arc basin was subsequently strongly deformed and is thought to be exposed in the present day Precordillera and Central Depression (section 6.5). The volcanic island arc now forms the Cordillera de la Costa (Chapter 3). This Mesozoic tectonic setting, precludes the presence of a Precambrian continental massif to the west of the island arc except in the form of an accreted terrane (Fig. 4.10).

Baeza and Venegas (1985), showed that amphibolites from the northern and central parts of the Peninsula have tholeiitic

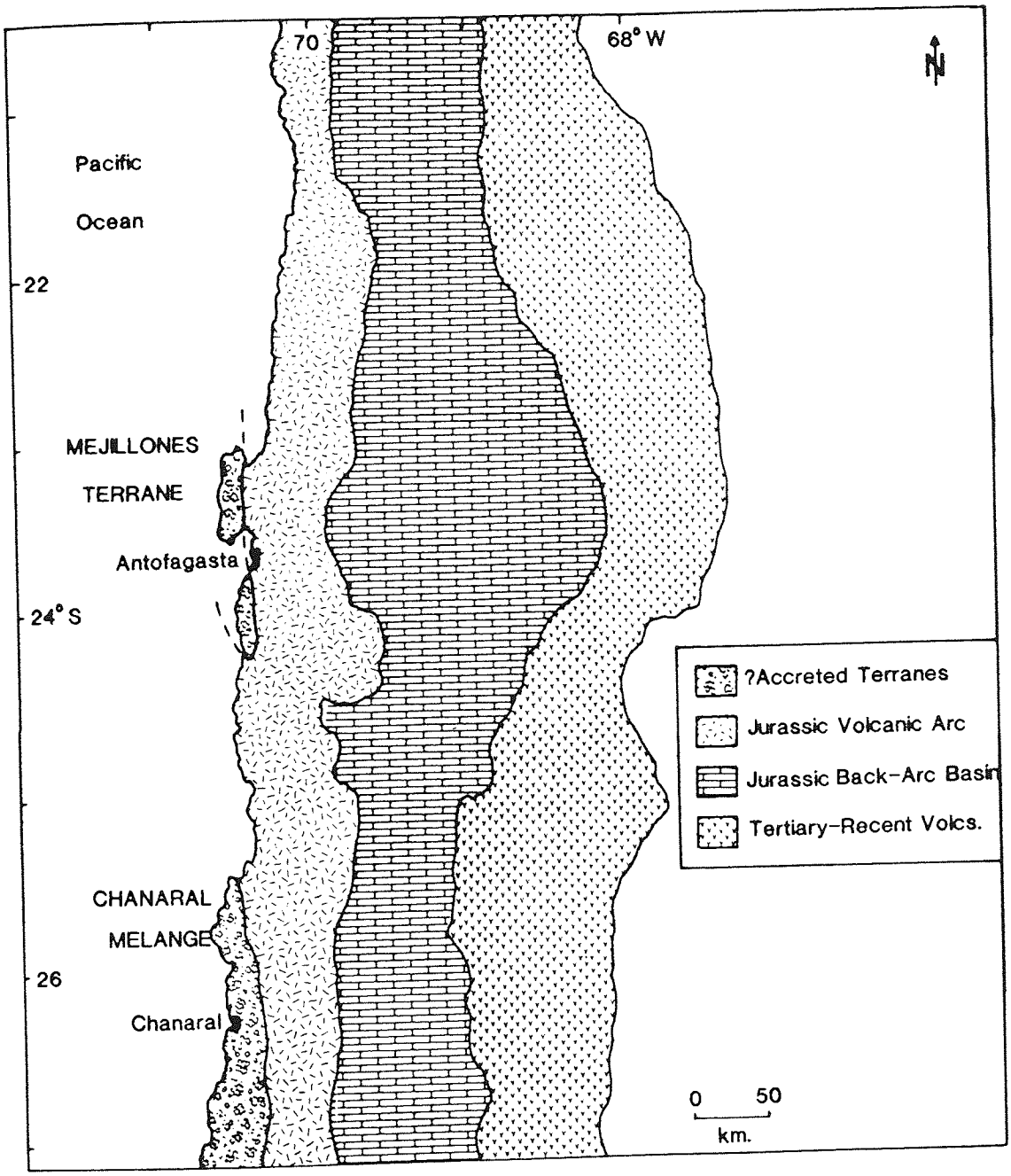

Fig. 4.10 Diagram showing the relationship of possible accreted terranes to the morphotectonic provinces of the Andean forearc.

compositions, a characteristic of oceanic crust, and a common feature of accreted terranes (Howell et al.,1985).

Other evidence for the allochthonous nature of the Mejillones terrane is the presence of the Coloso basin,the only north Chilean, Cretaceous continental basin. Formation of the Coloso basin is thought to have taken place, after emplacement of the Mejillones terrane, when extension and associated rotation of the forearc predominated. This resulted in the development of the Coloso basin along the suture between the terrane and the volcanic arc. The early sedimentary history of the basin was dominated by proximal alluvial-fan conglomerate deposition (Flint et al.,1986a; Flint and Turner,1988). Further extension resulted in more distal playa lake type sedimentation and finally a marine transgression represented by the El Way Formation, the only marine Cretaceous deposition in northern Chile (north of 27°S.). See Figure 4.11 for the envisaged tectonic development of the Coloso basin.

4.5.4 Age of Terrane Emplacement

The Mejillones terrane is closely associated with the Upper Jurassic coastal batholith. This is indicated by small pyroxenite and granodiorite stocks within the Peninsula (Fig. 4.2), which have been dated between 154-148Ma. (Damm et al.,1986; Fig. 4.8), and are present in both parts of the terrane. Also, the aforementioned resetting of radiometric dates through metamorphism is associated with batholith emplacement.

Outcrops of the extensive La Negra Formation (lavas of the volcanic arc, sections 2.4.2,3.5), have been identified on the Mejillones terrane (Baeza and Venegas,1984). Age dating of the

Fig. 4.11 Schematic diagram of the formation of the Coloso basin: a) accretion of the Mejillones terrane against the Jurassic volcanic arc, b) deposition of proximal conglomerates (Coloso Formation) in a narrow trough formed between the Mejillones Terrane and the mainland through forearc extension, c) basin width increases due to further forearc extension, resulting in an axially drained basin with more distal sedimention than Fig. 4.11b (Lombriz Formation), d) continued forearc extension, resulting in a marine transgression and the deposition of the shallow marine carbonates of the El Way Formation.

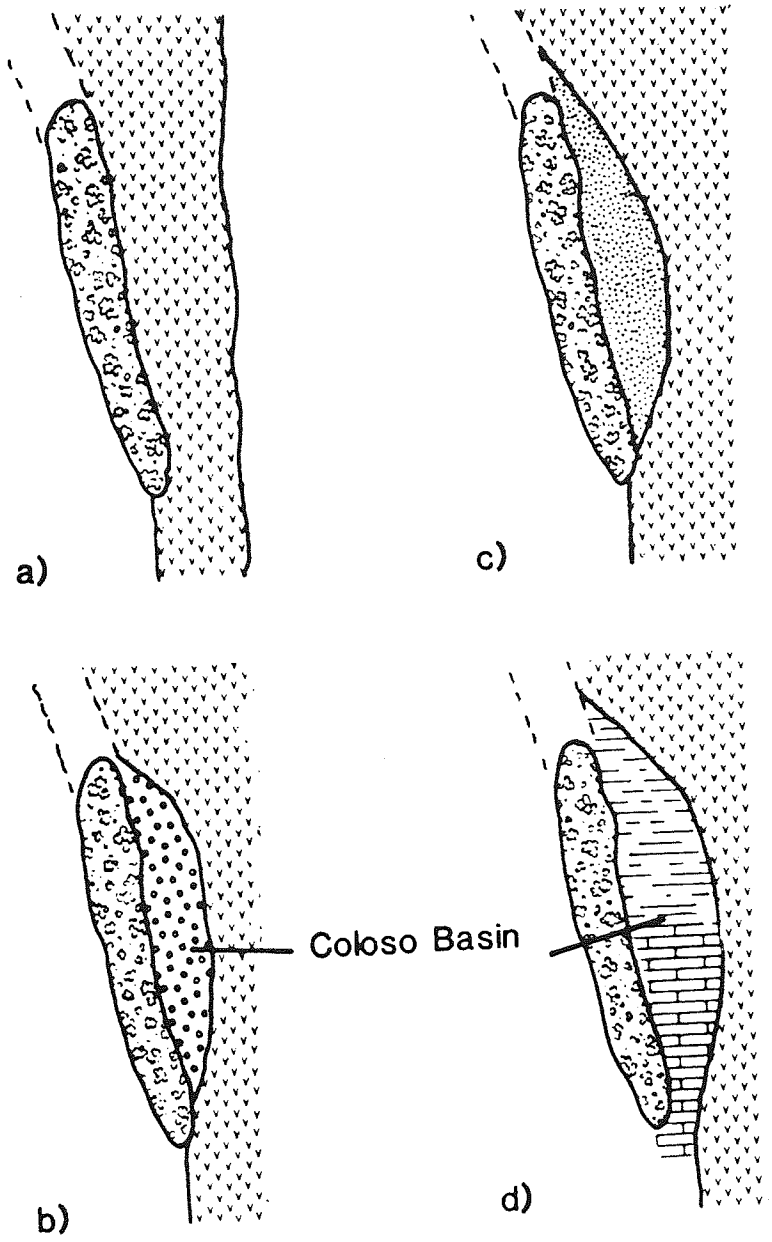
a)
c)
b)
Coloso Basin
d)
Distal Sands
Playa Muds and Sands
Marine Limestones
Mejillones Terrane
Island Arc
Proximal Conglomerates

Formation has yielded a 186+/-14Ma. Mid-Jurassic date (Rogers,1985). The La Negra Formation is however, 10km. thick (Garcia,1967), this thickness almost certainly reflects a long period of eruption possibly spanning most of the Jurassic. Consequently, the fact that the La Negra Formation overlies parts of the Mejillones terrane, does not conclusively prove that the terrane had been emplaced prior to 186Ma., but it is a possibility.

Two radiometric dates of 206 and 200Ma. (Ferraris and Di Biase,1978; Damm et al.,1986; Fig. 4.8), indicate that igneous/metamorphic activity took place in the terrane during the Lower Jurassic (Sinemurian). These dates may well reflect the beginning of igneous activity associated with the onset of the Jurassic volcanic-arc, coincident with the start of the Andean Cycle (section 2.4).

In summary, the Mejillones terrane may have been emplaced during the Sinemurian. It was probably in place by the mid-Jurassic, and certainly in place by the Upper Jurassic.

4.5.5 Conclusions

The Moreno Complex (Mejillones Peninsula) and the Bolfin Complex comprise a rigid block, as:

1) Palaeomagnetic poles from both areas are virtually identical, despite the fact that the forearc has undergone substantial clockwise rotation with respect to the stable shield area of South America (29+/-15 degrees).

2) Both areas display very similar lithological characteristics- the amphibolitization of a plutonic complex of originally gabbroic composition.

3) Remagnetization and acquisition of stable magnetic components for both areas was coincident with Mid-Upper Jurassic metamorphism thought to be associated with the activity of the Jurassic volcanic island-arc.

4) Fault trends are identical for both areas (NW-SE). These are at 90 degrees to the regional mainland normal fault trend, and coincident with the axis of the Coloso basin.

5) Both areas have yielded the only Precambrian/Lower Cambrian radiometric dates from the Central Andean Cordillera de la Costa (northern Chile).

The above rigid block has been interpreted as an accreted terrane (the Mejillones terrane) because:

1) The regional tectonic setting of the Andean forearc in the Sinemurian, of an island-arc/back-arc basin (the probable time of terrane emplacement), precludes the presence of a Precambrian/Lower Cambrian gabbroic coastal massif.

2) The affinity of amphibolites from the Peninsula with oceanic crust, negates the possibility that the terrane was simply a continental fragment rifted from the South American craton and accreted at a later date.

3) The Mejillones terrane formed a NW-SE oriented, elongate topographic high. Behind which, the only Lower Cretaceous continental and marine sediments were deposited in the Central Andean, Cordillera de la Costa.

4) Palaeocurrent, clast composition and sedimentological evidence

from the Coloso basin, requires the presence of a proximal, westerly-lying massif composed of amphibolitized and mineralized gabbro during the Lower Cretaceous.

CHAPTER 5

PALAEOMAGNETISM OF THE ANDEAN PRECORDILLERA, NORTHERN CHILE: EVIDENCE FOR INLAND FOREARC ROTATION

5.1 Introduction

Previous palaeomagnetic studies undertaken on the Andean forearc, have identified significant rotation of discrete crustal blocks, with respect to the stable shield area of South America (Palmer et al.,1980a,b; Turner et al.,1984; Heki et al.,1984,1985; May and Butler,1985; Beck,1985; Beck et al.,1986; Chapters 3 and 4). With the exception of Beck et al (1986), who worked in the Santiago area of Central Chile, all the above studies have been from the Pacific coast. The study of Beck et al. (1986), showed that significant crustal rotation of an area 200km. inland of the Pacific coast had taken place. It is possible that rotation is related to the dip of the subducting slab of the oceanic lithosphere (section 3.5). A palaeomagnetic study of the Precordillera (250km. inland) of northern Chile (Fig. 5.1), will clarify the validity of this theory, since the area overlies a steeply dipping subduction zone (40 degrees), in contrast to Central Chile, which overlies a shallow dipping subduction zone of 20 degrees (Barazangi and Isacks, 1976).

In this study the Andean Precordillera is defined as the narrow mountain range, located between the Central Depression and the Salar Depression (Figs. 2.1,5.1), and known locally as the Cordillera de Domeyko. A palaeomagnetic study of this area may resolve some of the

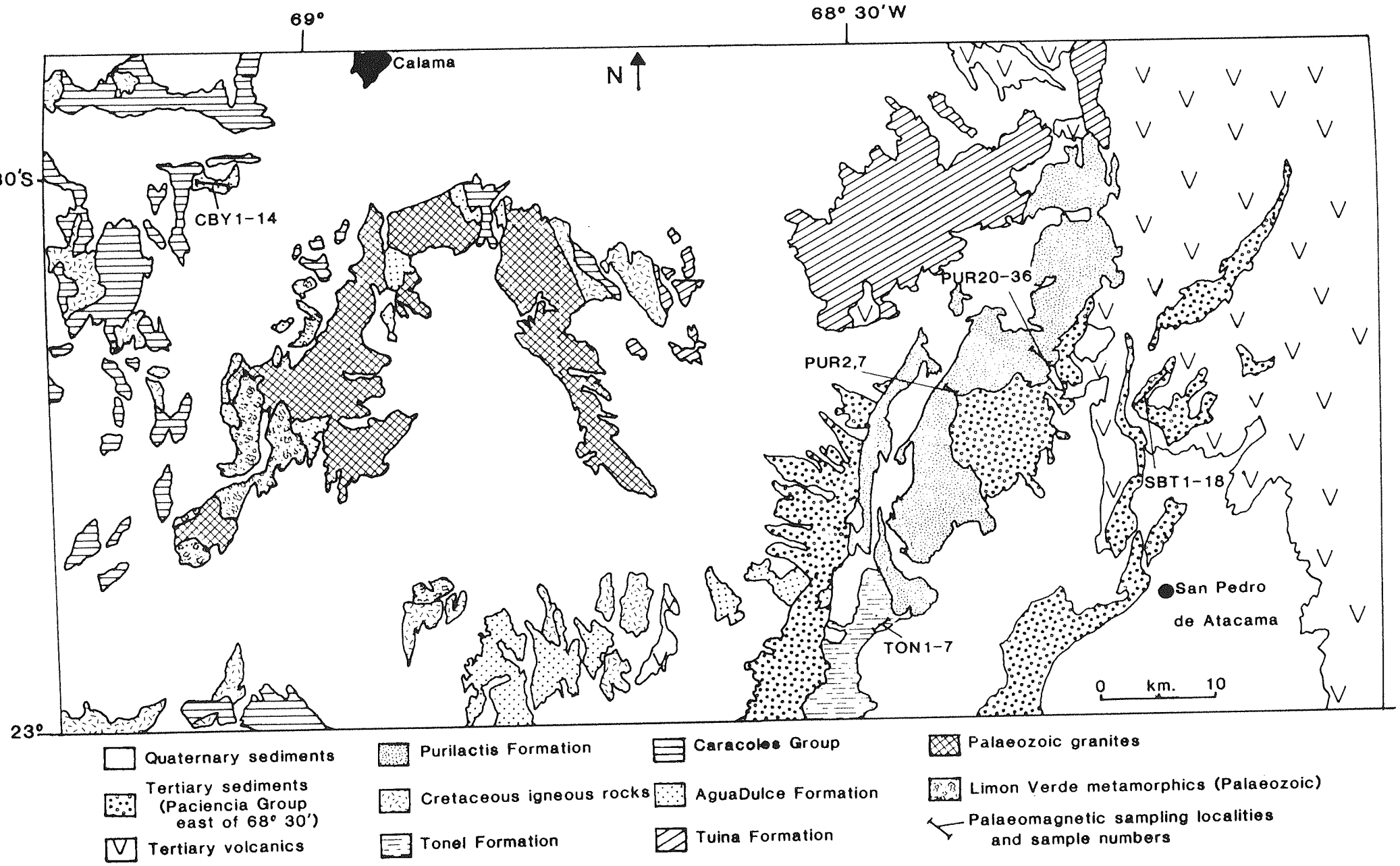

Fig. 5.1 Geological map of the Precordillera and eastern part of the Central Depression, with palaeomagnetic sampling localities.

problems outlined in section 3.5, regarding the dominant stress regime in the Andean forearc. This would also allow a comparison to be made between rocks of similar age from the Cordillera de la Costa (Chapter 3), and define the amount, age, extent and possible method of rotation of the Andean forearc.

5.2 Geology

The Andean Precordillera, Antofagasta Region, northern Chile, forms an extensive (600km.), N/S striking mountain range up to 4800m. high known as the Cordillera de Domeyko, of which the study area forms the northern part (Fig. 5.1).

Rocks exposed in the Precordillera range from Precambrian to Quaternary in age (Fig. 5.1). Pre-Mesozoic rocks include the Precambrian Limon Verde pluton (Damm et al.,1986; Fig. 5.1), which forms part of a N/S belt of Precambrian basement (section 2.2), and the Tuina Formation exposed in the eastern part of the area (Fig. 5.1). The Tuina Formation, thought to be Permian-Lower Triassic in age (Marinovic and Lahsen,1984), comprises a complex deformed sequence of interbedded volcanics and sediments. The Formation reflects a period when the tectonic history of the Central Andes is poorly understood (section 2.7).

Both the Limon Verde pluton and the Tuina Formation are overlain unconformably by the ?Upper Triassic Agua Dulce Formation (Marinovic and Lahsen,1984); an extensive sequence (750m; Baeza,1976), of arkosic sandstones and interbedded andesites, with a probable basal marine sequence (section 6.5). The Agua Dulce Formation outcrops on the

western flanks of the Cordillera de Domeyko and the eastern edge of the Central Depression (Fig. 5.1), and is thought to represent the onset of the Andean Orogenic cycle in the Precordillera of northern Chile (sections 2.3.5, 6.2). It forms the northern extension of the Upper Triassic-Lower Cretaceous marine back-arc basin developed further south (Chong,1977; sections 2.4.2, 6.3).

Other Mesozoic rocks from the area include the Tonel and Purilactis Formations (Bruggen,1932,1942,1950; Dingman,1963,1967), which outcrop on the eastern edge of the Cordillera de Domeyko. The Tonel Formation outcrops along the western edge of the Salar de Atacama (Fig. 5.1), and comprises a thick sequence of evaporites, mudstones and siltstones with minor sandstones. The Formation has been intruded by prominent green, hornblende rich dykes and sills, often extensively epidotised and chloritised.

The Purilactis Formation is exposed in the form of a NE-SW synclinal basin (Fig. 5.1), and is thought to be of Lower Cretaceous age, based on a derived Mid-Upper Jurassic fossil content (Felsch,1933; Dingman,1963,1967). It has a localised thrust faulted contact with the underlying Tonel and Tuina Formations in the south and north of the area respectively. The Formation comprises an extensive (3400m. thick), sequence of siltsones, sandstones and conglomerates representing aeolian, fluvial, lacustrine and alluvial fan environments. The facies relationships are complicated by marked variations across the limbs of the synclinal basin (section 6.3.3).

Both the Tonel and Purilactis Formations represent westerly equivalents of the Upper Triassic to Lower Cretaceous marine back-arc basin. The area must consequently have formed a topographic high during the first part of the Andean Orogenic cycle, as reflected by

the presence of continental facies throughout the Mesozoic. It is probable that the deposition of the Tonel and Purilactis Formations took place in a markedly different tectonic setting than that of the Agua Dulce Formation (see discussion, and section 6.5).

Further sedimentation is not recorded from the area, until the deposition of the Oligo-Miocene Paciencia Group, which unconformably overlies the Purilactis Formation (Fig. 5.1). A detailed sedimentological and diagenetic study of the Paciencia Group has been undertaken by Flint (1985b,1986). The Group consists of 2000m. of siltstones, sandstones and conglomerates, representing lacustrine, fluvial and proximal and distal alluvial fan facies, interbedded with occasional thin ash bands.

Extensive ignimbrite sheets developed from the Pliocene onwards and dominate the more recent geological history of the Precordillera. Sedimentation in the area is restricted to present day alluvial fan and plain conglomerates, together with thin conglomerates developed in intervals between ignimbrite eruption (Fig. 5.1). The ignimbrite sheets are thought to represent the onset of igneous activity associated with the formation of the Cordillera de los Andes.

In summary, sedimentation in the area studied has been continental in nature since the Upper Triassic, with the exception of the Jurassic marine back-arc basin developed in the south of the area (section 6.3). This has resulted in problems with dating of the studied units, as, with the exception of the Paciencia Group from which an interbedded ash flow has been dated at 28+/-6Ma. (Travisany,1978), age has been assigned through field relationships and derived fossil content.

5.3 Sampling and Laboratory Methods

Block and drilled samples oriented in the field were collected from the Agua Dulce and Tonel Formations, hornblende dykes intruded into the Tonel Formation (Tonel intrusives), the Purilactis Formation and the Paciencia Group (Fig. 5.1). Samples were orientated using both magnetic and sun compasses. Comparison of the two methods indicated that orientation was accurate to within 3 degrees. A fold test (McElhinney,1964) was applied to all sampled units, but, except for the Purilactis Formation, proved inconclusive (Tables 5.1-5.5).

The samples were demagnetized and analysed using the techniques outlined in sections 3.3 and 4.3, together with reflected light microscopy, in order to identify the magnetic mineralogy.

5.4 Palaeomagnetic Results

5.4.1 Agua Dulce Formation

Fourteen block samples yielding 37 specimen cores, were collected from the continental sediments and lower lava flows of the Agua Dulce Formation. The sampled area is situated to the west of the Precordillera, in the eastern edge of the Central Depression (Fig. 5.1).

The initial intensity of NRM varies between 0.126 and 32.3×10^{-3} Am^{-1}. Initial directions of NRM are well grouped with a small degree of scatter (Fig. 5.2a). It should be noted that the initial NRM directions, uncorrected for bedding, are nearly coincident with the present axial dipole field for the area. This implies possible

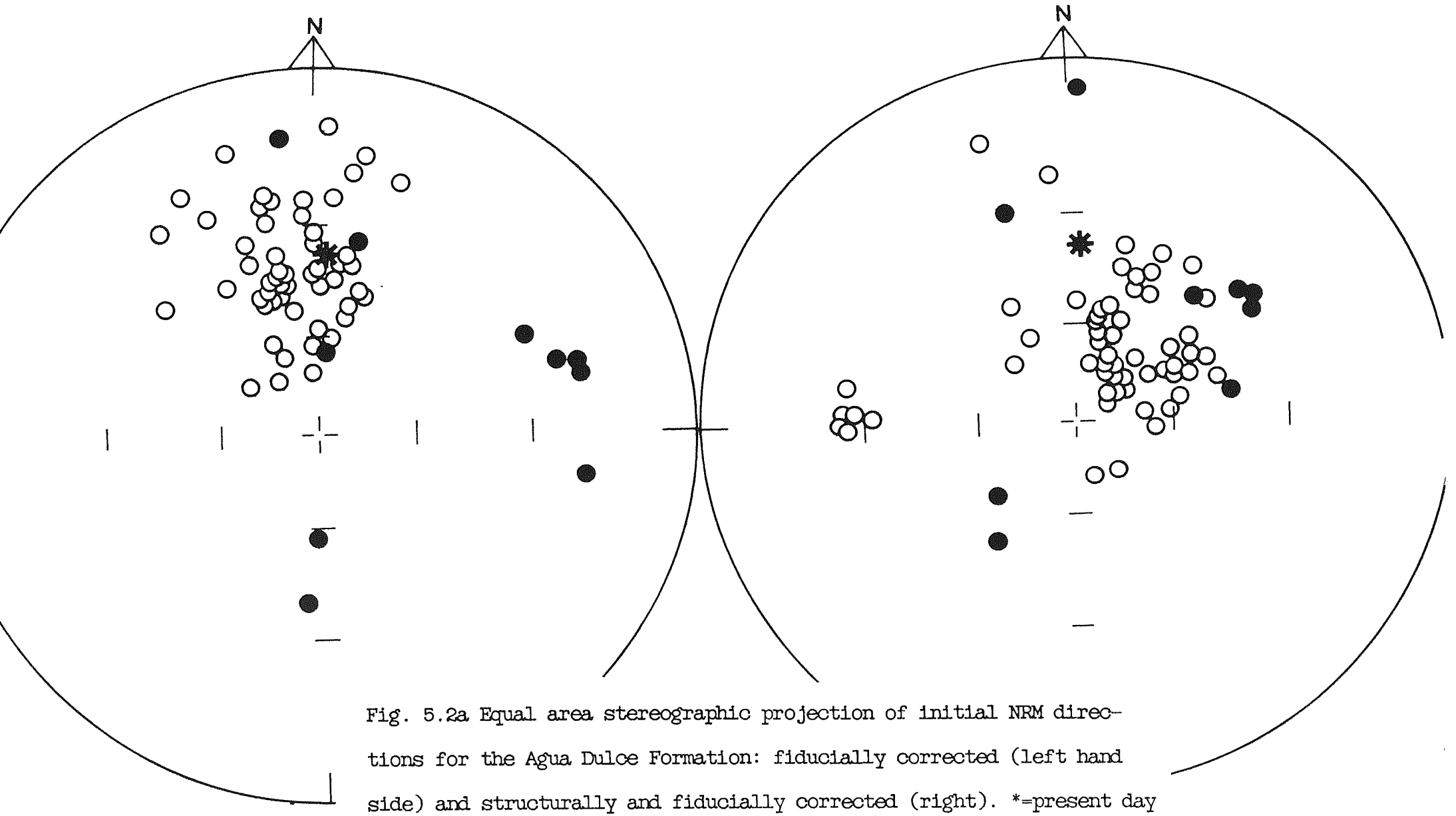

Fig. 5.2a Equal area stereographic projection of initial NRM directions for the Agua Dulce Formation: fiducially corrected (left hand side) and structurally and fiducially corrected (right). *=present day axial dipole field. Open symbols=upward inclination, closed symbols=downward inclination.

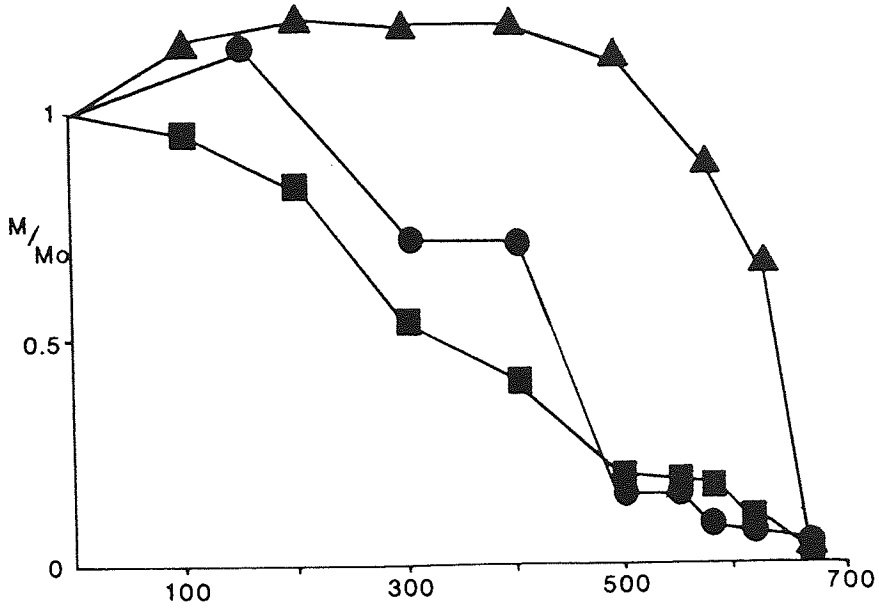

b)

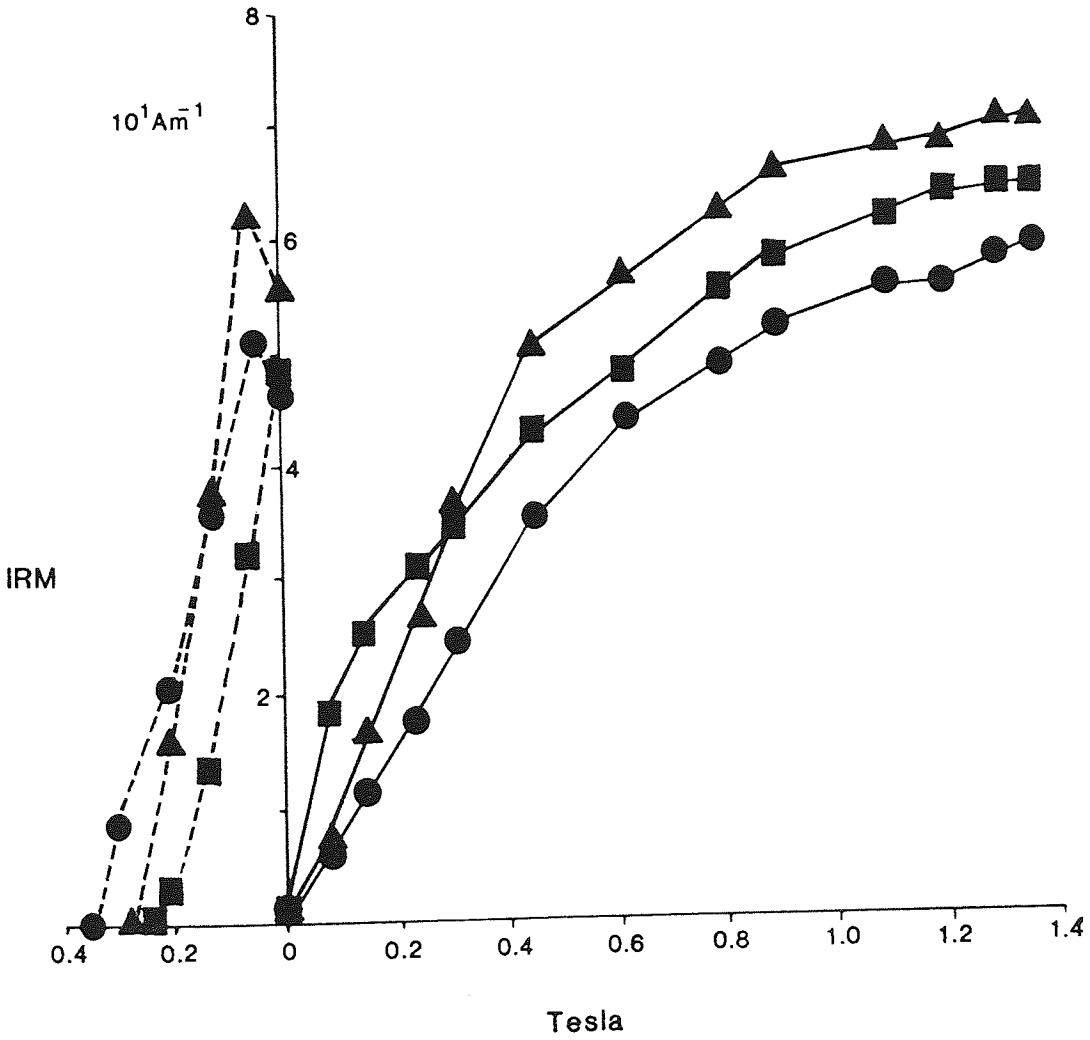

c)

Fig. 5.2b Normalised intensity decay curves for the Agua Dulce Formation: CBY1.2●, CBY8.3■ and CBY11.2▲.

Fig. 5.2c IRM acquisition curves for the Agua Dulce Formation, CBY7●, CBY9▲ and CBY12■.

remagnetization of the Formation in the present direction of the Earth's magnetic field. Although possible, this is considered unlikely for reasons outlined in the interpretation section below.

Figure 5.2b shows the variation in normalised intensity decay curves, for thermally demagnetized specimens. CBY8.2 (sandstone) shows a gradual decrease in the intensity of NRM, with half lost between 400 and 500 deg.C, 70-80% by 580 deg.C., and complete demagnetization by 680 deg.C. CBY11.2 (rhyolite) in contrast to CBY8.2, shows a small intensity increase up to 500 deg.C., with half the initial NRM lost by 620 deg.C. and complete demagnetization by 680 deg.C.

Specimens subjected to AF demagnetization show a rapid fall in intensity, with a MDF between 20 and 40mT. This is followed by a gradual decrease in NRM, in stronger fields. In some specimens however, only 40% of the original NRM may be removed at fields of up to 100mT.

Specimens from all 14 sites (both sandstones and lavas) have similar stereographic projections of directional change. Most specimens contain normal components of magnetization (grouped in the NE quadrant with upward inclination), throughout demagnetization up to temperatures of 550 deg.C and fields of 60mT. Above these temperatures and fields only random orientations were obtained, of no palaeomagnetic significance.

The Zijderveld orthogonal diagrams vary from site to site but contain one dominant component throughout demagnetization. This component has been extracted by LSF analysis. The isolated components have normal directions, confirming the observations made from the stereographic projections. The normal component was isolated between

TABLE 5.1

SPECIMEN	ISOLATED COMPONENT		RANGE
	DEC	INC	(DEG. C.)
CBY1.1	359 (336)	-57 (-35)	0-400
CBY1.2	40 (13)	-42 (-38)	300-500
CBY1.3	68 (7)	-60 (-63)	300-500
CBY2.2	33 (33)	-1 (-1)	300-400
CBY2.3	26 (351)	-56 (-43)	200-400
CBY2.4	33 (358)	-53 (-44)	620-680
CBY3.1	18 (347)	-56 (-40)	150-400
CBY3.2	31 (321)	-80 (-57)	300-500
CBY3.3	79 (53)	-35 (-54)	300-500
CBY4.2	30 (353)	-56 (-44)	400-500
CBY5.2	27 (358)	-50 (-39)	200-400
CBY5.3	20 (341)	-64 (-46)	100-300
CBY7.1	37 (11)	-44 (-25)	100-630
CBY7.2A	34 (9)	-46 (-27)	100-580
CBY7.3A	11 (6)	-23 (+4)	500-680
CBY8.2A	17 (349)	-60 (-29)	100-300
CBY8.3	28 (357)	-57 (-30)	200-400
CBY9.1A	43 (0)	-60 (-38)	100-300
CBY9.2	50 (3)	-59 (-41)	400-500
CBY9.2A	42 (8)	-52 (-33)	300-550
CBY11.2	72 (60)	-12 (-23)	400-500
CBY12.1	55 (19)	-46 (-35)	400-580
CBY12.1A	7 (351)	-49 (-17)	300-680
CBY13.2	26 (356)	-57 (-30)	630-675

CBY14.3	58	(10)	-50 (-37)	400-580
CBY14.3A	70	(23)	-42 (-41)	0-500
CBY4.1*	96	(68)	-41 (-66)	12-15
CBY10.2*	10	(354)	-45 (-14)	25-60
CBY12.3*	13	(351)	-55 (-24)	10-30
CBY13.3*	47	(0)	-62 (-41)	40-100
CBY14.1*	41	(10)	-43 (-23)	25-40

MEAN	N	R	K	CSD	DEC	INC	α_{95}
BEDDING CORRECTED	31	28.945	14.6	21.2	38.6	-51.4	6.5
UNCORRECTED	31	28.669	12.9	22.6	4.6	-36.5	7.5

Table 5.1 Extracted components from the Agua Dulce Formation, used for palaeomagnetic pole calculation (Table 5.5). *=AF demagnetized specimens, with range in mT. Figures in brackets are extracted components uncorrected for bedding. For explanation of symbols used see Table 3.2.

100-580 deg.C. and 10-60mT. The isolated components from the Agua Dulce Formation (Table 5.1), and resulting palaeomagnetic pole are discussed below.

Magnetic Mineralogy:

Sandstones: Discrete grains of haematite and martite are present in the volcaniclastic sandstones of the Agua Dulce Formation (section 7.2.1). Martite (Ramdohr,1969), is a common oxidation product of magnetite, formed through the growth of haematite along the octohedral (111) planes of the host magnetite crystal, resulting in a characteristic triangular texture (Plate 5.1). Haematite is also present as the oxidation product of biotite mica (Plate 5.2), and volcanic detritus (particularly ferromagnesian minerals). Haematite? and iron oxide stained clay minerals may be present as pore linings.

Lavas: Haematite is present as a brown alteration product, particularly in the more acidic flow-banded lavas.

IRM acquisition curves confirm the above observations. Figure 5.2c shows that neither the lavas or sandstones saturate in fields of up to 1.4 Tesla. This indicates that any magnetite originally present in martitised grains, has been completely replaced.

Interpretation: The NRM of both the lavas and sediments of the Agua Dulce Formation is carried by haematite, and is thought to have been acquired during a normal period of polarity of the Triassic magnetic field.

NRM acquisition of the lavas took place soon after eruption. A CRM was acquired during cooling through the oxidation of iron bearing minerals. The lavas cooled rapidly, as shown by the quenched nature of

Plate 5.1 PUR21 Martite. This grain contains the characteristic triangular martite texture. The light mineral is haematite, with dark relict lamellae of magnetite. Reflected light in oil, field of view=0.23mm. Purilactis Formation.

Plate 5.2 CBY5 Haematite alteration. Originally a grain of biotite mica, which has been completely pseudomorphed by haematite, but retains the characteristic phyllosilicate morphology. Reflected light in oil, field of view=0.23mm. Agua Dulce Formation.

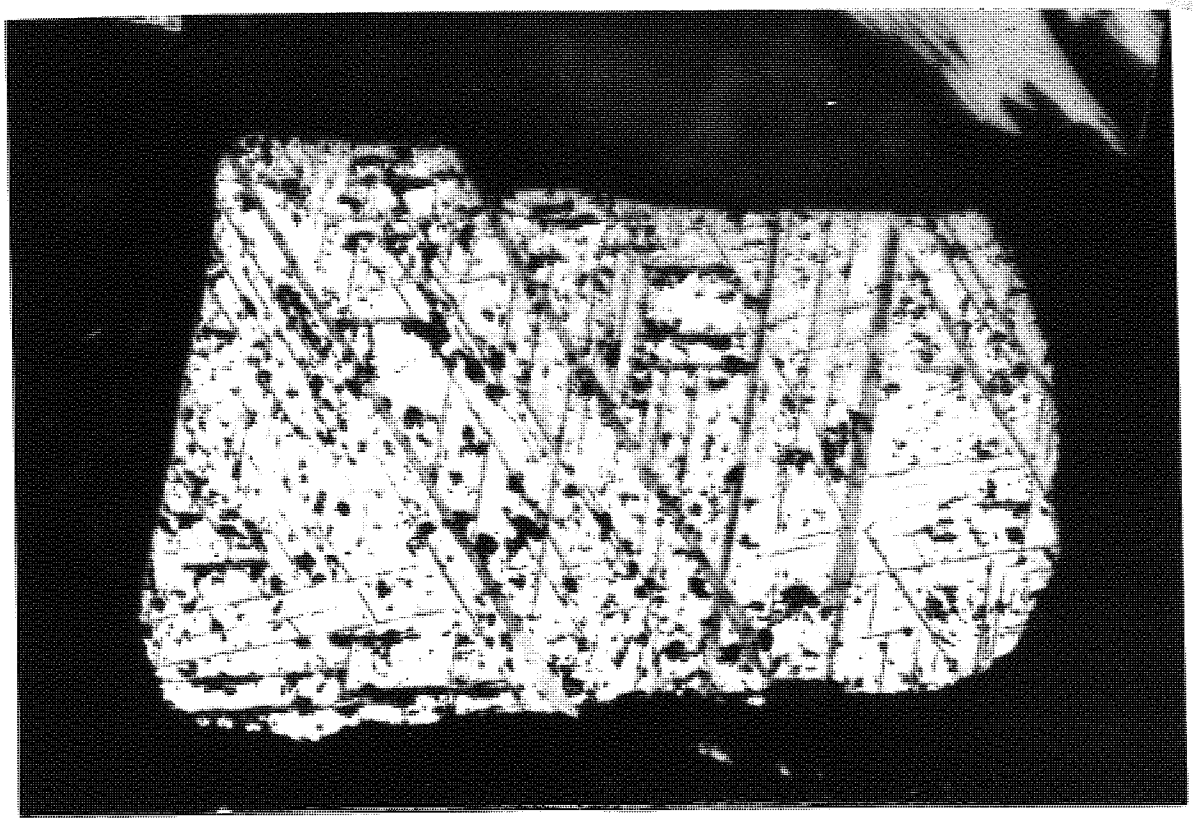

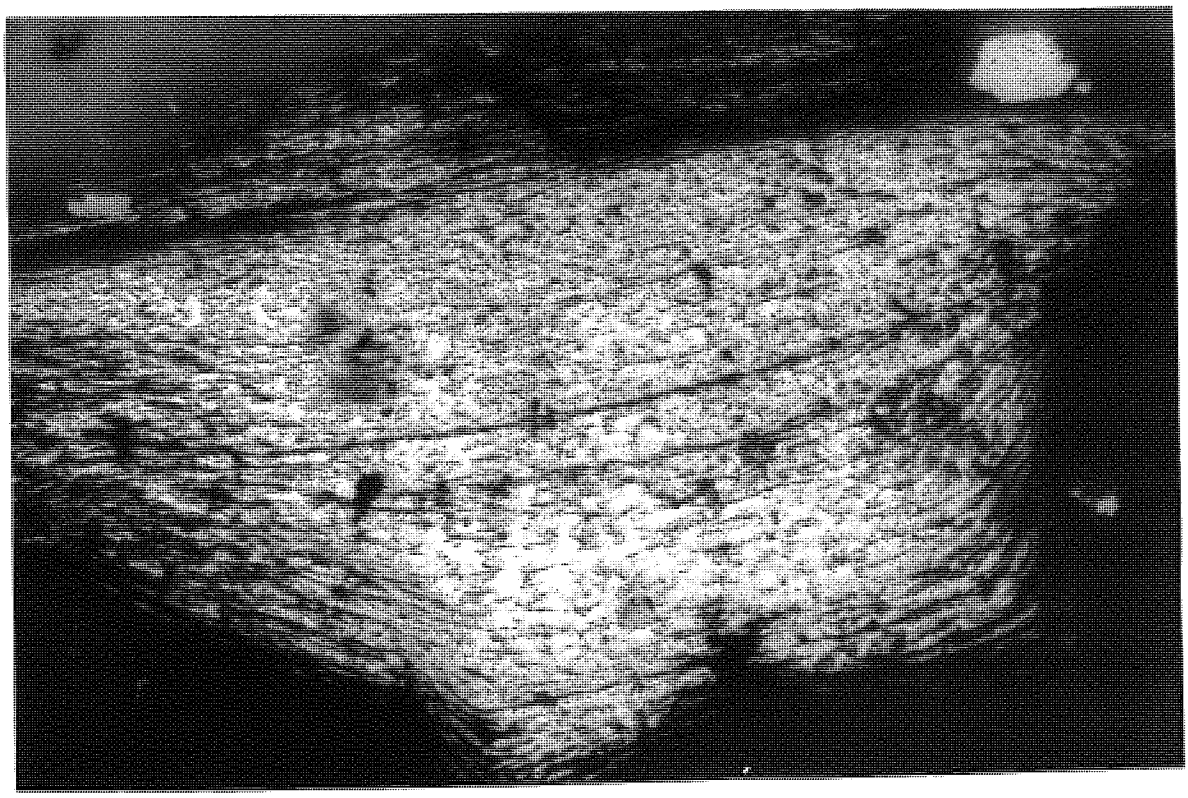

the groundmass (rapid cooling, would also prevent later alteration).

Diagenetic observations also indicate rapid remenance acquisition of the sediments, as a DRM/PDRM or early CRM. Rapid burial (marked pre-cement compaction), followed by early mono-mineralic (quartz) cementation (section 7.2.1). As no magnetite is present in the sandstones, it appears likely that the oxidation of magnetite and volcanic detritus took place in the source area, prior to deposition, resulting in a DRM.

Biotite oxidation is common (Plate 5.2), but this may take place relatively rapidly after deposition (Turner and Archer,1975). Iron oxide stained clay minerals present as pore linings in the sandstones, may originally have been infiltrated clay detritus (Walker et al.,1967), subsequently oxidised soon after deposition. Further burial of the sandstones resulted in the recrystallisation of the clay detritus to form illite or chlorite (both present on XRD traces, section 7.2.1). This process would release water and cations into the pore waters, resulting in a solution favouring further oxidation of any iron bearing minerals. This could result in a much later CRM than that recorded from a pre-burial near surface oxidative environment. However, as no other significant component has been isolated it can be assumed that either recrystallisation of the clay minerals took place soon after deposition indicating rapid burial, or no significant tectonic movement took place between deposition of the sediments and recrystallisation of the clay minerals.

In summary, the NRM of the Agua Dulce Formation was acquired rapidly after deposition or eruption, indicated by the identical components extracted from both the lavas and sandstones (Table 5.1).

Implying that NRM acquisition of the lavas and sediments took place at similar times.

5.4.2 Tonel Formation

A limited palaeomagnetic study was undertaken on the Tonel Formation, and associated high level intrusives (Fig. 5.1). Samples were collected from medium grained sandstones (2 sites, n=9) and green epidotised hornblende-rich dykes (4 sites, n=11). Although sampling of the Tonel Formation and associated intrusives was limited in terms of specimen/sample numbers, the palaeomagnetic results from these rocks are important in a stratigraphical context, as they bridge the gap between the underlying Agua Dulce Formation and overlying Purilactis Formation.

A tectonic correction was applied to TON6 and 7 (sandstones), but not to TON1, 2, 3 and 4, as they are exposed as apparently vertical dykes, relatively undisturbed by later tectonic events.

Sandstones: Two directions of initial NRM are present in the sandstones (Fig. 5.3a). Initial intensities are high ($98.6 \times 10^{-3} Am^{-1}$). Examination of the normalised intensity decay curves (Fig. 5.3b), indicates that during thermal demagnetization two thirds of the NRM is lost by 150 deg.C. Intensity remains constant up to 620 deg.C. where a marked blocking temperature is present, with complete demagnetization at 680 deg.C. Stereographic projections, Zijderveld orthogonal diagrams and LSF analysis all indicate the presence of one stable component of magnetization throughout demagnetization, with normal or reversed directions.

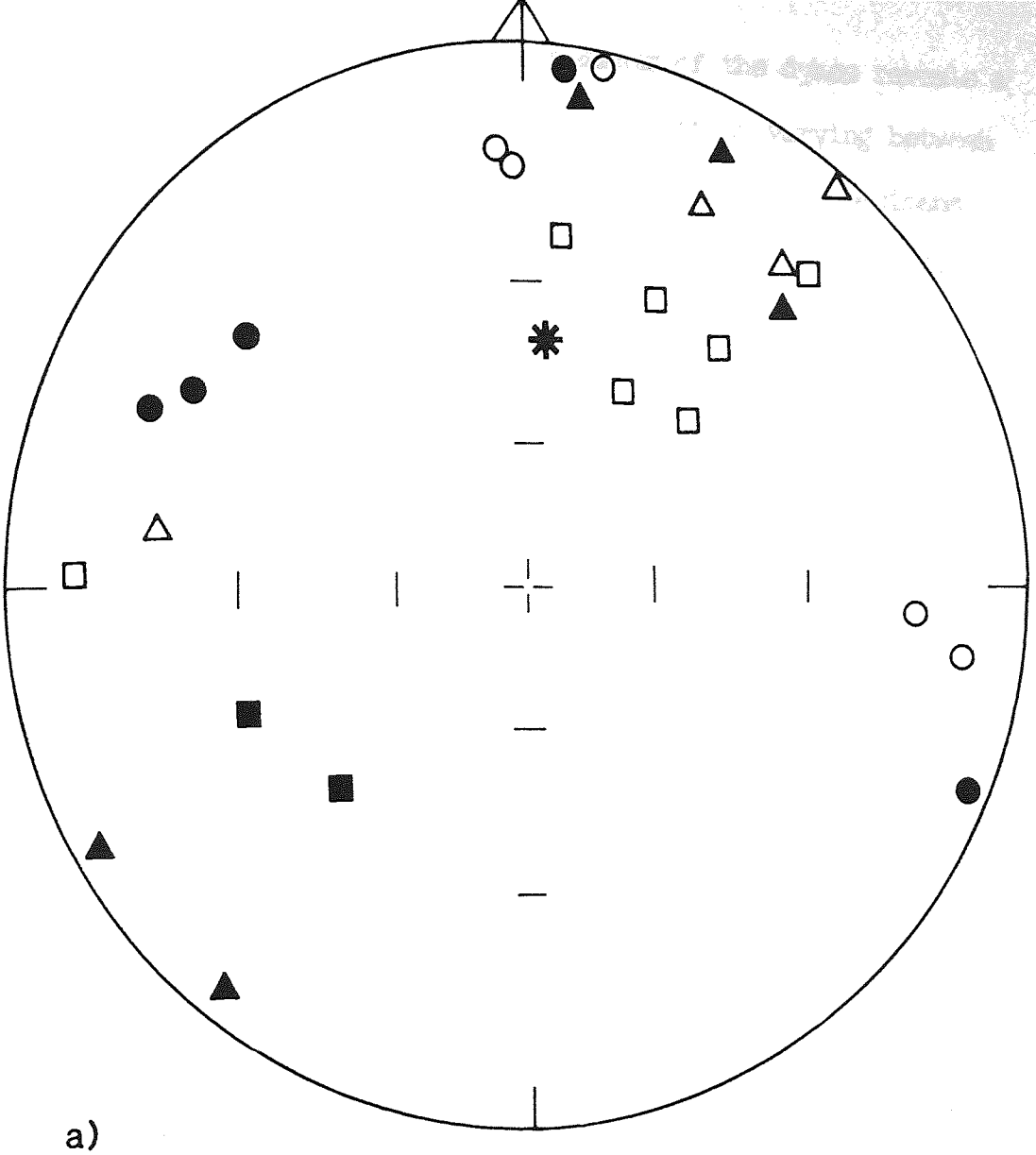

a)

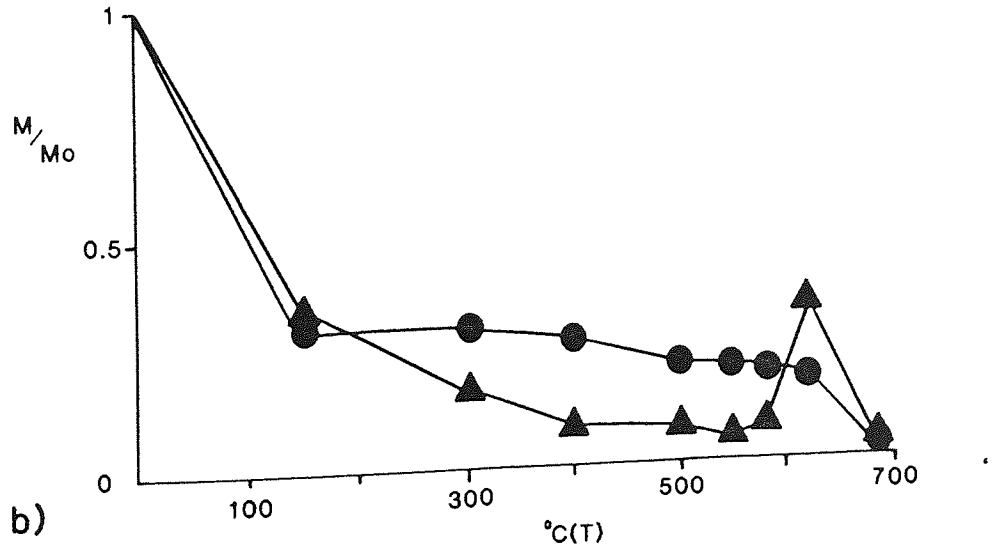

b)

Fig. 5.3a Equal area stereographic projection of initial NRM directions for the Tonel Formation. Tonel sandstones (▲) fiducially corrected, fiducially and structurally corrected (■), Tonel intrusives (●) fiducially corrected. Numbers=deg.C. Other details as Fig. 5.2a.

Fig. 5.3b Normalised intensity decay curves for Tonel sandstones (TON6.2●) and Tonel intrusives (TON2.2▲).

Tonel Intrusives: Initial NRM measurements of the dykes reveals a large degree of scatter (Fig. 5.3a), with intensities varying between 2.04 and 126.1x10^{-3}Am.$^{-1}$ During thermal demagnetization, all specimens lost 75% of their NRM by 150 deg.C., this was followed by a steady loss in intensity up to 580 deg.C. A marked increase in intensity is present at 620 deg.C. before complete demagnetization at 680 deg.C. (Fig. 5.3b). Stereographic projections, Zijderveld orthogonal diagrams and LSF analysis all indicate the presence of two components of magnetization (Table 5.2), these can be correlated with the normalised intensity curves. Up to 580 deg.C. a stable intermediate component of magnetization is present, this corresponds to a period of small intensity decrease or no decrease at all, on the decay curves (Fig. 5.3b). Above 580 deg.C and coincident with an intensity increase, a reversed or normal component is present (Table 5.2).

The magnetic mineralogy of the sandstones is characterised by the presence of haematite overgrowths on detrital haematite (possibly originally magnetite) and ilmenohaematites (Plate 5.3). Martitisation of original magnetite is also common.

The dykes contain discrete magnetite crystals and limonite (iron hydroxide), the oxidation product of original sulphide minerals.

Interpretation: TON6 and 7 (sandstones), acquired their NRM during a polarity reversal of the Earth's magnetic field. This follows as the specimens show very similar behaviour during demagnetization, whether containing normal or reversed components of magnetization. The NRM is thought to be a combination of DRM and PDRM(CRM). Preliminary diagenetic observations indicate relatively rapid cementation preventing extensive oxidation of any iron bearing minerals. This

TABLE 5.2

UNIT		N	R	K	CSD	DEC	INC	α_{95}	TEMP. (DEG. C.)
TONEL INTRUSIVES		11	9.262	6.5	28.3	233	+38	19.9	500-680
(TON1,2,3,4)		9	8.223	10.3	25.2	37	-30	16.8	150-500
SANDSTONES	CORR.	6	5.646	14.1	21.5	235	+21	18.5	500-680
(TON6,7)	UNCORR.	6	5.649	14.2	21.5	233	-6	18.5	
	CORR.	6	5.790	23.8	16.6	31	-30	14.0	0-400
	UNCORR.	6	5.792	24.2	16.5	30	+1	14.0	

Table 5.2 Extracted normal and reversed components from the Tonel Formation and associated intrusives, used for palaeomagnetic pole calculation (Table 5.5). CORR.=bedding corrected, UNCORR.=Components uncorrected for bedding. For explanation of symbols see Table 3.2.

theory is also supported by the relatively simple (one component) history of magnetization. Although complete remagnetization could also produce this behaviour, it would result in only one stable component, not the two antiparallel components present in the Tonel Formation (Table 5.2).

Authigenic haematite (not present in all samples) must contribute to the NRM of the sandstones as a PDRM. If the precipitation of haematite took place in a magnetic field of opposite polarity to the DRM of the sandstones, it may result in the phenomenon observed in site TON6. TON6 contains a reversed component in 3 specimens (possibly a DRM in origin), whereas, the three other specimens from the site contain a stable normal component (possibly a CRM in origin carried by authigenic haematite), which may have been superimposed on the original DRM. As the normal and reversed components are antiparallel (Table 5.2), no significant tectonic movement between the DRM and PDRM acquisition of the sandstones.

Two possibilities could explain the NRM acuisition of the Tonel intrusives:

1) Intrusion could have taken place during a period of fluctuating polarity of the Earth's magnetic field, indicated by the high temperature (>580 deg.C.) reversed and normal components. Subsequent cooling in an intermediate field led to the acquisition of an intermediate component of magnetization below 580 deg.C.

2) Alternatively it is possible that the dykes have been remagnetized, after cooling during changes of the ambient magnetic field. This is supported by the extensive alteration (epidotisation, chloritisation and limited sulphide mineralisation), of the rocks. As the normal and reversed components are only present above 580 deg.C. they may be

Plate 5.3 TON7 Haematite overgrowths. A detrital grain of ilmenite with haematite exsolution (c.f. Plate 4.4), which forms the darker part of the grain. The lighter parts of the grain (arrowed), are irregularly shaped overgrowths of haematite. Overgrowths would not be preserved, if the grain had been transported any distance, indicating that they formed "in situ". Reflected light in oil, field of view=0.23mm. Tonel Formation.

Plate 5.4 PUR21 Haematite alteration. The large grain (volcanic detritus?) in the centre and the small grain at the top of the photomicrograph, have been partially altered to haematite around the edges and along fractures. The smaller grain to the right of the large grain, displays the characteristic triangular martite texture. Haematite (light) has almost completely replaced magnetite (darker relict lamellae in the centre of the grain). Reflected light, field of view=0.56mm. Purilactis Formation.

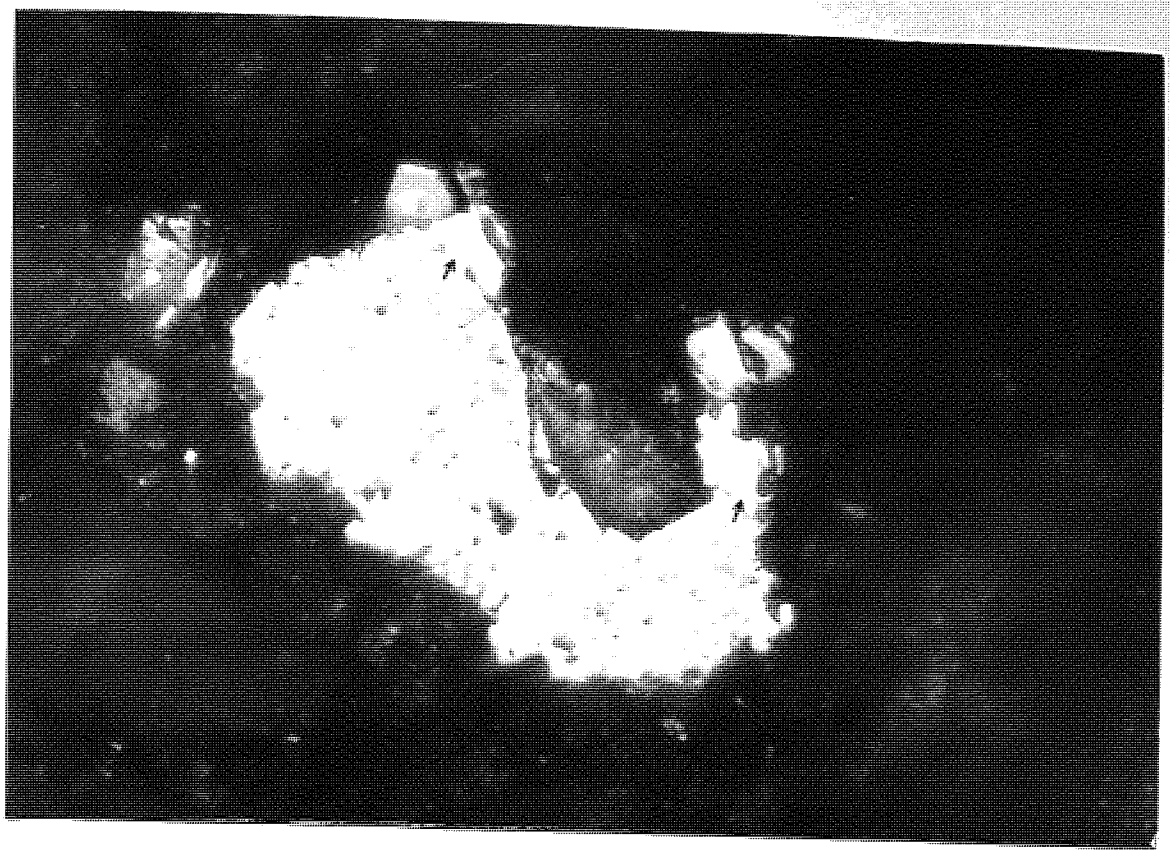

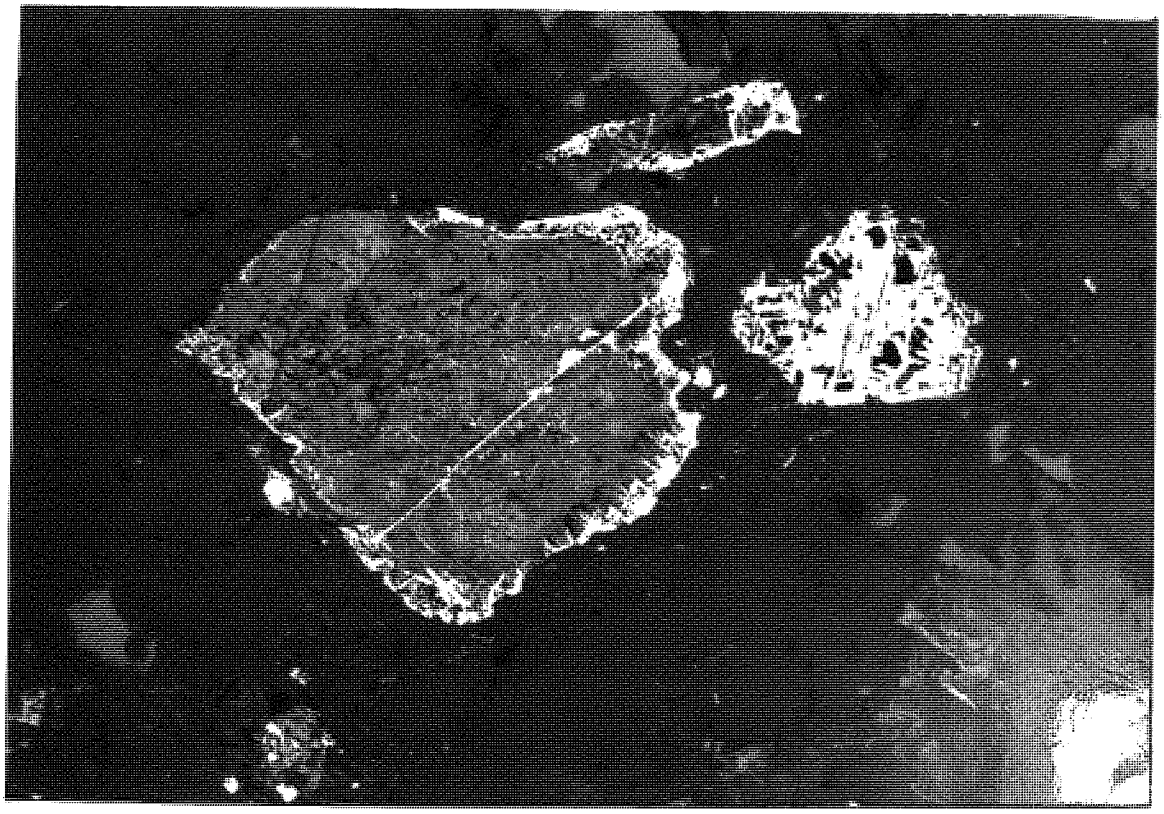

carried by haematite which may not necessarily be of primary magmatic origin (section 3.4.1), it could have formed through the secondary oxidation of magnetite associated with hydrothermal fluids, or surface weathering. The overlying Purilactis Formation contains extensive epidote cements (section 7.2.2). It is possible that epidotisation and ?remagnetization of the Tonel and Purilactis Formations took place at this time (see discussion).

In summary, the time of NRM acquisition of the Tonel intrusives is uncertain. It may have been relatively soon after intrusion, or post the deposition of the Purilactis Formation. However, the similarity between the isolated components from the dykes and sandstones (Table 5.2), indicates that whatever the time gap between NRM acquisition, no significant tectonic movement or shift in the Earth's magnetic field occurred, consequently the components were probably acquired at the same time.

5.4.3 Purilactis Formation

Sampling was undertaken on fine, medium and coarse grained sandstones (with the exception of PUR21 a granulestone), from an area of the Formation that has undergone limited epidotisation (Fig. 5.1). Sixteen sites yielded 81 specimen cores.

Initial NRM directions are scattered (Fig. 5.4a), but are located predominantly in the NW quadrant. Intensities of NRM vary greatly from 1.09 to 364.5x10^{-3}Am.$^{-1}$, but usually range between 3 and 50x10^{-3}Am.$^{-1}$

Examination of the normalised intensity decay curves for individual sites, reveals a wide variety of behaviour during demagnetization. For thermally demagnetized specimens two main groups (with gradations between the two), can be differentiated:

Group 1 (Fig. 5.4b): This group has a rapid initial intensity loss to 300 deg.C. (50-70% of NRM lost). The curve then remains constant, or shows a slight decrease in intensity up to 550/580/620 deg.C. (depending on individual sites), where a marked blocking temperature is present, after this the specimens remain demagnetized.
Group 2 (Fig. 5.4b): This group shows little loss of initial NRM until 400/500 deg.C., where a marked blocking temperature is present. A second blocking temperature is present at 550/580/620 deg.C. (depending on individual sites), after which the specimens remain demagnetized.

It must be emphasised that the groupings distinguished above represent "end member" type behaviour, and that most specimens display behaviour of a transitional nature between the two groups.

Specimens subjected to AF demagnetization show a rapid initial intensity decrease, with a MDF between 20 and 40mT. At higher fields (up to 100mT.) the intensity gradually decreases, where up to 40% of the original NRM may remain.

Examination of the stereographic projections of directional change reveals variable site behaviour. Most sites show stable reversed directions below 550 deg.C., and move to normal positions above 550 deg.C. (Fig. 5.4c). However, not all sites display this behaviour; some (PUR28,29,30,33) show little directional change and remain in a reversed position throughout demagnetization. Some sites (PUR21,31) contain intermediate components of magnetization positioned in the NW quadrant, similar to the initial NRM directions.

Examination of the Zijderveld orthogonal diagrams allows the definition of 1, 2 and 3 component systems of magnetization. A broad correlation can be made between stereographic projection analysis and

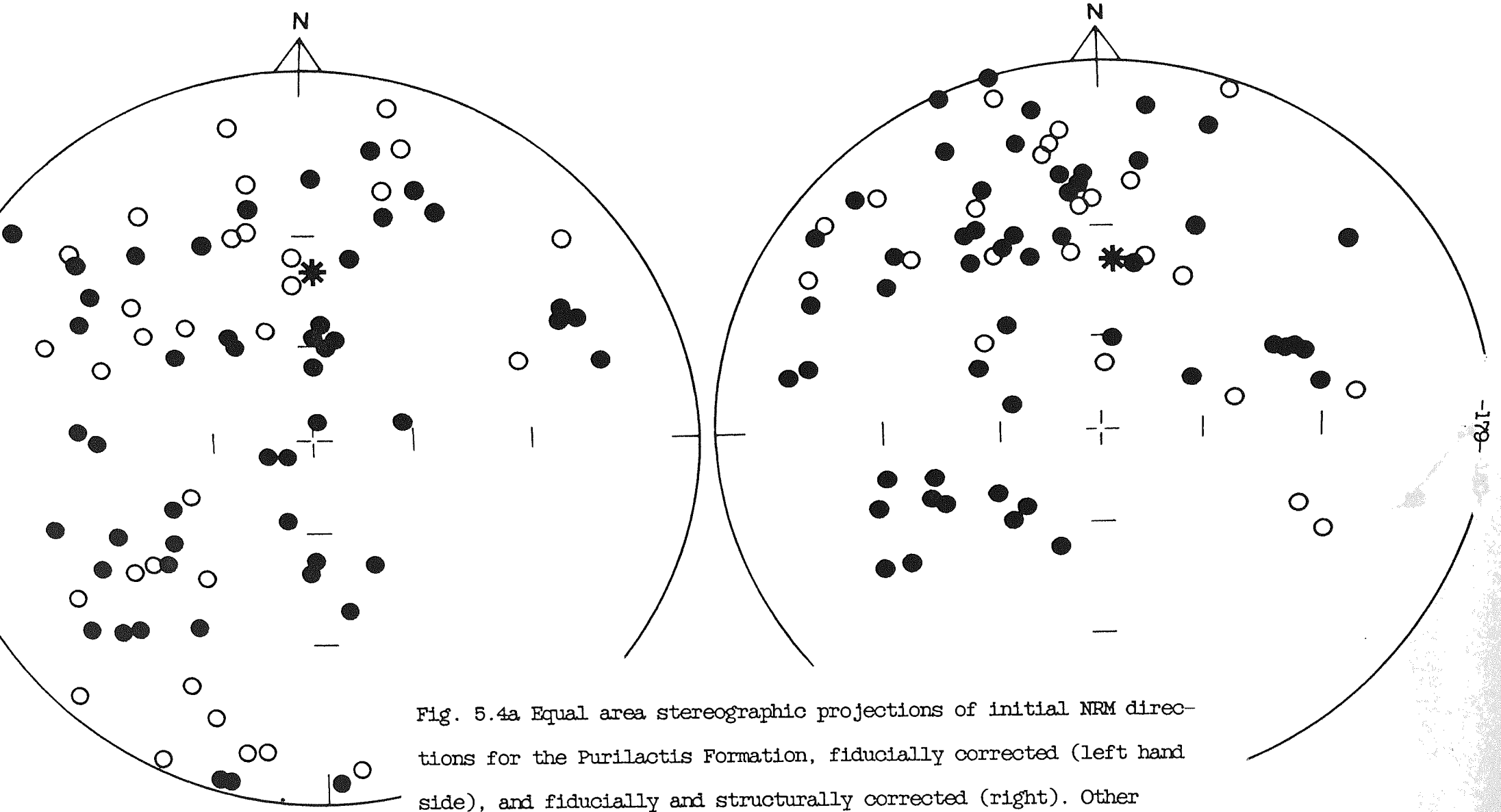

Fig. 5.4a Equal area stereographic projections of initial NRM directions for the Purilactis Formation, fiducially corrected (left hand side), and fiducially and structurally corrected (right). Other details as Fig. 5.2a.

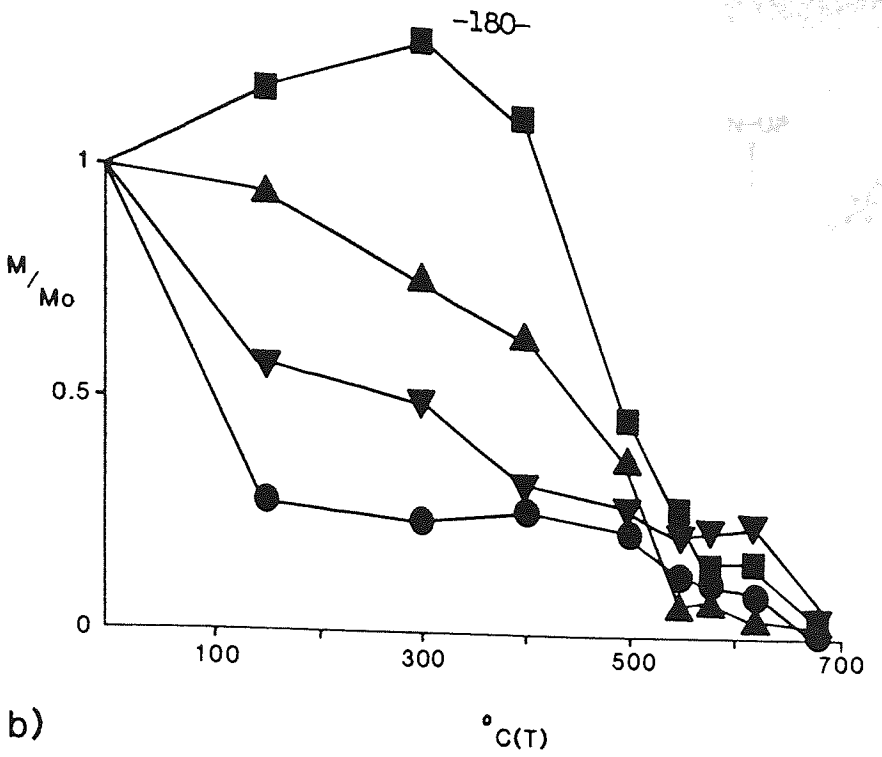
-180-
1
M/Mo
0.5
0
100
300
500
700
°C(T)

b)

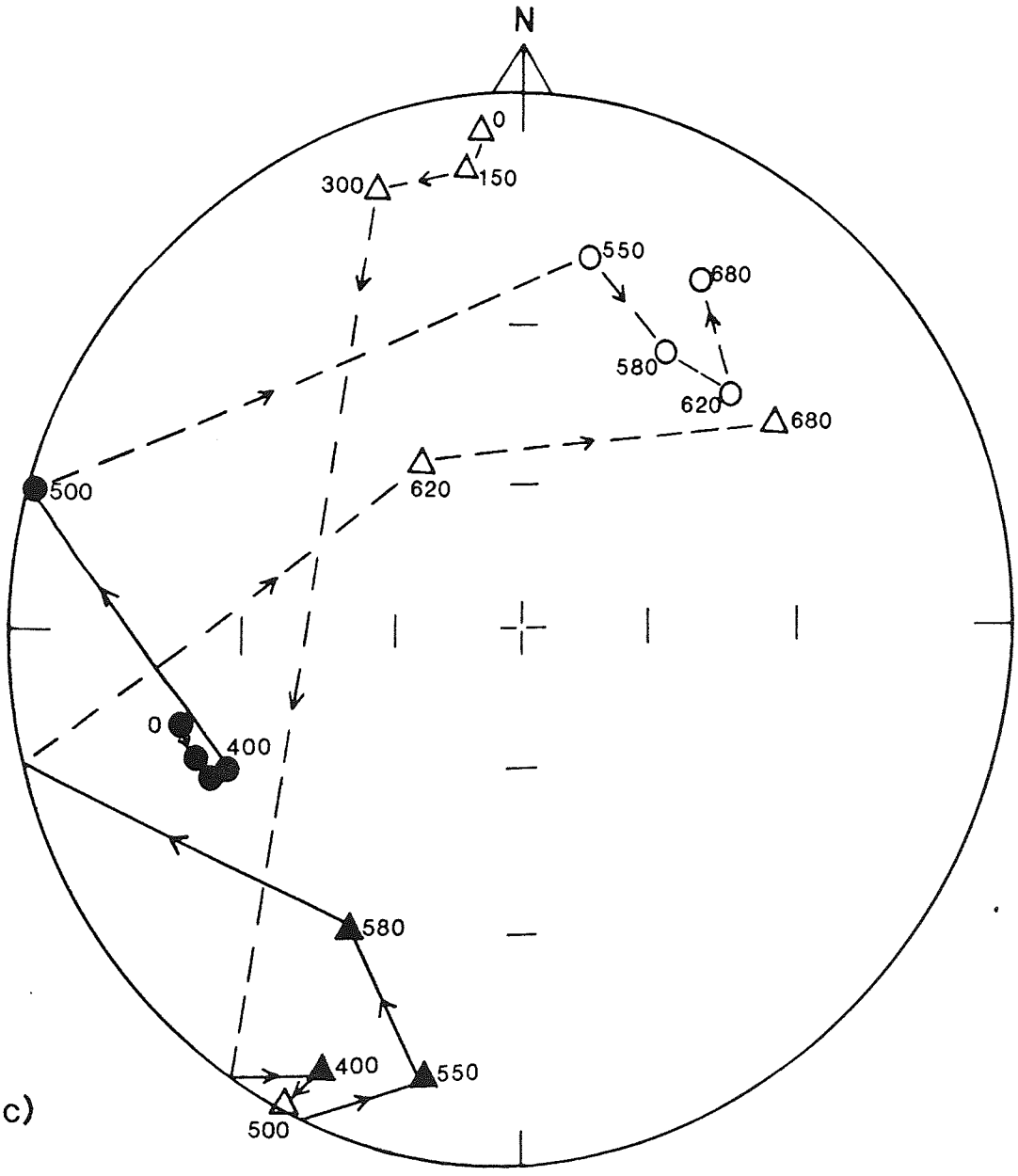
N
0
150
300
550
680
580
620
680
500
620
0
400
580
400
550
500

c)

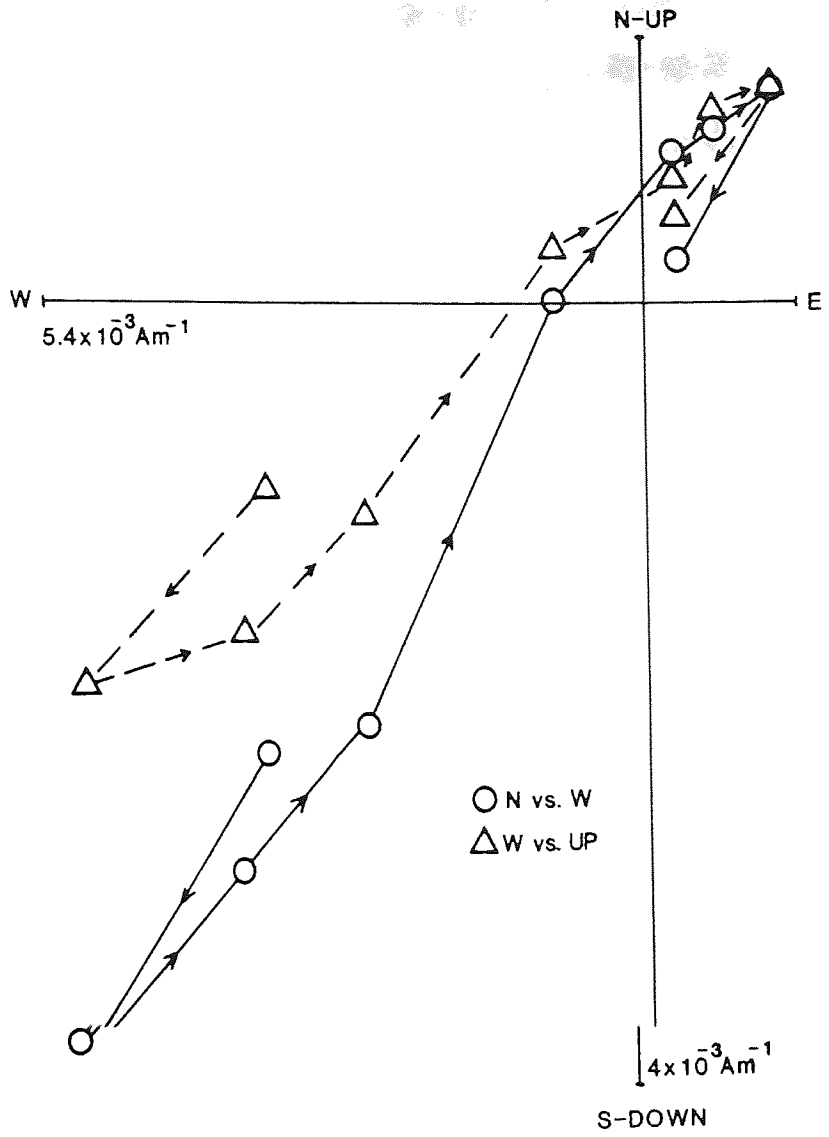

d)

Fig. 5.4b Normalised intensity decay curves for the Purilactis Formation, PUR26.4▼, PUR29.1■ and PUR31.1▲.

Fig. 5.4c Equal area stereographic projections of directional change for the Purilactis Formation, PUR26.1▲ and PUR32.3. Other details as Fig. 5.2a.

Fig. 5.4d Zijderveld orthogonal diagram for PUR32.3. Numbers=deg.C. .

Fig. 5.4e IRM acqisition curves for PUR2●, PUR27▲ and PUR36■.

Fig. 5.4f IRM acquisition curves for PUR7● and PUR21▲.

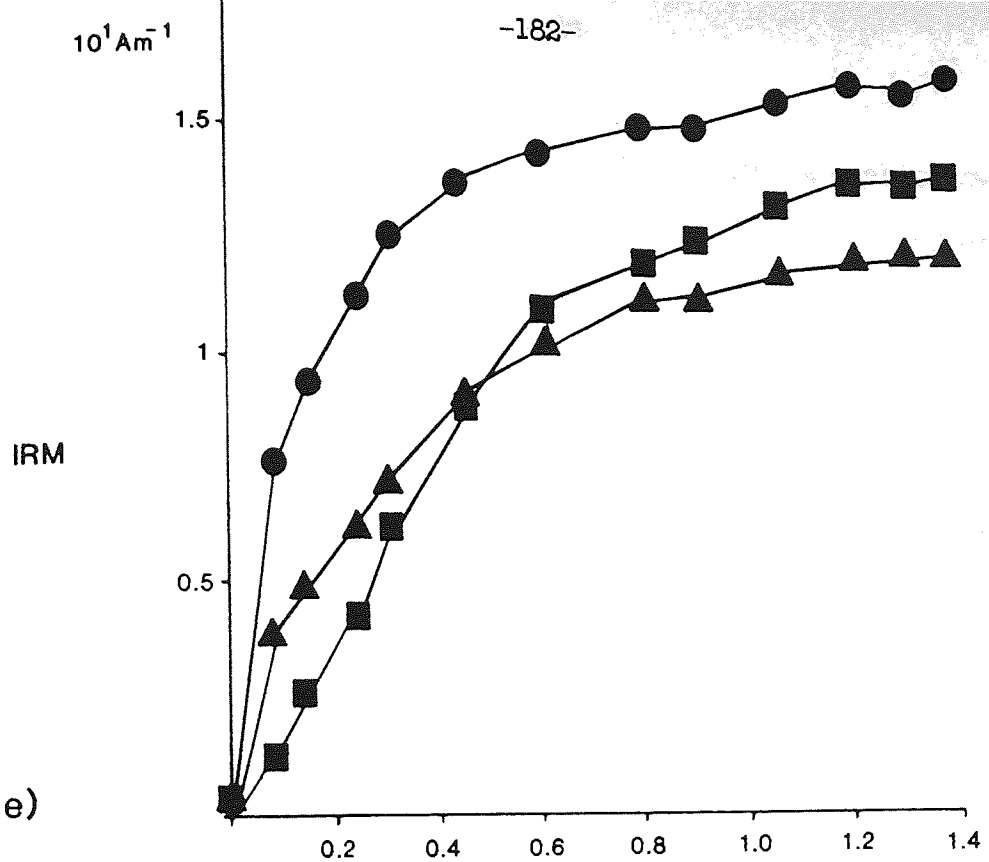
$10^1 Am^{-1}$
1.5
1
0.5
IRM
0.2
0.4
0.6
0.8
1.0
1.2
1.4
Tesla

e)

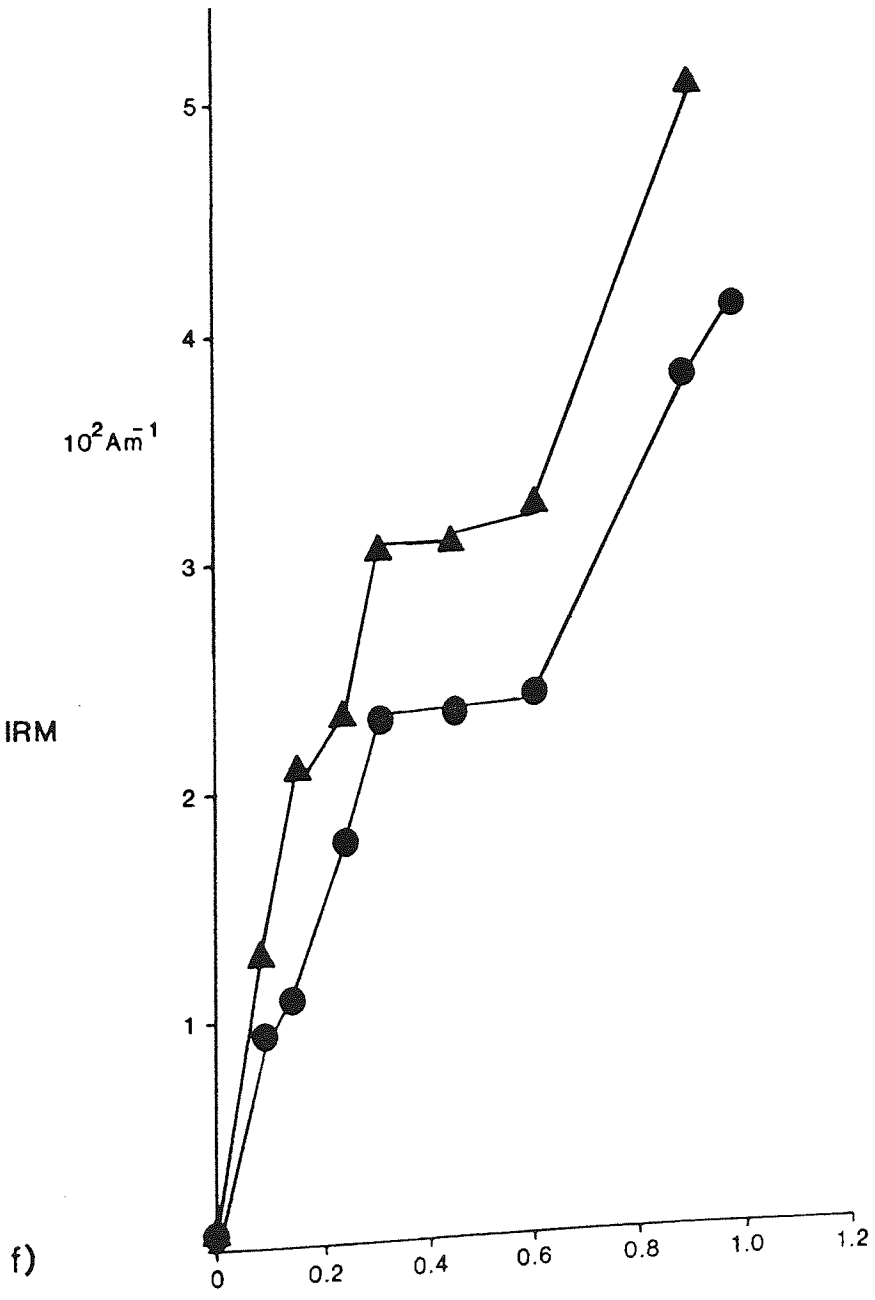
5
4
3
2
1
$10^2 Am^{-1}$
IRM
0
0.2
0.4
0.6
0.8
1.0
1.2

f)

the Zijderveld orthogonal diagrams. PUR32 contains a stable low temperature reversed component during demagnetization up to 550 deg.C., above this temperature a normal component is present. Zijderveld orthogonal diagrams for PUR32 contain two components of magnetization, which represent the normal and reversed components identified on the stereographic projections (Figs. 5.4c,d). A similar correlation can be seen for Zijderveld diagrams with one component, in which the stereographic projections show little or no directional change during demagnetization. This correlation is also present for sites with three component Zijderveld diagrams (PUR28,29,30 and 33). In these sites a low blocking temperature component is removed by 300 deg.C. before a stable reversed component is established between 300 and 550 deg.C., above 550 deg.C. a normal component of magnetization is dominant.

The isolated components (Table 5.3), reflect the above observations. Components identified below 550 deg.C. have dominantly reversed orientations, components above 550 deg.C. have mainly normal orientations. Both these components have been used to calculate a palaeomagnetic pole for the Purilactis Formation (Table 5.3).

Magnetic Mineralogy:

Haematite is the dominant magnetic mineral. It occurs as discrete detrital crystalline grains, and as an alteration product of magnetites and titanomagnetites (Plate 5.1). It is also common as an alteration product of volcanic detritus, particularly where original magnetite was present in the groundmass, commonly forming an authigenic rim around the original grain (Plate 5.4). It also forms as the oxidation product of detrital biotite micas and ferromagnesian

TABLE 5.3

SITEE	N	R	K	CSD	DEC	INC	α_{95}	RANGE (DEG. C.)
PUR2	6	5.52	10	17.2 (35.3)	20 (352)	-26 (-37)	19.9 (32.2)	500-620
PUR7	5	4.76	17	19.8 (26.5)	58 (71)	-46 (-15)	19.3 (26.4)	500-620
PUR23	5	4.82	23	17.1 (24.5)	201 (190)	+31 (+47)	16.5 (24.2)	300-580
PUR24	6	5.83	44	12.2 (16.5)	220 (215)	+34 (+41)	10.2 (14.0)	400-620
PUR25	6	5.88	40	12.7 (12.9)	215 (204)	+35 (+48)	10.7 (10.8)	300-580
PUR26	5	4.71	14	22.0 (24.5)	234 (229)	+39 (+52)	19.7 (24.2)	400-550
PUR28	7	6.49	12	23.7 (26.6)	236 (262)	+40 (+73)	18.5 (20.9)	500-620
PUR29	5	4.77	18	19.3 (35.9)	209 (210)	+34 (+50)	18.8 (37.7)	300-550
PUR30	3	2.99	999	2.5 (14.9)	209 (183)	+47 (+31)	3.8 (23.1)	300-550
PUR32	7	6.95	109	7.8 (7.0)	238 (233)	+39 (+33)	5.6 (5.5)	150-500
MEAN	10	9.74	35	13.8 (24.6)	219 (211)	+38 (+46)	8.6 (15.4)	

Table 5.3 Extracted normal and reversed components from the Purilactis Formation, used for palaeomagnetic pole calculation (Table 5.5). Excluded sites include PUR21 and 31 both of which contain dominantly intermediate components. For explanation of symbols see Tables 3.2 and 5.1.

An F-test (McElhinney,1964) was undertaken on the Purilactis Formation, and showed that at the 95% significance level the extracted components from both the bedding corrected and uncorrected populations were statistically different, consequently, the palaeomagnetic fold test is positive.

minerals. Magnetite rarely occurs as discrete detrital grains, but is sometimes present as relict cores to martitised grains.

Six sites were selected for IRM analysis. Four sites contained only haematite (Fig. 5.4e), whilst the other two contained both haematite and magnetite (Fig. 5.4f). This confirms the above petrographic observations, indicating that haematite is the main carrier of NRM in the Purilactis Formation, and also that most detrital magnetite had been converted to martite either prior to or during the early stages of diagenesis.

Interpretation: Three components of magnetization are present in the Purilactis Formation:

1) A low blocking temperature component removed by 300 deg.C. The component plots close to the present day axial dipole direction for the area, and its probable recent acquisition is supported by its similarity to the dominant initial direction of NRM (Fig. 5.4a), and its relatively rapid removal at low temperatures (coincident with a rapid initial intensity loss; Fig. 5.4b). The component is not present in all specimens, and in others may persist at temperatures higher than 300 deg.C.

The component is thought to be carried by authigenic haematite, which has formed through the oxidation of iron bearing minerals exposed at surface outcrop.

2) A stable reversed component present above 150/300 deg.C. and below 500/550 deg.C. The component is coincident with a period of little or no decrease in intensity on the normalised intensity decay curves (Fig. 5.4b), and must be carried by detrital magnetite (and any other

detrital magnetic minerals), as a reversed component is not present above 580 deg.C. (the curie temperature of magnetite).

In summary after removal of the low blocking temperature component, the remaining NRM is thought to be a DRM/PDRM, carried by detrital magnetite (martite) and haematite, present as discrete grains.

3) A stable normal component present between 500 and 620 deg.C., which must be carried by haematite. Detrital haematite is thought to carry a reversed component of magnetization (see above), therefore the normal component must be carried by authigenic haematite. The component may have formed as a CRM, whilst the sediments were still in an oxidising environment, prior to burial and cementation (section 7.2.2), as the normal and reversed components are antiparallel (Table 5.3), indicating that they may have been acquired within a short time span of each other.

In conclusion, a low blocking temperature component is thought to have been acquired in recent geological time, due to the oxidation of iron bearing minerals resulting from surficial exposure. This may result from uplift, however the similarity of the component to the present axial dipole field, indicates that the component is Recent in origin.

Important points regarding the above interpretation is the ability of magnetic minerals to be remagnetized and the identification of authigenic magnetic phases. Cleaning of samples (demagnetization), is undertaken to remove secondary components of magnetization acquired by the relaxation of single or multidomain particles, which have been

realigned in the Earth's magnetic field subsequent to the acquisition of the original NRM.

In line with this concept, high temperature components extracted from samples during demagnetization, should record an older magnetization since grains with lower blocking temperatures will be preferentially remagnetized. This "first in, last out" concept is true for both haematite and magnetite, but above 580 deg.C. (the Curie temperature of magnetite), only haematite retains any NRM. So, extracted components above 580 deg.C. must be carried by haematite. Consequently, if haematite formed later (as a CRM) than magnetite (as a DRM/PDRM), any component extracted above 580 deg.C., will not reflect the oldest magnetic component; as seen in the Purilactis Formation.

The variation from site to site in the temperature required to remove the low blocking temperature viscous component from the Purilactis Formation, is probably due to the ease at which oxidising fluids can penetrate strata, ie. impervious sandstones will suffer little oxidation, whereas porous, permeable sandstones will provide easy access to iron bearing minerals for oxidising fluids.

The reversed component is thought to represent an original DRM, carried by detrital haematite and magnetite (martite). The normal component is thought to be a CRM carried by authigenic haematite.

5.4.4 Paciencia Group

To complete the regional stratigraphical traverse of the Andean Precordillera, a palaeomagnetic collection was made from the Oligo-Miocene Paciencia Group (Fig. 5.1), from which 13 sites yielded 64 specimen cores. Samples were collected from medium and coarse grained

sandstone horizons throughout the Artolla Member (Flint,1985a) of the Paciencia Group.

The initial intensity of NRM varied between 7.5 and $114 \times 10^{-3} Am.^{-1}$, but is concentrated between 10 and $60 \times 10^{-3} Am.^{-1}$ Initial directions of NRM show a large degree of scatter (Fig. 5.5a).

Examination of the normalised intensity decay curves, indicates that one type of behaviour during demagnetization is dominant in 9 sites (Fig. 5.5b). This involves a rapid intensity decrease during thermal demagnetization, with 50% of NRM lost by 150 deg.C. and 75% by 300 deg.C. Between 300 and 500 deg.C.the intensity of NRM remains constant or shows a slight decrease. A marked blocking temperature is often present at 500/550 deg.C. A slight increase in intensity may take place at 580 deg.C. prior to complete demagnetization at 680 deg.C. Examination of the stereographic projections of these sites, reveals little directional change during demagnetization. The stable components may show normal (eg. sites SBT13,14,16), intermediate steeply inclined (eg. sites SBT1,2,5) or intermediate shallowly inclined (eg. sites SBT4,18) components of magnetization. This stable one component behaviour is also reflected by the isolated components (Table 5.4), and the Zijderveld orthogonal diagrams. The Zijderveld diagrams indicate the presence of one dominant stable component throughout demagnetization, but may reveal the presence of a viscous component between 0 and 300 deg.C. Above 580 deg.C. a second component of magnetization is present in some sites (Fig. 5.5c).

Sites SBT6 and 8 show similar behaviour during demagnetization to sites SBT1,2,4,5,13,14,16 and 18, but the normalised intensity decay curves do not show a rapid initial intensity loss (Fig. 5.5b). SBT10 and 15 show characteristics of both types of decay curve.

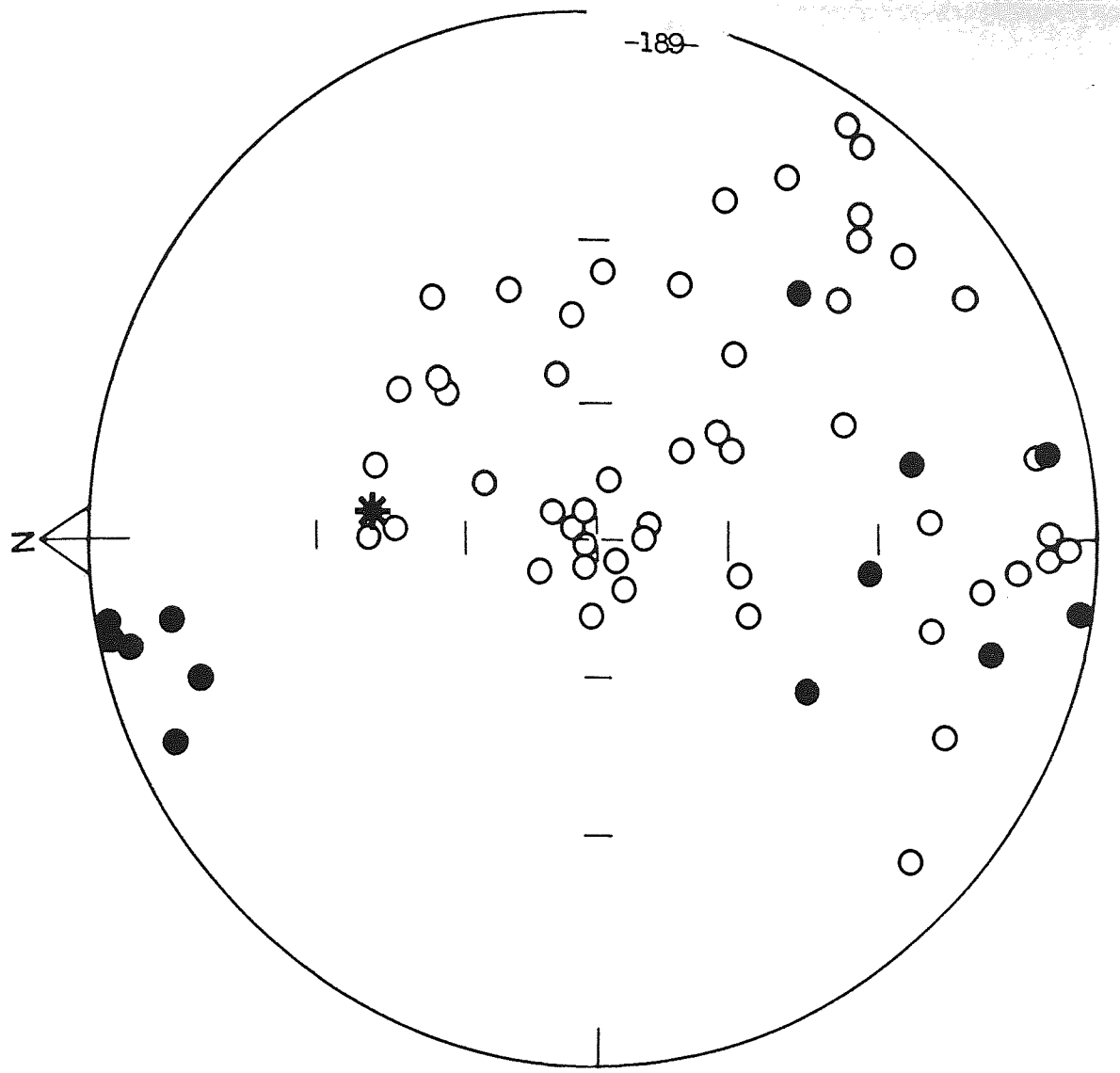
N

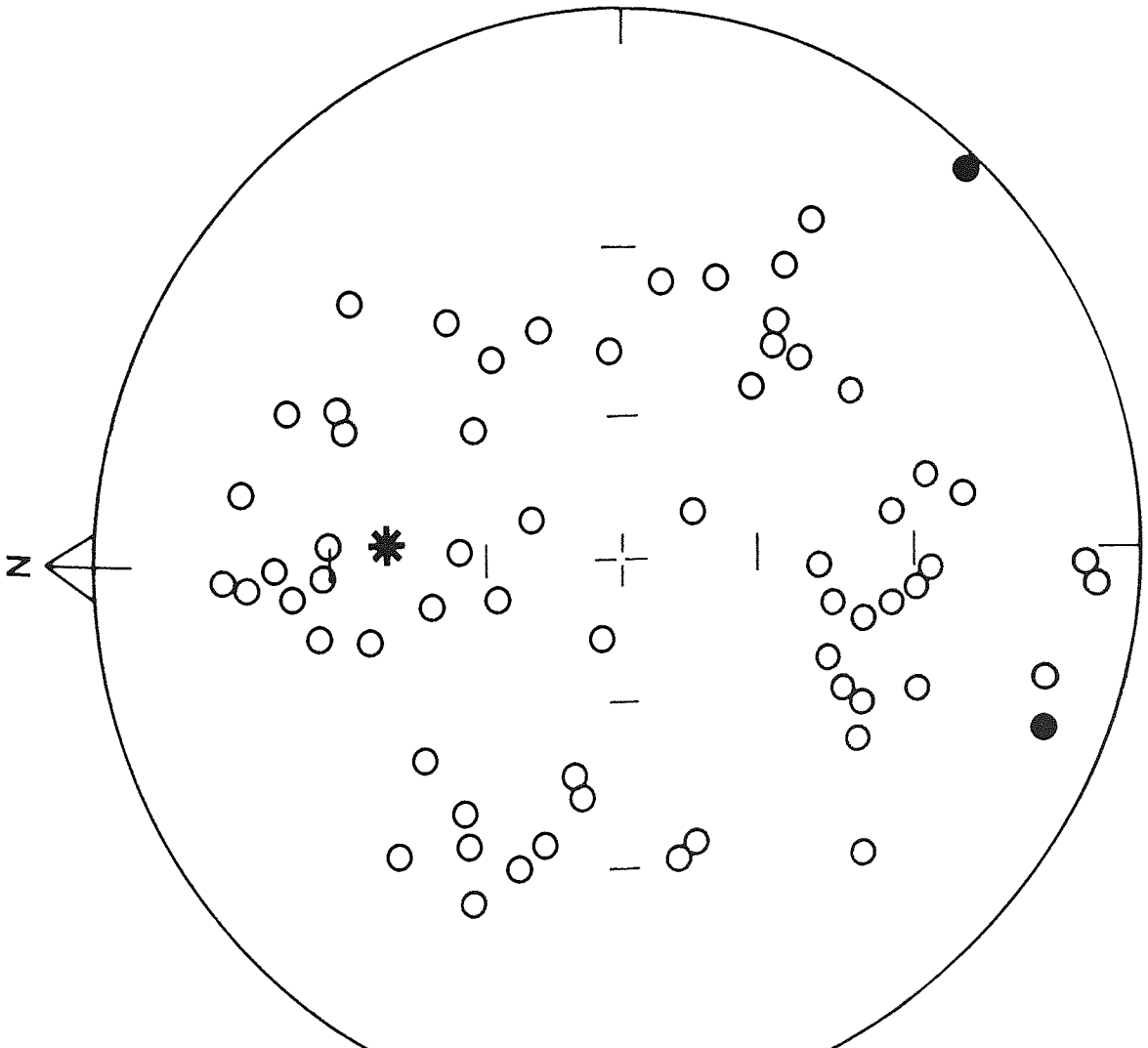
N

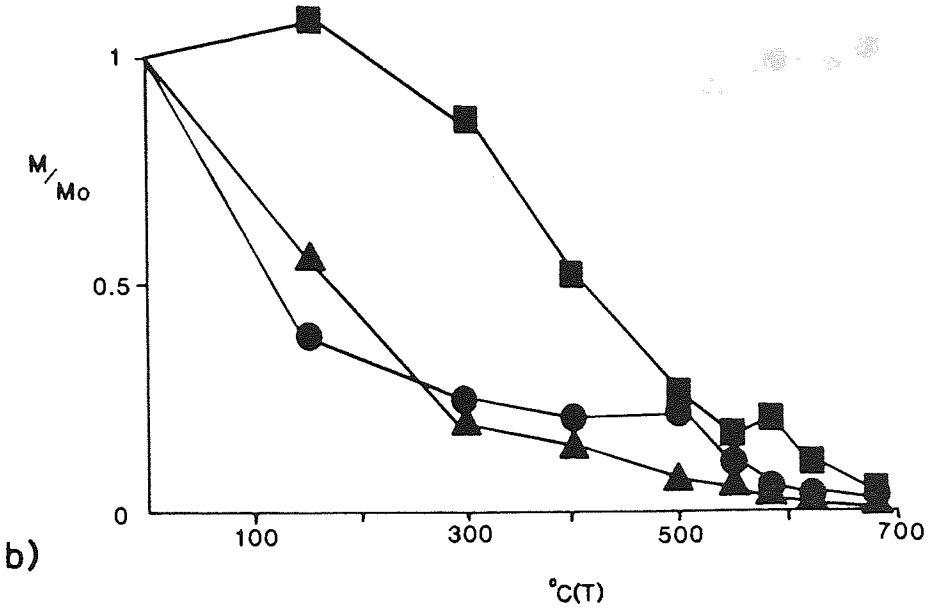
1
0.5
0
M/Mo
100
300
500
700
°C(T)

b)

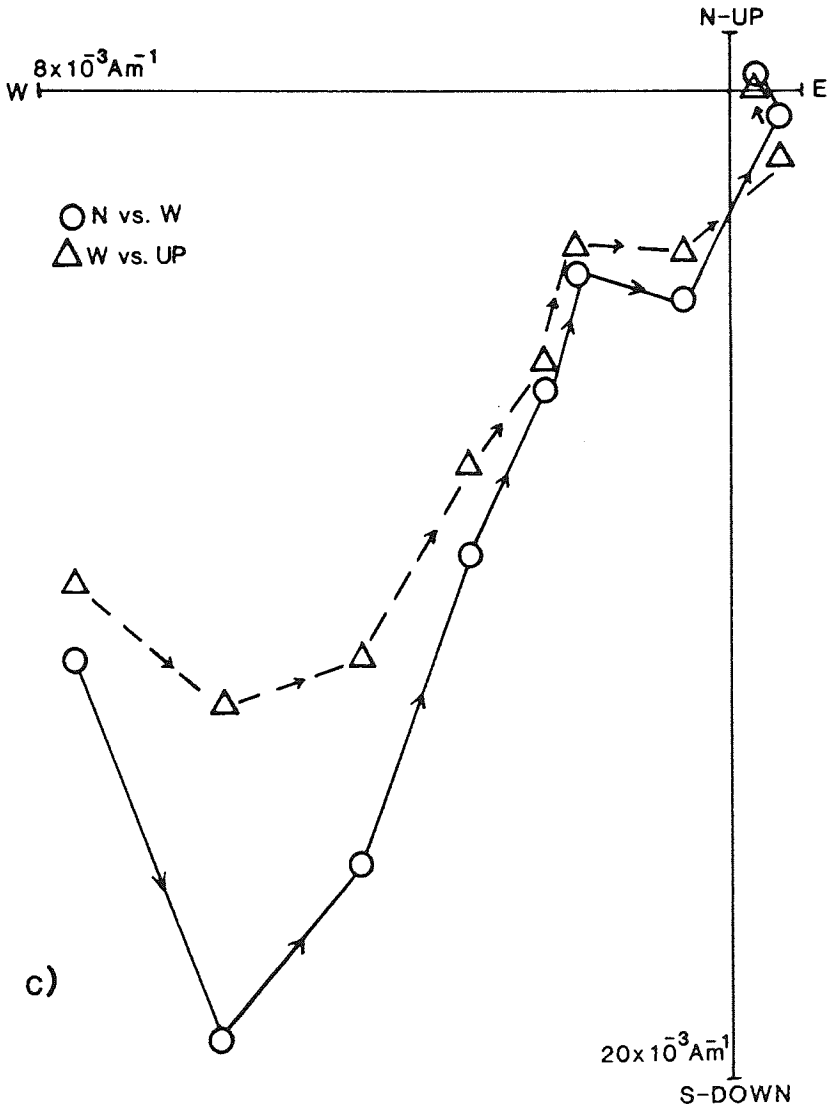
N-UP
8x10⁻³Am⁻¹
W
E
N vs. W
W vs. UP
20x10⁻³Am⁻¹
S-DOWN

c)

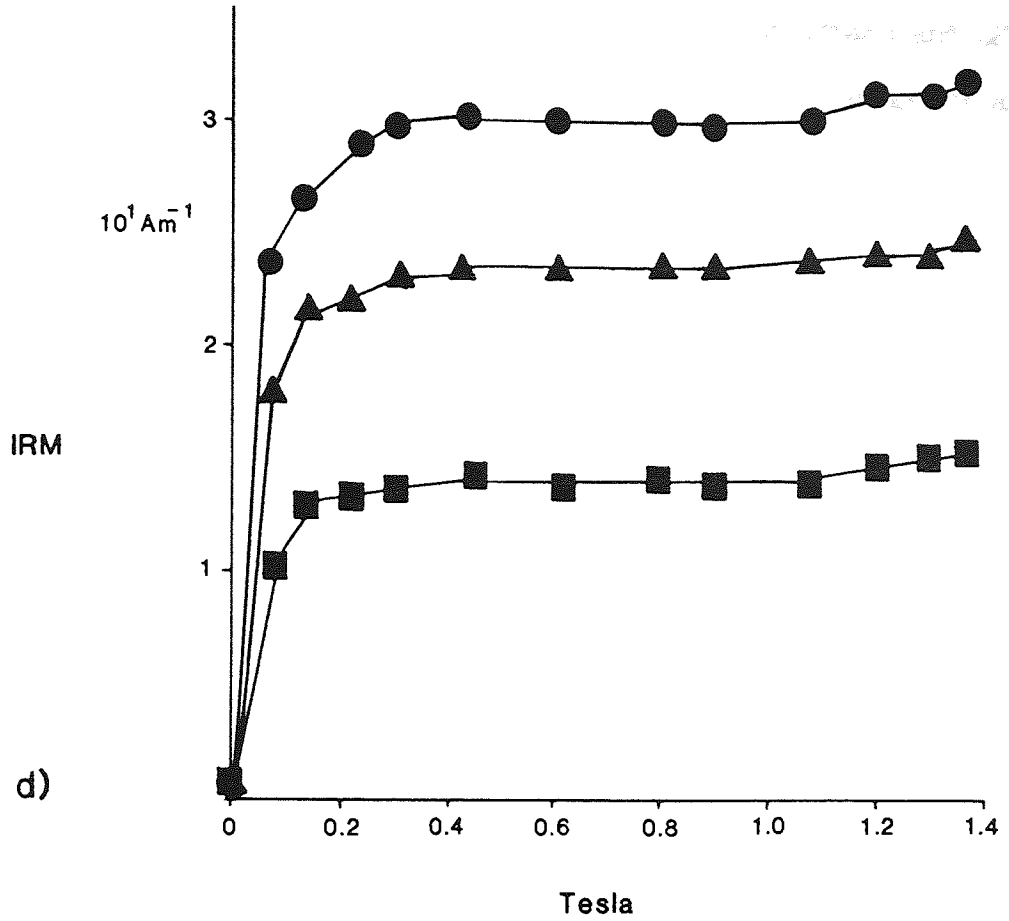

Fig. 5.5a Equal area stereographic projections of initial NRM directions for the Paciencia Group, fiducially corrected (left hand side), and fiducially and structurally corrected (right). Other details as Fig. 5.2a.

Fig. 5.5b Normalised intensity decay curves for the Paciencia Group, SBT1.1●, SBT6.2■ and SBT14.2▲.

Fig. 5.5c Zijderveld orthogonal diagram for SBT6.1.

Fig. 5.5d IRM acquisition curves for SBT10●, SBT15▲ and SBT18■.

Stereographic projections, Zijderveld orthogonal diagrams and LSF analysis for these sites (plus SBT17), reveals the presence of a stable reversed component. Extracted components are presented in Table 5.4.

Magnetic Mineralogy:

Flint (1985b) has previously described the petrology of the Paciencia Group and noted that magnetite and rare titanomagnetite are present as well rounded detrital grains commonly occurring in heavy mineral layers. Haematite is, however, the commonest iron oxide, it forms the earliest diagenetic phase occurring as an authigenic cement and overgrowths on detrital grains. Haematite also occurs as an oxidation product of: 1) detrital magnetite grains which are often completly replaced, forming the characteristic martite texture. 2) Volcanic detritus containing small magnetite grains in the groundmass. 3) Ilmenite grains often encompassed by a thin haematitic layer.

IRM acquisition curves (Fig. 5.5d), reveal that both magnetite and haematite (although there is only a small increase in IRM intensity above 0.6 Tesla), are present in the Paciencia Group, confirming the petrographic observations of Flint.

Interpretation: The Artolla Member of the Paciencia Group contains normal, intermediate and reversed components of magnetization. These formed as either a DRM or early PDRM, carried by relict magnetite and titanomagnetite (DRM) and authigenic haematite (PDRM).

According to Flint (1986), the Artolla Member of the Paciencia Group, was subjected to oxidising conditions shortly during and after

TABLE 5.4

NORMAL COMPONENTS

SITE	N	R	K	CSD	DEC	INC	α_{95}
SBT13	5	4.78 (4.72)	18 (14)	19 (21)	20 (23)	-38 (-14)	18.6 (21.1)
SBT14	6	5.78 (5.71)	22 (17)	17 (20)	7 (35)	-36 (-20)	14.5 (16.7)
SBT15	3	2.98 (2.78)	106 (9)	8 (27)	14 (6)	-29 (-31)	12.0 (43.7)
SBT16	3	2.99 (2.99)	356 (302)	4 (5)	40 (25)	-40 (-23)	6.7 (7.1)
MEAN	4	3.92 (3.92)	39 (35)	13 (14)	30 (23)	-36 (-23)	14.9 (15.7)

REVERSED COMPONENTS

SBT6	3	2.98 (2.98)	143 (140)	7 (7)	202 (188)	+49 (+15)	10.3 (10.5)
SBT8	2	1.99 (1.99)	248 (228)	5 (5)	190 (190)	+6 (-6)	15.9 (16.6)
SBT10	6	5.88 (5.73)	41 (19)	13 (19)	192 (190)	+22 (-12)	10.5 (15.9)
SBT15	3	2.99 (2.91)	247 (21)	5 (18)	211 (204)	+7 (-9)	7.9 (27.4)
SBT17	6	5.79 (5.79)	24 (24)	17 (17)	180 (180)	+11 (-15)	13.9 (14.1)
MEAN	5	4.84 (4.86)	27 (30)	16 (15)	205 (190)	+19 (-5)	15.4 (14.1)
MEAN	9	8.63 (8.49)	22 (16)	17 (20)	21 (16)	-27 (-7)	11.2 (13.4)

Table 5.4 Normal and reversed components extracted from the Artolla Member of the Paciencia Group (intermediate components have been excluded), and used in the palaeomagnetic pole calculation (Table 5.5). The normal component present in SBT10 has been omitted as error limits for the site are to large. For explanation of symbols used see Table 3.2. An F-test (McElhinney,1964) on the Paciencia Group proved that the bedding corrected and uncorrected extracted components were drawn from statistically different populations, consequently, the NRM of the Paciencia Group was acquired prior to folding.

deposition (haematite was the first authigenic cement). This occurred prior to burial and an associated change in porewater geochemistry from a neutral to alkaline fluid whilst moving out of an oxidising regime (Flint,1986). Consequently, the formation of authigenic haematite could only have taken place during the early stages of diagenesis of the Artolla Member.

The relatively rapid remanence acquisition of the Artolla sandstones, is also indicated by a comparison of isolated stable components from the sampled horizons and the sedimentary log for the member. This shows that the specimens define a good magnetostratigraphy documenting normal, reversed and intermediate polarities (Fig. 5.6). Sites displaying transitional normalised intensity decay curves (SBT10 and 15), are located close to a polarity change in the magnetostratigraphy of the Artolla Member (Fig. 5.6). SBT10 and 15 (Table 5.4) contain both normal and reversed components which have been superimposed on each other during a reversal of the Earth's magnetic field, another indication of rapid remanence acquisition. If the Artolla Member had been remagnetized after burial, the directions of remanence during demagnetization would be similar for all sites, and a magnetostratigraphy would not be present. It is therefore probable, that the NRM of the Artolla Member records an Oligo-Miocene magnetic field.

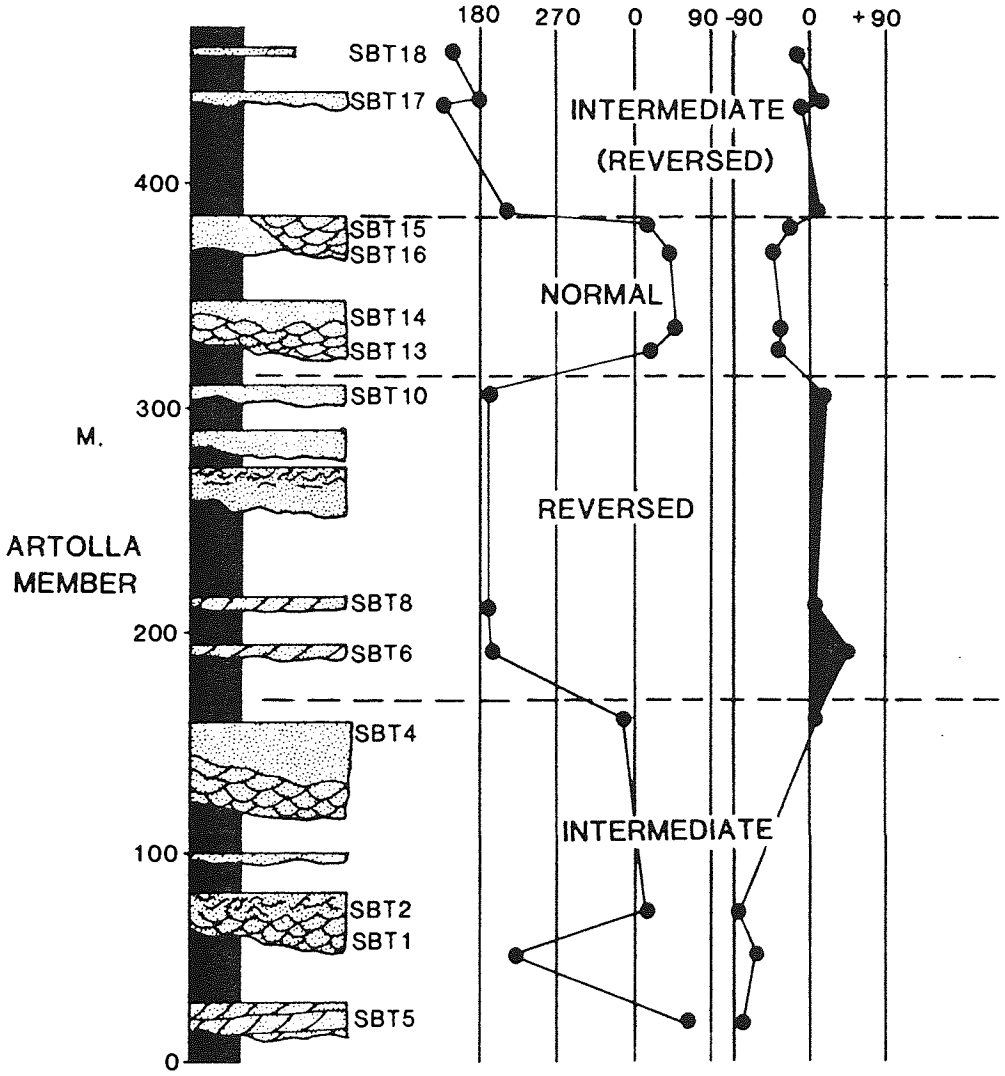

Fig. 5.6 Sedimentary log of the Artolla Member (Paciencia Group), showing the correlation between sampled horizons and extracted magnetic components.

5.5 Discussion

5.5.1 Palaeomagnetic Poles Derived from the Andean Precordillera and their Tectonic Implications

Figure 5.7 shows the relative positions of palaeomagnetic poles derived from the Andean Precordillera (using Tables 5.1-5.4, and summarised in Table 5.5), and reference poles derived from the stable shield area of South America (see Appendix A for reference pole derivation). It clearly shows that (with respect to their reference poles), the poles from the Precordillera have undergone significant clockwise rotation. The amount and error limits of rotation are presented in Table 5.5.

The youngest rocks studied, from the Oligo-Miocene Paciencia Group, have been rotated 22+/-14.5 degrees, this indicates that at least 22 degrees of rotation is post-Miocene in age, with respect to the present day South Pole (Appendix A).

Although the Tonel and Purilactis Formations have undergone different amounts of rotation (Table 5.5), overlapping error limits (Fig. 5.7), indicate that the differences are not statistically significant. The age of the two Formations is uncertain, but the differences could indicate that either the Tonel Formation was remagnetized in a similar magnetic field to the Purilactis Formation, and/or that no significant tectonic movement took place between the remanence acquisition of the two Formations.

As the Tonel and Purilactis Formations have undergone 41+/-17.5 and 33+/-12.5 degrees of clockwise rotation respectively, with respect to their reference poles, and the Paciencia Group has only rotated 22

TABLE 5.5

UNIT	LAT. AND LONG. OF UNIT	α_{95}	PALAEOPOLE LAT. LONG.	dp	dm	AMOUNT OF ROTATION
AGUE DULCE FORMATION	22.75S. 69.15W.	6.5	49S.233.4E.	6.7	8.7	30+/-9.2
PURILACTIS FORMATION	22.8S. 68.25W.	8.6	54.5S. 206E.	6.1	9.9	33+/-12.5
TONEL FORMATION	23.05S. 68.4W.	13.9	48S. 201E.	8.7	15.3	41+/-17.5
PACIENCIA GROUP	22.45S. 68.45W.	11.2	68.4S. 185E.	6.7	12.1	22+/-14.5

Table 5.5 Palaeomagnetic poles derived from the units studied, and the amount of rotation of the unit with respect to a reference pole derived from the stable shield area of South America (Appendix A). For explanation of symbols used see Tables 3.2 and 3.4.

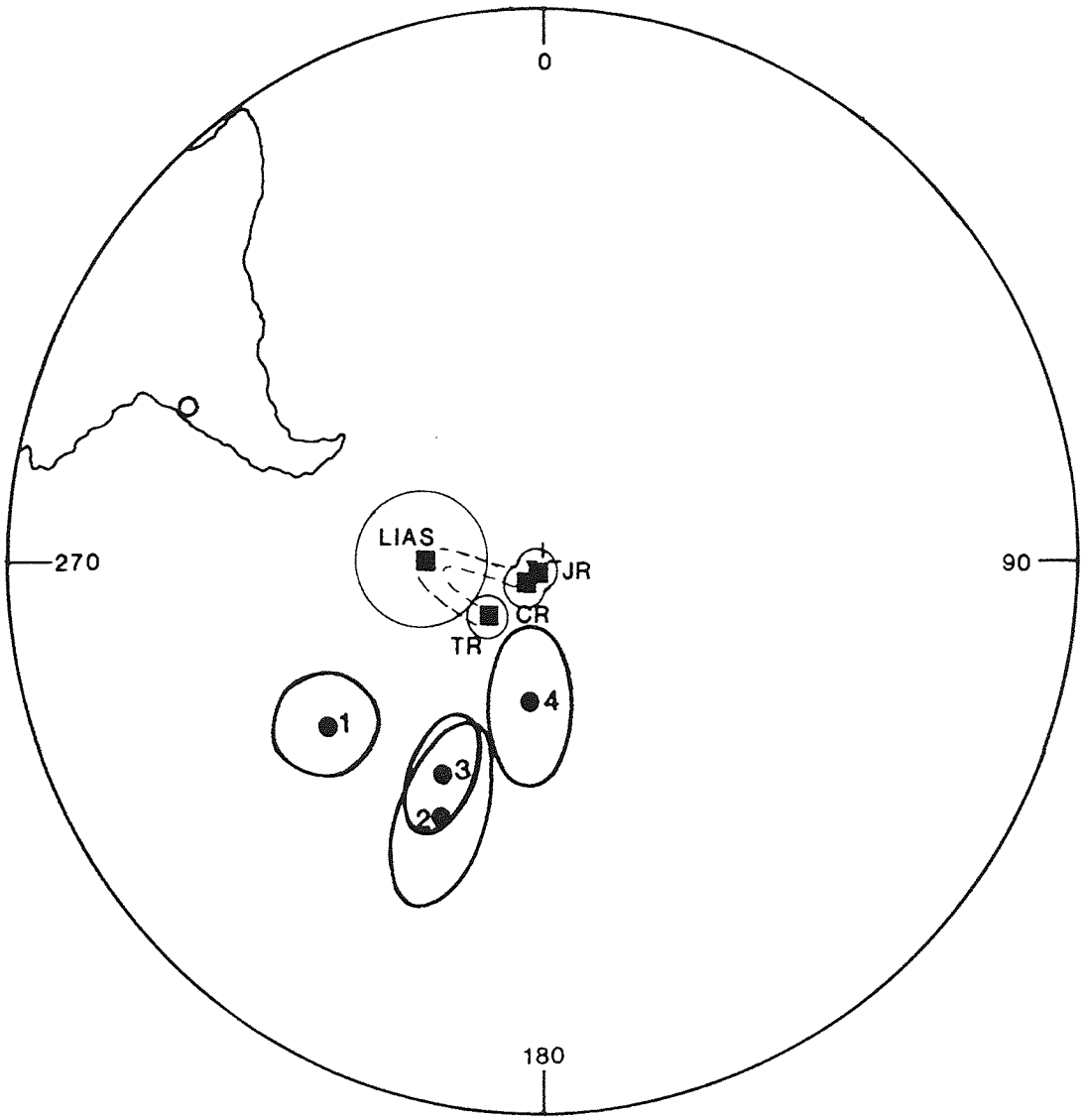

Fig. 5.7 Equal angle stereographic projection of palaeomagnetic poles and error limits of the units studied (from Table 5.5), indicating clockwise rotation, relative to the reference poles of Upper Triassic age (TR), Lower Jurassic age (LIAS), Upper Jurassic age (JR) and Early Mid-Mid Late Cretaceous age (CR), derived from the stable shield area of South America (Appendix A). 1=Agua Dulce Formation, 2=Tonel Formation and Intrusives, 3=Purilactis Formation, and 4=Paciencia Group.

degrees, approximately 11-19 degrees of clockwise rotation must have taken place prior to the NRM acquisition of the Paciencia Group.

The Agua Dulce Formation has undergone 30+/-9.2 degrees of clockwise rotation, with respect to an Upper Triassic reference pole. This amount of rotation is less than that of the younger Tonel and Purilactis Formations. It is possible therefore, that prior to the clockwise rotation of the Precordillera, the Agua Dulce Formation had been rotated anticlockwise. Alternatively, as the sampling locality of the Agua Dulce Formation is situated to the west of the Precordillera in the Central Depression (Fig. 5.1), rotation of the Formation may not have been as extensive as that of the Precordillera.

Extent, Method and Timing of Rotation

It is clear that rotation of the Andean forearc has affected the Cordillera de la Costa (Chapter 3), the eastern edge of the Central Depression (Agua Dulce Formation) and the Precordillera, and may even extend further east. Questions which arise from this observation include:

1) Is the rotation in the Cordillera de la Costa and the Precordillera connected in any way, and if so by what method?

2) Why has the Precordillera been rotated in a stepwise fashion, whereas rotation of the Cordillera de la Costa appears to have been continuous?

3) If rotation is not connected, what tectonic regime could account for two/three discrete areas of rotation in the Andean forearc?

1) It is unlikely that the Precordillera and Cordillera de la Costa have any crustal connection as no major E-W trending stuctures are

apparent, also, any E-W trending structures would have to cross the dominant N/S trending morphological and geological provinces of the Andean forearc (Fig. 2.1). Any crustal connection would also imply that the area has moved as a single rigid block, again requiring major E-W trending structural features.

The difference in the style of rotation, between the continuous rotation of the Cordillera de la Costa and the stepwise rotation of the Precordillera, may simply be a function of time. There is a major time gap between the NRM acquisition of the Purilactis Formation and the Paciencia Group (approximately 85Ma. assuming the Purilactis formation is Lower Cretaceous in age). The Precordillera had started to rotate clockwise after deposition of the Tonel and Purilactis formations, undergoing 11-19 degrees of rotation prior to the deposition of the Paciencia Group, after which a further 22 degrees of rotation took place.

3) The model and resulting tectonic setting created to account for the rotation of the Cordillera de la Costa presented in section 3.5 and shown schematically in Fig. 3.11, could be modified to take into account the rotation present in the Precordillera. The model involves placing the Andean forearc in an extensional regime, through a combination of subduction roll back, slab pull and absolute motion of the overriding South American plate. Where extension due to roll back and slab pull is at an angle to the absolute motion of the South American plate, resulting in a stress regime accommodated through the clockwise rotation of discrete crustal blocks. The modification of this model requires a detailed examination of the Andean forearc.

The forearc can be split into 3 geological provinces west of and including the Precordillera (Fig. 2.1). Each of these provinces has a distinct geological history and all are bounded by a thrust or fault zone. Palaeomagnetic evidence indicates that the Cordillera de la Costa has rotated approximately 29+/-15 degrees (Chapter 3), that the eastern part of the Central Depression has rotated approximately 30 degrees (Agua Dulce Formation) and that the Precordillera has rotated between 41 and 22 degrees (Table 5.5). These provinces when subjected to an extensional tectonic regime will almost certainly respond differently due to differences in lithology, structure, depth and extent. This may well account for the variation in rotation between the provinces.

An important feature present in the Cordillera de la Costa but not present in the Precordillera, is the NE-SW fault orientation thought to be associated with rotation (section 3.5). This feature should be present in the Precordillera, if the rocks of the Precordillera had responded in the same way to an extensional stress regime as those of the Cordillera de la Costa. However, close examination of the orientation of the major basins of the Precordillera and Central Depression does reveal a NE-SW trend (Purilactis and Tuina Formations; Fig. 5.1). This may imply that rotation is on a larger scale in the Precordillera and Central Depression than in the Cordillera de la Costa, as in the Cordillera de la Costa rotation has been taken up by a sequence of "en echelon" small-scale faults (Chapter 3), whereas rotation in the Precordillera is on a basin-wide scale.

The models of both Dewey (1980), and Bott (1982), which involve the stressing of a continental crust, contain zones of weakness inland

of the plate margin, due to high heat flow associated with the volcanic arc. It is possible that rotation may be influenced by the high heat flow which would create an area of weakness/mobility in the continental crust (Dewey,1980), favouring greater mobility of an area close to the volcanic arc ie. the Precordillera.

Another possible influencing factor on inland crustal rotation, is the 40 degree angle of dip of the subducting slab in this area of the Central Andes. The higher the angle of dip, the more influence slab pull and subduction roll back should have on the overriding continental plate (section 3.5). This would create a larger amount of extensional stress in the continental plate and consequently a larger amount of rotation than in area overlying a shallow dipping subduction zone such as Central Chile, where Beck et al. (1986) found only 14 degrees of clockwise rotation in rocks of a similar age to the Purilactis Formation, 250km. inland of the coast.

Mercier (1981) working in Peru, also found that areas overlying relatively steeply dipping subduction zones, were subject to extensional stress regimes, and that areas overlying relatively shallow subduction zones were dominated by compressional tectonic regimes ie. favouring more extensive rotation in the Central Andes than in northern Peru.

Points of intrest to note, include the rate and extent of rotation. The rate of rotation has increased from the interval between the deposition of the Purilactis Formation and the Paciencia Group when approximately 11-19 degrees of rotation took place in 85Ma., to 22 degrees of post-Paciencia Group rotation in approximately 28Ma.

The extent of rotation is also interesting, in that although the Precordillera is relatively close to an area of active compression-the

Subandean thrust belt approximately 500km. to the east (Fig. 2.1), an extensional regime is still dominant. These points need to be addressed in future work on the Andean forearc.

5.5.2 Conclusions

1) Rotation is thought to be associated with an extensional forearc stress regime created through the interaction of slab pull, subduction roll back and the absolute motion of the South American plate at the subduction zone, this has resulted in placing the top of the South American plate in an extensional stress regime.

2) Rotation in the Precordillera is thought to result in the movement of discrete crustal blocks, confined to the Precordillera.

3) Rotation is thought to be a continuous process, interrupted periodically by compressional deformation phases.

4) Rotation may be associated with the angle of dip of the subducting slab, the steeper the dip the larger the amount of extensional stress can be placed on the continental crust.

CHAPTER 6

STRATIGRAPHY, SEDIMENTATION, PALAEOGEOGRAPHY AND BASIN EVOLUTION DURING THE ANDEAN OROGENIC CYCLE, (22-24°S, NORTHERN CHILE)

6.1 Introduction

Dickinson (1974) and Dickinson and Seely (1979), classified the principal basins formed in an Andean-type mountain belt into: forearc, intra-arc and retroarc foreland basins. Considerable work has been undertaken on the evolution of foreland basins (see Allen et al.,1986), but the current understanding of the origin of intra-arc and forearc basins is limited.

In this chapter, the evolution of the Andean forearc is examined through a detailed analysis of the wide variety of sedimentary basins currently exposed in the Andean forearc. These formed in response to major tectonic events, and have been split into three distinct orogenic episodes: 1) Permian to Triassic,
2) Jurassic to Mid-Cretaceous, and
3) Mid-Cretaceous to Recent.

Eleven basins/formations are discussed (Fig. 6.1), with particular attention focussed on the Agua Dulce, Purilactis, Coloso and San Pedro basins. These basins are distributed across the forearc and range in age from the Upper Triassic to the present day. Although some detailed studies of the individual formations and basins have been previously undertaken, the inter-relationship of the basins within a regional context has not been addressed.

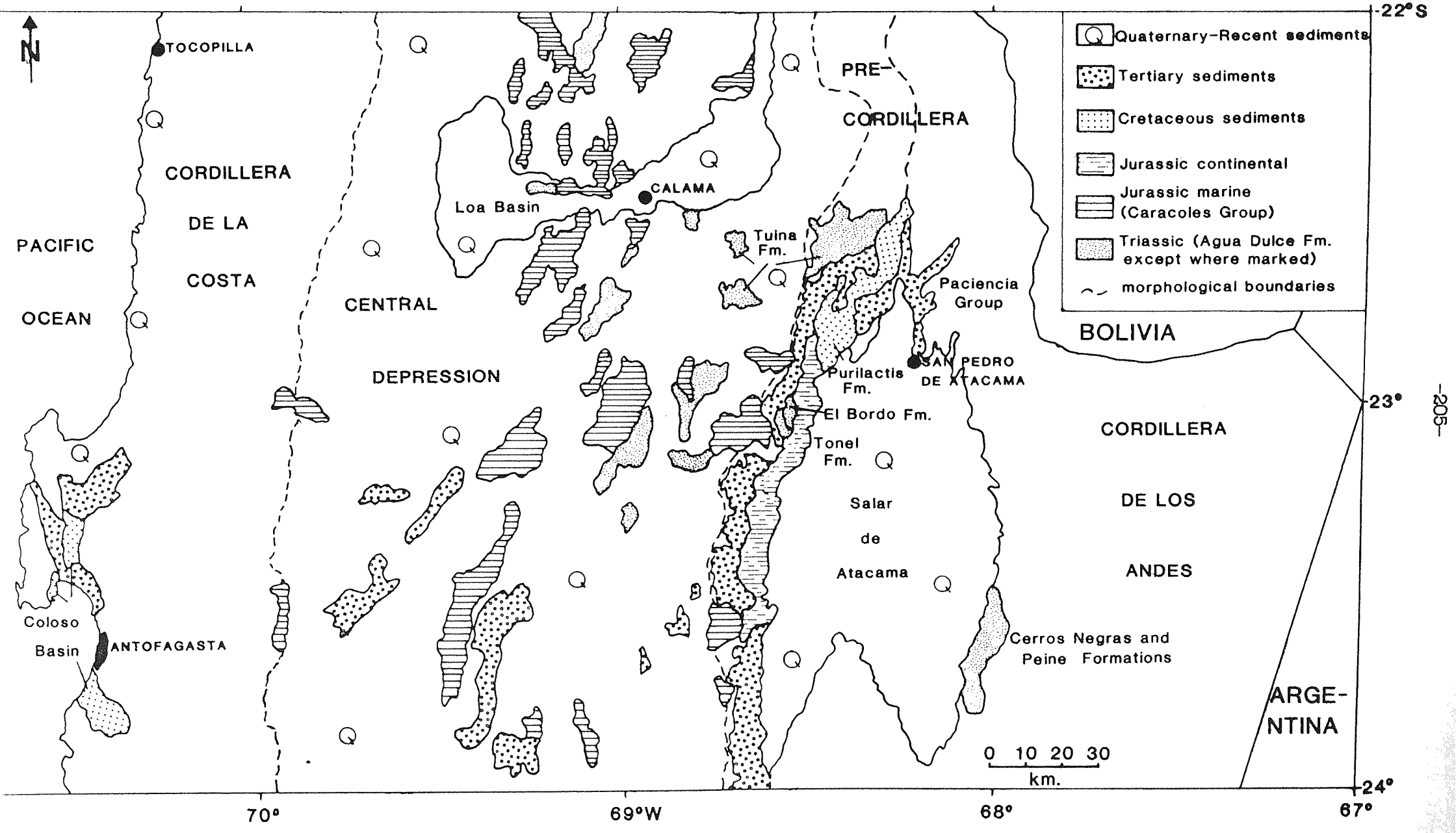

ig. 6.1 Location map showing the distribution of Mesozoic-Recent sediments and sedimentary basins in the Andean forearc, northern Chil

6.2 Permian to Triassic Basin Evolution

6.2.1 The Tuina Formation

The Tuina Formation outcrops in the centre of the Cordillera de Domeyko (Fig. 6.1), and, based on regional lithostratigraphy, has been assigned a ?Permo-?Triassic age (Marinovic and Lahsen,1984). The base of the Formation is not exposed, and the top is overlain unconformably by the Purilactis Formation (Fig. 6.2a). Faulting is extensive in the Tuina Formation, making a true estimation of thickness difficult. Marinovic and Lahsen (1984) have estimated a thickness of approximately 2500m.

The Tuina Formation comprises a complexly deformed sequence of interbedded red sandstones, siltstones, mudstones, green conglomerates and brecciated and unbrecciated acidic lava flows. These lithologies are commonly interbedded on the scale of a few metres. A summary log is presented in Figure 6.2b.

The main outcrop of the Tuina Formation was originally mapped as containing NW/SE oriented fault-bounded blocks of conglomerates belonging to the Purilactis Formation (Marinovic and Lahsen,1984; Fig. 6.2a). Field evidence indicates that despite having a superficial similarity to conglomerates from the Purilactis Formation, these strata within the fault blocks have stronger affinities to the Tuina Formation. The conglomerates in the blocks are distinctly different from those of the Purilactis Formation as: 1) the degree of lithification is much greater, 2) the overall clast size is much larger, and 3) the clast composition is markedly different (the Tuina Formation contains clasts of sedimentary rock types, which are absent from the Purilactis Formation).

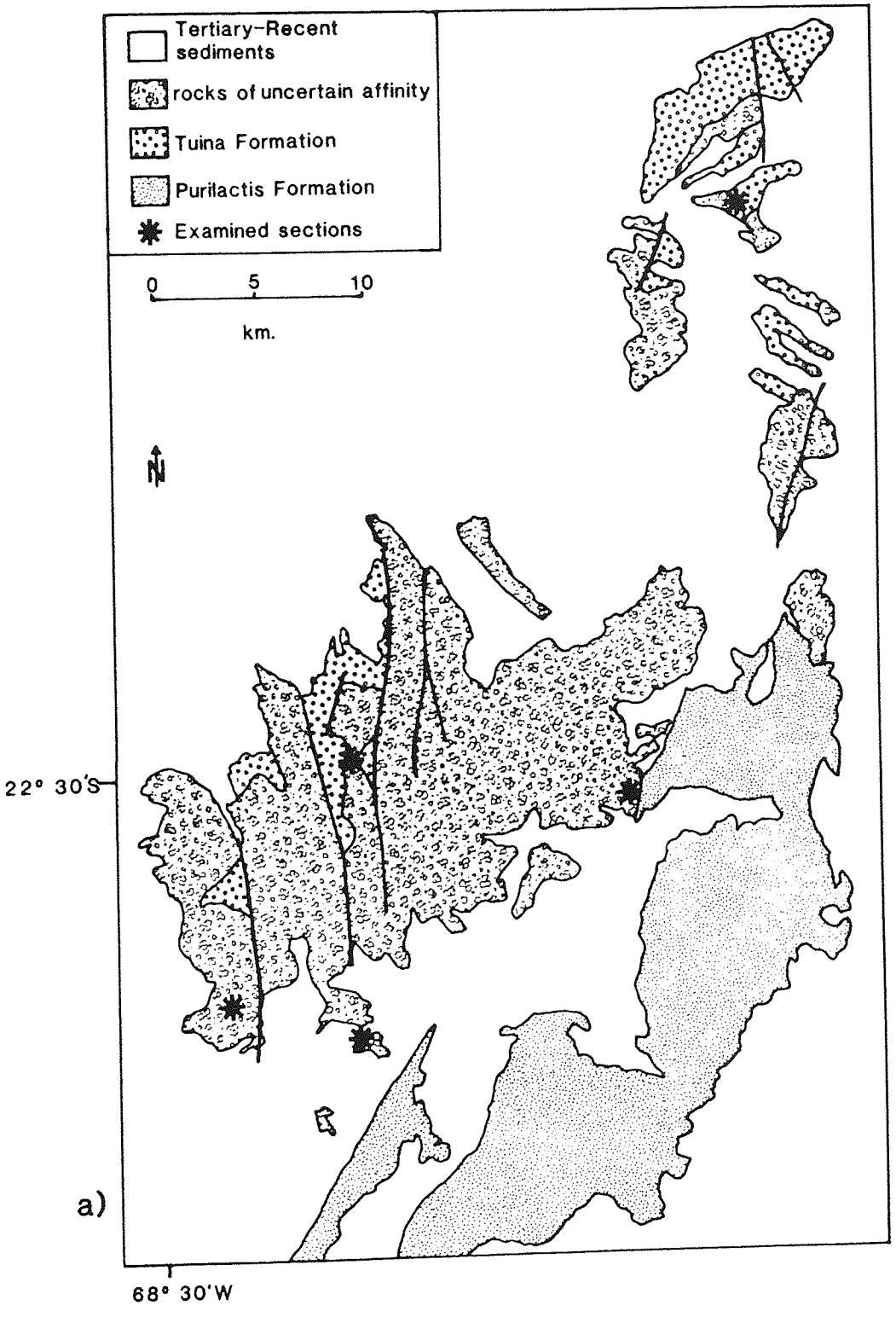

Fig. 6.2a Main outcrop distribution, showing the location of fault-bounded blocks of the Purilactis Formation (after Marinovic and Lahsen, 1984)

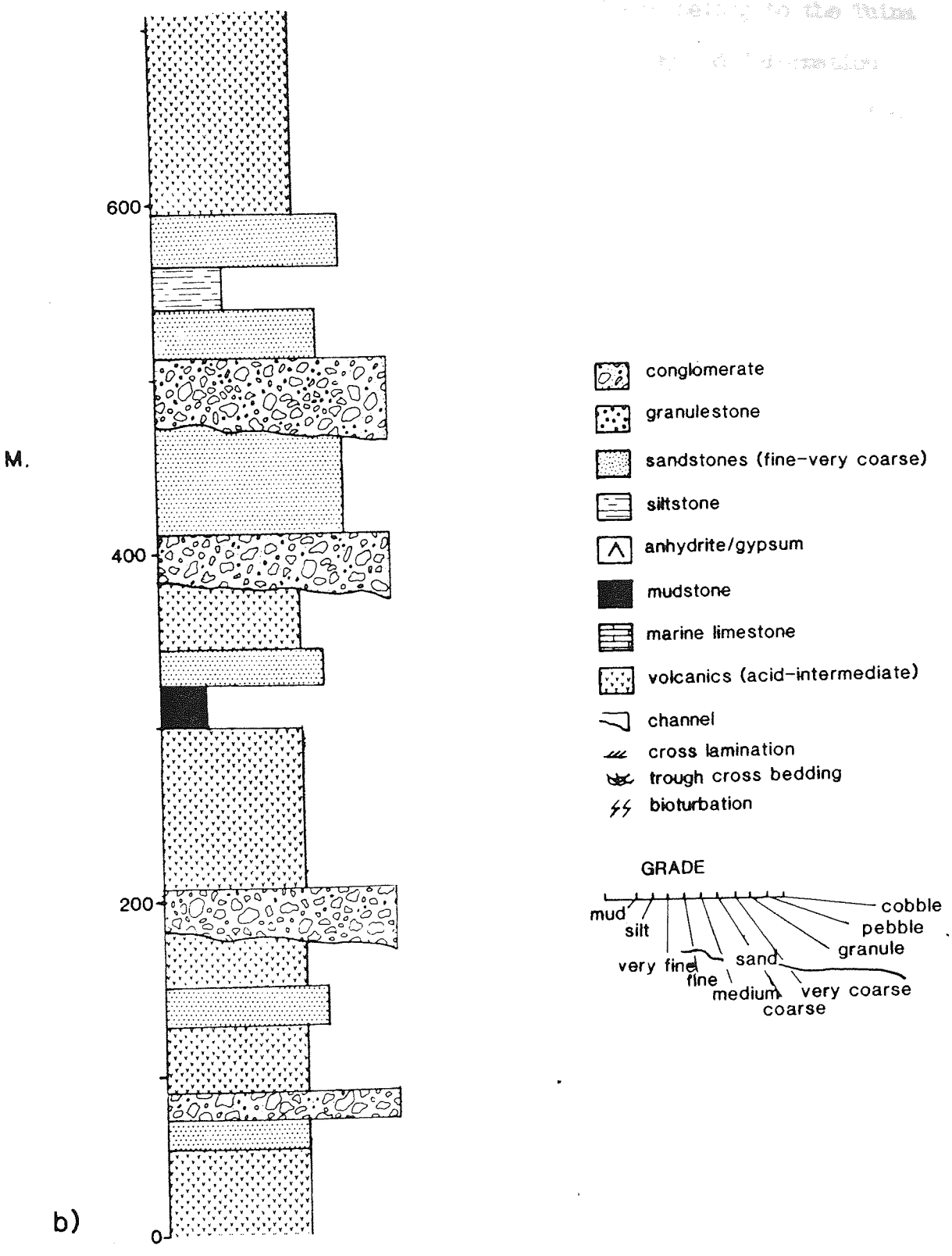

Fig. 6.2b Summary log of the Tuina Formation, modified from Marinovic and Lahsen (1984), and key to the following figures.

A further indication that the faulted blocks belong to the Tuina Formation is provided by the regional stratigraphy and deformation history of the area. The Purilactis Formation unconformably overlies the Tuina Formation and has suffered only minor post-depositional deformation, unlike the Tuina Formation. Furthermore, no fault blocks of the Agua Dulce or Tonel Formations are present in the Tuina Formation, both of which are older than the Purilactis Formation and would almost certainly have been caught up in any regional deformation.

The Tuina Formation also contains extensive hydrothermal copper deposits, which are absent from all overlying or adjacent Formations (Marinovic and Lahsen,1984). It is probable therefore, that extensive deformation and mineralisation of the Tuina Formation took place prior to the deposition of the Agua Dulce Formation, possibly in the mid-Permian (Saalian) deformation phase (Table 2.1).

Interpretation: The Tuina Formation represents a faulted sequence of proximal and distal continental sediments and volcanics, deposited prior to the development of the Jurassic volcanic arc (section 2.4.2). It is possible that the Tuina Formation may record the beginning of volcanic activity associated with the origin of the volcanic arc. However, this period of geological history in the Central Andes is extremely poorly understood (section 2.3.6), and more work is required in order to characterise the Formation, and to unravel the stratigraphy, facies relationships and basin fill sequence.

6.2.2 The El Bordo Formation

The 1200m. thick El Bordo Formation is exposed in the south of

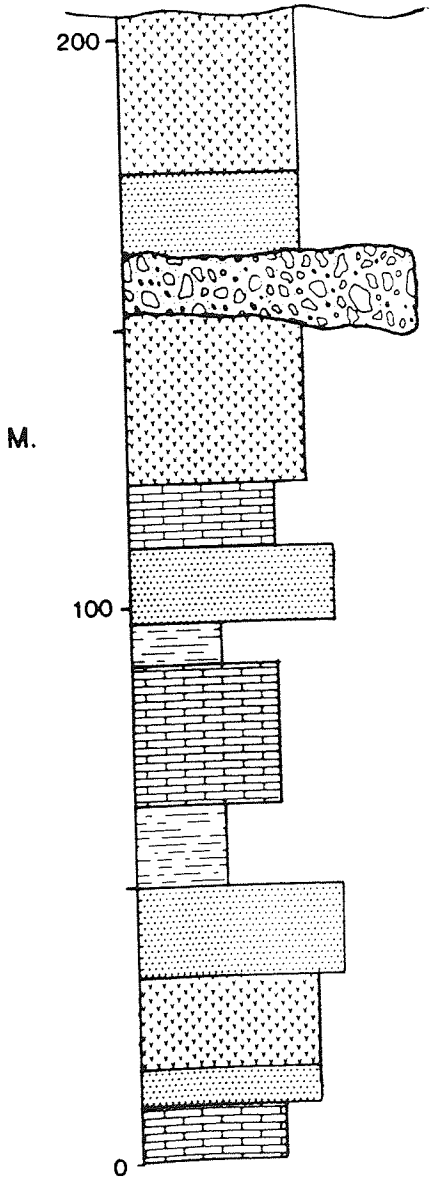

Fig. 6.3 Summary log of the El Bordo Formation, for key see Fig. 6.2b.

the study area (Fig. 6.1). Based on regional lithostratigraphy it is thought to be of ?Lower Triassic age (Ramirez and Gardeweg,1982), as it is overlain by the ?Upper Triassic Agua Dulce Formation, and has a faulted contact with the ?Jurassic Tonel Formation (Plate 6.1).

Preliminary field work indicates the presence of a shallow marine sequence of interbedded muddy and porcellaneous limestones, quartz arenites and horizontally stratified chert and haematite horizons. Ramirez and Gardeweg (1982) described a continental sequence from the same area, comprising andesites, brecciated andesites, rhyolites and coarse red sandstones with a vertebrate and invertebrate fauna. A generalized sedimentary log is presented in Figure 6.3.

Although the El Bordo Formation is not regionally extensive, it is important stratigraphically as it records the first marine interval associated with the onset of the Andean Orogenic cycle. The Formation is essentially flat lying and cut by minor extension faults.

Interpretation: The El Bordo Formation comprises a sequence of shallow marine and continental rocks, deposited in a low-lying basin subject to periodic sea-level fluctuations, possibly related to tectonic events. Although knowledge of the El Bordo Formation is limited, it contains similar lithological associations to both the Tuina and Agua Dulce Formations (sections 6.2.1, 6.2.3). These Formations are thought to have been deposited under an extensional tectonic regime, possibly associated with the formation of the Jurassic back-arc basin and volcanic arc. Again like the Tuina Formation, more work must be undertaken on the El Bordo Formation to determine the stratigraphy and facies relationships of the basin fill sequence and origin of the volcanics.

Plate 6.1 Field photograph from the top of the Precordillera, looking south. To the left (behind the figure) are the red and green mudstones and sandstones of the Tonel Formation (dipping 30 degrees east). The Tonel Formation unconformably overlies the El Bordo Formation, seen in the foreground to the right, which dips 50 degrees to the east and is distinguished from the Tonel Formation by its light brown colour. The Agua Dulce Formation is seen at the top right of the photograph (arrowed), it has a faulted contact with the El Bordo Formation.

Plate 6.2 Field photograph taken from the Llano de Paciencia (Salar de Atacama), looking west at the Precordllera. This photograph shows the unconformable contact between the Tonel Formation (red and white, to the left), and Member 1 of the Purilactis Formation (light green/brown, to the right). Arrowed are the green hornblende-rich dykes, sampled for palaeomagnetic work (Chapter 5).

6.2.3 The Agua Dulce Formation

The Agua Dulce Formation (Garcia,1967), outcrops extensively in the eastern margin of the Central Depression (Plate 6.1). Aspects of the Formation have previously been studied by Wetzel (1927, in Baeza,1976), Biese (1957), Perez and Levi (1961), Garcia (1967), Baeza (1976), Ramirez and Gardeweg (1982) and Marinovic and Lahsen (1984), but little attention has been paid to the sedimentology of the Formation.

The Agua Dulce Formation has an erosive contact with the Limon Verde pluton and unconformably overlies the El Bordo Formation (Plate 6.1). It is unconformably overlain by Hettangian limestones (Biese,1957; Chong,1977), and has been assigned an ?Upper Triassic age on this lithostratigraphic basis (Garcia,1967). Equivalent sequences to the Agua Dulce Formation outcrop further south (25°S) on the eastern flanks of the Cordillera de Domeyko and include: the Bardas Negras and Portezuelo de la Sal Formations (Chong,1973), and on the eastern side of the Salar de atacama, the Peine and Cerros Negros Formations (Fig. 6.1). A summary log of the Agua Dulce Formation is presented in Figure 6.4.

In the Limon Verde area (Fig. 6.1), the Agua Dulce Formation is approximately 1200-1600m. thick (Ramirez and Gardeweg,1982). The bulk of the Formation in this area is composed of acidic lavas, particularly flow-banded rhyolites, commonly interbedded with thin beds of red arkosic sandstones. The basal part of the Formation consists of 100m of sandstones and shales. The lower 15m., comprising a basal conglomerate overlain by purple and green shales with siderite nodules, is thought to represent a marine incursion (P. Turner, pers. comm.,1985). Above this horizon, the shales are interbedded with

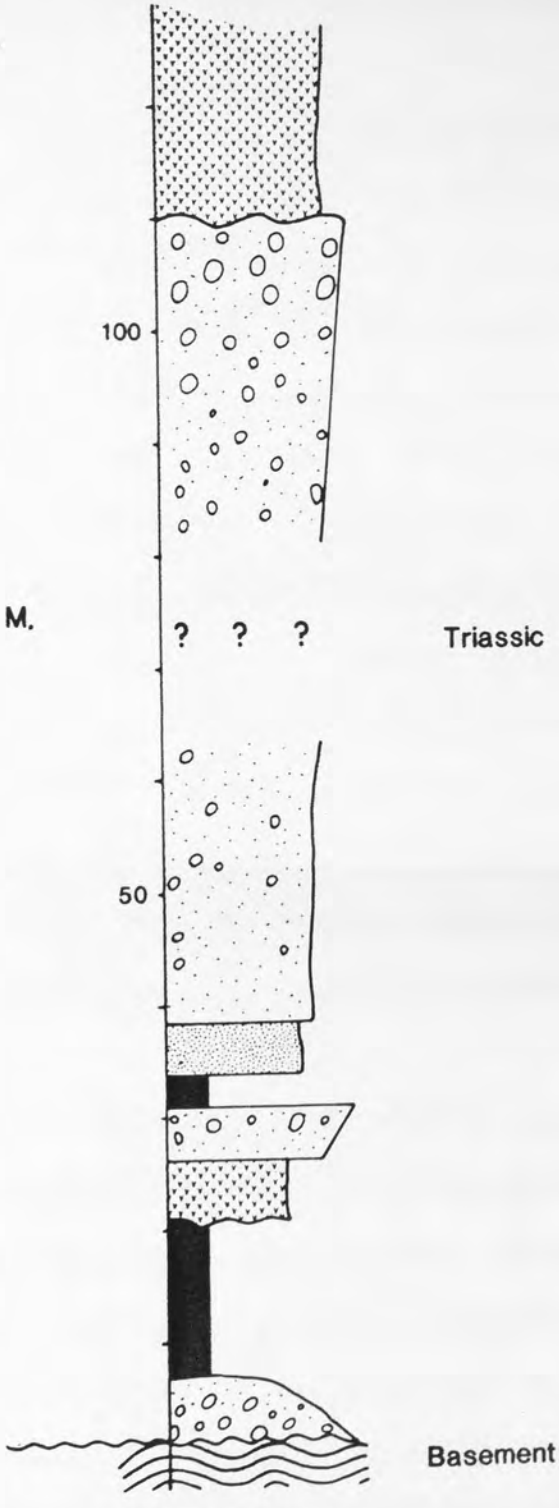

Fig. 6.4 Summary log of the Agua Dulce Formation, for key see Fig. 6.2b.

coarse sandstones and conglomerates, which eventually pass into coarse red arkosic sandstones, with a high percentage of volcanic detritus (30-50%; section 7.2.1).

Despite the limited exposure of the Agua Dulce Formation, most sections are thought to have been deposited subaerially (Baeaza,1976). With the exception of the Limon Verde area, no other sections of marine sediments have been recorded from the Formation. However, further work may well reveal their presence, particularly as the stratigraphically equivalent Portezuelo de la Sal Formation to the south, contains a good marine fauna (Bogdanic,1983).

Although the Agua Dulce Formation is essentially flat lying, minor extension and later thrust faults cut the Formation, making correlation between outcrops difficult. Deformation is probably associated with the closure of the Jurassic back-arc basin (section 6.3). Further south similar deformation has affected the Portezuelo de la Sal Formation, together with the younger Caracoles Group and Cretaceous and Palaeocene volcanics (Chong and Reutter,1985).

Interpretation: The Agua Dulce Formation records a marine transgression, followed by localised uplift, resulting in continental sedimentation and contemporaneous acid volcanism. Overlying Hettangian carbonates of the Caracoles Group, record the inception of back-arc basin sedimentation (see below). This implies that the Agua Dulce Formation is associated with the crustal extension required for the initial formation of a back-arc basin. Rifting has been postulated by Noble et al. (1978) and Pitcher (1984) to account for the geochemical characteristics of Permo-Triassic plutons and volcanics of the Mitu

Group from southern Peru and Bolivia. The Agua Dulce Formation could thus represent a southerly extension of this rift association.

6.2.4 Discussion of Permian to Triassic Basin Evoltion

The Tuina and El Bordo Formations are thought to range from the ?Permian-?Lower Triassic in age and, as the Andean Orogenic cycle commenced in the Upper Triassic (Coira et al.,1982; Chapter 2), they form part of the transitional period prior to the development of the Andean Orogenic cycle (section 2.3.5).

The Agua Dulce Formation is thought to represent the onset of the Andean Orogenic cycle. The Formation records the end of a major regression (possibly similar to the El Bordo Formation), with uplift resulting in the deposition of arkosic sandstones and extensive associated acid volcanics. Uplift would imply a dominantly compressive tectonic regime, but, as the Agua Dulce Formation precedes the formation of the back-arc basin, it is probably related to extension. Extension and localised uplift prior to subsidence occur in rift related settings, where doming of the continental crust is a common feature (Bott,1981). Doming of the crust is often associated with high level intrusions, commonly of acidic composition (eg. the North American Cordillera, Wernicke et al.,1987). Localised crustal uplift would account for the marine to continental transition and the acidic volcanics of the Agua Dulce Formation. It is interesting to note that the Cerros Negros Formation (Fig. 6.1), is lithologically similar to the Agua Dulce Formation as well as being of the same age (Ramirez and Gardeweg,1982). Consequently, the Cerros Negros Formation may also have a rift association, and as it is situated on the east side of the Salar de Atacama, the possibility exists that the Salar de Atacama

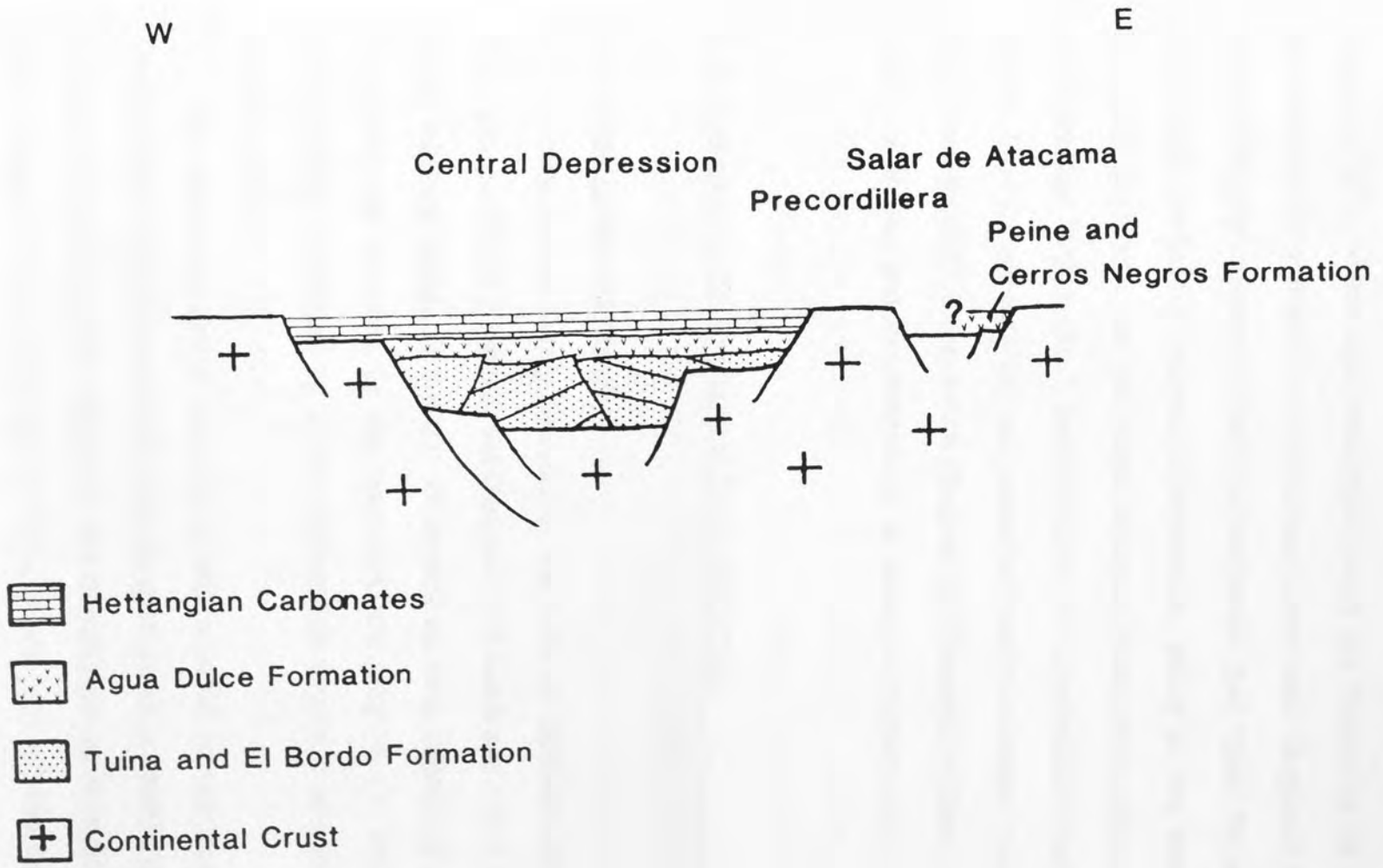

Fig. 6.5 Schematic diagram of the evolution during Permian to Lower Jurassic times in the Andean forearc.

basin marks the position of a failed Mesozoic rift.

The probability that ?Upper Triassic rocks of northern Chile represent a period of rift basin formation is supported by observations at 25°S, where the Portezuelo de la Sal Formation is disconformably overlain by Hettangian limestones (Bogdanic,1983). The small time gap between deposition indicates that Upper Triassic rocks are almost certainly related to extension, prior to the formation of the back-arc basin. As the Permo-Triassic rocks of northern Chile all have similar lithological associations, it is possible that an extensional (rift) tectonic regime prevailed over the Andean forearc during this time period. A schematic diagram of ?Permian to Lower Jurassic basin evolution and sedimentation is shown in Figure 6.5.

6.3 Jurassic to Mid-Cretaceous Basin Evolution

6.3.1 The Caracoles Group

The Caracoles Group represents the bulk of sedimentation which took place directly behind the Jurassic volcanic arc, in a back-arc basin setting (section 2.4.2). It covers an area extending from the Cordillera de la Costa to the Precordillera (Fig. 6.1), which has been considerably shortened by later compressive tectonic events (Chong and Reutter,1985).

The Caracoles Group contains a well studied marine fauna (Chong,1977; Hillebrandt,1973; Hillebrandt et al., 1986). The Group is exposed in the southern ranges of the Cordillera de Domeyko (24-26°S), and, between 21-24°S outcrops in the eastern part of the Central Depression (Fig. 6.1). A summary of the sedimentary history of the

basin has been given in section 2.4.2. Consequently, only facts relevant within the context of this chapter will be discussed. Particular attention will be paid to tectonic events as deduced from the sedimentary record. A generalised sedimentary log of the Group is presented in Figure 6.6.

Recent detailed mapping of the Jurassic back-arc basin has been undertaken by Baeza (1976), Chong (1977), Bogdanic (1983), Hillebrandt et al. (1986) and Quinzio Sinn (1986). These workers have concentrated on characterising the fauna and defining the aerial extent of the basin throughout its history.

The onset of marine sedimentation began in Hettangian times (Chong,1977), with the deposition of transgressive shallow marine shelf limestones over the Agua Dulce and El Bordo Formations. Continued subsidence led to deeper water black shale sedimentation during the Sinemurian; the largest aerial extent of the back-arc basin. Following the Sinemurian a gradual shallowing of the basin took place through to the Callovian, as reflected by the deposition of shelf limestones and subordinate sandstones and conglomerates. The shallowing of the basin culminated in extensive evaporite deposition during the Oxfordian and Kimmeridgian (Chong,1977).

A further marine transgression occurred during the Tithonian-Neocomian, when a smaller basin developed mainly in the south (25^{o}S) of the area. The sea began to retreat in the lower part of the Neocomian, resulting in the interfingering of marine, lagoonal and continental sediments (Chong,1977).

Intermediate-acidic volcanic rocks occur sporadically throughout the Caracoles Group, and volcanic activity was particularly voluminous towards the end of the Neocomian.

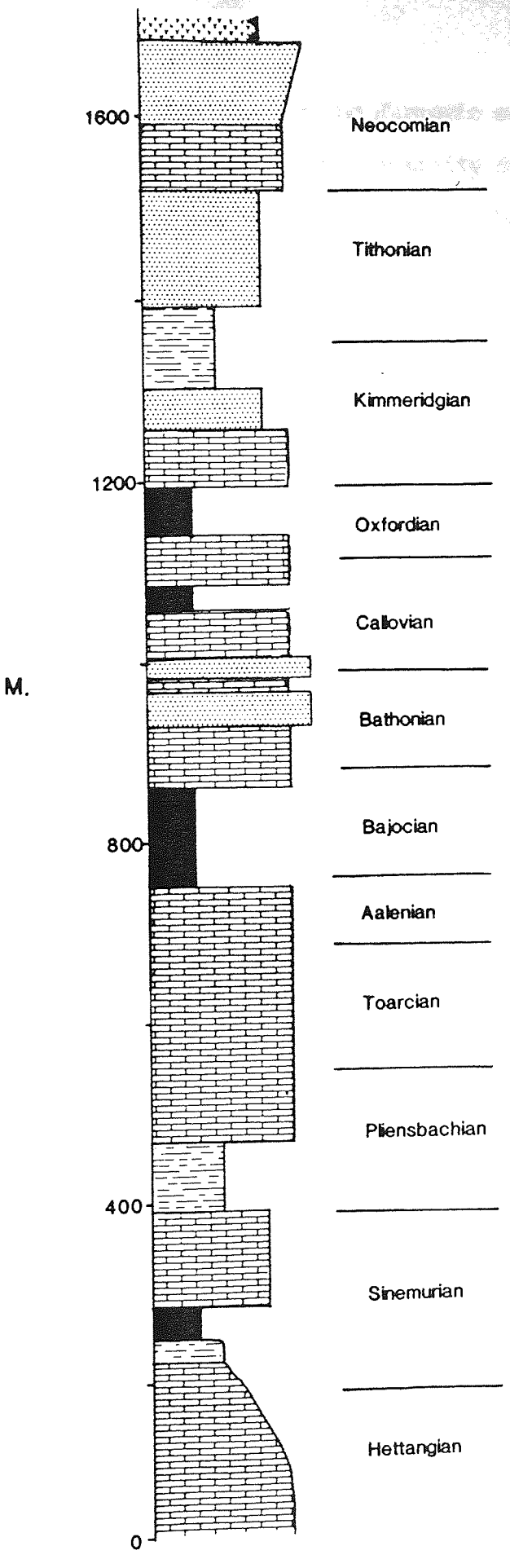

Fig. 6.6 Summary log of the Caracoles Group, modified from Chong (1977) and Bogdanic (1983), for key see Fig. 6.2b.

Several minor unconformities separate the Jurassic stages (Chong,1977), testifying to continued tectonic activity during back-arc basin sedimentation. After closure of the basin at the end of the Lower Cretaceous, later compressive tectonism has resulted in considerable shortening of the basin-fill sequence. The major period of deformation has been placed at 40Ma. by Chong and Reutter (1985), and has resulted in Palaeozoic granites being thrust over Oxfordian evaporites (Fig. 6.7). The age of the collapse of the back-arc basin is however, uncertain, and maybe as late as the Pliocene (G. Williams, pers. comm.,1987).

Interpretation: Deposition of the Caracoles Group in a back-arc basin setting commenced in the Hettangian. Further extension and subsidence of the basin continued up to the Sinemurian, where the volcanic arc must have been at its furthest point westwards from the back-arc basin depocentre, as indicated by the deposition of deep water sediments. Subsequently, subsidence ceased and uplift predominated in the basin. This period from the Sinemurian to the Kimmeridgian probably saw either an eastward movement of the volcanic arc (and gradual closure of the basin), or the westwards movement of South America, recorded by the transition from shallow marine to continental sedimentation. A smaller basin developed from the Tithonian-Neocomian, indicating a minor period of extension prior to complete closure at the end of the Neocomian (Hauterivian). The occurrence of volcanic rocks throughout the Caracoles Group indicates the relatively close proximity of the volcanic arc during the Andean Orogenic cycle.

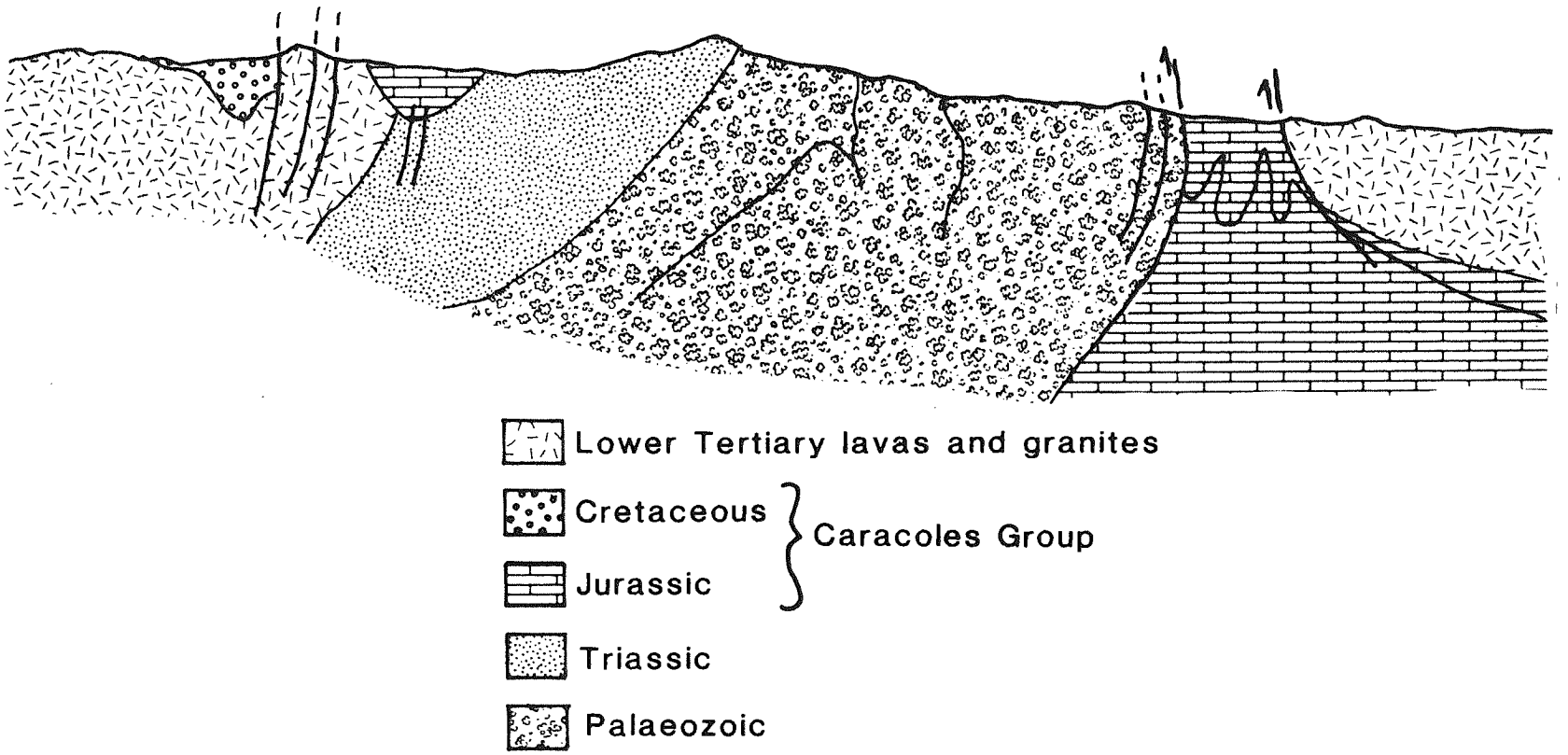

Fig. 6.7 Structural cross-section of the Caracoles Group at 25S.

(after Chong, 1977; Chong and Reutter, 1985).

6.3.2 Tonel Formation

The Tonel Formation (Dingman,1967), outcrops on the eastern flanks of the Cordillera de Domeyko (Fig. 6.1), forming a spectacular fault scarp along the western edge of the Salar de Atacama.

The Formation was first described as the Salinas de Purilactis Formation by Bruggen (1942,1950). Dingman (1967) renamed the unit the Tonel Formation, to avoid confusion with the overlying Purilactis Formation. Subsequent workers (Maranovic and Lahsen,1984) have reverted to considering it part of the Purilactis Formation.

Field evidence indicates however, that the two units should be considered separate Formations, for the following reasons:

1) The Purilactis Formation is composed of coarse sandstones and conglomerates. The Tonel Formation is composed dominantly of mudstones and siltstones.

2) The Tonel Formation is intruded by green hornblende rich dykes and sills. Clasts of these intrusives are found throughout the Purilactis Formation.

3) No evaporites are present in the Purilactis Formation. The Tonel Formation contains extensive evaporites.

4) The Tonel Formation dips to the west and strikes N-S. The Purilactis Formation forms a NE-SW oriented plunging syncline (with dips of up to 60 degrees), the southern nose of which unconformably overlies the Tonel Formation, with a minor, thrusted contact (Plate 6.2).

The Tonel Formation is, consequently, considered to be older than the Purilactis Formation, and has been assigned a Jurassic age (?Oxfordian) on the basis of its lithology and stratigraphic position

(Dingman,1967). It unconformably overlies the Agua Dulce and El Bordo Formations, a further indication of a probable Jurassic age.

The Tonel Formation consists dominantly of interbedded mudstones (commonly with desiccation cracks), siltstones with minor evaporites (halite and gypsum) and fine sandstones. A generalised log of the Formation is presented in Figure 6.8.

The Formation is relatively undisturbed by later tectonic events. However, a period of extension and associated magmatism, resulting in high level intrusions, occurred after deposition (section 5.4.2). Otherwise, deformation is limited to normal and thrust faults at the contact with the Purilactis Formation (where the presence of evaporites would aid movement), and the western boundary of the Formation (Ramirez and Gardeweg,1982).

Interpretation: The Tonel Formation was deposited in a continental setting, and probably represents a distal alluvial fan/sand flat/playa lake environment, as indicated by the fine grain size of the sediments and the presence of evaporites.

Owing to the uncertainty in the age of the Tonel Formation its exact relationship to the Caracoles Group is uncertain. It may be a lateral equivalent of the Group, or represent a northern extension of the continental sedimentation, associated with the final closure of the back-arc basin. Preliminary work indicates that the Formation does not contain any limestone clasts, consequently the Caracoles Group could not have been uplifted to form a westerly source area during the deposition of the Tonel Formation. Further work however (particularly palaeocurrent evidence), is required to determine the source area of the Tonel Formation.

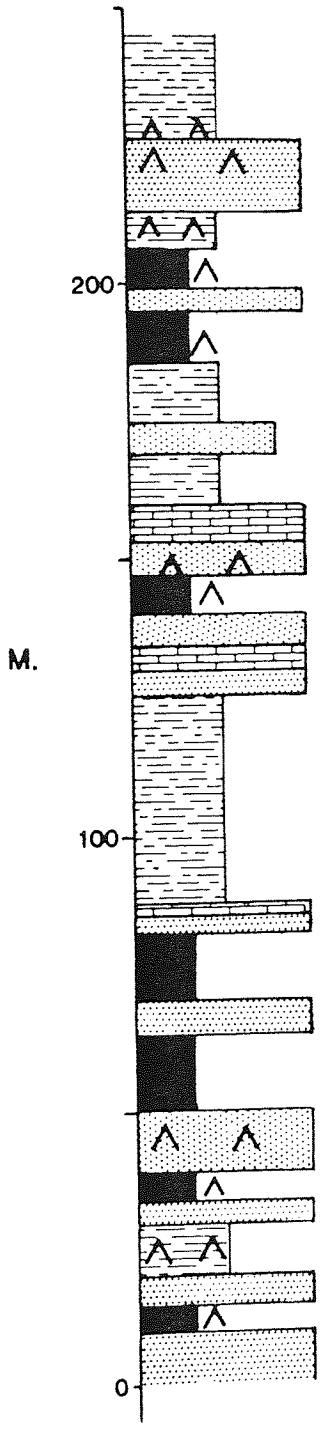

Fig. 6.8 Summary log of the Tonel Formation, for key see Fig. 6.2b.

6.3.3 The Purilactis Formation

The Purilactis Formation outcrops in the form of a folded plunging syncline, closing to both the north and south (Fig. 6.9a). It forms the eastern edge of the Cordillera de Domeyko, adjacent to the Llano de Paciencia (Fig. 6.1). The Purilactis Formation unconformably overlies the Tonel and Tuina Formations. Where the contact is seen, small scale thrust faulting is usually present (Plate 6.2). It is unconformably overlain by the Paciencia Group (Plate 6.3).

Only a broad description of the sedimentology of the Purilactis Formation is possible within the scope of this chapter, although more detailed studies have been undertaken. Therefore, the sedimentology of the Formation is briefly summarised, and a broad facies analysis of the basin fill sequence presented.

The Purilactis Formation was first defined by Bruggen (1934,1950), and subsequently described by Harrington (1961), Dingman (1963,1967), Hollingworth and Rutland (1968) and Marinovic and Lahsen (1984). Dingman (1963,1967) described the Formation in detail, producing a generalised log for the southern part of the eastern limb of the syncline, and assigned a Cretaceous age to the Purilactis Formation, based on a derived Mid-Upper Jurassic fossil content (Felsch,1933).

The Formation is approximately 3500m. thick, and displays considerable sedimentological variation, making correlation across the limbs of the syncline particularly difficult. Consequently, the Formation is discussed within a regional context.

Figure 6.9a shows the locations of sedimentary logs measured in the Purilactis Formation. The Formation comprises a variety of fluvial facies (Miall, 1987), with associated aeolian, lake margin sabkha and

Plate 6.3 Field photograph taken from the northeastern part of the Purilactis basin (Fig. 6.9a), looking south. On the right, are the light coloured sandstones of the Rio Salado Member of the Paciencia Group, which unconformably overlie red mudstones (and light brown sandstones), from the lowest part of the Purilactis Formation.

Plate 6.4 Field photograph from Quebrada Seilao (Fig. 6.9a), looking east across the Llano de Paciencia. In the distance are the volcanoes of the Cordillera de los Andes. In front of these the red and white ridge of the Cordillera de la Sal is exposed. The light brown rocks in the far foreground comprise part of a Pliocene ignimbrite flow. in the near foreground, Member 1 of the Purilactis Formation is exposed (Fig. 6.9b), coarse red and green sandstones. Stratigraphically, this is the lowest exposure of the Purilactis Formation in Quebrada Seilao.

lacustrine intercalations. The Quebrada Seilao section has been taken as the type section for the Formation. The base of the Formation is not seen at this locality. However, similar facies to the basal member are involved in localised thrust faulting, at the contact with the Tonel Formation.

Quebrada Seilao section:

Based on lithological variation this section has been split into 8 Members (Fig. 6.9b):

Member 1 (160m. thick) consists of a sequence of stacked channelised coarse sandstones, with palaeocurrents derived from the SE, interpreted as a braided fluvial system (Plate 6.4).

Member 2 (430m. thick) is characterised by isolated sandstone channels in bioturbated mudstones and siltstones. The channels were derived from the N/NE (in contrast to Member 1), and are thought to represent an anastomosing or meandering fluvial system (Plate 6.5).

Member 3 (210m. thick) is similar to Member 2 having palaeocurrents derived from the N/NE, but is generally coarser grained. It contains isolated conglomerate packets in bioturbated mudstones and siltstones, representative of a braided fluvial system (Plate 6.6).

Member 4 (40m. thick) consists of a sequence of poorly channelised conglomerates and very coarse sandstones, with no mudstones or siltstones (Plate 6.6).

Member 5 (440m. thick) comprises a sequence of stacked, large scale trough cross bedded, green sandstones; with palaeocurrents derived from the NW (Plates 6.6,6.7). The sandstones commonly contain thin horizons of grain fall laminae, indicative of aeolian deposition (Hunter,1977)

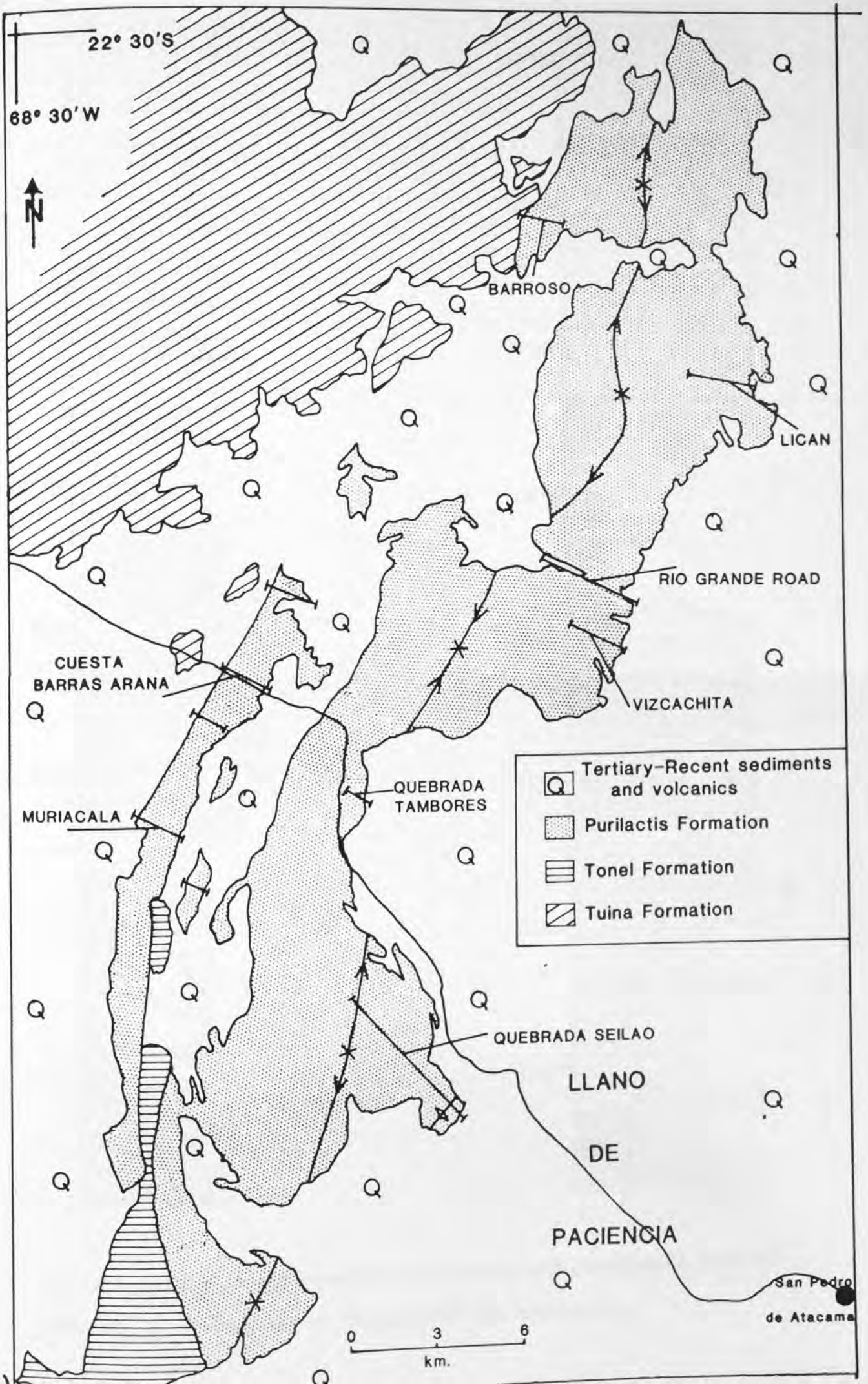
22° 30'S
68° 30'W
N
BARROSO
LICAN
RIO GRANDE ROAD
CUESTA
BARRAS ARANA
VIZCACHITA
QUEBRADA
TAMBORES
MURIACALA
QUEBRADA SEILAO
LLANO
DE
PACIENCIA
San Pedro
de Atacama
0
3
6
km.
Tertiary-Recent sediments and volcanics
Purilactis Formation
Tonel Formation
Tuina Formation

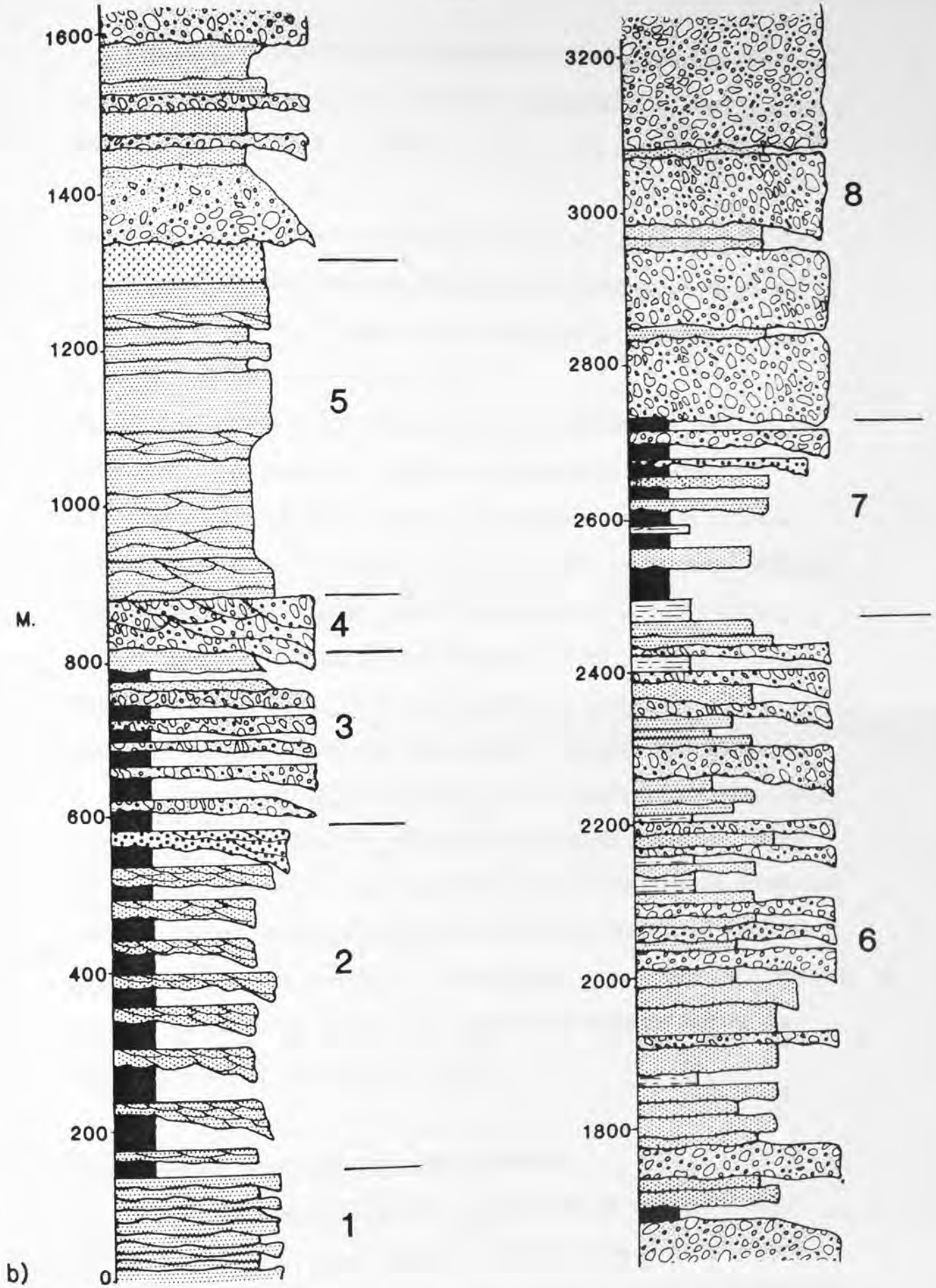

Fig. 6.9 The Purilactis Formation: a) outcrop and location of measured sections, b) summary log of the Quebrada Seilao section,

The lower five members of the Quebrada Seilao section are overlain by a 40m. thick (often brecciated) andesite lava. The lava has a weathered and eroded top, indicating that it is not a high level intrusion.

Member 6 (1100m. thick) is characterised by a complex sequence of channelised conglomerates, sandstones and siltstones which generally fine upwards and are thought to be related to proximal and distal alluvial fan deposition (Plate 6.7).

Member 7 comprises finely laminated (on a millimetre scale), bioturbated, purple siltstones, thought to represent a lacustrine environment. Coarse sandstone and conglomerate horizons increase towards the top of the member, and are thought to represent alluvial fan discharge into a lake, possibly in the form of a fan-delta.

Member 8 consists of coarse conglomerates often poorly channelised, with thin interbedded laterally impersistent sandstones and mudstones, representing relatively proximal braided, alluvial fan deposition.

Throughout the Quebrada Seilao section clast composition rarely varies, it is dominated by purple, red and black andesites, green Tonel intrusives, white acid plutonics, red porphyries and less commonly Mid-Upper Jurassic limestone clasts. The limestone clasts are present from Member 3 upwards. Consequently, except for the limestone clasts, no change in source area composition occurred during the deposition of the Purilactis Formation.

Cuesta Barros Arana and equivalent sections:

A measured section from the western limb of the syncline at Cuesta Barros Arana (Fig. 6.9c), is thought to be the approximate stratigraphical equivalent of Members 1 to ?5 from the Quebrada Seilao

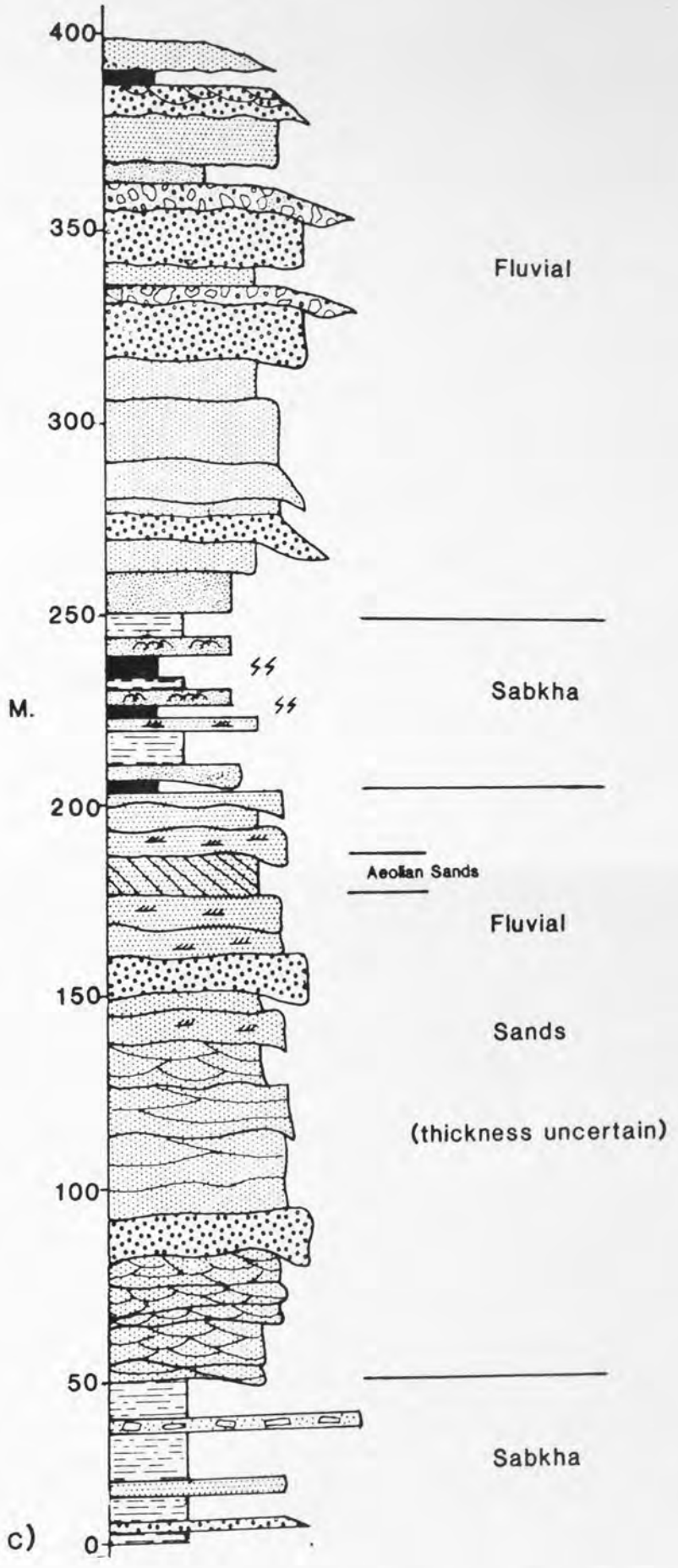

c) summary log of the Cuesta Barras Arana section,

Plate 6.5 Field photograph from Quebrada Seilao (Fig. 6.9a). Member 2 of the Purilactis Formation (Fig. 6.9b), consisting of channels comprised of a series of thin pinching and swelling units of coarse sandstone, interbedded with red bioturbated mudstones and siltstones. The main channel in the centre of the field of view is 8m. thick

Plate 6.6 Field photograph from Quebrada Seilao (Fig. 6.9a). Members 3, 4 and 5 (Fig. 6.9b) of the Purilactis Formation. Member 3 is exposed on the left of the photograph and consists of thin sheet-like coarse sandstones and conglomerates, interbedded with red sandstones and siltstones. Member 4 (the prominent outcrop in the centre and right, between the arrows), consists of a series of stacked channels of conglomerate and very coarse sandstone, with no siltstones or mudstones. To the right of Member 4 (extreme right of the photograph), the green sandstones of Member 5 can be seen. On the extreme top right of the picture, the western limb of the Purilactis syncline can be seen. On the extreme left is on outcrop of light brown Pliocene ignimbrite. The distance between the arrows is 40m.

section. The section is 400m.+ thick, and from the base upwards comprises:

1) Finely laminated red mudstones and siltstones with occasional anhydrite nodules, thought to represent a playa lake type environment. This seqence is at least 50m. thick, however, the base is not seen.

2) Medium-coarse light grey sandstones (150m. thick). High angle foresets and abundance of grainfall laminae in one horizon indicates deposition in an aeolian environment. However, most of the sands are thought to be fluvial in origin as they commonly contain mud rip-up clasts. Locally the sandstones are highly fractured.

3) Grey mudstones which are finely laminated and contain adhesion ripples, burrows, anhydrite nodules and thin laterally extensive beds of coarse sandstone (Plate 6.8), which eventually dominate the succession. This sequence is approximately 50m. thick, and thought to represent an inland sabkha environment, with increased fluvial? input towards the top.

4) Massive coarse brown and grey sandstones (approximately 70m. thick), which contain isolated pebbles and mud clasts, and may sometimes be normally graded. These sandstones are fluvial in origin.

5) Interbedded brown conglomerates and trough cross bedded coarse brown sandstones again of fluvial origin. This sequence is 80m.+ thick, however, it may be thicker, as the top is not exposed.

At this point in the succession, a loss of exposure occurs (which may be due to erosion of easily weathered siltstones and mudstones), before Members 5 and 6 are seen forther east, close to the synclinal axis (Fig 6.9d).

Another section in the west limb, about 6km. north of Cuesta Barros Arana (Fig. 6.9a), contains similar grey, structureless, well

Plate 6.7 Field photograph from Quebrada Seilao (Fig. 6.9a). Members 5 and 6 of the Purilactis Formation (Fig. 6.9b). The green sandstones of Member 5 are present in the centre and bottom left of the field of view. The prominent red horizon above Member 5, is weathered andesite. The prominent white beds above the andesite, are sandstones of Member 6, covered by secondary anhydrite. Above these white sandstones conglomerates dominate the succession.

Plate 6.8 Field photograph from Cuesta Barros Arana (Fig. 6.9a). Laterally extensive sheet-like medium grey sandstones are interbedded with, and overlie the grey lake margin sabkha facies illustrated in Figure 6.9c. Height of cliff=35m.

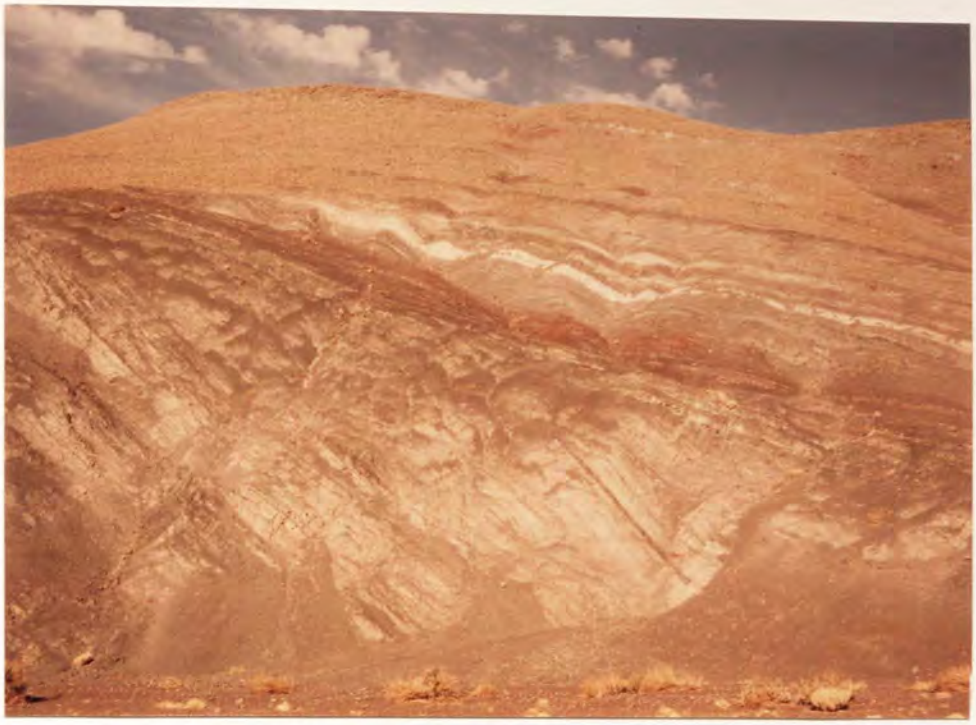

sorted sand bodies to the Lican and Vizcachita sections (see below), interpereted as reworked aeolian sand bodies. The lower part of this section (overlying basal siltstones and mudstones), contains interbedded red and green sandstones similar to those of Member 1 (Quebrada Seilao). Above the sandstones, mudstones and siltstones predominate, interpreted as a playa lake facies, possibly laterally equivalent to the Cuesta Barros Arana section. The top of this section is dominated by interbedded conglomerates and large scale, low angle trough cross bedded sandstones, laterally equivalent to the upper part of the Cuesta Barros Arana section, and probably deposited in a braided fluvial environment.

The sandstones and conglomerates seen at the top of the section north of Cuesta Barros Arana, can be traced 7km. to the south of Cuesta Barros Arana (Muriacala section; Fig. 6.9a), where they overlie massive, coarse grey sandstones of probable fluvial origin, deposited over the characteristic basal facies of red siltstones and mudstones.

Barroso section:

In this area (Fig. 6.9a), red siltstones, mudstones and occasional sandstones and thin limestones, unconformably overlie the Tuina Formation, with a poorly exposed, locally thrusted contact. At this point the mudstones and siltstones are much thicker than in the Cuesta Barros Arana section (approximately 700m.). Above this unit, poorly accessible coarse sandstone units are present (approximately 600m. thick).

Vizcachita and Rio Grande road sections:

The Vizcachita section (Fig. 6.9a), has a basal sequence of thin red and brown sandstones and mudstones, overlain by massive coarse grey sandstones of probable fluvial origin. These are overlain by green conglomerates similar to Member 6, which in turn are overlain by purple siltstones and green sandstones equivalent to Member 7. Owing to the plunging nature of the syncline, the synclinal axis falls within Member 7.

In the Rio Grande road section (Fig. 6.9a), the grey sandstones of fluvial origin from the Vizcachita section are equivalent to 600m. of aeolian sandstones, which formed aeolian dunes up to 30m. high (P. Turner, pers. comm.,1987). It is probable, that the structureless nature of the Vizcachita sandstones, results from the fluvial reworking of the well sorted aeolian dune sandstones, also indicated by the presence of well rounded quartz grains.

Members 6, 7 and 8 (and possibly 5), can be traced throughout the basin. On the western limb of the syncline above the Cuesta Barros Arana sections, similar facies to Members 6 and 7 are interbedded in a complex fashion. Member 7 appears to thicken going both north and west. Member 8 is extremely well exposed in Quebrada Tambores (Fig. 6.7a), and represents the final basin fill sequence.

Interpretation and Correlation of the Purilactis Basin Fill Sequence

Figure 6.9d shows the distribution and possible correlation of identified Members and equivalent facies, between logged sections, based mainly on sedimentological similarities. Members 1 to 5 appear to be laterally impersistent, although a possible correlation can be made between Member 5 (containing cross bedded sandstones with

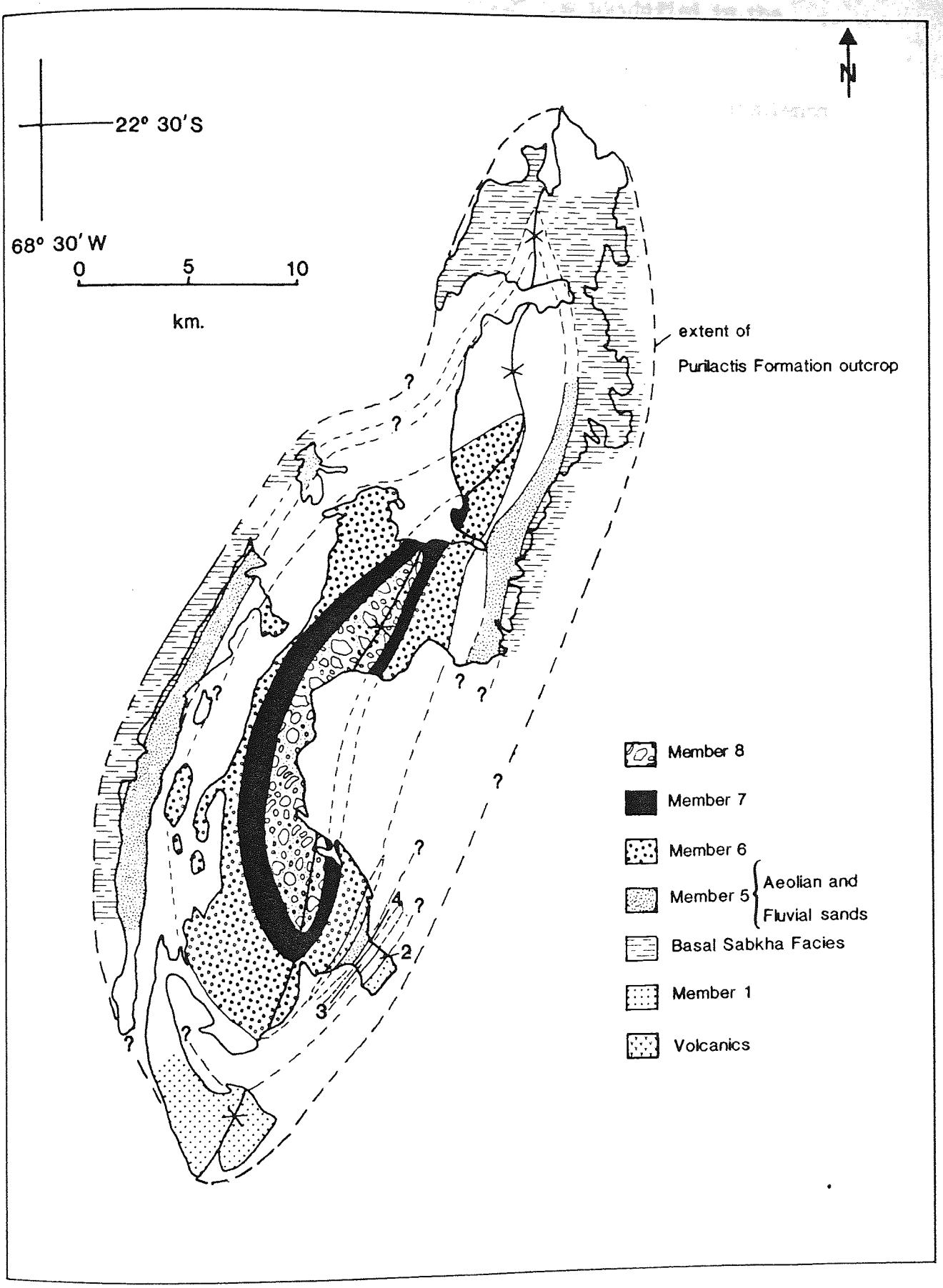

d)

d) possible facies distribution. Numbers correspond to Members defined in the Quebrada Seilao section (see text and Fig. 6.9b).

grainfall laminae), and the aeolian sandstones identified in the Cuesta Barros Arana and Rio Grande road sections.

It is thought that Members 1 to 5 and their lateral equivalents represent localised depositional environments, as inferred by the large facies variations from rocks of apparently the same age (Fig 6.9d).

The probable basin-wide distribution of Members 6 to 8, and increasing grain size over Members 1 to 5 and their lateral equivalents, indicate that the basin was actively shallowing during the latter part of its history (after eruption of an andesite lava; Fig. 6.9b).

The Purilactis Formation comprises a coarsening upward basin-fill sequence, implying that sediment supply exceeded subsidence and was tectonically mediated.

6.3.4 The Coloso Basin

The Coloso basin (Fig. 6.1), includes the Coloso, Lombriz and El Way Formations, and is the only basin to have formed in the Cordillera de la Costa of the study area during the Andean Orogenic cycle. The events resulting in the formation of the Coloso basin, have previously been discussed in Chapter 4. It is thought to have a unique evolution, related to the accretion of the Mejillones terrane. A brief sedimentologically orientated summary will be given here.

The Coloso Formation was deposited unconformably on the Mejillones Peninsula, the Jurassic La Negra Formation and the Bolfin Complex (Table 3.1; section 3.2; Chapter 4). The Coloso and overlying Lombriz Formation are thought to be of Lower Cretaceous age as they are overlain conformably by the Hauterivian El Way Formation.

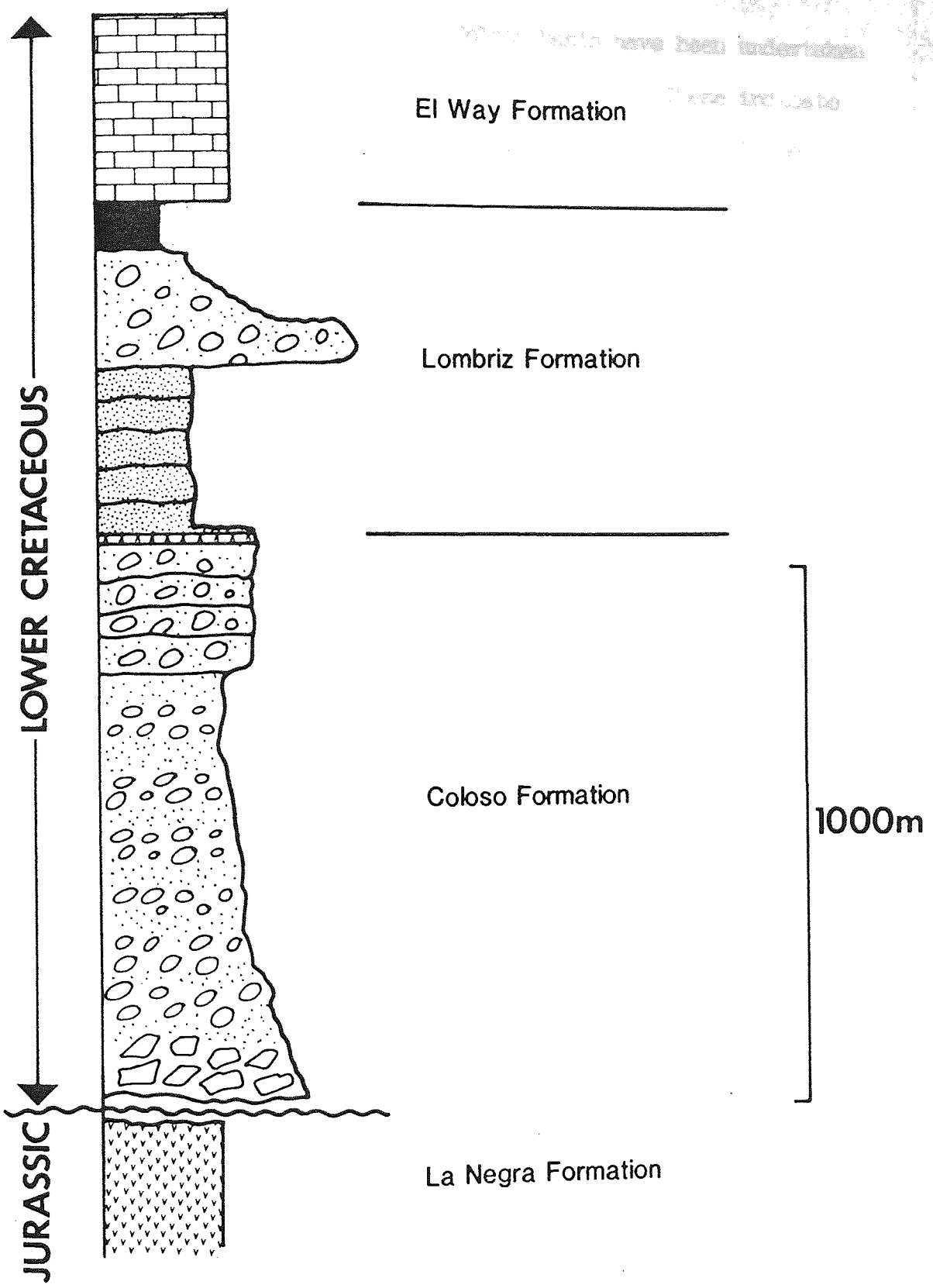

Fig. 6.10 Summary log of the Coloso basin. For key see Fig. 6.2b.

Sedimentological studies on the Coloso basin have been undertaken by Flint et al. (1986a), and Flint and Turner (1988). These indicate that the basin fill generally fines upwards (Fig 6.10). The Coloso Formation consists of coarse poorly confined proximal conglomerates, which grade into finer grained more distal, channelised conglomerates. The overlying Lombriz Formation is dominated by purple siltstones and fine grained sandstones which often contain dewatering structures, and are commonly interbedded with gypsum. This sequence is thought to represent a playa lake environment. The Lombriz Formation also contains a major proximal conglomerate horizon, which has a different source area to the Coloso Formation conglomerates, as indicated by palaeocurrents and clast composition (Flint and Turner,1988). Above the conglomerate, playa lake sedimention resumed, with thin sandstones, which in ths section commonly have thin oolitic grain coatings (Flint et al.,1986a). This sequence eventually passes into the shallow marine limestones of the El Way Formation.

The top part of the basin fill sequence has been interpreted by Flint et al. (1986a) and Flint and Turner (1988), as an alluvial fan-fan delta complex, complicated by facies variations associated with fan and inter fan sedimentation, and synsedimentary faulting. A schematic palaeogeography for the Coloso basin is presented in Fig. 6.11.

Interpretation: The Coloso basin is thought to have formed landward of the accreted Mejillones terrane (Chapter 4). Extension and subsidence at the edge of the forearc, along the suture between the South American continent and the accreted terrane, caused the formation of the basin. Sedimentation in the basin began with the deposition of the

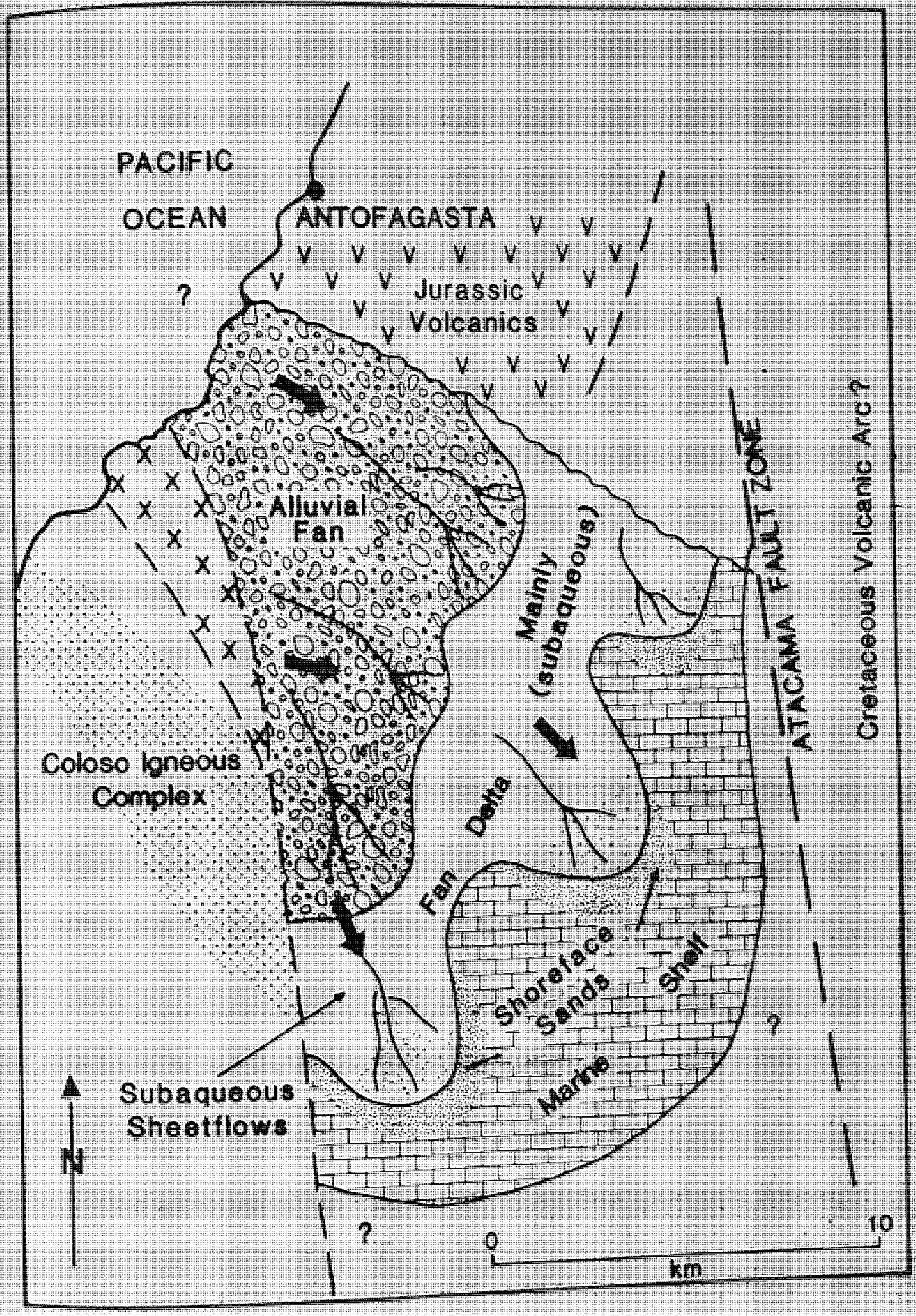

Fig. 6.11 Schematic palaeogeography for the Coloso Basin (after Turner and Flint, 1988).

proximal alluvial fans of the Coloso Formation and was succeeded by the dominantly distal alluvial fan and playa sediments of the Lombriz Formation. Further extension resulted in the alluvial fan-fan delta association, continuous subsidence resulted in the complete flooding of the basin and deposition of the El Way Formation.

6.3.5 Discussion of Jurassic to Mid-Cretaceous Basin Evolution

Jurassic marine strata, unconformably overlie the Agua Dulce Formation, but have not been recorded east of the Precordillera or Salar de Atacama. This implies that a significant topographical feature was present in the Precordillera throughout this period of time, restricting the marine transgression.

The sedimentological history of this Jurassic back-arc basin suggests that the basin continued opening until the Sinemurian, at this time the volcanic arc was at its furthest point west of the South American craton. After the Sinemurian, the back-arc basin gradually closed due to the accretion of the volcanic arc against the South American craton. This event resulted in the and uplift of the back-arc basin, and the deposition of shallow marine and continental sediments from the late Jurassic to Mid-Cretaceous.

A comparable tectonic setting is seen in Southern Chile during the Lower to mid-Cretaceous (Bruhn and Dalziel,1977), where a back-arc basin developed behind a volcanic arc with continental crust to the east.

The accretion of the volcanic arc in northern Chile (and probably along the entire western margin of South America; Dalziel,1986), may be due to the initiation of the break-up of Gondwanaland, or westwards movement of Gondwanaland. Either theory would result in the accretion

of the arc against the South American craton. Although it appears probable that Gondwanaland split in the early Cretaceous (Linares and Valencio,1975; Vilas,1976; Valencio et al.,1977; Rabinowitz and La Brecque,1979), activity in the Lower Jurassic could have preceeded the break, possibly associated with the accretion of the Mejillones terrane (Chapter 4).

Deposition of the Tonel Formation is thought to have taken place during the Oxfordian (Dingman,1967). Further work on the Formation is required to determine its source area and relationship to the back-arc basin. However, it is possible to reconstruct some aspects of Oxfordian palaeogeography. Evaporite deposition took place in the back-arc basin centre to the west of the Tonel Formation during the Oxfordian, as recorded by the Caracoles Group. It is possible therfore, that the Tonel Formation is laterally equivalent to the Oxfordian sediments of the Caracoles Group. This theory is supported by the facies associations of the two units, with the distal sand flats and occasional evaporites of the Tonel Formation passing southwards and westwards into a thicker sequence of evaporites in the basin centre. However, until further work is undertaken on the Tonel Formation any palaeogeographic reconstruction must remain tentative.

The above observations indicate that the Tonel Formation was unlikely to have been derived from a westerly-lying source area. As previously noted, the back-arc basin was restricted to the east by a palaeogeographic high, located close to the present day Precordillera. It is possible that this positive feature may have formed the source area for the Tonel Formation. However, the Tonel Formation currently forms the western edge of the Precordillera. Therefore, if the Tonel

Formation lay to the west of and was sourced by the "palaeo-Precordillera", it must have been transported eastwards to its present position by subsequent tectonic movements, a theory considered below.

Following contraction of the back-arc basin and deposition of the Tonel Formation, the Lower Cretaceous Coloso and Cretaceous Purilactis basins formed in the Andean forearc (both with distinctly different origins). The formation of the Coloso basin has been outlined in Chapter 4 and summarised above (Fig. 4.11, shows a schematic development history of the basin).

The evolution of the Coloso basin is similar to that envisaged by Bluck (1978), for the Old Red Sandstone in the Midland Valley of Scotland. In the latter, extension at the end of the Caledonian Orogeny, produced a fining upward sequence from coarse, thick, proximal conglomerates dominated by marginal palaeocurrents, to thinner, finer grained sandstones and calcrete beds, with axial palaeocurrent directions.

The formation of the Purilactis basin is much more problematical. The basin formed over the Tonel Formation and may have extended further eastwards than at present (the eastern basin margin is not exposed). It formed after a period of extension associated with the intrusion of hornblende rich-dykes and sills into the Tonel Formation. The basal member of the Purilactis Formation (Quebrada Seilao section), is sourced from the southeast, implying the presence of positive area (relicts of the source area of the Tonel Formation?). However, the rest of the Formation has northwesterly derived palaeocurrents. This evidence coupled with a clast content including: 1) Tonel intrusives, 2) fossiliferous Jurassic limestones, 3) andesites, and 4) acid plutonics (possibly from the Limon Verde

complex), indicates that the carbonate basin, the Tonel Formation and basement lying to the west and north of the basin had been uplifted, probably resulting from the closure of the back-arc basin by Purilactis times.

The Purilactis basin-fill sequence of distal to proximal sediments, and the change from easterly to northwesterly derived palaeocurrents, implies continuous uplift and relative movement of the source area basinwards, and/or decreasing subsidence of the basin. Uplift may be related to the eastward transport of the Tonel Formation (see above), as the Purilactis Formation unconformably overlies the Tonel Formation, any eastward movement would also affect the Purilactis Formation. It is possible that deposition in the Purilactis basin took place during this eastwards movement, ie. a "piggy-back" basin carried on the back of an eastwardly propagating thrust system.

Both the Purilactis and Tonel Formations have probably been transported eastwards to comprise part of the Precordillera. This would imply that a stable block existed in the Precordillera, against which the Purilactis and Tonel Formations were emplaced. The presence of buoyant continental crust below the Precordillera would account for this, and would also account for the palaeogeographic high present during the deposition of the Caracoles Group, and the easterly source area required for the Tonel Formation and lower member of the Purilactis Formation. Schematic diagrams of Jurassic to mid-Cretaceous basin evolution sedimentation and deformation are shown in Figures 6.12a,b.

It should be noted that palaeomagnetic data (section 5.5.1) indicate approximately 33 degrees of post-depositional clockwise rotation of the Purilactis Formation. This implies that the measured

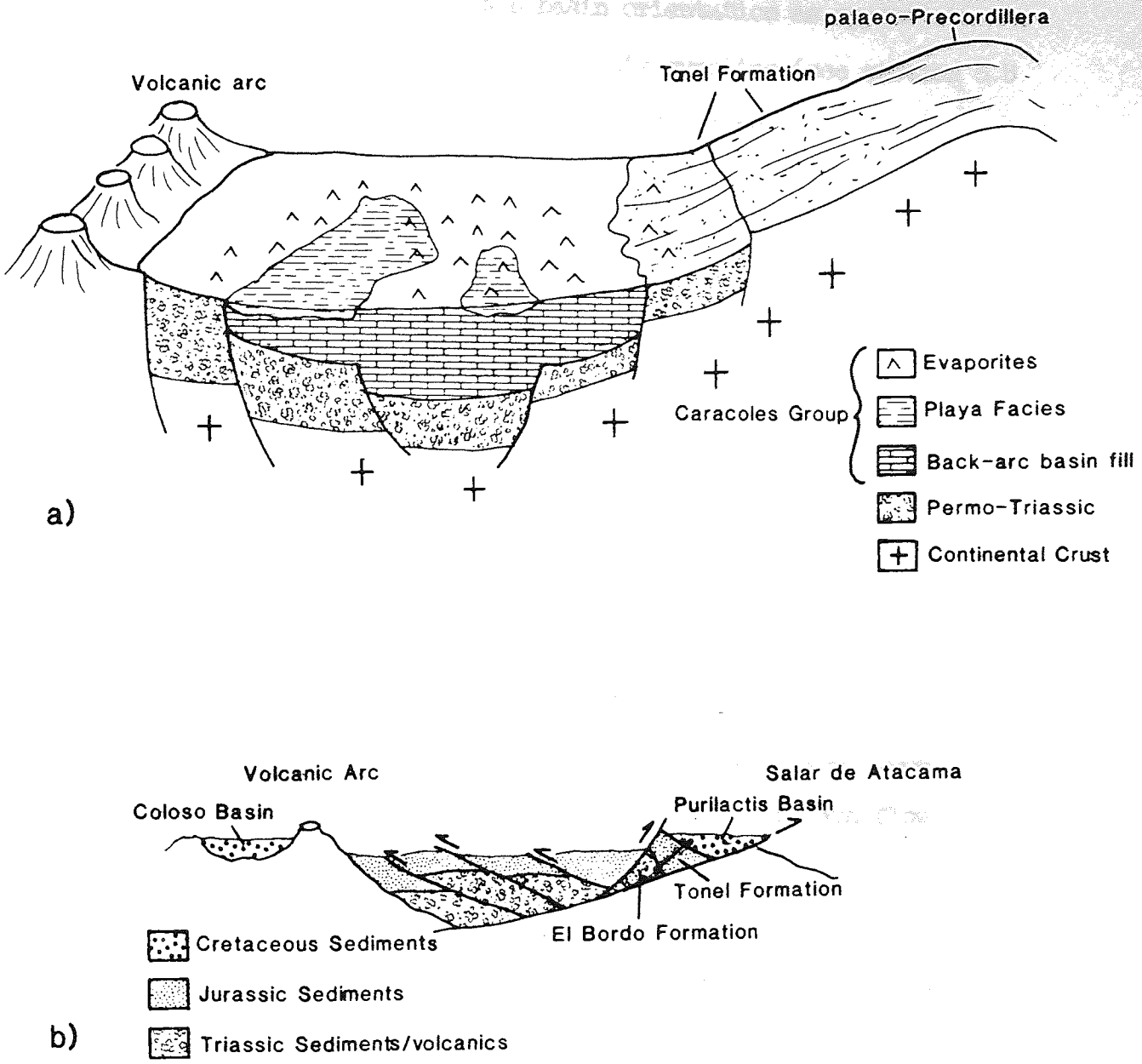

Fig. 6.12a Schematic diagram of Lower Jurassic to Upper Jurassic basin evolution in the Andean forearc.

Fig. 6.12b Lower Cretaceous to Mid-Cretaceous basin evolution. Note the compression of the back-arc basin sequence (Caracoles Group).

N/NE derived palaecurrents were in fact derived from the N/NW; this would also give an approximate N/S basin orientation as opposed to the present NE/SW orientation of the Purilactis syncline (see section 5.5 for an explanation of the present basin orientation).

6.4 Mid-Cretaceous to Recent Basin Evolution

6.4.1 The Paciencia Group

The Paciencia Group outcrops on the eastern edge of the Cordillera de Domeyko (where it unconformably overlies the Purilactis Formation; Plate 6.3), and extends further eastwards where it infills the northern part of the Salar de Atacama depression (Fig. 6.1). The Group is thought to be Oligocene-Lower Miocene in age based on a radiometric date derived from an interbedded ash flow (28+/-6Ma., Travisany,1978), and the 17+/-2Ma age of an overlying lava flow (Ramirez,1979).

The sedimentology of the Paciencia Group has been described by Flint (1985a,b), who distinguished two source areas for the 2000m. thick continental sequence.

Westerly derived sediments:

These consist of the Barros Arana and Rio Salado Members (Fig. 6.13). The Barros Arana Member comprises clast-supported conglomerates, interpreted as distal fan/pebbly braided stream sediments deposited along the western margin of the San Pedro basin (Flint,1985a). The Rio Salado Member was widely deposited and overlies the easterly derived succession (Fig. 6.13). The mudstones and

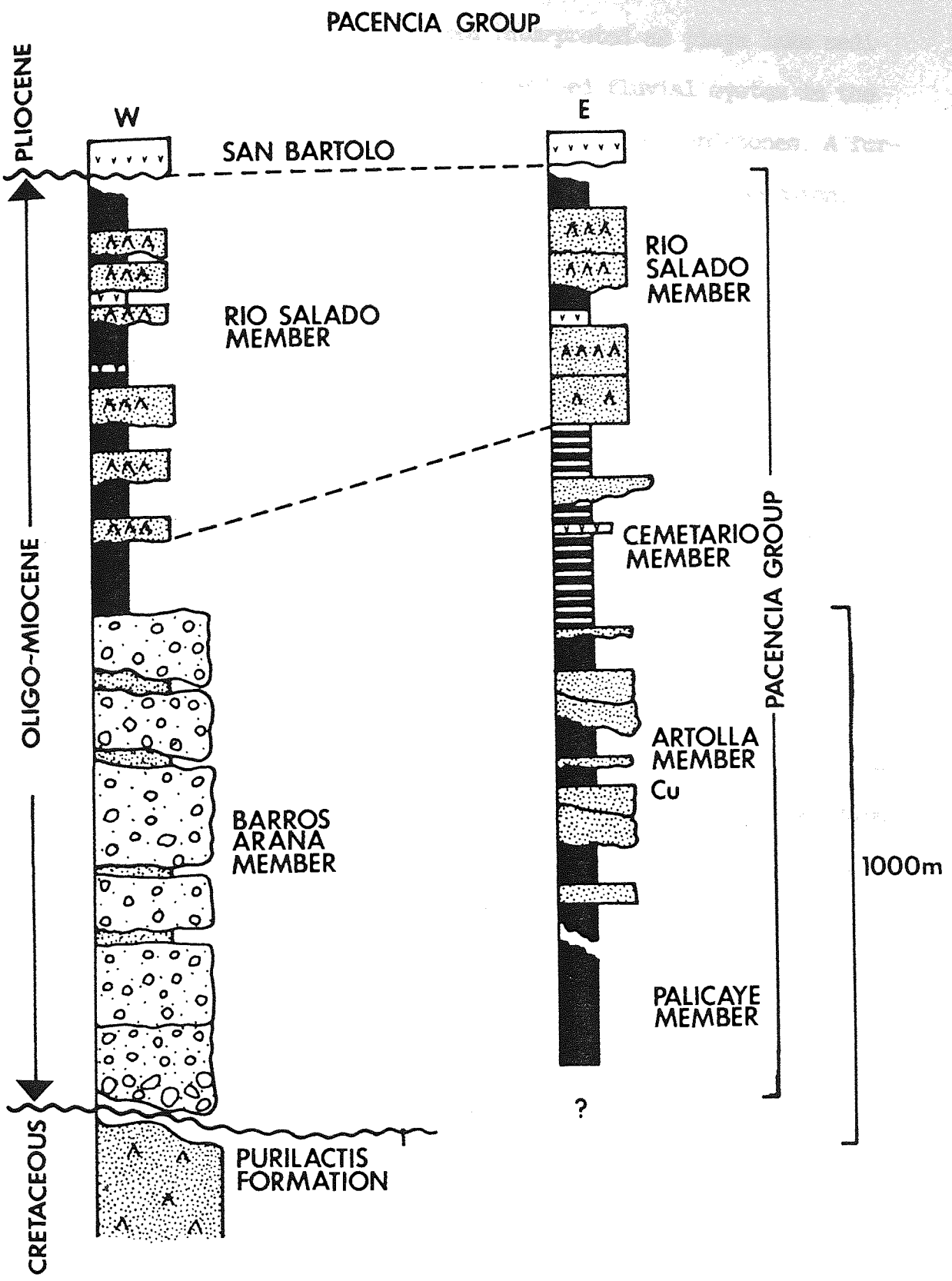

Fig. 6.13 Summary log of the Paciencia Group (after Flint,1985a). For key see Fig. 6.2b

evaporites of this member have been interpreted as playa lake sediments (Flint, 1985a), with a locally derived fluvial system in the west of the basin represented by thin channelised sandstones. A further sequence of Barros Arana conglomerates tops the succession, testifying to later source area rejuvenation.

Easterly derived sediments:

The eastern part of the basin was dominated by playa lake and marginal sandflat depositional environments (with occasional thin sandstones of fluvial origin, with easterly derived palaeocurrents), represented by the Palicaye, Artolla and Cementario Members (Fig. 6.13). The sequence is overlain by the westerly derived Rio Salado Member.

Interpretation: Based on facies associations, Flint (1985a,b) interpreted the Paciencia Group as being deposited in a half-graben type basin, with sediments derived from both foot-wall and hanging-wall blocks. Later fault movement resulted in western source area rejuvenation reflected by the deposition of the extensive Rio Salado Member and the top sequence of the Barros Arana Member. The easterly source area has subsequently been covered by Pliocene to Recent volcanics (Fig. 6.1).

6.4.2 The Salar de Atacama

The Salar de Atacama forms part of a N/S striking depression located between the Precordillera and the Cordillera de los Andes (Figs. 2.1,6.1). Sedimentation in the Salar is similar to many of the continental sedimentary formations previously described. Sedimentation

at the edge of the salar is dominated proximal and distal alluvial fan facies. Fluvial sediments, related to the ephemeral Rio Grande are found in the northern and western parts of the basin. The centre of the Salar contains extensive sand flats and halite deposits, together with mudstones and siltstones deposited in ephemeral plaka lakes. Estimates of the basin thickness have been put at 8km. based on seismic evidence (G. Chong, pers. comm.,1987).

The history of the basin is unknown, but Flint (1985b) suggested that the Salar de Atacama, possibly represents a modern analogue to the older San Pedro basin, as the focus of sedimentation and subsidence appears to have moved south with time. The probable 8km. thickness of sedimentary pile, indicates that the basin may in fact have originated prior to the late Tertiary. Further discussion of the origin of the basin is presented below (section 6.11).

6.4.3 The Central Depression

This basin forms a major geomorphological and geological province (Fig. 6.1), and encompasses the area between the Precordillera and the Cordillera de la Costa. It is bounded by the extensional Atacama Fault zone to the west (which is over 1000km. long), and the Domeyko thrust front to the east.

Like the Salar de Atacama, the age of initiation of the basin is unknown, but it may have originated through Pliocene-Recent forearc extension (see below). Sedimentation in the studied segment of the Central Depression is limited to proximal and distal alluvial fan deposition, with extensive sand flats and salt pans. Three Recent fault scarps (up to 2.5m. high) cut the alluvial fans, producing a stepped morphology. These scarps can be traced for over 30km.

Deposition in the studied area is limited to small isolated basins (with the exception of the Loa basin, see below), located between uplifted areas of Mesozoic-Lower Tertiary sediments and Palaeozoic basement (Fig. 6.1).

The Loa Basin: Active deposition in the Central Depression is currently limited to the Loa basin in the east of the studied segment of the Central Depression (Fig. 6.1). The basin contains Pliocene sediments, testifying to the longevity of the Rio Loa, currently the only permanent fluvial system in northern Chile.

6.4.4 The Cordillera de la Costa

Sedimentation on the western flanks of the Cordillera de la Costa has been active from the late Teriary onwards, and is represented by the Hornitos, La Portada and Mejillones Formations (Ferraris and Di Biase,1978; Table 3.1). These are comprised of interbedded shallow marine gravels and fossiliferous limestones, aeolian sandstones and alluvial fan conglomerates derived from the Cordillera de la Costa. These sediments were deposited and preserved due to the isostatic uplift of the Cordillera de la Costa after the Pleistocene glaciation (Paskoff,1977).

6.4.5 Discussion of Mid-Cretaceous to Recent Basin Evolution

Sedimentation ceased at the end of the ?mid-Cretaceous. The locus of deposition moved eastwards to the San Pedro basin after the deposition of the Purilactis Formation. Assuming the Purilactis Formation is Lower Cretaceous in age, a time gap of 85Ma. separates periods of

active sedimentation. This is in contrast to the Lower Tertiary succession of Eocene red beds and volcanics of the Cinchado Formation (Marinovic and Lahsen,1982), to the south of the study area.

Uplift and ?folding of the Purilactis Formation or subsidence of the area to the east of the Purilactis Formation, resulted in it forming the source area for the westerly derived members of the Paciencia Group. The finer grained nature of the Paciencia Group Members (except the Barros Arana Member) and the easterly derived palaeocurrents, testifies to the lack of a permanently elevated source area to the west during deposition of the Paciencia Group, except for periodic uplift resulting in the final basin fill sequences of the Rio Salado and Upper Barros Arana Members.

The present day basins of the Andean forearc (with the exception of the Salar de Atacama), result from the recent extension of the forearc in the Central Depression (the old back-arc basin). Extension may have occurred along pre-existing thrust faults, and resulted in the present day topography of the Central Depression, producing many small basins in the central and western parts of the Central Depression. These basins are scattered between areas of basement, which are thought to represent the surface expression of tilted fault blocks. Subsidence in the Central Depression appears to be more active in the east, where deposition is taking place in the Loa basin related to the Rio Loa floodplain.

A schematic diagram of mid-Cretaceous to Recent basin evolution and sedimentation is shown in Figures 6.14a,b.

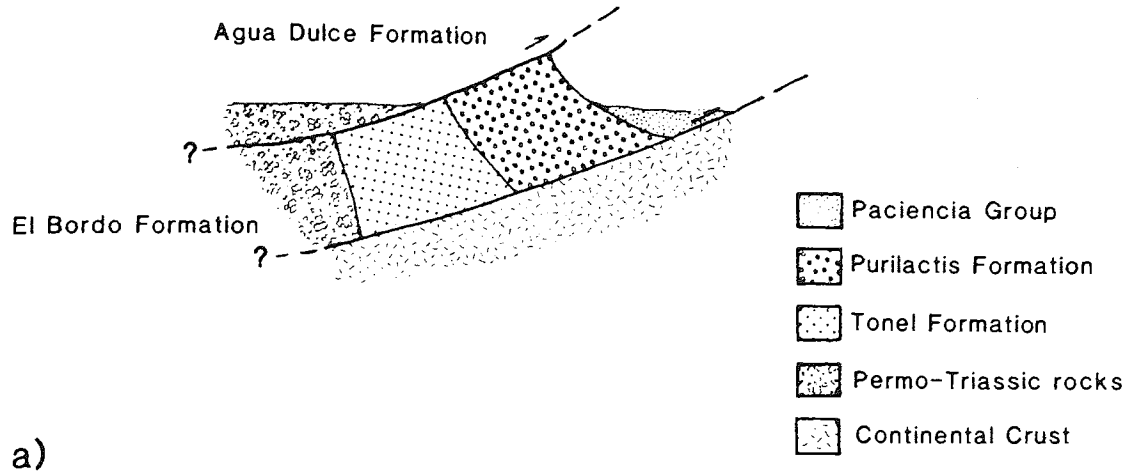

a)

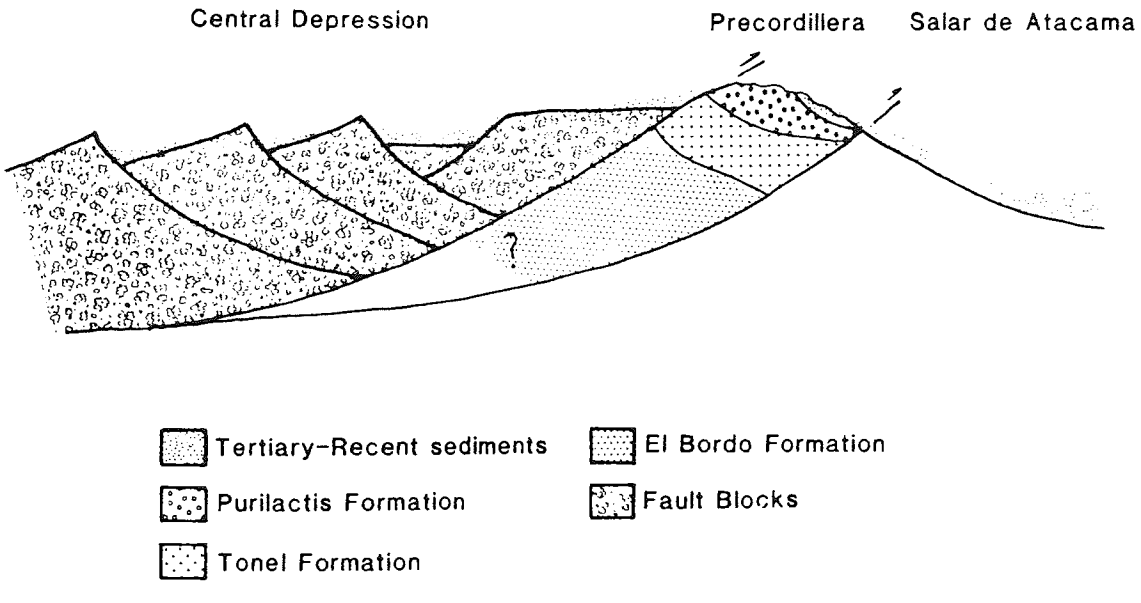

b)

Fig. 6.14a Schematic diagram Mid-Cretaceous to Miocene basin evolution in the Andean forearc (Precordillera).

Fig. 6.14b Miocene to Recent basin evolution. The tilted fault blocks are composed of Precambrian basement (eg. Limon Verde schists; Chapter 2), Triassic sediments and volcanics (Agua Dulce Formation) and the Hettangian-Hauterivian back-arc basin fill.

6.5 Discussion

Sedimentary basin formation and basin fill sequences in the Precordillera indicate that from the Tonel Formation to the Paciencia Group the locus of sedimentation has moved eastwards. Throughout this period fine grained sediments were consistently derived from the east and coarse grained sediments from the west, in the Purilactis Formation and the Paciencia Group. This indicates that the westerly source area was periodically uplifted to supply coarse grained detritus to the basins. Considering that the back-arc basin was being continually compressed/uplifted (probably from the late Jurassic onwards), the Purilactis and San Pedro basins are thought to be foreland basins, formed in front of an eastwardly propagating thrust front. This interpretation is supported by the eastwards movement of basins, and the continuous uplift of a proximal source area to the west of the basins. Deposition in the basins ceased through extended compression which resulted in the coarsening upwards basin fill sequences, but eventually cut off sediment sources.

A similar tectonic setting to the mid-Cretaceous to Lower Tertiary sequences of the Andean forearc is seen in the late Tertiary to Recent succession of NW Argentina. In San Juan Province (27°S), a foreland basin lay to the east of an active thrust zone and volcanic arc (Johnson et al.,1986), resulting in a sedimentary sequence similar to the Purilactis Formation. The sequence contains basal fluvial sediments overlain by alluvial-fan sediments, indicating continued source area uplift during deposition (Johnson et al.,1986).

The eastward movement of the locus of sedimentation effectively resulted in the encroachment of sedimentary basins across the Salar de

Atacama. However, this eastwards movement is periodic, as indicated by the large time gap between basin formation (Lower cretaceous-Oligocene). Also, eastward thrust propagation would not be aided by the probable presence of buoyant continental crust beneath the Precordillera, indicated by the lack of deformation east of the Precordillera, adjacent to the Salar de Atacama. yet to the north and south of the Salar, the position of the thrust front as shown by the location of the Precordillera, is much further to the east (Fig. 6.1).

6.5.1 Summary of Events

1) Permian-Triassic: Deposition of the shallow marine, continental and volcanic Tuina, El Bordo and Agua Dulce Formations took place in an extensional tectonic setting, in basins possibly formed through the rifting of the South American craton. The Peine and Cerros Negros Formations also record this extensional event, which may have been responsible for the initiation of the Salar de Atacama.

2) Jurassic: Deposition of the Caracoles Group took place in a back-arc basin, behind an active volcanic arc; represented by the present day Cordillera de la Costa. The Caracoles Group records the opening and closure of the back-arc basin through the presence of continental, shallow and deep marine sediments. The Tonel Formation was deposited on the eastern edge of the receeding ocean during the late Jurassic (?Oxfordian).

3) Lower Cretaceous-Eocene: The back-arc basin extended slightly in the Lower Cretaceous, as recorded by a minor marine transgression, however the basin was completely closed by the Hauterivian. Closure

took place due to the accretion of the Jurassic volcanic arc and Mejillones terrane, coupled with the westwards movement of South America away from Africa. The closure of the basin resulted in the deformation of the back-arc basin sequence and the formation of a foreland basin to the east of the deformation front, where deposition of the Purilactis Formation took place. The continued movement of the deformation front eastwards is recorded by the upward coarsening nature of the Purilactis Formation. Also at this time, extension dominated the western margin of the study area, as indicated by the formation of the Coloso basin behind the accreted Mejillones terrane. As shown in Chapters 3 and 5, extension and compression can act synchronously at an active plate margin.

4) Eocene-Miocene: Deformation of the back-arc basin was still active up to this period, with the movement of the deformation front eastwards over the Purilactis Formation, and the deposition of the Paciencia Group in a foreland basin. The sediments of the Paciencia Group record the periodic eastwards movement of the deformation front through the presence of westerly derived conglomerates towards the top of the Group. The mid-Miocene Quechua deformation phase (Table 2.1), testifies to continued compression within the forearc, and was followed by extensive ignimbrite eruption.

5) Pliocene-Recent: Compression was still active in the forearc during this period, as recorded by locally thrust faulted Pliocene ignimbrites to the east of the Precordillera. However, west of and including the Precordillera extension dominated the forearc, as indicated by the formation of the Central Depression and the clockwise

rotation of the forearc (Chapters 3 and 5). The formation of the Central Depression is thought to have taken place through the reactivation of thrust faults formed during the compression of the back-arc basin sequence, this has resulted in a series of tilted fault blocks separated by small isolated sedimentary basins (Fig. 6.14b).

The above work has shown that Mesozoic-Recent sedimentary basin formation in the Andean forearc is complex and related to the interaction of compression and extension at a destructive plate margin.

CHAPTER 7

DIAGENESIS OF ANDEAN ALLUVIUM, NORTHERN CHILE

7.1 Introduction

A model for the diagensis of continental sediments in arid climatic zones has been well established for some time (Walker,1967; Walker et al.,1978; Turner,1980). In the model, emphasis is placed on the dissolution of framework grains in oxidising groundwater, frequently near neutral pH and under shallow burial conditions, resulting in a distinctive suite of authigenic minerals including quartz, alkali feldspar, haematite, zeolites and clays. The authigenic phases precipitate as discrete crystals, replacements and syntaxial overgrowths under suitable interstitial conditions. The formation of authigenic haematite has important palaeomagnetic implications, as the time at which haematite precipitation took place can be identified palaeomagnetically.

Red bed deposition has dominated throughout much of the Mesozoic in the Central Andes, northern Chile, and provides a good opportunity to make comparative studies of the diagenesis of continental sediments of differing ages, deposited in basins formed in different tectonic settings.

Four stratigraphic units have been included in the study. These are: the Agua Dulce Formation, the Purilactis Formation, the Coloso Formation and the Paciencia Group (Fig. 7.1). The sedimentology, basin fill sequence and evolution of these units has been discussed

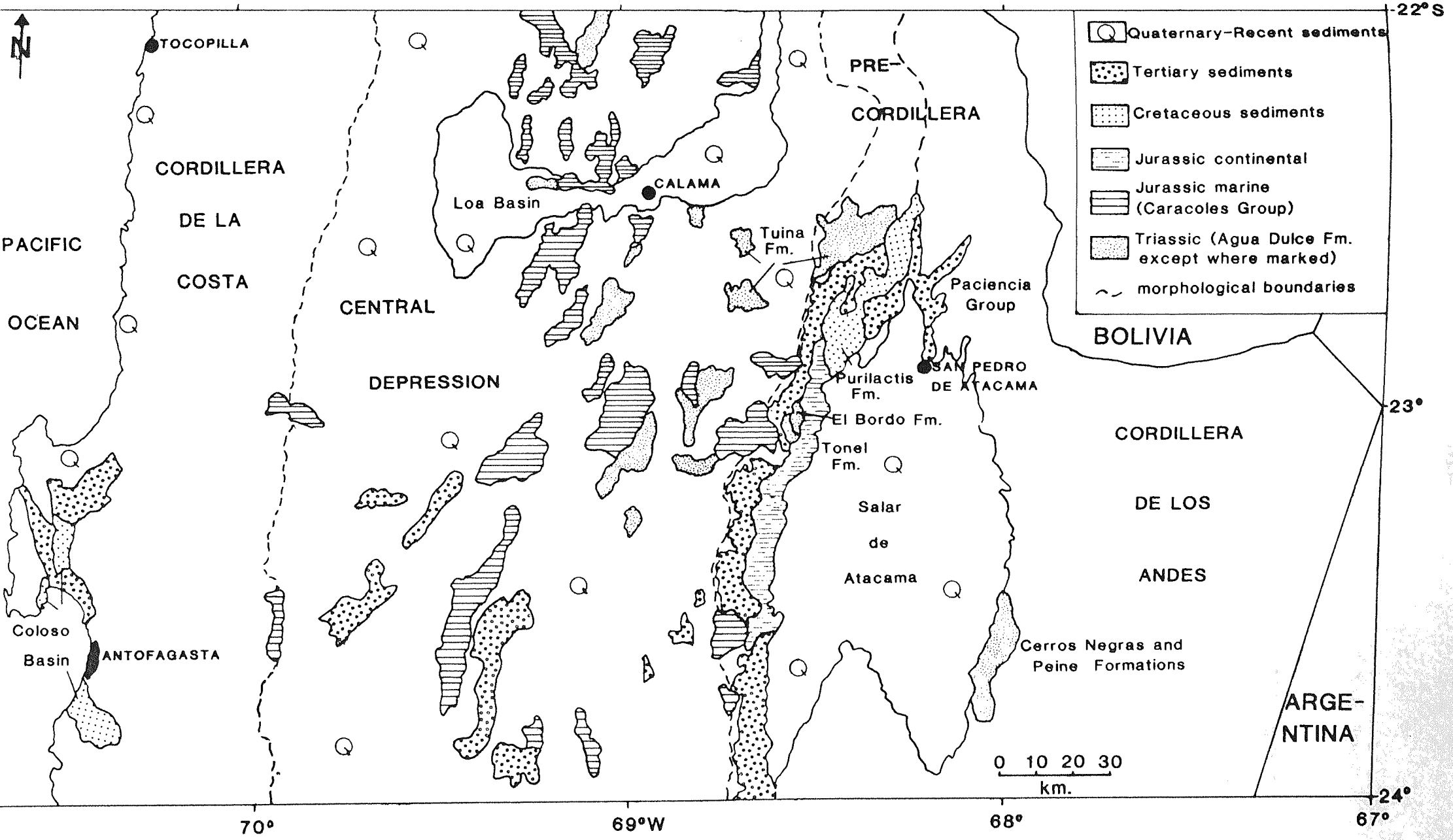

Fig. 7.1 Location map of the units studied.

TABLE 7.1

UNIT	THICKNESS (M.)	LITHOLOGY	FACIES	CLAST CONTENT	BASIN TYPE, EVOLUTION AND REMARKS
Agua Dulce Formation	1200	coarse sands.	fluvial?	acidic volcanics	Rift? with interbedded andesites
Purilactis Formation	3500	congloms. sands. silts. muds.	alluvial-fan fluvial lacustrine	andesite limestone Tonel intrusives acid plutonics	coarsening upwards foreland basin
Coloso Formation	1000	congloms.	alluvial-fan	intermediate volcs basic plutonics	fining upwards basin, formed through extension after terrane emplacement
Paciencia Group	2000	congloms. sands. silts. muds.	alluvial-fan fluvial playa	andesites sands.	foreland basin with easterly and westerly lying source areas

Table 7.1 summarises data presented in Chapter 6, which is relevant to the diagenesis of the studied units.

previously in Chapter 6. Factors relevant to the diagenesis of these units are presented in Table 7.1.

Analytical techniques used in this study include the petrographic examination of thin sections, XRD analysis of clay minerals, SEM with EDAX analysis, cathode luminescence and electron probe microanalysis. In the following sections the results for each of the 4 studied units will be discussed and a general synthesis based on the observed evidence presented.

7.2 Petrography and Diagenesis

7.2.1 The Agua Dulce Formation

The sandstones of the Agua Dulce Formation are mineralogically immature plotting in the lithic arkose/feldspathic litharenite fields (Fig. 7.2) of Pettijohn et al. (1973). Plagioclase and K-feldspars occur in relatively equal proportions with minor amounts of perthitic feldspar. Volcaniclastic detritus is also abundant (particularly volcanic glass; Plate 7.1).

Compaction is significant, as indicated by sutured and concavo-convex grain contacts, together with fractured feldspars and micas. There is no visible porosity. Early diagenesis involved the infiltration of detrital clay and subsequent oxidation and recrystallisation of clay grain coatings. Dissolution and replacement of feldspars is common, and ferromagnesian minerals are absent. The oxidation of iron bearing grains is common, particularly detrital magnetite, biotite mica (Plate 5.2) and volcanic detritus.

The main authigenic phase is quartz, occurring as syntaxial

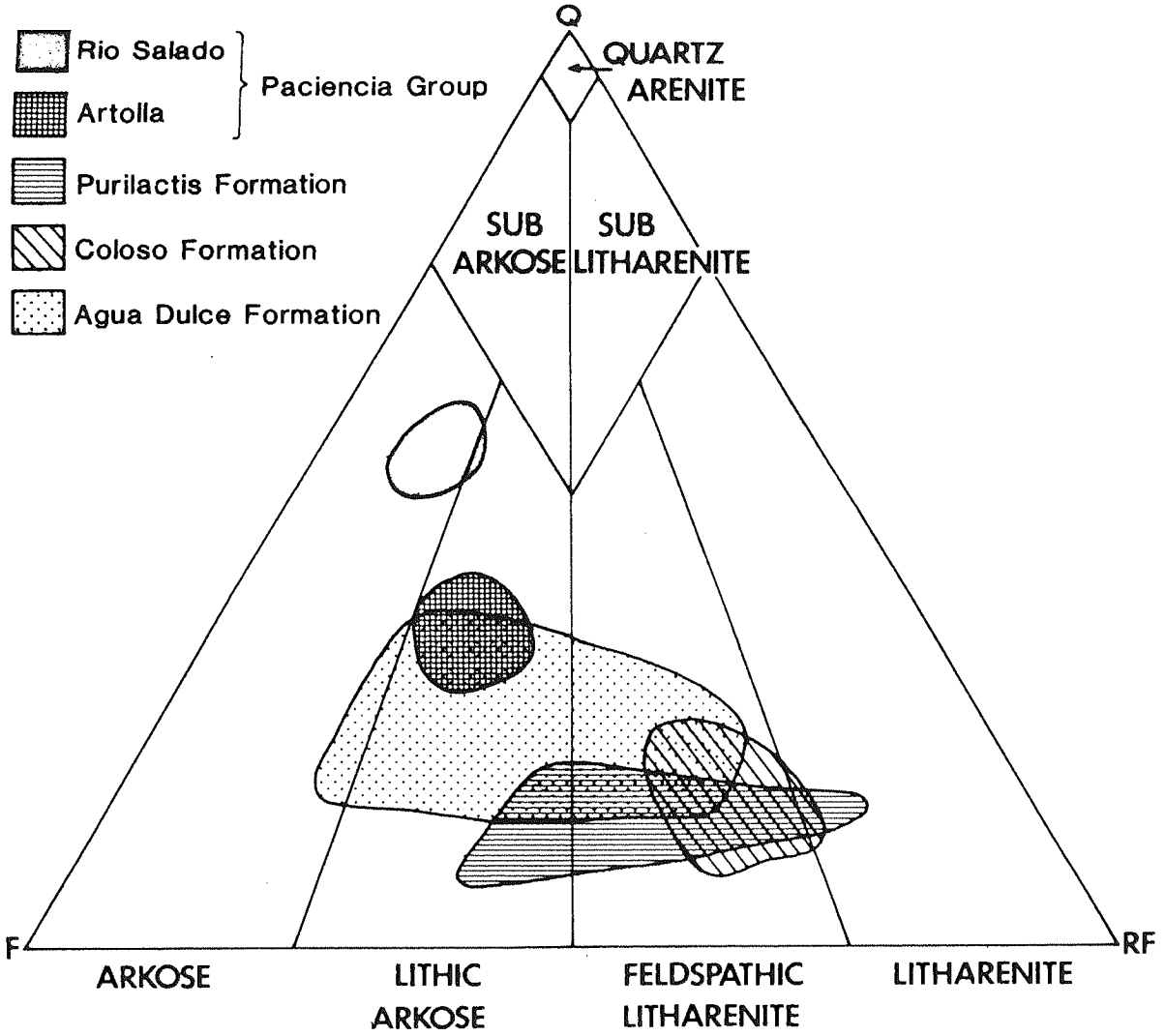

Fig. 7.2 Compositional variation of the studied units (after Pettijohn et al.,1973).

overgrowths, euhedral microcrystalline pore fills and replacive cement. Quartz is commonly intergrown with authigenic chlorite and crystalline illite (Plate 7.2), as identified by XRD analysis (Fig. 7.3). The clays occur as pore linings and alteration products of detrital rock fragments, feldspars and volcaniclastic detritus. Non-ferroan calcite occurs as a late-stage, pervasive cement.

Interpretation: During deposition and early diagenesis the Agua Dulce Formation was subject to oxidising conditions. At this time, iron bearing detritus and infiltrated clays were oxidised to haematite. This is indicated by palaeomagnetic work, as authigenic and detrital haematite carry the same magnetic component (section 5.4.1). Syntaxial overgrowths of quartz were precipitated before or after clay grain coatings developed. Volcanic glass is only partially altered indicating that the Agua Dulce Formation did not long remain under oxidising conditions. It follows therefore, that the Formation was rapidly buried. Burial is probably associated with the large volumes of lava which interbedded with the sandstones, and subsidence associated with an extensional (rift related) tectonic setting (section 6.2). After burial quartz and clay precipitation took place around fractured and sutured grains. The abundance of quartz could be due to the presence of large amounts of silica associated with the interbedded acidic volcanics. Although the Agua Dulce Formation is the oldest unit studied, it appears that cementation was rapid, as much of the early diagenetic components have been preserved.

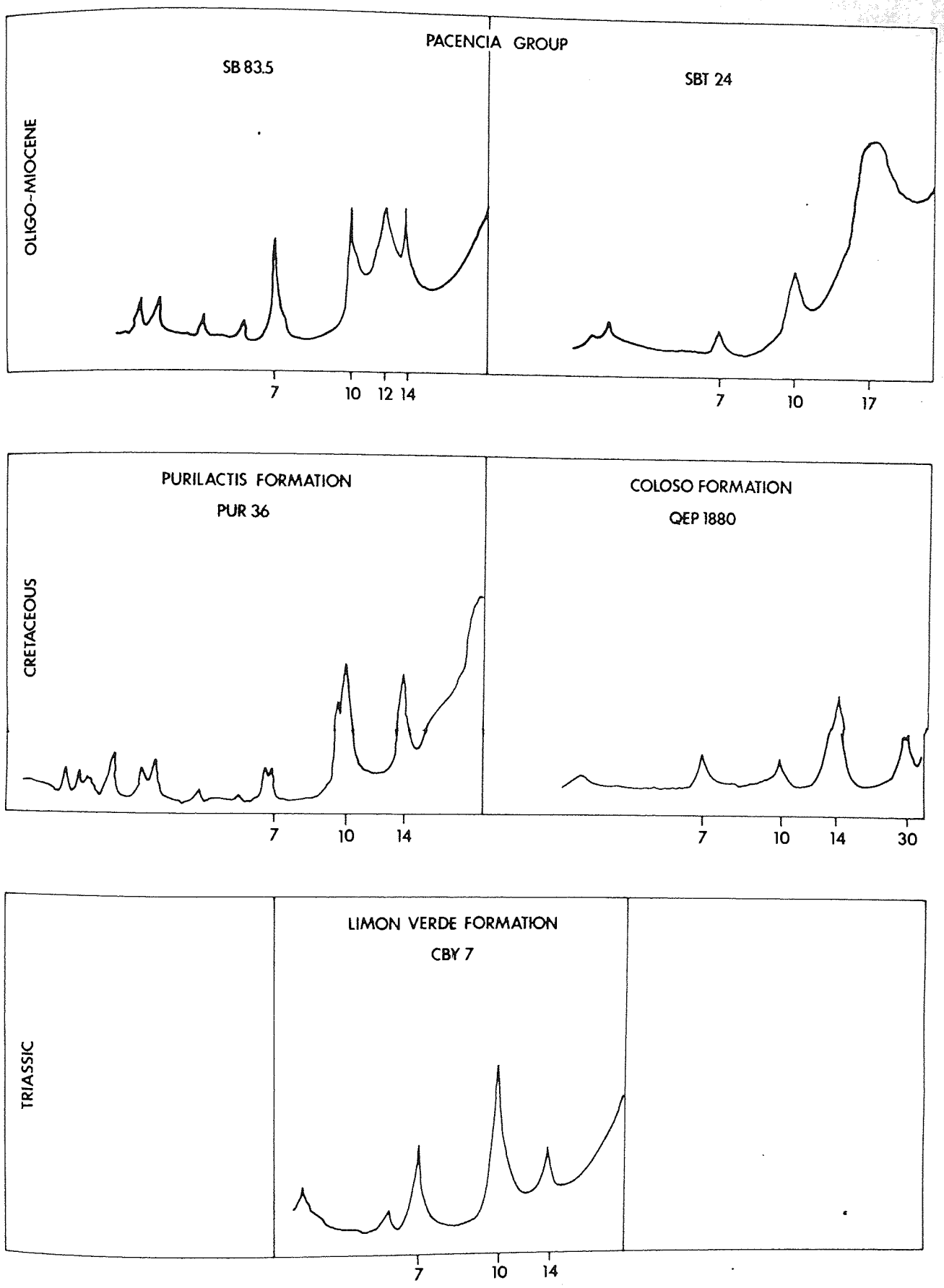

Fig. 7.3 XRD analysis of clay size fractions from the studied units. Numbers=Angstroms. 14=Chlorite, 10=Illite, 30=Corrensite, 7=Kaolinite or Chlorite, between 10 and 17 broad peaks=mixed layer Illite-Smectite clay, below 7=secondary peaks of clays, feldspars, quartz and

Plate 7.1 CBY9 Agua Dulce Formation. A photomicrograph of a partially altered volcanic glass shard. Haematite forms undulose ribbons across the shard. The shard contains a virtually unaltered phenocryst of plagioclase feldspar (F), testifying to the unaltered nature of the rock. the matrix of the sandstone is composed dominantly of haematite. Transmitted light, field of view=0.89mm.

Plate 7.2 CBY7 Agua Dulce Formation. Authigenic pore lining clay (illite), intergrown with pore filling quartz crystals. Transmitted light, field of view=0.35mm.

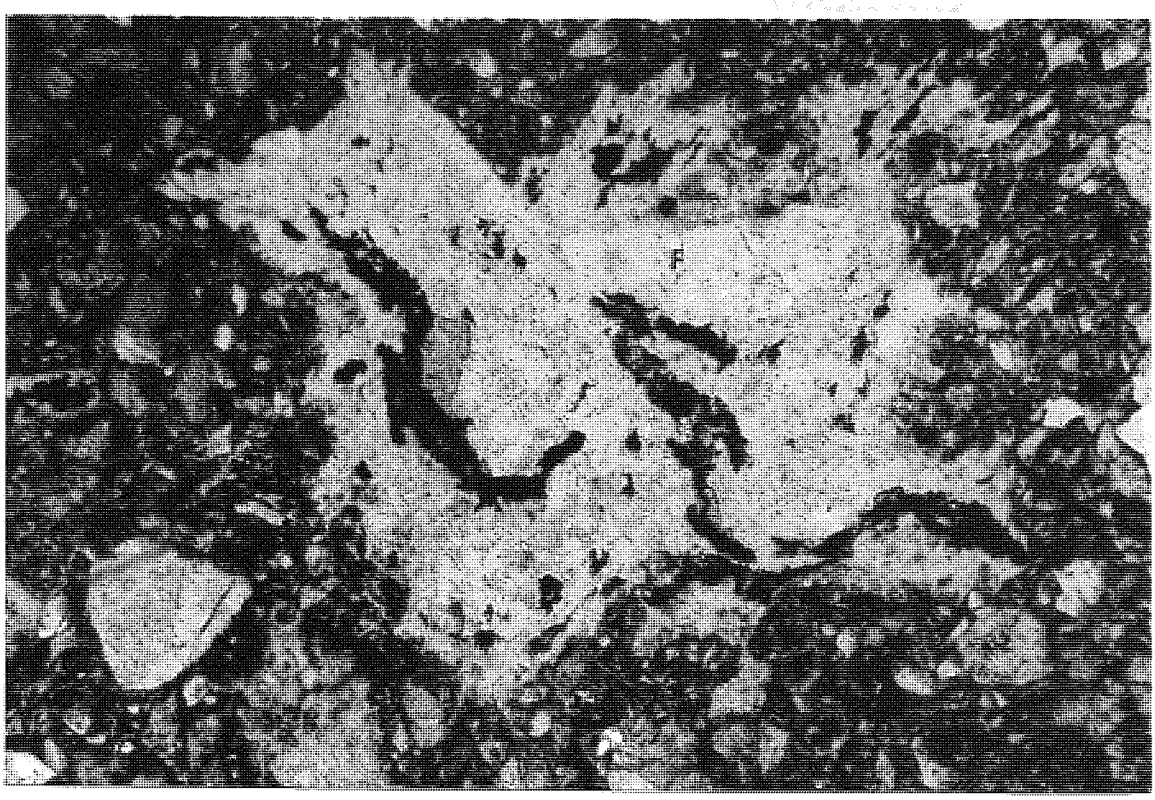

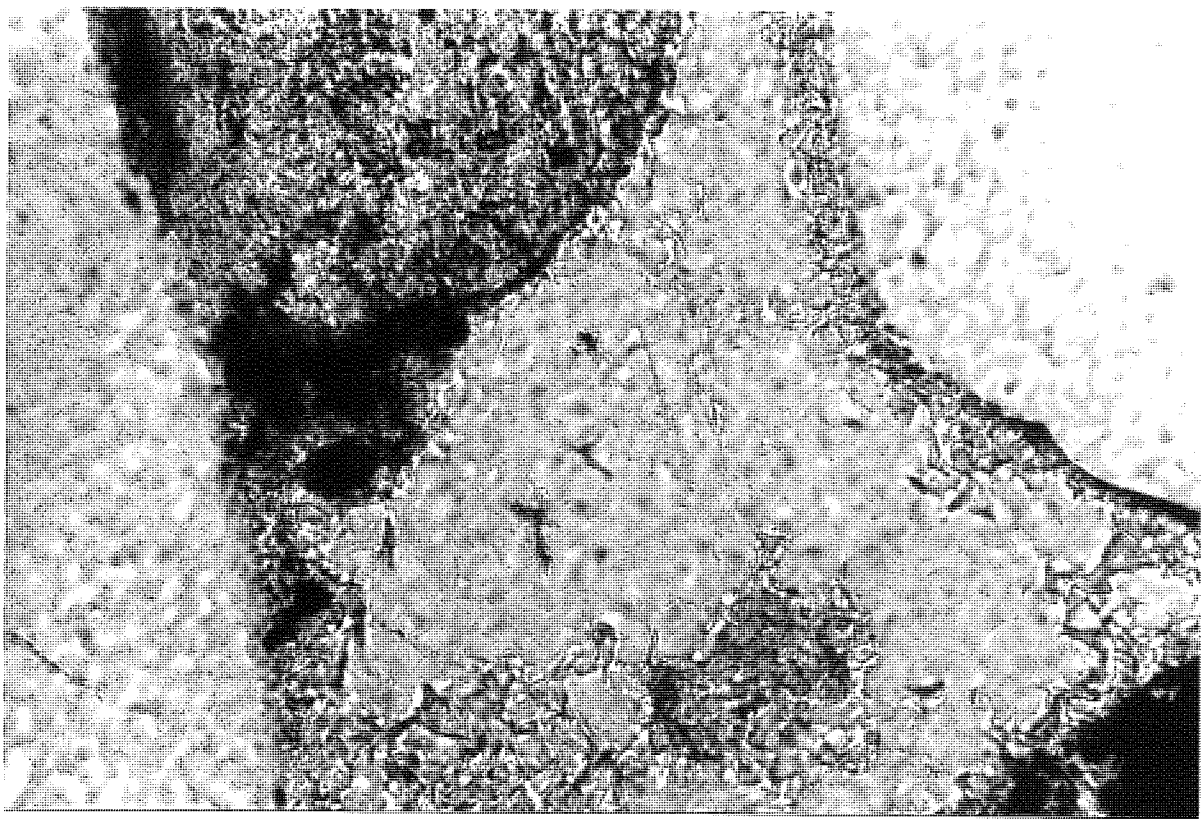

7.2.2 The Purilactis Formation

The Purilactis sandstones are mineralogically immature (Fig. 7.2), with a high percentage of igneous rock fragments (25-45%), particularly andesitic and dacitic volcanics and granitic plutonics, almost certainly derived from the westerly lying Limon Verde Complex (Fig. 7.1). Detrital feldspars (15-30%) are generally albitic in composition, and commonly contain dissolution voids (Plate. 7.3). Many of the framework components (particularly volcanic rock fragments and detrital plagioclase grains), have been altered to clay minerals and haematite. The sandstones are well compacted exhibiting concavo-convex grain contacts, and contain no visible porosity.

The main cementing phases are analcime, quartz, non-ferroan calcite, epidote and authigenic clay minerals. All of these are present in varying proportions, with the exception of epidote, the distribution of which is restricted to certain horizons. Analcime occurs commonly as small euhedral pore-lining crystals and more rarely as a coarse pore-fill. Quartz is present as a chalcedonic pore-fill and a pervasive microcrystalline typee, replacing grains and filling pore spaces. Non-ferroan calcite forms small euhedral crystals un-etched by analcime, with luminescent rims containing up to 1% Mn^{2+}. It also occurs as a coarse pore-fill and replacive cement, and cathode luminescence indicates at least three separate phases of precipitation (Plate 7.4). Fine grained authigenic clay minerals identified as illite and mixed layer illite-smectite (Fig. 7.3), are present as alteration products of detrital silicate grains. Coarse authigenic clays fill pores and have been identified petrographically as chlorite. Overgrowths of quartz and K-feldspar form minor cementing phases which may pre- or post-date the iron oxide stained clay grain

Plate 7.3 PUR32 Purilactis Formation. Replaced detrital grain (centre), with an iron oxide stained grain coating. The inside of the grain is lined by quartz (Q), and infilled by non-ferroan calcite, and small needle-like crystals of quartz. Transmitted light, field of view=0.45mm.

Plate 7.4 PUR36 Purilactis Formation. Photomicrograph of a coarse grained sandstone under cathode luminescence. Three separate phases of calcite cement (orange) are present. The calcite occurs between detrital grains of volcaniclastic material. The first phase (1) is revealed by small euhedral crystals of calcite with non-luminescing cores and brightly luminescing manganiferous rims, generally present as a pore-lining. The second phase (2) is brightly luminescing, but contains no, non-luminescing cores, and again is present as a pore-lining. The final stage (3) of calcite cement is pore-filling and dully luminescing. Field of view=1.7mm.

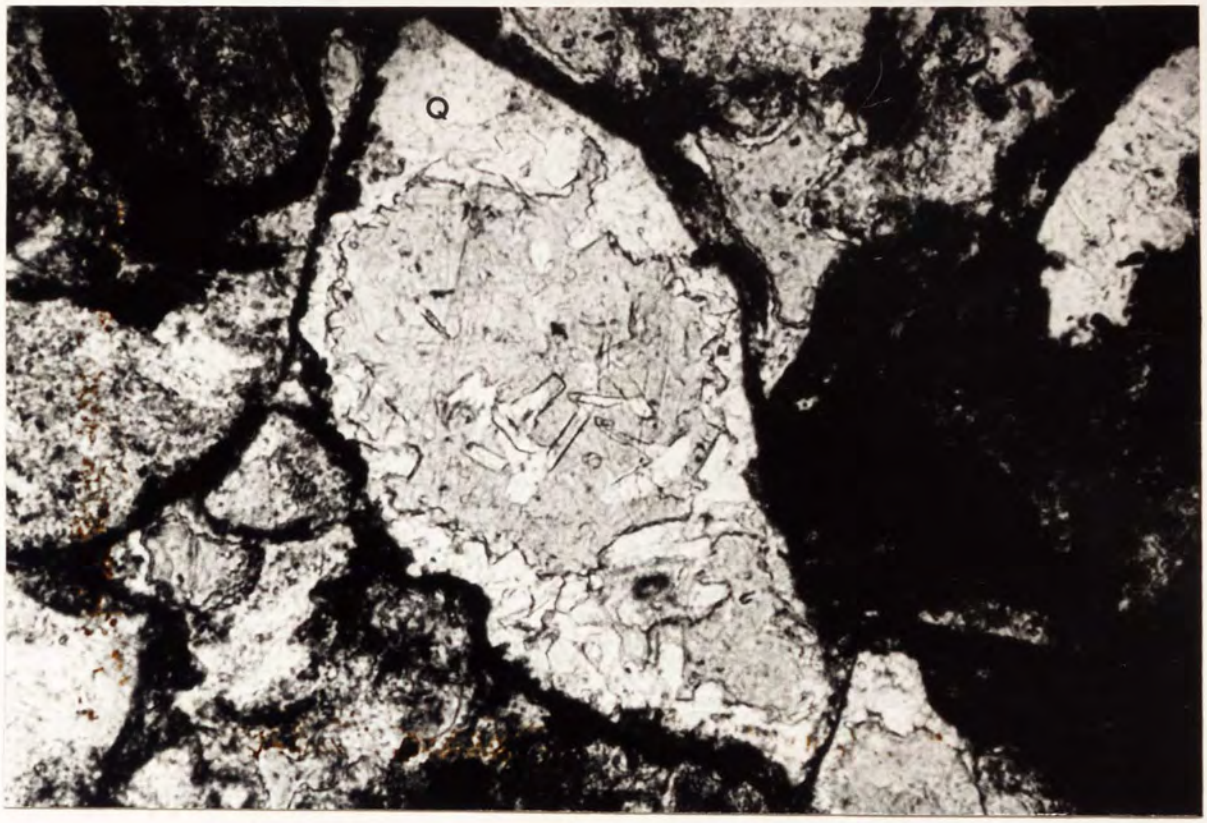
Q

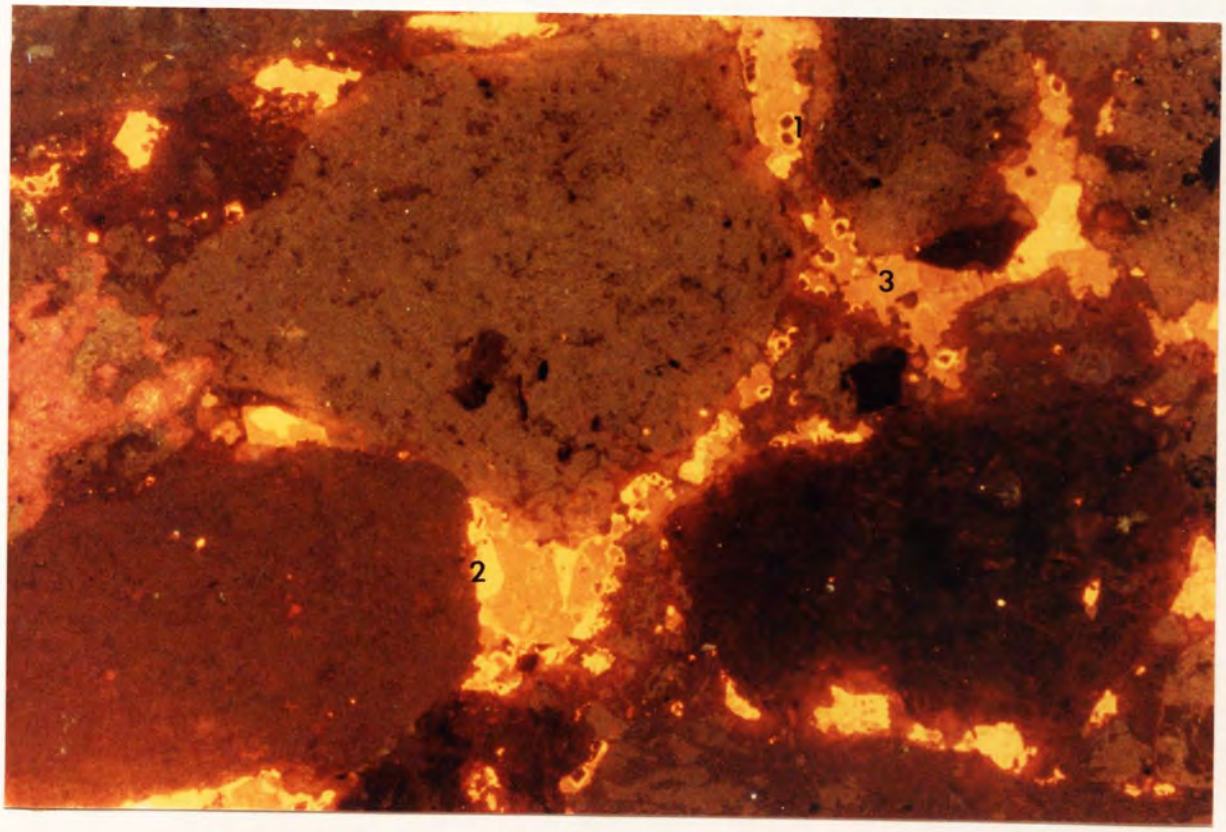
1
3
2

coatings present in all samples. Epidote occurs as a coarse pore fill (Plate 7.5), and appears to post-date a secondary porosity generation event. Samples containing epidote are often slightly porous. Framework grains are commonly corroded, and in some cases the rock may be totally cemented by epidote. In some samples, late-stage veins of analcime cross-cut all earlier diagenetic phases.

The relationship of the authigenic phases is complex, and no certain paragenetic sequence can be determined as analcime, non-ferroan calcite and quartz may pre- or post-date each other in different samples. However, epidote when present, is always the final cementing phase (if analcime veins are absent).

Interpretation: The Purilactis Formation was deposited in an oxidising freshwater regime. During shallow burial, iron-bearing detritus and clay grain coatings were oxidised to form haematite. Minor syntaxial overgrowths of quartz and K-feldspar were also precipitated at this time. The oxidising regime ended with increased burial, resulting in a diagenetic regime where quartz, analcime and non-ferroan calcite were deposited as pore-linings. Conditions continued to favour non-ferroan calcite, quartz, chlorite and less commonly analcime precipitation, resulting in pore-filling cements of these phases (for a discussion of the geochemical significance of analcime see below). Following the precipitation of pore-filling cements, a phase of secondary porosity generation took place in some samples, possibly associated with corrosive hydrothermal fluids from which epidote was precipitated.

7.2.3 The Coloso Formation

Mineralogically the Coloso sandstones are dominated by feldspar (intermediate-basic plagioclase) and rock fragments (Fig. 7.2), derived from the basic plutonic rocks of the Bolfin and Moreno Complexes and the andesitic La Negra Formation (Chapters 3, 4 and 6). The sandstones show considerable diagenetic alteration. Dissolution voids are abundant particularly in intermediate plagioclases and labile rock fragments. A wide range of authigenic minerals include analcime, haematite, non-ferroan calcite, quartz, alkali feldspars, clays and small amounts of clinoptilolite.

Haematite occurs as the oxidation product of detrital iron bearing grains, particularly magnetite. K-feldspar and quartz are minor phases occurring as syntaxial overgrowths on detrital grains. They formed at an early stage of diagenesis, prior to compaction. Analcime is common and occurs as discrete crystals and large areas of pore-filling cement (Plate 7.6).

Non-ferroan calcite occurs as a pore-fill, and as euhedral crystals apparently unetched by analcime. The crystals are zoned as revealed by cathode luminescence (Plate 7.7), with cores of non-ferroan calcite and outer zones containing up to 1% Mn^{2+} (c.f. the Purilactis Formation). There is also a later phase of non-ferroan calcite cementation which is pervasive and replaces framework grains and earlier authigenic minerals. The authigenic clay mineralogy of the Coloso Formation is characterised by mixed layer illite-smectite, illite and chlorite phases and limited amounts of corrensite (Fig. 7.3).

Interpretation: A freshwater oxidising regime predominated during deposition and in the early stages of diagenesis of the Coloso

Plate 7.5 PUR27 Purilactis Formation. A coarse grained sandstone with pore-filling epidote (E) cement, surrounding a quartz overgrowth (QO), and associated with porosity development (P). Two partially altered detrital grains are present in the bottom right and left of the photomicrograph. Transmitted light, field of view=0.35mm.

Plate 7.6 QEP3 Coloso Formation. Coarse euhedral analcime pore-lining (white), with a non-ferroan calcite (stained) pore-fill in the centre of the photomicrograph. A partially altered feldspar grain with an iron oxide stained clay grain coating is present at the bottom centre of the photomicrograph. The two grains at the top left and right consist of volcanic detritus which has been partially oxidised. Transmitted light, field of view=0.9mm.

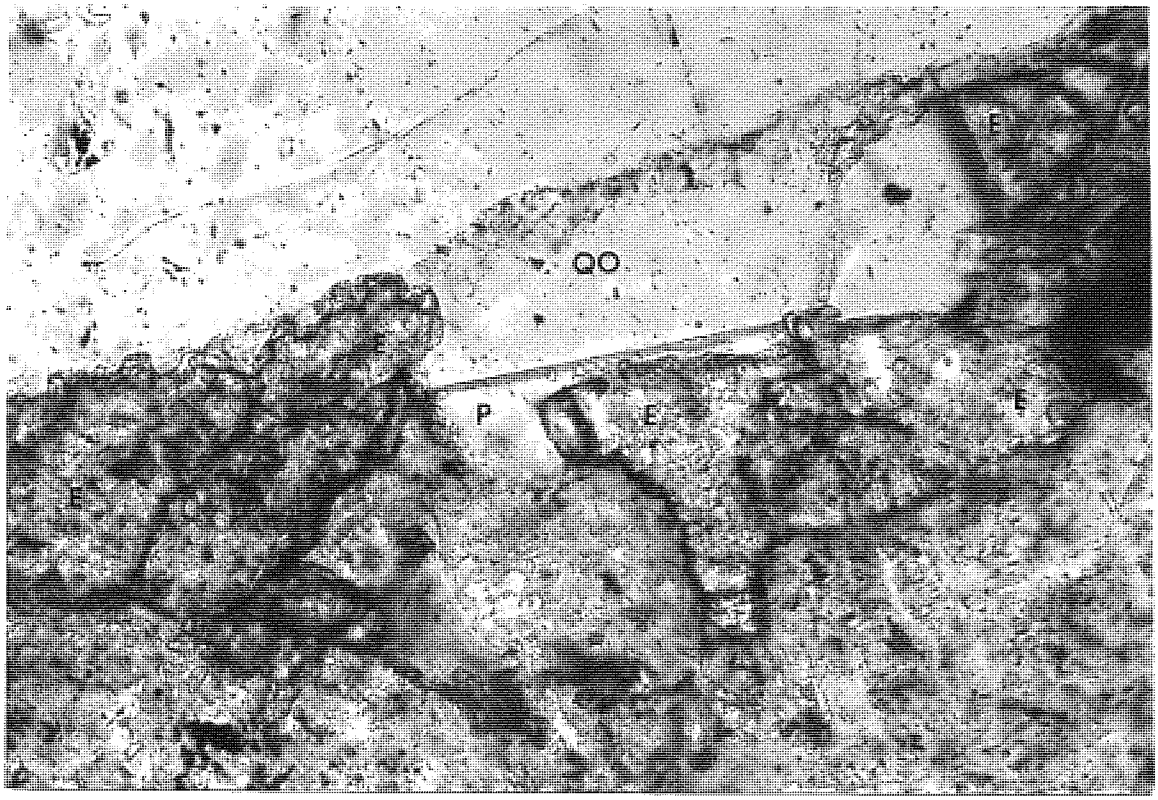
QO
P
E
E
E
E

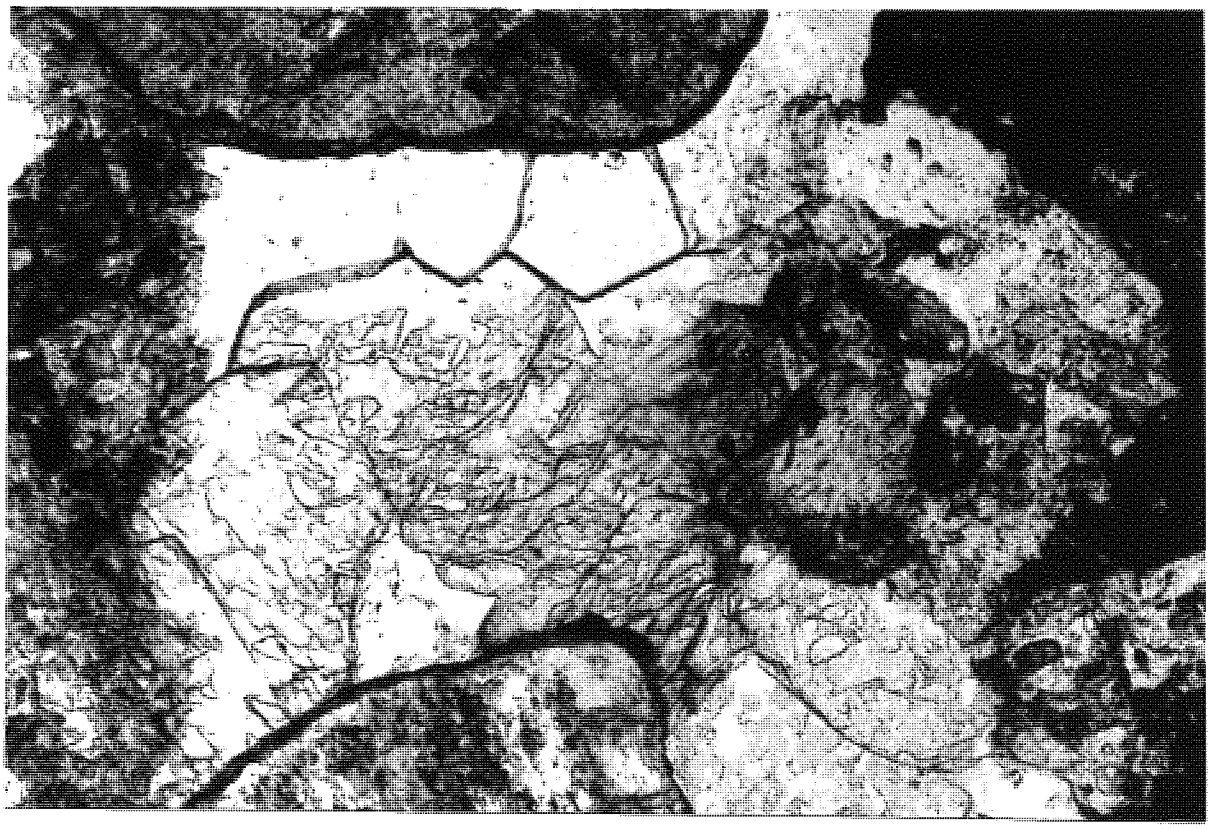

Formation. At this time, the oxidation of iron-bearing detritus, the precipitation of haematite and syntaxial overgrowths of quartz and K-feldspar took place. Burial of the Formation was associated with an increase in pH. and temperature, and resulted in a regime favouring the precipitation of analcime, quartz, non-ferroan calcite and clay minerals (the diagenetic significance of analcime is discussed below). As in the Purilactis Formation, the paragensis of the authigenic phases is complicated, and difficult to determine.

7.2.4 The Paciencia Group

The diagenesis of the Paciencia Group has previously been described by Flint (1985b,1987), and has been related to the different Members of the Group (section 6.4.1), based on source area derivation.

Westerly derived sediments: The Barros Arana sandstones have the composition of arkosic wackes (Fig. 7.2). Present porosity is 5-10%. Feldspars comprise a mixture of fresh orthoclase and microcline (60-65%) and partially dissolved plagioclase. Lithic fragments include first cycle andesitic and granitic material, but are dominated by clasts of fine grained brown sandstone (85%) derived from the purilactis Formation.

Easterly derived sediments: The sandstones of the Artolla Member are finer grained than those of the Barros Arana Member, with porosities of 3-5%. They are more feldspathic than the westerly derived material, plotting in the arkose field (Fig. 7.2). Feldspar is dominated by acid-intermediate commonly zoned plagioclase (90%). Lithic fragments are solely of andesitic composition, with no sedimentary material present.

Compaction is limited in both members. Dissolution and/or

Plate 7.7 QEP9 Coloso Formation. Photomicrograph of a coarse grained sandstone under cathode luminescence. The sandstone consists of poorly luminescing volcanic detritus (bluey-green), which has a pore-lining cement of euhedral calcite crystals, with non-luminescing cores and manganiferous rich luminescing (orange) rims (c.f. Plate 7.4). Analcime occupies the non-luminescing dark, pore-filling area (centre). Field of view=1.7mm.

Plate 7.8 SBT18 Paciencia Group. Photomicrograph of a coarse grained sandstone using a SEM. Euhedral (dodecohedral), crystals of analcime are present on a sodium feldspar with dissolution voids (D). Clay grain coatings are also present (C). Field of view=0.13mm.

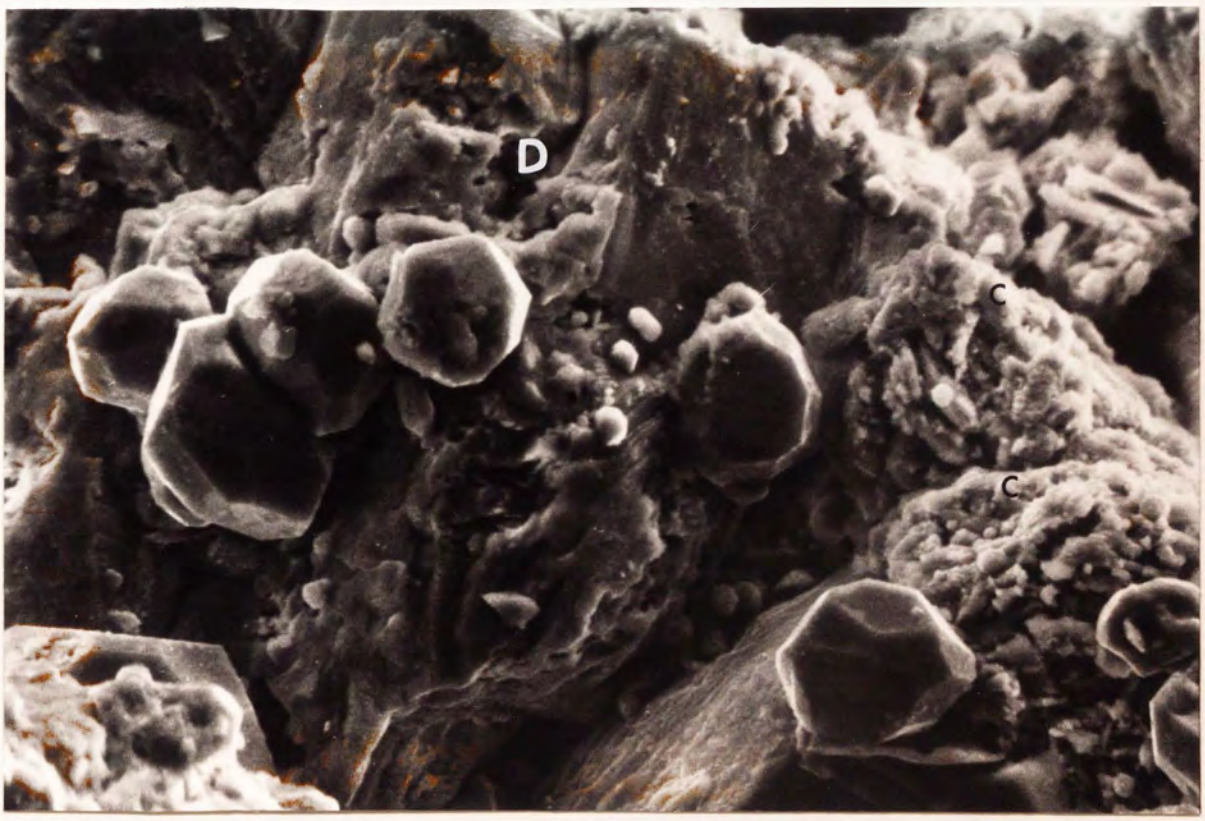
D
C
C

alteration of framework grains is extreme. Iron oxide stained grain coatings are present and haematite may also form early pore-filling cement. Quartz, and both alkali and plagioclase feldspar occur as syntaxial overgrowths. Analcime (with a higher silica content than the previously described units, see below) and very rare clinoptilolite are present as pore-lining euhedral crystals (Plate 7.8). Sparry non-ferroan calcite forms the most extensive cement in the Group with anhydrite/gypsum occurring as minor components. Authigenic clay minerals are rare, but do replace plagioclase grains. SEM and XRD analysis indicates that the clays present include: illite, smectite and mixed layer illite-smectite (Fig. 7.3).

Interpretation: In common with the previously described units the Paciencia Group was subjected to an oxidising regime prior to and during shallow burial. This promoted the oxidation of iron-bearing detritus, the precipitation of haematite and limited syntaxial overgrowths of quartz and K-feldspar. The sequence was not completely oxidised during shallow burial indicated by the preservation of abundant magnetite, which records a magnetostratigraphy (section 5.4.4; Fig. 5.6). Increased burial resulted in the precipitation of pore-lining analcime (see below) and, much more rarely, clinoptilolite. Pore-filling cements are mostly non-ferroan calcite, with gypsum and anhydrite dominant in evaporitic facies.

7.2.5 Summary of the Diagenesis of the Studied Units

A general diagenetic scheme for the studied units, can be established from the previous descriptions:

1) Early Diagenesis (pre and shallow burial): This took place in oxidising conditions under the influence of depositional groundwater. It resulted in the precipitation of haematite and the oxidation of detrital iron bearing grains notably: magnetite, biotite mica and volcaniclastic detritus, to form haematite. Early diagenesis also involved the mechanical infiltration of clay particles, forming clay grain coatings and limited clay pore-fills (Walker et al.,1978). Clay grain coatings may or may not preceed syntaxial overgrowths of quartz and alkali/plagioclase feldspars, which are, however, volumetrically unimportant.

2) Late Diagenesis (deeper burial): Burial of the studied units resulted in a change in porewater geochemistry, to fluids favouring the precipitation of analcime (except for the Agua Dulce Formation), quartz, non-ferroan calcite (which may be zoned with manganiferous rich crystal rims) and clay minerals, as pore-lining and pore-filling cements.

The main differences between the four studied units, appears to be related to burial, and the presence of contemporaneous volcanics. The abundance of quartz cements in the Agua Dulce Formation, can be related to the interbedded volcanics (see discussion), this distinguishes it from the other studied units. Compaction features and epidote cements indicate that the Purilactis Formation was most deeply buried, with the Coloso Formation intermediate and the Paciencia Group the most shallowly buried, of the studied units.

Analcime is present in the Purilactis and Coloso Formations, and the Paciencia Group. These units are distributed across the Andean forearc (Fig. 7.1), and range in age from the Lower Cretaceous to Miocene (Table 7.1). Consequently, conditions favouring analcime

precipitation are likely to be related to burial, rather than the age or distribution of the units. The paucity of analcime in the Agua Dulce Formation is thought to be related to differences in the diagenesis of the unit rather than its age (see Discussion). Conditions favouring analcime precipitation are limited (see below), consequently determination of these conditions would allow constraints to be placed on the diagenetic porewater geochemistry of Andean alluvium.

7.3 The Origin and Significance of Analcime

Analcime is a characteristic diagenetic phase in Andean red beds. This is unusual in red bed sequences, as feldspar usually forms the dominant sodium/potassium authigenic silicate phase. An understanding of the conditions under which the formation of analcime takes place, should lead to a better understanding of the pore water geochemistry of Andean alluvium. Analcime has been shown to occur in a wide variety of geological and hydrographic environments favouring zeolite formation (Hay,1966,1978). Environments applicable to an Andean setting include:

1) Saline, alkaline lakes (Surdam and Sheppard,1978). The largest known analcime bearing deposits are the "analcimolites", reviewed by Hay (1966). They consist of silty claystones and sandstones containing up to 40% analcime, deposited in playa/lacustrine environments. Although the common presence of montmorillonite has led some authors to suggest an indirect volcanic origin (Vernet,1961; High and

Picard,1965), there is little direct evidence for the derivation of analcime from volcanic material (Hay, 1966; Oesterlen,1979).

Phillipsite, clinoptilolite, erionite, chabazite and mordenite form directly from volcanic glass in the saline, alkaline lake environment (Hay,1964; Sheppard and Gude, 1968; Mariner and Surdam,1970; Surdam and Eugater,1976; Surdam and Sheppard,1978). With an increase in pore water salinity these zeolites characteristically alter to analcime. Further diagenesis results in albite or K-feldspar formation, giving rise to a lateral zonation of authigenic silicate minerals (Sheppard and Gude,1968; Surdam and Eugster,1976; Surdam and Sheppard,1978).

2) Open hydrological systems (Walton,1975; Hay,1978). Horizontal zeolite zonation is also well documented in open hydrological systems, where, through the progressive evolution of meteoric water by reaction with solid materials in its flow path, a characteristic mineral zonation is encountered. Such zones may be several hundreds of metres wide, again ranging from volcanic glass through zeolites to albite (Walton,1975).

3) Burial diagenesis/metamorphism (Coombs et al.,1959; Iijima and Utada,1972). A similar zeolite zonation to open hydrological systems is found in areas subject to low grade metamorphism/burial diagenesis, but on a larger scale of up to 10km. depth (Coombs,1954; Boles and Coombs,1977).

4) Hydrothermal alteration (Hay,1978). The zonation associated with zeolites of hydrothermal origin, is commonly restricted to a few hundred metres and usually complex (Iijima,1974; Utada et al.,1974).

In all of these reported analcime occurrences the original presence of volcanic glass, and the subsequent zonation of zeolites are major factors. Analcime however, does not form directly from volcanic glass (Hay,1978), but commonly forms from either a Na-Al-Si gel, such as those found at Lake Magadi, Kenya (Surdam and Eugster,1976) or from an alkalic, silicic zeolite precursor such as erionite (Surdam and Eugster,1976), clinoptilolite or phillipsite (Sheppard and Gude,1969,1973).

7.3.1 Analcime Geochemistry

The formation of analcime from a zeolite precursor has been well documented (Sheppard and Gude,1969,1973; Surdam and Eugster,1976) and experimental work and theoretical considerations, have enabled the formulation of three main geochemical parameters for the precipitation of analcime in the aqueous environment:

1) A high Na^+/H^+ ratio, that is a gain in Na^+ and depletion of K^+ and Ca^{++}, reflecting the more extreme saline environments for zeolite formation (Hess,1966).

2) A relatively low Si/Al activity. This may be achieved through the dissolution of labile rock fragments at a high pH. Despite the high Si activity, the Al concentration increases more rapidly due to the dissolution of feldspar rich rock fragments, resulting in a net decrease in the Si/Al ratio with increasing pH (Boles,1971).

3) A relatively low activity of H_2O (Surdam and Sheppard,1978).

The above geochemical parameters are met through an increase in alkalinity and salinity. Although the above parameters have only been determined for the formation of analcime from a zeolite precursor, they are obviously applicable to other modes of analcime formation, for example from a gel or direct precipitation from a pore fluid.

As noted by Surdam and Sheppard (1978), kinetic factors such as activation energies, nucleation rates, crystal growth rates and rates of reaction may also be important. For example, reaction time can control the H O content of analcime (Arima and Edgar,1980).

Further refinement of the conditions required to precipitate analcime in Andean alluvium, have been possible using microprobe analysis to determine the exact composition of analcime. The results show (Fig. 7.4), that, when the Na:Si ratio is plotted against Si:Al ratio, Andean analcimes display an affinity with other documented sedimentary analcimes. Figure 7.4 also reveals a marked bimodal distribution, with analcime from the Paciencia Group being more siliceous than analcime from the Purilactis and Coloso Formations. Analysis of the microprobe results also reveals a large compositional variation in the analcimes when calculated to 96 oxygens per unit cell:

$$Na_{12.06-13.69}Al_{13-14.41}Si_{33.75-35.76}O_{96}.nH_2O$$

This variation spans all 3 groups of Coombs and Whetten (1967), indicating that the origin of analcime from Andean red beds is unlikely to be determined through compositional variation. However, the silica rich nature of the analcimes suggests a high silica activity at the time of formatiom (Coombs and Whetten,1967). This is

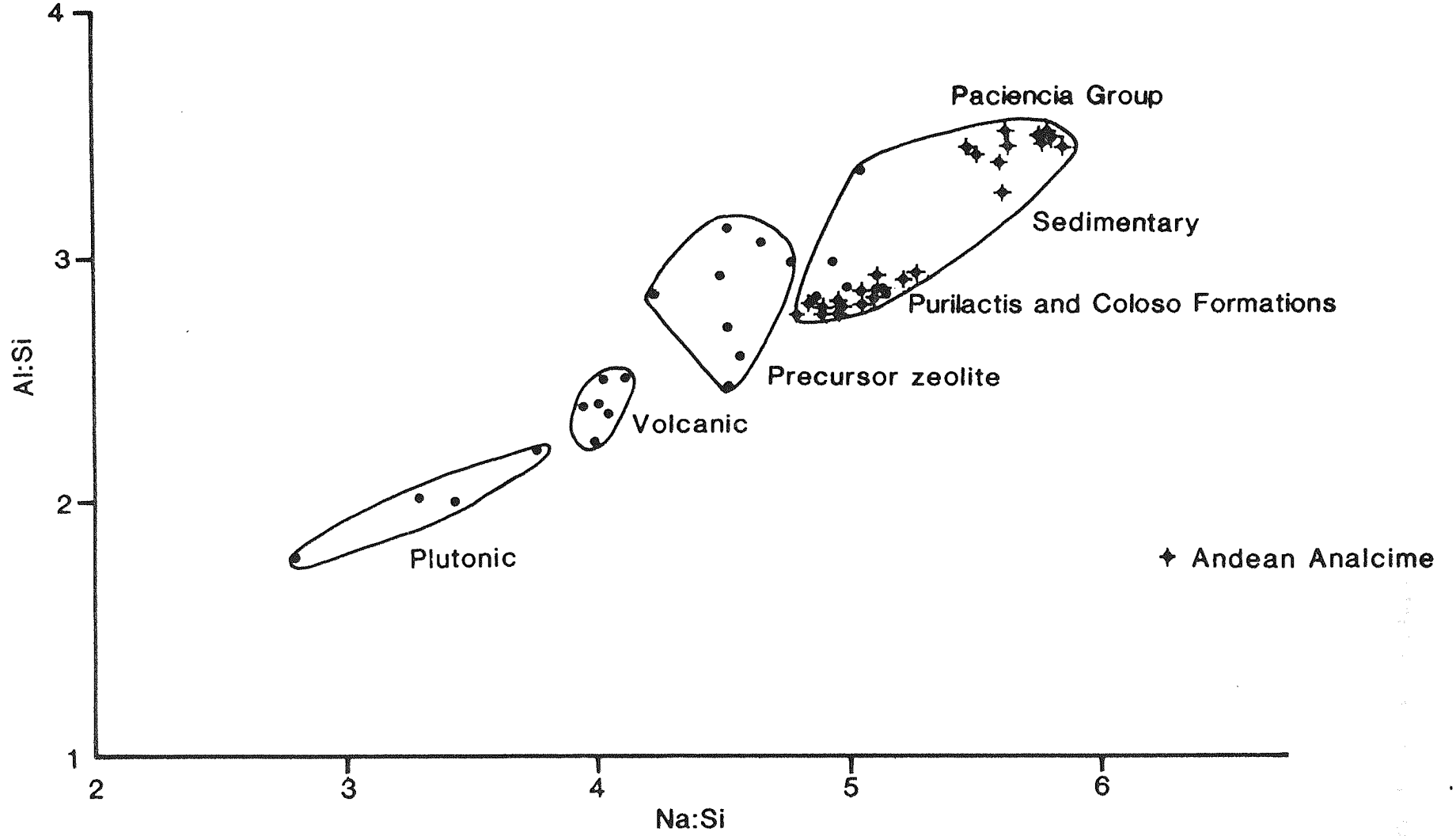

7.4 Composition (Na:Si/Al:Si) of authigenic analcime crystals
the Purilactis Formation, the Coloso Formation and the Paciencia
, compared with analcimes of other affinities (derived from
electron microprobe analyses). Plutonic analcime (Deer et al.,1966;
Coombs and Whetten,1967), volcanic analcime (Deer et al.,1966; Coomb
and Whetton,1967; Walton,1975),zeolite precursor and sedimentary
analcime (Coombs and Whetten,1967).

confirmed by the common coexistence of chalcedonic quartz and analcime as pore-filling phases. The high silica content may also reflect relatively low temperature burial conditions, as the silica content of zeolites decreases with increasing temperature (Velde,1985).

7.3.2 Textural Characteristics of Andean Analcime

In Andean analcime, clear textural evidence for the original presence of volcanic glass or for analcime formation from a zeolite precursor was not found (in the Paciencia Group extremely rare fan-shaped clinoptilolite crystals are present, but bear no textural relationship to analcime). Oversize pore spaces indicating dissolution of glass shards, zeolite pseudomorphs after volcanic glass, relict clay grain coatings after glass shards or analcime pseudomorphs after other zeolites are all absent. Textural evidence such as a fine mesh like structure (Nashar,1978), for formation from a Na-Al-Si gel is also absent. The perfectly euhedral nature of the analcime crystals (Plates 7.3,7.4), suggests direct precipitation from a pore fluid, supporting the experimental evidence of Donahoe and Liou (1985) for zeolite precipitation directly from solution.

The paucity of associated zeolites and zeolite zonation, the presence of analcime in Andean red bed sequences located in geologically similar, but widespread (250km. apart) basins, the lack of clear textural evidence for formation from a zeolite precursor or for the original presence of volcanic glass, points to an alternative origin for the formation of analcime to that invoked for previously described analcime occurrences.

7.4 Discussion

Petrographic observations of Andean alluvium indicate that the pore waters were originally oxidising and mildly alkaline prior to and during shallow burial. Further burial resulted in the evolution of more saline, alkaline pore waters, which would favour the precipitation of analcime. The change in pore water geochemistry is thought to be influenced by the following factors:

1) A lithic arkose or lithic arenite framework mineralogy, derived from intermediate igneous source areas.

2) A prevailing evaporitive climate, resulting in a dessicating basin.

3) Deposition in a closed hydrographic basin.

However, the diagenesis of Andean alluvium is complex, and any theory concerned with the pore water geochemistry, must take into account: 1) the close association of complex authigenic carbonates with analcime, 2) the paucity of feldspar precipitation in Andean alluvium, and 3) the lack of analcime in the Agua Dulce Formation.

7.4.1 A Model for the Diagenesis of Andean Alluvium

The sedimentology and tectonic setting of the four basins studied (Chapter 6), indicates that deposition took place in hydrographically closed basins. All the studied basins are fault bounded, and thought to be internally drained. The presence of extensive playa lake sediments in the studied units, indicates that evaporation exceeded precipitation. A basinal setting known to be characterised by saline, alkaline brines (Surdam and Sheppard,1978).

Pre-burial diagenesis of Andean alluvium took place under an oxidising regime at near neutral pH, conditions favouring the

precipitation of authigenic quartz and K-feldspar (Coloso Formation) as syntaxial overgrowths (Walker et al.,1978). Concentration of the originally oxidising pore waters is thought to have taken place initially through evaporation, and continued through reaction with materials encountered in its flow path, due to the closed hydrographic nature of the basins. The main diagenetic reaction was the dissolution of intermediate plagioclase as shown by widespread dissolution textures. This reaction can be written:

$$NaAlSi_2O_6 + 6H_2O + 2H^+ \longrightarrow 3Si(OH)_4 + Na^+ + Al(OH) + 2HCO_3^- \quad (1$$

$$CaAl_2Si_2O_8 + 4H_2O + 4H^+ \longrightarrow 2Si(OH)_4 + Ca^{2+} + 2Al(OH)_2 \quad (2$$

The reactions for albite and anorthite are written separately for convenience. There is a wide range of feldspar compositions present in the studied red beds and an average composition of An_{50} is realistic.

The effect of feldspar dissolution was to both raise alkalinity and provide a source for both Na and Al for analcime precipitation. These dissolution reactions took place in depositional meteoric porewaters. Following the above dissolution reactions, intrastratal solutions would evolve into saline, alkaline brines, as the fluid moved basinwards due to the pieziometric head and groundwater recharge. With further concentration calcite would be precipitated when the thermodynamic solubility product was exceeded according to:

$$Ca^{2+} + HCO_3^- \longrightarrow CaCO_3 + H^+$$

(3

The early crystals of calcite with outer manganiferous zones in the Coloso and Purilactis Formations record this increase in salinity and alkalinity of the interstitial solutions. When conditions were sufficienly alkaline analcime was precipitated according to the reaction:

$$2Si(OH)_4 + Na^+ + Al(OH)_3 \longrightarrow NaAlSi_2O_6.H_2O + 3H_2O + 2H^+$$

(4

Texturally the analcime appears to have been precipitated after the main physical compaction of the sandstones (which varied in degree between the studied units). Its euhedral and inclusion free nature suggest that no intermediate phase such as sodium smectite was present.

The absence of analcime from the Agua Dulce Formation may be due to its diagenetic replacement. Although there is no clear textural evidence of such "in situ" replacement, a generalised reaction can be written: analcime —> quartz + sodium smectite, which is consistent with the abundance of authigenic quartz and clay minerals in the Agua Dulce Formation. However, clay mineral analyses indicate that any smectite present must have been converted to illite.

Alternatively, owing to the large amount of silica present in the Agua Dulce Formation derived from interbedded acidic volcanics, the pore fluids may have become supersaturated with respect to quartz.

This would account for the lack of later diagenetic events in the Agua Dulce Formation, compared to the other units studied.

The coexistence of analcime, authigenic clays (chlorite or illite), quartz and non-ferroan calcite, as both pore-lining and pore-filling cements, indicates that the composition of the pore fluid was constantly fluctuating between these diagenetic phases, but never exceeded the solubility product of K-feldspar, due to the high ionic mobility of Na^+ in solution.

7.4.2 Conclusions

In three spatially and temporally separate basins, virtually identical diagenetic regimes prevailed. Diagenesis in the basins involved a change from freshwater oxidising to saline, alkaline pore waters, through reaction with Na-rich feldspathic and volcaniclastic detritus. This diagenetic regime was favoured by an igneous source area of intermediate composition and deposition in a desiccating, closed hydrographic basin, where evaporation exceeded precipitation (Fig. 7.5).

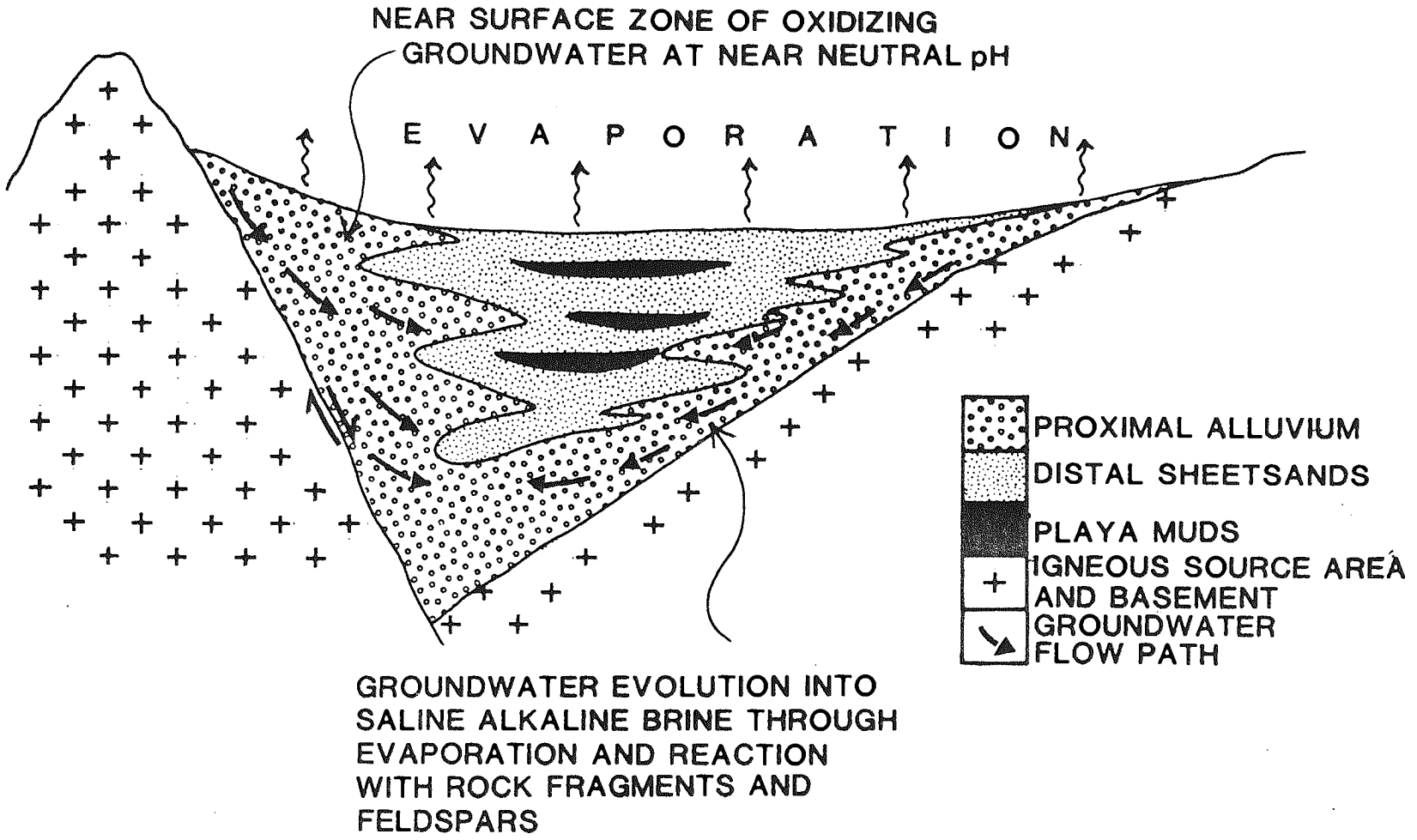

Fig. 7.5 Schematic diagram for analcime precipitation in a hydrographically closed basin, showing the envisaged groundwater circulation. Modified after Surdam and Sheppard (1978) and Walker (1976).

CHAPTER 8

THESIS CONCLUSIONS

1) The Andean forearc is not a simple compressive orogen. It is composed of a number of discrete morphotectonic provinces, each with a separate geological evolution, not neccessarily related to compression.

2) Extensional stress regimes have dominated the Mesozoic history of the Andean forearc, interrupted periodically by compressive events. The interaction between extensional and compressional tectonic regimes, has resulted in the present day segmentation of the forearc.

3) Palaeomagnetism is a useful analytical technique in the study of forearc regions. In the Andean forearc, palaeomagnetism has allowed the definition of structural trends, enabling the response of the overriding South American Plate to an extensional stress regime to be determined, giving an insight into processes active at a convergent plate margin. Palaeomagnetism has also aided in partially defining the extent and age of the response of the continental crust to an extensional tectonic regime.

4) The Andean Orogenic cycle was and is, a complex teconic episode, which can split into three main phases:

a) ?Permian-Triassic. This period involved the extension and possible rifting of the South American craton in northern Chile (roughly along longitude 69°E.). A rift association which may extend as far north as Central Peru.

b) Jurassic-Lower Cretaceous. During this period, formation of a volcanic arc and associated back-arc basin took place. Sediments in the back-arc basin record the movement of the volcanic arc, with the deposition of deep marine sediments (when the arc was at its furthest point from the South American craton), through shallow marine and continental sediments (closure of the basin due to the movement of the arc towards the craton, or vice-versa), up to the end of the Neocomian.

The accretion of the Mejillones terrane took place during the Jurassic (?Lower), and may be asociated with the closure of the back-arc basin.

c) Mid-Cretaceous to Recent. Accretion of the volcanic arc coupled with the Mejillones terrane, against the South American craton (the eastern edge of which is thought to be represented by the Precordillera, in northern Chile), resulted in the compression and episodic deformation of the back-arc basin sequence. This produced an eastwardly propagating thrust system, in front of which sedimentation took place in foreland basins. The period of closure of the back-arc basin and accretion of the volcanic arc is coincident with the break-up of South America and Africa in the Lower-Mid Cretaceous, which resulted in the movement of South America westwards.

The end of the Miocene recorded the uplift of the forearc, the development of the present day volcanic arc, and the initiation of an eastwardly propagating thrust front on the eastern side of the volcanic arc. Volcanism was relocated from the late Jurassic/early Cretaceous position in the Cordillera de la Costa, 250km. inland to its present day position. The movement of the locus of volcanism is thought to be due to the shallowing of the angle of subduction through the westward movement of South America and collision with the volcanic arc, after the opening of the South Atlantic. This resulted in the eastward movement of the depth at which andesitic magma generation takes place.

After accretion of the volcanic arc and deformation of the back-arc basin, extension again dominated in the forearc, resulting in subsidence and the formation of the Central Depression, characterised by small sedimentary basins located between isolated tilted fault blocks, formed through extension along previous thrust faults.

APPENDIX A

A.1 Reference Pole Derivation

Palaeomagnetic poles derived from the stable shield area of South America, their ages and method of derivation are presented in Table A.1. These poles (used in Figs. 3.8, 4.9 and 5.7), allow a comparison to be made between similarly aged palaeomagnetic poles derived from the Andean forearc, enabling the identification of forearc rotation.

The age range covered by the reference poles is small, in order to minimise the effect of apparent polar wander of the South American craton.

Palaeomagnetic poles derived from the Eastern Andean foothills have been excluded from the reference pole calculations, as they are located in the Andean thrust belt and may not give a reliable direction.

Some of the poles presented below are poorly defined, however, palaeomagnetic data for the South American craton (particularly pre Mid-Jurassic) are sparse. Also, some of the poles presented below have been used by other workers allowing a comparison to be made between data sets.

TABLE A.1

AGE	RANGE(Ma)	POLE LAT.	POLE LONG.	α_{95}	REFERENCE
Mid Early-Mid Late Cretaceous	115-85	87	235	5.0	Beck et al. (1986) from 20 poles
Mid-Upper Jurassic	164-160	89	217	4.6	Combined from Schult and Guerreiro (1979) and Vilas (1974).
Lower Jurassic	204-195	72	271	15.0	MacDonald and Opdyke (1974), derived from 3 poles, including Valencio and Vilas (1972).
Late Triassic	232-224	79	226	4.4	Combined from Veldekamp et al. (1971), Valencio and Vilas (1972) and Valencio et al. (1975).

Table A.1 Palaeomagnetic reference poles derived from the stable shield area of South America, and used for comparison with palaeomagnetic poles derived from the Andean forearc.

APPENDIX B

B.1 Access to Palaeomagnetic Files and Results

All palaeomagnetic data used in this thesis is available for inspection, and is lodged with the Departmental Superintendent at the Department of Geological Sciences, Aston University, Aston Triangle, Birmingham.

REFERENCES

Acenolaza, G.F., Benedetto, J.L., Vieira, O., Koukharsky, H. and Salfity, J.A. 1972. Presencio de sedimentitas Devonicas en la Puna de Atacama, Prov. de Salta, Argentina. Assoc. Geol. Argent. Rev., 27: 345-346.

Acenolaza, G.F. and Durand, F.R. 1984. The trace fossil Oldhamia. Its interpretation and occurence in the Lower Cambrian of Argentina. N. Jahrb. Geol. Palaont. Munster., 12: 728-740.

Acenolaza, G.F. and Durand, F.R. 1986. Upper Precambrian-Lower Cambrian biota from the northwest of Argentina. Geol. Mag., 123: 367-375.

Allen, P.A., Homewood, P. and Williams, G.D. 1983. Foreland basins: an introduction. Spec. Publ. Int. Ass. Sediment., 8: 3-12.

Allmendinger, R.W., Ramos, V.A., Jordan, T.E., Palma, M. and Isacks, B.L. 1983. Palaeogeography and Andean structural geometry, northwest Argentina. Tectonics, 2: 1-16.

Arabasz, W.J. 1968. Geologic structure of the Taltal area, northern Chile; in relation to the earthquake of December 28, 1966. Bull. Seism. Soc. America, 58: 835-842.

Arabasz, W.J. 1970. Geological and geophyisical studies of the Atacama fault zone in northern Chile. Unpubl. Ph.D. thesis. Calif. Inst. Tech. 175pp.

Arima, M. and Edgar, A.D. 1980. Importance of time and H_2O content on the analcime-H_2O system at 465°C and 1Kb pH_2O. N. Jahb. Miner. Min., 12: 543-544.

Atherton, M.P., Pitcher, W.S. and Warden, V. 1983. The Mesozoic marginal basin of Central Peru. Nature, 305: 303-306.

Baeza, L. 1976. Geologia de Cerritos Bayos y areas adyacentes entre los 22°30'-22°45' L. S. y los 68°55'-69°25' L. W. II Region, Antofagasta, Chile. Unpubl. thesis, Depto. Geol. Univ. del Norte, Antofagasta. 182pp.

Baeza, L. and Venegas, R. 1984. Geological map of the Mejillones Peninsula, northern Chile. Univ. del Norte, Antofagasta, Chile. Unpubl.

Baeza, L. and Venegas, R. 1985. Petroligia de las anfibolitas de la Peninsula de Mejillones, norte de Chile. Actas IV Congresso Geol. Chileno, Antofagasta. Tomo 3: 31-51.

Bahlberg, H. 1985. sedimentological aspects of the El Toco Formation (Palaeozoic; Coastal Cordillera) NW of Quillagua, northern Chile. Actas IV Congresso Geol. Chileno, Antofagasta. Tomo 1: 17-29.

Bahlberg, H., Breitkreuz, C. and Zeil, W. 1986. Palaeozoische Sedimente Nord-Chiles. Berliner Geowiss. Abh., 66: 147-168.

Barazangi, M. and Isacks, B.L. 1976. Spatial distribution of earthquakes and subduction of the Nazca Plate beneath South America. Geology, 4: 686-692.

Barth, W. 1972. Das Permakarbon bei Zudanez (Bolivien) und einer ubersicht das Jungpalaeozoikums im Zentralen Teil der Anden. Geol. Rund., 61: 249-270.

Beck, M.E. 1980. Palaeomagnetic record of plate margin tectonic processes along the western margin of North America. J. Geophys. Res., 84: 7115-7131.

Beck, M.E. 1985. Palaeomagnetic data from active plate margins of South America. Presented at the I.G.C.P. final symposium, Santiago, November 1985. In press.

Beck, M.E., Drake, R.E. and Butler, R.F. 1986. Palaeomagnetism of Cretaceous volcanic rocks from Central Chile and implications for the tectonics of the Andes. Geology, 14: 132-136.

Berg, K., Breitkreuz, C., Damm, K.W., Pichowiak, S. and Zeil, W. 1983. The North Chilean coast range-an example of the development of an active continental margin. Geol. Rund., 72: 715-731.

Berg, K. and Breitkreuz, C. 1983. Mesozoische Plutone in der Nord-Chilenischen Kustenkordillere: Petrogenese, Geochronlogie, Geochemie und Geodynamik Mantelbetonter Magmatite. Geotekt. Forsch., 66: 107pp.

Biese, W. 1957. Der Jura von Cerritos Bayos, Calama, provincia de Antofagasta. Geol. Jahrb., 72: 439-494.

Bluck, B. 1978. Sedimentation in a late orogenic basin: the Old Red Sandstone of the Midland Valley, Scotland. In: Bowes, D.R. and Leake, B.E. (eds.): Crustal evolution in northwestern Britain and adjacent regions. Geol. J. Spec. Iss., 10: 249-278.

Bogdanic, T. 1983. Antecedentes generales y biostratigraphica del sisteme Jurassico en la zona Preandina, entre los 24°30' y los 25°30' de latitud sur y los 69° y 69°30' de longitud oeste. II Region de Antofagasta, Chile. Unpubl. thesis, Depto. Geosciencias, Univ. del Norte. 243pp.

Boles, J.R. 1971. Synthesis of analcime from natural heulandite and clinoptilolite. Am. Mineral., 56: 1724-1734.

Boles, J.R. and Coombs, D.S. 1977. Zeolite facies alteration of sandstones in the Southland Syncline, New Zealand. Am. J. Sci., 277: 982-1012.

Bott, M.H.P. 1981. Crustal doming and the mechanism of continental rifting. Tectonophysics, 73: 1-8.

Bott, M.H.P. 1982. Origin of the lithospheric tension causing basin formation. Phil. Trans. R. Soc. London, A305: 319-324.

Breitkreuz, C. 1985. Presentation of a marine volcano-sedimentary sequence of presumably pre-Devonian age in the Sierra de Argomedo (24°45'S-69°22'W), northern Chile. Actas IV Congresso Geol. Chileno, Antofagasta. Tomo 1: 1-76.

Breitkreuz, C. 1986. Plutonism in the Central Andes. Zbl. Geol. Palaont., 9/10: 1283-1293.

Breitkreuz, C. and Zeil, W. 1984. Geodynamic and magmatic stages on a traverse through the Andes between 20 and 24°S. (N. Chile, S. Bolivia, N.W. Argentina). J. Geol. Soc. London, 141: 861-868.

Bruggen, J. 1934. Las formaciones de sal y petroleo de la Puna de Atacama. Minas y Petroleo Bol. (Santiago, Chile), 4.

Bruggen, J. 1942. Geologia de la Puna de San Pedro de Atacama y sus formaciones de areniscas y arcillas rojas. An. 1° Congr. Panam. Ing. Minas y Geol., 2: 342-360.

Bruggen, J. 1950. Fundamentos de la geologia de Chile. Inst. Geogr. Militar, 374pp.

Bruhn, R.L. and Dalziel, I.W.D. 1977. Destruction of the Early Cretaceous marginal basin in the Andes of Tierra del Fuego. In Talwani, M. and Pittman, W.C. (eds.): Island arcs, deep sea trenches and back-arc basins. Am. Geophys. Union (Washington D.C.). Maurice Ewing Series 1: 395-405.

Buchelt, M. and Zeil, W. 1986. Petrographische und Geochemische untersuchungen an Jurassischen Vulkaniten der Porphyrit-Formation in der Kustenkordillere Nord-Chiles. Berliner Geowiss. Abh., 66: 191-204.

Chase, C.G. 1978. Plate kinematics: the Americas, East Africa and the rest of the world. Earth Planet. Sci. Lett., 37: 355-368.

Chong, G. 1973. Reconocimiento geologica del area Catalina-Sierra de Varas y Estratigrafica del Jurassico del Profeta. Unpubl. thesis, Dept. Geol. Univ. Chile. 294pp.

Chong, G. 1977. Contribution to the knowledge of the Domeyko Range in the Andes of northern Chile. Geol. Rund., 66: 374-404.

Chong, G. and Reutter, K. 1985. Fenomenos de tectonica compressiva en las Sierras de Varas y de Argomedo, Precordillera Chilena, en el ambito del Paralela 25° Sur. Actas IV Congresso Geol. Chileno, Antofagasta. Tomo 4: 219-238.

Cobbing, E.J., Pitcher, W.S., Wilson, J.J., Baldock, J.W., Taylor, W.P., McCourt, W. and Snelling, N.J. 1981. The geology of the Western Cordillera of northern Peru. Overseas Mem. Inst. Geol. Sci. London, 5: 143pp.

Coira, B., Davidson, J., Mpodozis, C. and Ramos, V. 1982. Tectonic and magmatic evolution of the Andes of northern Argentina and Chile. Earth Sci. Rev., 18: 303-332.

Coney, P.J., Jones, D.L. and Monger, J.W.H. 1980. Cordilleran suspect terranes. Nature, 288: 329-332.

Cowen, D.S., Botros, M. and Johnson, P.H. 1986. Bookshelf tectonics: rotated crustal blocks within the Sovanco fracture zone. Geophys. Res. Lett., 13: 995-998.

Coombs, D.S. 1954. The nature and alteration of some Triassic sediments from Southland, New Zealand. Royal Soc. New Zealand Trans., 82: 65-109.

Coombs, D.S., Ellis, A.J. Fyfe, W.S. and Taylor, A.M. 1959. The zeolite facies, with comments on the interpretation of hydrothermal synthesis. Geochim. Cosmochim. Acta., 17: 53-107.

Coombs, D.S. and Whetten, J.T. 1967. Composition of analcime from sedimentary and burial metamorphic rocks. Geol. Soc. Am. Bull., 78: 269-282.

Cuerda, A. 1974. Zur Stratigraphie des Altpalaozoikums in Argentina. Geol. Rund., 63: 1261-1277.

Dalmayrac, B., Laubacher, G., Marocco, R., Martinez, C. and Tomasi, P. 1980. La chaine Hercynienne d'Amerique du Sud. Structure et evolution d'un orogene intracratonique. Geol. Rund., 69: 1-21.

Dalziel, I.W.D., De Wit, M.J. and Palmer, K.F. 1974. A fossil marginal basin in the Southern Andes. Nature, 250: 291-294.

Dalziel, I.W.D. 1986. Collision and Cordilleran orogenesis: an Andean perspective. In: Coward, M.P. and Ries, A.C. (eds.): Collision tectonics. Geol. Soc. Spec. Publ., 19: 389-404.

Damm, K.W., Pichowiak, S. and Zeil, W. 1981. The plutonism in the north Chilean coast range and its geodynamic significance. Geol. Rund., 70: 1054-1076.

Damm, K.W., Pichowiak, S. and Todt, W. 1986. Geochemie, Petrologie und Geochronologie der Plutonite und des metamorphen Grundgebirges in Nordchile. Berliner Geowiss. Abh., 66: 73-146.

Darwin, C. 1876. geological observations on the volcanic islands and part of South America visited during the voyage of H.M.S. "Beagle". Smith, Elder and Co., London. 647pp.

Davidson, J., Mpodozis, C. and Rivano, S. 1981. Palaeozoico de Sierra Almeida, al oeste de Monturaqui; Alta Cordillera de Antofagasta, Chile. Rev. Geol. Chile, 12: 3-23.

Deer, W.A.., Howie, R.A. and Zussman, J. 1966. An introduction to the rock-forming minerals. Longman, London. 528pp.

Dewey, J.F. 1980. Episodicity, sequence and style at convergent plate boundaries. In: Strangway D.W. (ed.): The continental crust and its mineral deposits. Geol. Ass. Canada Spec. Paper, 20: 553-573.

Dickinson, W.R. 1974. Plate tectonics and sedimentation. In: Dickinson, W.R. (ed.): Tectonics and sedimentation. Soc. Econ. Palaeont. Miner. Spec. Publ., 22: 1-27.

Dickinson, W.R. and Seely, R.C. 1979. Structure and stratigraphy of forearc regions. Bull. Am. Ass. Pet. Geol., 63: 2-31.

Dingman, R.J. 1963. Cuadrangulo Tulor, Provincia de Antofagasta. Instituto de Investigaciones Geologicas. Carta Geologica de Chile 14, 29pp.

Dingman, R.J. 1965. Pliocene age of the ash flow deposits of the San Pedro area, Chile. U.S. Geol. Surv. Prof. Pap., 525-C: C63-67.

Dingman, R.J. 1967. Geology and groundwater resources of the northern part of the Salar de Atacama, Antofagasta Province, Chile. Bull. U.S. Geol. Surv. 1219.

Donahoe, R.J. and Liou, J.G. 1985. An experimental study on the process of zeolite formation. Geochim. Cosmochim. Acta., 49: 2349-2360.

Dunlop, D.J. 1972. Magnetic mineralogy of unheated and heated red sediments by coercivity spectrum analysis. Geophys. J., 27: 37-55.

Dunlop, D.J. 1979. On the use of Zijderveld diagrams in multicomponent palaeomagnetic studies. Phys. Earth Planet. Inter., 20: 12-24.

England, P. and Wortel, R. 1980. Some consequences of the subduction of young slabs. Earth Planet. Sci. Lett., 47: 403-415.

Espinoza, S.R. 1983. Geologia y genesis de la mineralization cupifera del sector de Caleta Coloso, al sur de Antofagasta. Rev. Geol. Chile., 20: 81-91.

Farrar, E., Clark, A.H., Haynes, S.J., Quirt, G.S., Conn, H. and Zentilli, M. 1970. K/Ar evidence for the post-Palaeozoic migration of the granite intrusion foci in the Andes of northern Chile. Earth Planet. Sci. Lett., 10: 60-66.

Feininger, T. 1986. Allochthonous terranes in the Andes of Ecuador and northwestern Peru. Can. J. Earth Sci., 24: 266-288.

Felsch, J. 1933. Informe preliminar sobre los reconocimientos geologicos de los yacimientos petroleros en la cordillera en la provincia de Antofagasta. Minas y Petroleo Bol. (Santiago, Chile), 3: 411-422.

Ferraris, B. and Di Biase, F. 1978. Hoja Antofagasta, Region de Antofagasta, Chile. Instituto de Investigaciones Geologicas. Carta Geologica de Chile 33, 48pp.

Fisher, R.A. 1953. Dispersion on a sphere. Phil. Trans. R. Soc. London, A217: 295-305.

Flint, S.S. 1985a. Alluvial fan and playa sedimentation in an Andean arid closed basin: the Paciencia Group, Antofagasta province, Chile. J. Geol. Soc. London, 142: 533-546.

Flint, S.S. 1985b. The sedimentology, diagenesis and copper mineralisation of continental sediments in the Central Andes. Unpubl. Ph.D. thesis Univ. of Leeds. 403pp.

Flint, S.S. 1987. Diagenesis of Tertiary playa sandstones of northern Chile. Implications for Andean uplift and metallogeny. Sedimentology, 34: 11-29.

Flint, S.S., Clemmey, H. and Turner, P. 1986a. The Lower Cretaceous Way Group of northern Chile: an alluvial fan-fan delta complex. Sed. Geol., 46: 1-22.

Flint, S.S., Clemmey, H. and Turner, P. 1986b. Conglomerate hosted copper mineralisation in Cretaceous Andean molasse: the Coloso Formation of northern Chile. Geol. Mag., 123: 525-536.

Flint, S.S. and Turner, P. 1988. Alluvial-fan and fan-delta sedimentation in a forearc extensional setting: the Cretaceous Coloso basin of northern Chile. In: Nemec D. and Steel, R.J. (eds.): Fan Deltas. Blackie, London. (In press).

Garcia, F. 1967. Geologia del Norte Grande de Chile. Simp. Geosincl. Andino 1962. Soc. Geol. Chile Publ., 3, 183pp.

Halpern, M. 1978. Geological significance of Rb-Sr isotopic data of northern Chile crystalline rocks of the Andean orogen between 23 and 27'S. Geol. Soc. Am. Bull., 89: 522-532.

Halpern, M. and Latorre, C.O. 1973. Estudio geocronologico inicial de rocas del noroeste Argentino. Ass. Geol. Argent. Rev., 28: 195-205.

Harrington, H. 1961. Geology of parts of Antofagasta and Atacama provinces of northern Chile. Am. Ass. Pet. Geol. Bull., 45: 169-197.

Harrington, H. 1967. Devonian of South America. Int. Symp. Devonian System (Calgary), Proceedings 2: 551-671.

Hay, R.L. 1964. Phillipsite of saline lakes and soils. Am. Miner., 49: 1366-1387.

Hay, R.L. 1966. Zeolites and zeolite reactions in sedimentary rocks. Geol. Soc. Am. Spec. Pap., 85, 130pp.

Hay, R.L. 1978. Geologic occurrence of zeolites. In: Mumpton, F.A. (ed.): Natural zeolites: occurrence, properties and use. Pergammon Press, New York. p. 135-143.

Hayes, D.E. 1966. A geophysical investigation of the Peru-Chile trench. Marine Geol., 4: 309-351.

Heki, K., Hamono, Y. and Kono, M. 1983. Rotation of the Peruvian block from palaeomagnetic studies of the Central Andes. Nature, 305: 514-516.

Heki, K., Hamono, Y., Kinoshita, H., Taira, A. and Kono, M. 1984. Palaeomagnetic study of Cretaceous rocks of Peru, South America: Evidence for rotation of the Andes. Tectonophysics, 108: 267-281.

Heki, K., Hamono, Y., Kono, M. and Ui, T. 1985. Palaeomagnetism of Neogene Ocros dyke swarm, the Peruvian Andes: Implications for the Bolivian Orocline. Geophys. J., 80: 527-534.

Herve, F., Davidson, J., Godoy, E., Mpodozis, C. and Covacevich, V. 1981. The late Palaeozoic in Chile: stratigraphy, structure and possible tectonic framework. An. Acad. Brasil. Ciencias, 53: 361-373.

Hess, P.C. 1966. Phase equilibria of some minerals in the K_2O-Na_2O-Al_2O_3-Si O_2-H_2O system at 25°C and 1 atmosphere. Am. J. Sci., 264: 289-309.

Heute, C., Maksaev, V., Moscoso, R., Ulriksen, C. and Vergara, C. 1977. Antecedentes geocronologicas de rocas intrusivas y volcanicas en

la Cordillera de los Andes comprendida entre la Sierra Moreno y el Rio Loa y los 21 y 22° latitud Sur. II Region. Rev. Geol. Chile, 4: 35-41.

High, L.R. and Pickard, M.D. 1965. Sedimentary petrology and origin of the analcime rich Popo Agie Member, Chugwater Formation (Triassic), west-central Wyoming. J. Sed. Pet., 35: 49-70.

Hillebrandt, A.v. 1973. Neue Ergibnisse uber den Jura von Chile und Argentinien. Munstersche Forsch. Geol. Palaont., 31/32: 167-199.

Hillebrandt, A.v., Groschke, M., Prinz, P. and Wilke, H-G. 1986. Marines Mesozoikum in Nordchile zwischen 21 und 26°S. Berliner Geowiss. Abh., 66: 169-190.

Hollingworth, S.E. and Rutland, R.W.R. 1968. Studies of Andean uplift. Part 1-post Cretaceous evolution of the San Bartolo area, N. Chile. Geol. J., 6: 49-62.

Howell, D.G., Jones, D.L. and Schermer, E.R. 1985. Tectonostratigraphic terranes of the Circum-Pacific region. In: Howell, D.G. (ed.): Tectonostratigraphic terranes of the Circum-Pacific region. Earth Science series (Houston), 1: 3-32.

Hunter, R.E. 1977. Basic types of stratification in small aeolian dunes. Sedimentology, 24: 361-387.

Iijima, A. 1974. Clay and zeolite alteration zones surrounding Kuroko deposits in the Hokuroko district, northern Akita, as submarine hydrothermal-diagenetic alteration products. In: Ishihara, S., Kanehira, K., Sasaki, A., Saro, T. and Shimazaki, Y. (eds.): Geology of the Kuroko deposits. Soc. Mining Geologists Jap. Tokyo, p.267-289.

Iijima, A. and Utada, M. 1972. A critical review on the occurrence of zeolites in sedimentary rocks in Japan. Jap. J. Geol. Geog., 42: 61-84.

Isaakson, D.E. 1975. Evidence for an extra continental land source during the Devonian period in the Central Andes. Geol. Soc. Am. Bull., 86: 37-46.

Jackson, J. and McKenzie, D. 1986. A block model of distributed deformation by faulting. J. Geol. Soc. London, 143: 349-354.

James, D.E. 1971. Plate tectonic model for the evolution of the Central Andes. Geol. Soc. Am. Bull., 82: 3325-3346.

James, D.E. 1978. Subduction of the Nazca Plate below Central Peru. Geology, 6: 174-178.

James, D.E. 1982. A combined O, Sr, Nd and Pb isotopic and trace element study of crustal contamination in Central Andean lavas. 1 local geochemical variation. Earth Planet. Sci. Lett., 57: 47-62.

Jarrard, R.D. 1986. Causes of compression and extension behind trenches. Tectonophysics, 132: 89-102.

Johnson, N.M., Jordan, T.E., Johnsson, P.A. and Naeser, C.W. 1986. Magnetic polarity stratigraphy, age and tectonic setting of fluvial sediments in an eastern Andean foreland basin, San Juan Province, Argentina. In: Allen, P.A. and Homewood, P. (eds.): Foreland basins. Spec. Publ. Int. Ass. Sediment., 8: 63-75.

Jones, D.L., Silberling, W. and Coney, P.J. 1986. Collision tectonics in the Cordillera of western North America: examples from Alaska. In: Coward, M.P. and Ries, A.C. (eds.): Collision tectonics. Geol. Soc. Spec. Publ., 19: 367-387.

Jordan, T.E., Isacks, B.L., Allmendinger, R.W., Brewer, J.A., Ramos, V.A. and Ando, C.J. 1983. Andean tetonics related to the geometry of the subducted Nazca Plate. Geol. Soc. Am. Bull., 94: 341-361.

Jordan, T.E. and Alonso, R.N. 1987. Cenozoic stratigraphy and basin tectonics of the Andes Mountains, 20-28° South latitude. Am. Ass. Pet. Geol. Bull., 71: 49-64.

Jurgan, H. 1974. Die Marine Kalkfolge der Unterkreide in der Quebrada El Way, Antofagasta, Chile. Geol. Rund., 63: 490-516.

Kirschvink, J.L. 1980. The least-squares line and plane and the analysis of palaeomagnetic data. Geophys. J., 62: 699-718.

Kominz, M.A. 1984. Oceanic ridge volumes and sea-level change-an error analysis. In: Schlee, J. (ed.): Inter-regional unconformities and hydrocarbon accumulations. Mem. Am. Ass. Pet. Geol., 34: 109-127.

Kussmaul, S.L., Hoerman, P.K., Ploskonka, E. and Subieta, T. 1977. Volcanism and structure of southwestern Bolivia. J. Volcan. Geotherm. Res., 2: 73-111.

Linares, C. and Valencio, D.A. 1975. Palaeomagnetism and K/Ar ages of some trachybasalt dykes from Rio de las Molinas, Province of Cordoba, Republica Argentina. J. Geophys. Res., 86: 3315-3321.

MacDonald, W.D. and Opdyke, N.D. 1974. Triassic palaeomagnetism of northern South America. Am. Ass. Pet. Geol. Bull., 58: 205-215.

Marinovic, C. and Lahsen, D. 1984. Hoja Calama. Region de Antofagasta. Carta Geologica de Chile no. 58. 1:250,000. Serv. Nac. Geol. Chile. 140pp.

May, S.R., Coney, P.J. and Beck, M.E. 1983. Palaeomagnetism and suspect terranes of the North American Cordillera. U.S. Geol. Surv. Open-File Report, 83, 799pp.

May, S.R. and Butler, R.F. 1985. Palaeomagnetism of the Puente Piedra Formation, Central Peru. Earth Planet. Sci. Lett., 72: 215-218.

McBride, S.L., Robertson, R.C.R., Clark, A.H. and Farrar, E. 1983. Magmatic and metallogenic episodes in the northern tin belt, Cordillera Real, Bolivia. Geol. Rund., 72: 685-713.

McCourt, W.J., Aspden, J.A. and Brook, M. 1984. New geological and geochronological data from the Columbian Andes: continental growth by multiple accretion. J. Geol. Soc. London, 141: 831-845.

McElhinney, M.W. 1964. Statistical significance of the fold test in palaeomagnetism. Geophys. J., 8: 338-340.

McFadden, P.L. and Jones, D.L. 1981. The fold test in palaeomagnetism. Geophys. J., 67: 53-58.

McGeary, S. and Ben-Avaraham, Z. 1985. The accretion of Gorgona Island, Columbia. Multichannel seismic evidence. In: Howell, D.G. (ed.): Tectonostratigraphic terranes of the Circum-Pacific region. Earth Sci. Series (Houston), 1: 543-544.

Mariner, R.H. and Surdam, R.C. 1970. Alkalinity and formation of zeolites in saline, alkaline lakes. Science, 170: 977-980.

Megard, F., Noble, D.C., Mckee, E.H. and Belkon, H. 1984. Multiple phases of Neogene compressive deformation in the Ayacucho intermontane basin, Andes of Central Peru. Geol. Soc. Am. Bull., 95: 1108-1117.

Megard, F., Noble, D.C., Mckee, E.H. and Cuenod, Y. 1985. Tectonic significance of silicic dykes contemporaneous with latest Miocene Quechua 3 tectonism in the Rimac Valley, Western Cordillera of Central Peru. J. Geol., 93: 373-376.

Mendiguren, J.A. and Richter, F.M. 1978. On the origin of intraplate compressional stresses in South America. Phys. Earth Planet. Inter., 16: 318-326.

Mercier, J.L. 1981. Extensional-compressional tectonics associated with the Aegean arc: comparison with the Andean Cordillera of South Peru-North Bolivia. Phil. Trans. R. Soc., A300: 337-355.

Miall, A.D. 1987. Recent developments in the study of fluvial facies models. In: Ethridge, F.C., Flores, R.M. and Harvey, M.D. (eds.): Recent developments in fluvial sedimentology. Soc. Econ. Palaont. Miner. Spec. Publ. 39: 1-9.

Miller, H. 1970. Vergleichende studien aus pre-Mesozoischen Gesteinen Chiles unter besonderer Berucksichtigung ihrer Kleintektonik. Geotekt. Forsch., 36: 64pp.

Mingramm, A., Russo, A., Pozzo, A. and Cazau, L. 1979. Sierras Subandinas. 2nd. Symp. Geol. Region Argent., 1: 95-138.

Minster, J.B. and Jordan, T.H. 1978. Present day plate motions. J. Geophys. Res., 83: 5331-5354.

Molnar, P. and Atwater, T. 1978. Interarc spreading and Cordilleran tectonics as alternates related to the age of the subducted oceanic lithospere. Earth Planet. Sci. Lett., 41: 330-340.

Moraga, B., Chong, G., Fortt, M.A. and Henrique, H. 1974. Estudio geologico de Salar de Atacama, Provincia de Antofagasta, Chile. Instituto del Investigaciones Geologica Chile Bol., 29: 56pp.

Nashar, B. 1978. Sedimentary analcime at Murrurundi, New South Wales, Australia. Min. Mag., 42: 241-243.

Noble, D.C., McKee, E.H., Farrar, E. and Peterson, U. 1974. Episodic Cenozoic volcanism and tectonism in the Andes of Peru. Earth Planet. Sci. Lett., 21: 213-220.

Noble, D.C., Miles, L.S., Megard, F. and Bowman, H. 1978. Comendite (peralkaline rhyolite) and basalt in the Mitu Group, Peru: evidence for Permian-Triassic lithospheric extension in the Central Andes. J. Res. U.S. Geol. Surv., 6: 453-457.

Noble, D.C., Farrar, E. and Cobbing, E.J. 1979. The Nazca Group of South-Central Peru: age, source, and regional volcanic and tectonic significance. Earth planet. Sci. Lett., 45: 80-86.

Oesterlen, M. 1979. Karoo-system und Prakambrische unterlage im nordlichen Angola. Geol. Jahrb., B36: 3-41.

Okada, A. 1971. On the neotectonics of the Atacama fault zone region-Preliminary notes on late Cenozoic faulting and geomorphic development of the coast range of northern Chile. Bull. Dep. Geogr. Univ. Tokyo, 3: 47-65.

Omarini, R., Cordani, U.G., Viramonte, J.A., Salfity, J.A. and Kawashita, K. 1979. Estudio isotopico Rb/Sr de la Faja Eruptiva de la Puna a los 22°35' lat. Sur, Argentina. Actas II Congresso Geol. Chileno, Santiago. Tomo 3: 257-269.

Palmer, H.C., Hayatsu, A. and MacDonald, W.D. 1980a. Palaeomagnetic and K-Ar age studies of a 6km. thick Cretaceous section from the Chilean Andes. Geophys. J., 62: 133-153.

Palmer, H.C., Hayatsu, A. and MacDonald, W.D. 1980b. The Middle Jurassic Camaraca Formation, Arica, Chile. Palaeomagnetism, K-Ar dating and tectonic implications. Geophys. J., 62: 155-157.

Paskoff, R. 1977. Quaternary of Chile: the state of research. Quaternary Res., 8: 2-31.

Perez, E. and Levi, D. 1961. Relacion estratigraphica entre la Formacion Moctezuma y el granito subyacente, Calama, Prov. de Antofagasta, Chile. Santiago Inst. Ing. Min. Chile. Minerales, 74: 39-48.

Pettijohn, F.J. Potter, P.E. and Siever, R. 1973. Sand and sandstones. Springer-Verlag, Berlin. 518pp.

Pichowiak, S. and Breitkreuz, C. 1984. Volcanic dykes in the North Chilean coast range. Geol. Rund., 73: 853-868.

Pitcher, W.S. 1984. Phanerozoic plutonism in the Peruvian Andes. In: Harmon, R.S. and Barreiro, B.A. (eds.): Andean magmatism-chemical and isotopic constraints. Shiva, London. p.152-167.

Prince, R.A. and Kulm, L.D. 1975. Crustal rupture and the initiation of imbricate thrusting in the Peru-Chile trench. Geol. Soc. Am. Bull., 86: 1639-1653.

Quinzio Sinn, L.A. 1986. Biostratigraphische untersuchungen im Marinen Unterjura der Kustenkordillere zwischen Antofagasta und Chanaral, Nord Chile. Berliner Geowiss. Abh. Sonderband, 37-38.

Rabinowitz, P.D. and La Brecque, J. 1979. The Mesozoic South Atlantic ocean and the evolution of its continental margins. J. Geophys. Res., 84: 5973-6002.

Ramdohr, P. 1969. The ore minerals and their intergrowths. Pergamon, New York. 3rd. Ed.

Ramirez, C.E. 1979. Edades potasio/argon de rocas volcanicas Cenozoicas en la zona de San Pedro de Atacama y El Tatio, Region de Antofagasta. Actas II Congr. Geol. Chileno, Arica, Chile., 1: 31-41.

Ramirez, R. and Gardeweg, M. 1982. Hoja Toconao, Region de Antofagasta. Carta Geol. Chile no. 54; 1:250,000. Serv. Nac. Geol. Miner. Chile. 117pp.

Ramos, V.A., Jordan, T.E., Allmendinger, R.W., Mpodozis, C., Kay, S.M., Cortes, J.M. and Palma, M. 1986. Palaeozoic terranes of the Central Argentine-Chilean Andes. Tectonics, 5: 855-880.

Rapela, C.W., Heaman, L.M. and McNutt, R.H. 1982. Rb/Sr geochronology of granitoid rocks from the Pampean Ranges, Argentina. J. Geol., 90: 574-582.

Rogers, G. 1985. A geochemical traverse across the North Chilean Andes. Unpubl. Ph.D. thesis, Open Univ. Milton Keynes. 333pp.

Ron, H., Freund, R. and Garfunkel, Z. 1984. Block rotation by strike-slip faulting: structural and palaeomagnetic evidence. J. Geophys. Res., 89: 6256-6270.

Rutland, R.W.R. 1971. Andean Orogeny and sea-floor spreading. Nature, 233: 252-255.

Schult, A. and Guerreiro, S.D.C. 1980. Palaeomagnetism of Mesozoic igneous rocks from the Maranhao basin, Brazil, and the timing of the opening of the South Atlantic. Earth Planet. Sci. Lett., 42: 427-436.

Shackleton, R.M., Ries, A.C., Coward, M.P. and Cobbold, P.R. 1979. Structure, metamorphism and geochronology of the Arequipa Massif of Coastal Peru. J. Geol. Soc. London, 136: 195-214.

Sheppard, R.A. and Gude, A.J. 1968. Distribution and genesis of authigenic silicate minerals in tuffs of Pleistocene Lake Tecopa, Inyo County, California. U.S. Geol. Surv. Prof. Paper, 597, 38pp.

Sheppard, R.A. and Gude, A.J. 1969. Diagenesis of tuffs in the Barstow Formation, Mud Hills, San Bernadino County, California. U.S. Geol. Surv. Prof. Paper, 634, 35pp.

Sheppard, R.A. and Gude, A.J. 1973. Zeolites and associated authigenic minerals in tuffaceous rocks of the Big Sandy Formation, Mohave County, Arizona. U.S. Geol. Surv. Prof. Paper, 830, 35pp.

Sillitoe, R.H. 1974. Tectonic segmentation of the Andes: implications for magmatism and metallogeny. Nature, 250: 542-545.

Stephenson, A. 1967. The effect of heat treatment on the magnetic properties of the Old Red Sandstone. Geophys J., 13: 425-440.

Surdam, R.C. and Eugster, H.P. 1976. Mineral reactions in the sedimentary deposits of the Lake Magadi region, Kenya. Geol. Soc. Am. Bull., 87: 1739-1782.

Surdam, R.C. and Sheppard, R.A. 1978. Zeolites in saline, alkaline lake deposits. In: Sand, L.B. and Mumpton, F.A. (eds.): Natural zeolites: occurrence, properties and use. Pergamon, New York. p.145-174.

Thorpe, R.S., Francis, P.W., Hammil, M. and Baker, M.C.W. 1982. The Andes. In: Thorpe, R.S. (ed.): Andesites. Wiley and Sons, London. p.187-205.

Tosdal, R.M., Clark, A.H. and Farrar, E. 1984. Cenozoic polyphase landscape and tectonic evolution of the Cordillera Occidental, southernmost Peru. Geol. Soc. Am. Bull., 95: 1318-1382.

Travisany, V. 1978. Mineralizacion cuprifera en areniscas de la Formacion San Pedro en el districto San Bartolo. Unpubl. thesis, Univ. of Chile, Santiago, Chile. 78pp.

Turner, J.C.M. 1970. The Andes of Northwestern Argentina. Geol. Rund., 59: 1028-1063.

Turner, J.C.M. and Mon, R. 1979. Cordillera Oriental. In: Segundo Simposio de Geologica Regional Argentina, (Cordoba). Acad. Nac. Ciencias, 1: 57-94.

Turner, P. 1980. Continental Red Beds. Elsevier, Amsterdam. 562pp.

Turner, P. and Archer, R. 1975. Magnetisation history of Lower Old Red Sandstones from the Gamrie outlier, Scotland. Earth Planet. Sci. Lett., 27: 240-250.

Turner, P. Clemmey, H. and Flint, S.S. 1984a. Palaeomagnetic studies of a Cretaceous molasse sequence in the Central Andes (Coloso Formation, Northern Chile). J. Geol. Soc. London, 141: 869-876.

Turner, P., Hirst, J.P.P. and Friend, P.F. 1984b. A palaeomagnetic analysis of Miocene fluvial sediments at Pertusa, near Huesca, Ebro Basin, Spain. Geol. Mag., 121: 279-290.

Ulriksen, C. 1979. Regional geology, geochronology and metallogeny of the Coastal Cordillera of Chile, between 25°30' and 26° S. Unpubl. M.Sc. thesis, Dalhousie Univ. Canada. 180pp.

Utada, M., Minato, H., Ishikawa, T. and Yoskizaki, Y. 1974. The alteration zones surrounding Kuroko-type deposits in the Nishi-Aizu district, Fukushima Prefecture, with emphasis on the analcime zone as an indicator in exploration of ore deposits. Mining Geol. Spec. Issue, p.291-302.

Valencio, D.A. and Vilas, J.F.A. 1972. Palaeomagnetism of Late Palaeozoic and Early Mesozoic rocks of South America. Earth Planet. Sci. Lett., 15: 75-85.

Valencio, D.A., Mendia, J.E. and Vilas, J.F.A. 1975. Palaeomagnetism and K-Ar ages of Triassic igneous rocks from the Ischigualasto-Ischichuca basin and Puesta Viejo Formation, Argentina. Earth Planet. Sci. Lett., 26: 319-330.

Valencio, D.A., Mendia, J.E., Giudici, A. and Gascon, J.O. 1977. Palaeomagnetism of the Cretaceous Piruga Subgroup (Argentina) and the age of the opening of the South Atlantic. Geophys. J., 51: 47-58.

Veldkamp, J., Mulder, F.G. and Zijderveld, J.D.A. 1971. Palaeomagnetism of Suriname dolerites. Phys. Earth Planet. Inter., 4: 370-380.

Velde, B. 1985. Clay Minerals. Elsevier, Amsterdam. 427pp.

Vernet, J.P. 1961. Concerning the association montmorillonite-analcime in the series of Stanleyville, Congo. J. Sed. Pet., 31: 293-295.

Vilas, J.F.A. 1974. Palaeomagnetism of some igneous rocks of the Middle Jurassic Chon Aike Formation from Estancia la Reconquista, Province of Santa Cruz, Argentina. Geophys. J., 39: 511-522.

Vilas, J.F.A. 1976. Palaeomagnetism of the Lower Cretaceous Sierra de los Condores Group, Cordoba Province, Argentina. Geophys. J., 46: 295-305.

Walker, T.R. 1967. Formation of red beds in modern and ancient deserts. Geol. Soc. Am. Bull., 78: 353-368.

Walker, T.R. 1976. Diagenetic origin of continental red beds. In: Faulke, H. (ed.): The Continental Permian in Central, West and South Europe. Dordrecht, Holland. p.240-282.

Walker, T.R., Waugh, B. and Crone, A.J. 1978. Diagenesis in first cycle desert alluvium of Cenozoic age, South Western United States and North Eastern Mexico. Geol. Soc. Am. Bull., 89: 19-32.

Walton, A.W. 1975. Zeolite diagenesis in Oligocene volcanic sediments Trans-Pecos, Texas. Geol. Soc. Am. Bull., 86: 615-624.

Wernicke, B.P., Christiansen, R.L., England, P.C. and Sonder, L.J. 1987. Tectonomagmatic evolution of Cenozoic extension in the north American Cordillera. In: Coward, M.P., Dewey, J.F. and Hancock, P.L. (eds.): Continental Extensional Tectonics. Geol. Soc. Spec. Publ., 28: 203-221.

Wetzel, W. 1927. In: Baeza, L. 1976. Geologia de Cerritos Bayos Y areas adyacentes entre los 22°30'-22°45' L.S. y los 68°55'-69°25' L.W., II Region, Antofagasta, Chile. Unpubl. thesis, Univ. del Norte, Antofagasta, Chile. 182pp.

Widdowson, J.W. and de Sa, A. 1975. A digitally controlled AF demagnetiser for peak fields of up to 0.1T. J. Physics London, E8: 302-304.

Zeil, W. 1979. The Andes: a geological review. Borntraeger, Berlin. 260pp.